

1988

The Inorganic Geochemistry Of Two Western Us Coals: Emery Coal Field, Utah And Powder River Coal Field, Wyoming

Michael A. Powell

Follow this and additional works at: <https://ir.lib.uwo.ca/digitizedtheses>

Recommended Citation

Powell, Michael A., "The Inorganic Geochemistry Of Two Western Us Coals: Emery Coal Field, Utah And Powder River Coal Field, Wyoming" (1988). *Digitized Theses*. 1711.
<https://ir.lib.uwo.ca/digitizedtheses/1711>

This Dissertation is brought to you for free and open access by the Digitized Special Collections at Scholarship@Western. It has been accepted for inclusion in Digitized Theses by an authorized administrator of Scholarship@Western. For more information, please contact tadam@uwo.ca, wlsadmin@uwo.ca.



National Library
of Canada

Bibliothèque nationale
du Canada

Canadian Theses Service

Service des thèses canadiennes

Ottawa Canada
K1A 0N4

NOTICE

The quality of this microform is heavily dependent upon the quality of the original thesis submitted for microfilming. Every effort has been made to ensure the highest quality of reproduction possible.

If pages are missing, contact the university which granted the degree.

Some pages may have indistinct print especially if the original pages were typed with a poor typewriter ribbon or if the university sent us an inferior photocopy.

Previously copyrighted materials (journal articles, published tests, etc.) are not filmed.

Reproduction in full or in part of this microform is governed by the Canadian Copyright Act, R.S.C. 1970, c. C-30.

AVIS

La qualité de cette microforme dépend grandement de la qualité de la thèse soumise au microfilmage. Nous avons tout fait pour assurer une qualité supérieure de reproduction.

S'il manque des pages, veuillez communiquer avec l'université qui a conféré le grade.

La qualité d'impression de certaines pages peut laisser à désirer, surtout si les pages originales ont été dactylographiées à l'aide d'un ruban usé ou si l'université nous a fait parvenir une photocopie de qualité inférieure.

Les documents qui font déjà l'objet d'un droit d'auteur (articles de revue, tests publiés, etc.) ne sont pas microfilmés.

La reproduction, même partielle, de cette microforme est soumise à la Loi canadienne sur le droit d'auteur, S.R.O. 1970, c. C-30.

The Inorganic Geochemistry of Two Western U.S. Coals:
Emery Coal Field, Utah and Powder River Coal Field, Wyoming

By

Michael A. Powell

Department of Geology

Submitted in partial fulfillment of the requirements
for the degree of Doctor of Philosophy

Faculty of Graduate Studies
The University of Western Ontario
London, Ontario, Canada

© Michael A. Powell 1987

Permission has been granted to the National Library of Canada to microfilm this thesis and to lend or sell copies of the film.

The author (copyright owner) has reserved other publication rights, and neither the thesis nor extensive extracts from it may be printed or otherwise reproduced without his/her written permission.

L'autorisation a été accordée à la Bibliothèque nationale du Canada de microfilmer cette thèse et de prêter ou de vendre des exemplaires du film.

L'auteur (titulaire du droit d'auteur) se réserve les autres droits de publication; ni la thèse ni de longs extraits de celle-ci ne doivent être imprimés ou autrement reproduits sans son autorisation écrite.

ISBN 0-315-40789-1

ABSTRACT

The inorganic geochemistry of coals from the Cretaceous, Emery Coal Field, Utah and the Paleocene, Powder River Coal Field, Wyoming have been determined using XRF, various neutron activation techniques and SEM/EDS. Differences in deposition environments for the two coal deposits results in a higher ash content in the Utah coal (avg., 8.2%) relative to the Wyoming coal (avg., 4.4%). The Utah coal contains higher concentrations of 27 of the 40 elements detected in both coals. The geochemistry of overburden and clinker associated with the Wyoming coal and Fe-sulfide nodules (selected elements) from within the Utah coal is also reported.

Specific mineral phases within the two coals have been identified using SEM/EDS. Discrete grains contained in the surfaces of pellets prepared from crushed whole coal were analyzed and their mineralogies determined based on stoichiometry.

The oxidation of Fe-sulfide to hydrous Fe-sulfates is documented. Paragenesis results in szomolnokite developing on "clean" Fe-sulfide while halotrichite is the typical secondary phase which forms in the presence of clays.

The environmental aspects of coal utilization are discussed. A new term, "The Effective Coal Concentration (ECC)" is proposed to better assess the amounts of potentially harmful (as well as economically important) elements released to the environment as a result of coal utilization.

Some new conclusions regarding the organic/inorganic affinities of the elements are presented based on the physicochemical nature of the element at the time of emplacement. Elements with ionic potentials (IP) >0.05 tend to favor organic association while elements with $IP < 0.05$ tend towards inorganic combination. Elements which exhibit multiple oxidation states with resulting IP values above and below 0.05 show the largest variations in organic/inorganic affinity.

ACKNOWLEDGEMENTS

During my first meeting with W.S. Fyfe in the spring of '82' he suggested the possibility of me doing a thesis with him related to the geochemistry of coal, a subject I knew little about at the time. Since then Bill has supported this project financially but more importantly I have appreciated his patience and counsel throughout the study. Thanks Bill!

For technical advice and help I would like to thank the following: Tsai W. Wu for much advice and assistance with XRF; Y. Chang for performing XRD; and the staff at Surface Science Western, present and past, Bill, Darlene, Dietmar, Tammy and Doug, for all manner of help.

I am especially indebted to those who have shown so much patience as I fumbled through the day-to-day life of grad school. To the secretarial staff, Joan, Shiela, Marg and especially Jackie, who knows all the answers (angles), or at least where to find them, a heart-felt, thank you!

Thanks to Alan Noon for his patience during the numerous "last minute" photographic needs in the completion of this and other works in the past years.

The past five years at U.W.O. have provided much more than an education. The eclectic nature of graduate-life leads to the formation of many friendships. I am convinced that they are as important as the work itself. I will always treasure the memories.

Thanks to my friends in Detroit, Roman, Kenny, Steve, Michael, Gordon, Wendy and all the others. Your faith in my endeavors has meant more than you might imagine (not to mention the fun we've had).

Bill and A.J., what can I say? Each of you in your own way has helped me immensely. I look forward to our continued friendships!!!

Lysbeth, the six months you were suppose to be in Canada has turned into three years, got ya! Thanks for having enough faith in me to leave your secure life to share in this experience. Oh yes, thanks for Matthew too!

Mom, as usual, I owe you more than thanks, not only for financial support but also for "being there" whenever I've needed you.

This thesis is dedicated to,

Dr. S.E. White, Professor Emeritus,
The Ohio State University

If there was one single person during my undergraduate career who's influence has contributed to my desire to attain higher levels, it was Dr. White.

"I've had good days
and bad days
and going half mad days"

Jimmy Buffett,
Last Mango in Paris,
1985

TABLE OF CONTENTS

	Page
CERTIFICATE OF EXAMINATION	ii
ABSTRACT	iii
ACKNOWLEDGEMENTS	v
DEDICATION	vii
TABLE OF CONTENTS	viii
LIST OF FIGURES	xiii
LIST OF TABLES	xviii
CHAPTER I:	
INTRODUCTION AND OBJECTIVES	1
I.1 Introduction	1
I.2 Objectives	2
CHAPTER II:	
GENERAL DESCRIPTION OF FIELD AREAS	4
II.1 Utah: Emery Coal Field	4
II.1.1 Introduction	4
II.1.2 Upper Cretaceous History	4
II.1.3 Upper Cretaceous (Turonian) Stratigraphy	10
II.1.4 Paleoenvironment	10
II.1.5 Sample Collection	13
II.2 Wyoming: Powder River Coal Field	19
II.2.1 Introduction	19
II.2.2 Early Tertiary (Paleocene) History ...	22
II.2.3 Upper Paleocene Stratigraphy	26
II.2.4 Paleoenvironment	29
II.2.5 Sample Collection	30

CHAPTER III:		
DATA PRESENTATION; RESULTS AND DISCUSSION		34
III.1 Ash		34
III.1.1 Utah		34
III.1.2 Wyoming		34
III.1.3 Summary		37
III.2 Chemical and Mineralogical Analyses (By Method)		38
III.2.1 Introduction		38
III.2.2 Instrumental Neutron Activation Analysis		39
III.2.2.1 Introduction		39
III.2.2.2 Utah: Whole Coal		39
III.2.2.3 Utah: Fe-sulfide Nodules .		40
III.2.2.4 Wyoming: Whole Coal		42
III.2.3 X-Ray Fluorescent Spectroscopy		44
III.2.3.1 Introduction		44
III.2.3.2 Utah: Whole Coal		44
III.2.3.3 Wyoming: Whole Coal		47
III.2.4 Multiple-Technique Analysis		50
III.2.4.1 Introduction		50
III.2.4.2 Utah: Whole Coal		53
III.2.4.3 Wyoming: Whole Coal		54
III.2.4.4 Wyoming: Overburden Sediment and Clinker		54
III.2.4.4.1		
Introduction		56
III.2.4.4.2		
Overburden Sediment		58

	III.2.4.4.3		
	Clinker	61	
	III.2.4.4.4		
	Comparison of Clinker vs Overburden	64	
III.3	Scanning Electron Microscopy / Energy Dispersive Spectroscopy (SEM/EDS)	65	
III.3.1	Introduction	65	
III.3.2	Utah: Whole Coal	76	
	III.3.2.1 Introduction	76	
	III.3.2.2 Clays	81	
	III.3.2.3 Silicates (Other Than Clays)	84	
	III.3.2.4 Carbonates	86	
	III.3.2.5 Oxides	88	
	III.3.2.6 Sulfides	89	
	III.3.2.7 Sulfates	90	
III.3.3	Wyoming: Whole Coal	91	
	III.3.3.1 Introduction	91	
	III.3.3.2 Interpretation	94	
	III.3.3.3 Summary	95	
III.3.4	Utah: Fe-sulfide Nodules	97	
	III.3.4.1 Introduction	97	
	III.3.4.2 Mineralogy and Geochemistry	100	
	III.3.4.3 Summary	113	
 CHAPTER IV:			
	SPONTANEOUS OXIDATION OF FE-SULFIDE TO FE-SULFATE ...	115	
IV.1	Introduction	115	

IV.2	Geochemistry of Secondary Mineral Phases	117
IV.2.1	Szomolnokite	117
IV.2.2	Halotrichite	118
CHAPTER V:		
	DATA COMPARISONS (OVERALL GEOCHEMISTRY)	136
V.1	Introduction	136
V.2	Utah	136
V.3	Wyoming	140
V.4	Utah vs Wyoming	142
V.4.1	Correlation Data	151
CHAPTER VI:		
	COAL UTILIZATION / FLY ASH; ENVIRONMENTAL CONSIDERATIONS	166
VI.1	Introduction	166
VI.2	The Problem	167
VI.3	Resources - Consumption - Waste	169
VI.4	Mode of Occurrence of Potentially Harmful Trace Elements in Coal	172
VI.5	Element Partitioning; The Coal Combustion Facility	173
VI.6	Mechanisms of Fly Ash Formation	178
VI.7	"Dangerous" Characteristics of Fly Ash	179
VI.8	Health Considerations	187
VI.9	Summary: A New Term	190
CHAPTER VII:		
	OBSERVATIONS ON THE GEOCHEMISTRY OF COAL	196
VII.1	Introduction	196
VII.2	The Relative Abundances of the Geochemical Elements in Coal vs Other Rock Types	199

VII.2.1	Introduction	199
VII.2.2	Comparisons of Like Lithologies	200
VII.2.3	Coal vs Rock	204
VII.2.4	Summary	209
VII.3	Organic/Inorganic Affinities of the Elements in Coal	210
VII.3.1	Introduction	210
VII.3.2	The Role of Ionic Potential (IP) in Determining the Organic/Inorganic Affinity of the Elements	221
VII.4	Summary	233
CHAPTER VIII:		
	CONCLUSIONS	236
	BIBLIOGRAPHY	241
	VITA	252

LIST OF FIGURES

FIGURE	DESCRIPTION	PAGE
II.1	LOCATION MAP, SHOWING THE POSITION OF THE EMERY COAL FIELD IN SOUTH-CENTRAL UTAH	6
II.2	TOP: GENERALIZED X-SECTION OF CRETACEOUS STRATA ALONG A NE-SW LINE RUNNING THROUGH THE EMERY COAL FIELD. BOTTOM: GENERALIZED STRATIGRAPHIC COLUMN OF ROCKS IN THE EMERY COAL FIELD	9
II.3	GENERALIZED STRATIGRAPHY OF COAL BEDS WITHIN THE FERRON SANDSTONE MEMBER OF THE MANCOS SHALE	12
II.4	A - SIMPLIFIED SCHEMATIC OF THE TURONIAN LAST CHANCE DELTA OF SOUTHERN UTAH. B - PREDICTIVE MODEL FOR THE SHAPE AND ORIENTATION OF FERRON SANDSTONE PEATS	15
II.5	SCHEMATIC OF THE SUBSURFACE ROOM AND PILLAR MINE FROM WHICH SAMPLES OF UTAH COAL WERE COLLECTED FOR THIS STUDY	18
II.6	LOCATION MAP SHOWING THE POSITION OF THE POWDER RIVER COAL/STRUCTURAL BASIN IN NE WYOMING AND SE MONTANA	21
II.7	OUTLINE OF THE POWDER RIVER COAL BASIN IN WYOMING: GENERALIZED GEOLOGY, STRIPPABLE COAL DEPOSITS AND POWDER RIVER COAL FIELD ..	24
II.8	GENERALIZED STRATIGRAPHY OF COAL BEDS WITHIN THE PALEOCENE FORT UNION FORMATION IN THE POWDER RIVER	28
II.9	SCHEMATIC OF THE OPEN-PIT BENCH MINE FROM WHICH SAMPLES OF WYOMING COAL WERE COLLECTED FOR THIS STUDY	33
III.1	A - PHOTOMICROGRAPH OF A TYPICAL PELLET OF WHOLE COAL FROM WHICH EDS ANALYSES WERE COLLECTED. B - PHOTOMICROGRAPH OF ONE OF THE DISCRETE GRAINS SHOWN IN "A"	69
III.2	A TO P - REPRESENTATIVE EDS SPECTRA OF INDIVIDUAL GRAINS CONTAINED IN WHOLE COAL PELLETS OF UTAH COAL	79

III.3	A TO D - REPRESENTATIVE EDS SPECTRA OF INDIVIDUAL GRAINS CONTAINED IN PELLETS OF WYOMING COAL	93
III.4	PHOTOMICROGRAPH OF ONE OF THE FE-SULFIDE NODULES FROM THE UTAH COAL	99
III.5	A - PHOTOMICROGRAPH OF THE INTERIOR OF ONE OF THE FE-SULFIDE NODULES FROM THE UTAH COAL. B - PHOTOMICROGRAPH OF SOME OF THE CELLS, WITH INFILLINGS, FROM "A"	102
III.6	A - PHOTOMICROGRAPH OF A BRECCIATED VEINLET FROM WITHIN THE "COALY" ZONE OF ONE OF THE FE-SULFIDE NODULES. B - EDS SPECTRUM FROM A GRAIN IN THE FAR RIGHT OF "A". C - EDS SPECTRUM FROM A GRAIN IN THE CENTER OF "A". D - EDS OF THE CEMENT ADJACENT TO THE CENTRAL GRAIN IN "A"	104
III.7	A - PHOTOMICROGRAPH OF A CLAY BLEB FROM WITHIN THE "COALY" ZONE ADJACENT TO ONE OF THE FE-SULFIDE NODULES. B - EDS SPECTRUM FROM THE CLAY BLEB IN "A". C - EDS SPECTRUM FROM THE FE-SULFIDE CRYSTALS CONTAINED IN THE CLAY BLEB	108
III.8	A - PHOTOMICROGRAPH OF THE BANDED ZONE CLOSEST TO THE FE-SULFIDE NODULE. B - PHOTOMICROGRAPH OF THE BANDED ZONE FARTHER FROM THE FE-SULFIDE NODULE THAN SHOWN IN "A". C - PHOTOMICROGRAPH SHOWING THE MICRO-FAULTS WHICH DEVELOPED IN THE COAL BANDS WITHIN THE BANDED ZONE. D - PHOTOMICROGRAPH OF A CALCITE RHOMBUS FROM WITHIN ONE OF THE CALCITE LAYERS IN THE BANDED ZONE. E - TYPICAL EDS SPECTRUM FROM ANY OF THE FE-SULFIDE SHOWN IN "B" AND "C". F - TYPICAL EDS SPECTRUM FROM ANY OF THE CALCITE SHOWN IN "A", "B", "C" AND "D"	111

IV.1	<p>A - PHOTOMICROGRAPH OF THE INTERIOR OF AN FE-SULFIDE NODULE AFTER OXIDATION TO FE-SULFATE HAS OCCURRED.</p> <p>B - PHOTOMICROGRAPH OF AN EUBEDRAL ROSETTE OF SZOMOLNOKITE OBSERVED GROWING ON THE SURFACE OF ONE OF THE ISOLATED SPHERES OF FE-SULFIDE AT THE PERIFERY OF ONE OF THE NODULES.</p> <p>C - TYPICAL EDS SPECTRUM FROM THE SZOMOLNOKITE SHOWN IN "A" AND "B" 120</p>
IV.2	<p>A TO F - SERIES OF PHOTOMICROGRAPHS SHOWING THE PROGRESSIVE ALTERATION OF FE-SULFIDE TO FE-SULFATE AND THE ATTENDED VOLUME CHANGE 122</p>
IV.3	<p>A - PHOTOMICROGRAPH OF THE "FOREST" OF ACICULAR HALOTRICHITE WHICH FORMED AT THE RIM OF ONE OF THE FE-SULFIDE NODULES.</p> <p>B - PHOTOMICROGRAPH OF HALOTRICHITE WHICH FORMED ON THE ISOLATED SPHERES OF FE-SULFIDE ADJACENT TO THE RIM OF THE NODULE 125</p>
IV.4	<p>A - PHOTOMICROGRAPH OF ONE OF THE BUNDLES OF HALOTRICHITE WHICH FORMED IN THE INTERIOR OF THE NODULES.</p> <p>B - EDS SPECTRUM FROM THE HALOTRICHITE.</p> <p>C - EDS SPECTRUM OF THE MATERIAL CAPPING THE HALOTRICHITE 127</p>
IV.5	<p>A - PHOTOMICROGRAPH OF ACICULAR HALOTRICHITE GROWING FROM CRACKS IN THE SURFACE OF THE COAL IN THE INTERIOR OF THE NODULE.</p> <p>B - PHOTOMICROGRAPH OF HALOTRICHITE GROWING THROUGH/AROUND/FROM A CRYSTAL OF SZOMOLNOKITE.</p> <p>C - PHOTOMICROGRAPH OF ONE OF THE CRYSTALS OF SZOMOLNOKITE WHICH BECAME ATTACHED TO THE HALOTRICHITE AS IT GREW FROM THE SURFACE OF THE NODULE 130</p>
IV.6	<p>A - PHOTOMICROGRAPH OF ONE OF THE "RIBBONS" OF HALOTRICHITE OBSERVED GROWING ON GYPSUM IN THE INTERIORS OF THE NODULES (AS SHOWN IN FIGURE IV-1).</p> <p>B - TYPICAL EDS SPECTRUM OF THE HALOTRICHITE.</p> <p>C - EDS SPECTRUM OF THE GYPSUM SUBSTRATE ON WHICH THE HALOTRICHITE IS GROWING 134</p>

V.1	GRAPHS OF THE FIVE GROUPS OF ELEMENTS COMPARED IN THE UTAH AND WYOMING COALS: GROUP I - CONCENTRATIONS >0.5% GROUP II - CONCENTRATIONS 0.01-0.5% GROUP III - CONCENTRATIONS 10-100 PPM GROUP IV - CONCENTRATIONS 1-10 PPM GROUP V - CONCENTRATIONS <1 PPM	147
V.2	A TO Q - GRAPHS OF THE CORRELATION COEFFICIENTS OF THE INDIVIDUAL ELEMENTS FOR THE UTAH AND WYOMING COALS TAKEN TOGETHER	156
VI.1	SCHEMATIC OF A COAL COMBUSTION FACILITY	175
VI.2	SCHEMATIC SHOWING THE PROCESS OF FLY-ASH FORMATION AND THE FATE OF THE ELEMENTS	181
VI.3	GRAPH SHOWING THE RELATIONSHIP BETWEEN PARTICLE SIZE AND TRACE ELEMENT CONCENTRATION FOR PARTICULATE MATTER COLLECTED FROM A COAL BURNING FACILITY	185
VI.4	GRAPH SHOWING THE CONCENTRATION OF TRACE ELEMENTS AS A FUNCTION OF DEPTH BELOW THE SURFACE FOR PARTICULATE MATTER FROM A COAL BURNING POWER PLANT	185
VI.5	GRAPH SHOWING THE PERCENTAGE OF INHALED PARTICULATES RETAINED IN THE VARIOUS AREAS OF THE RESPIRATORY SYSTEM AS A FUNCTION OF PARTICLE SIZE	189
VII.1	GRAPHS SHOWING THE RELATIVE ABUNDANCES OF 38 ELEMENTS IN TYPICAL CRUSTAL AND BASALTIC MATERIAL	202
VII.2	GRAPHS SHOWING THE RELATIVE ABUNDANCES OF 38 ELEMENTS IN UTAH COAL FROM THIS STUDY AND TYPICAL CRUSTAL AND BASALTIC MATERIAL ...	206
VII.3	GRAPHS SHOWING THE RELATIVE ABUNDANCES OF 38 ELEMENTS IN WYOMING COAL FROM THIS STUDY AND TYPICAL CRUSTAL AND BASALTIC MATERIAL ...	208
VII.4	GRAPH OF THE IONIC POTENTIALS OF THE ELEMENTS DETECTED IN BOTH COALS FROM THIS STUDY	213
VII.5	A - GRAPH OF THE IONIC RADII VS IONIC POTENTIALS OF THE ELEMENTS DETECTED IN BOTH COALS FROM THIS STUDY	215

VII.6

GRAPHS OF THE IONIC POTENTIALS OF SOME OF THE ELEMENTS FOR WHICH THERE ARE DATA ON ORGANIC/INORGANIC AFFINITIES:
A - ELEMENTS OCCURRING IN ONLY ONE OXIDATION STATE,
B - ELEMENTS OCCURRING IN TWO OXIDATION STATES,
C - ELEMENTS OCCURRING IN MORE THAN TWO OXIDATION STATES 223

VII.7

GRAPHS OF THE IONIC POTENTIALS OF THE ELEMENTS DETECTED IN BOTH COALS FROM THIS STUDY:
A - CHALCOPHILE ELEMENTS,
B - SIDEROPHILE ELEMENTS,
C TO F - LITHOPHILE ELEMENTS 229

LIST OF TABLES

TABLE	DESCRIPTION	PAGE
III.1	% ASH IN 21 SAMPLES OF COAL FROM THE EMERY COAL FIELD, UTAH	35
III.2	% ASH IN 24 SAMPLES OF COAL FROM THE POWDER RIVER COAL FIELD, WYOMING	36
III.3	INAA OF 7 ELEMENTS IN WHOLE COAL AND PYRITE NODULES FROM THE EMERY COAL FIELD, UTAH	41
III.4	INAA OF 7 ELEMENTS IN WHOLE COAL FROM THE POWDER RIVER COAL FIELD, WYOMING	43
III.5	XRF OF 19 ELEMENTS IN WHOLE COAL FROM THE EMERY COAL FIELD; UTAH	46
III.6	XRF OF 19 ELEMENTS IN WHOLE COAL FROM THE POWDER RIVER COAL FIELD, WYOMING	48
III.7	ANALYSES OF 56 ELEMENTS (WHOLE COAL BASIS) FROM THE EMERY COAL FIELD, UTAH	51
III.8	ANALYSES OF 40 ELEMENTS IN COAL FROM THE POWDER RIVER COAL FIELD, WYOMING	55
III.9	ANALYSES OF 40 ELEMENTS IN OVERBURDEN SEDIMENT AND CLINKER FROM THE POWDER RIVER COAL FIELD, WYOMING	57
III.10	GEOCHEMISTRY (39 ELEMENTS) OF SEDIMENT AND CLINKER ASSOCIATED WITH COAL FROM THE POWDER RIVER COAL FIELD, WYOMING. DATA FOR OTHER NORTHERN GREAT PLAINS SEDIMENTS ARE SHOWN FOR COMPARISON	59
III.11	LIST OF ELEMENTAL ASSEMBLAGES DETECTED BY EDS IN DISCRETE MINERAL PHASES IN PELLETS OF UTAH COAL	77
V.1	COMPARISON OF THE GEOCHEMISTRY (49 ELEMENTS) OF EMERY COAL FIELD COALS FROM THIS STUDY WITH OTHER EMERY COALS AND OTHER UTAH COALS	137
V.2	COMPARISON OF THE GEOCHEMISTRY (36 ELEMENTS) OF POWDER RIVER BASIN COALS FROM THIS STUDY WITH OTHER POWDER RIVER BASIN COALS AND OTHER WYOMING COALS	141

V.3	COMPARISON OF THE GEOCHEMISTRY OF EMERY COAL FIELD COALS WITH POWDER RIVER COAL FIELD COAL FIELD COALS	143
V.4	COMPARISON OF THE RATIOS OF 39 ELEMENTS DETECTED IN BOTH COALS FROM THIS WORK	145
V.5	CORRELATION COEFFICIENTS FOR 17 ELEMENTS PLUS ASH IN THE UTAH COALS	152
V.6	CORRELATION COEFFICIENTS FOR 17 ELEMENTS PLUS ASH IN THE WYOMING COALS	153
VI.1	COAL CONSUMPTION FOR THE U.S., CANADA AND THE WORLD (1982)	168
VI.2	COAL RESOURCES FOR THE U.S., CANADA AND THE WORLD	168
VI.3	AVERAGE CONCENTRATIONS AND PENETRATION FIGURES FOR SOME OF THE MORE HARMFUL TRACE ELEMENTS ASSOCIATED WITH COAL	193
VI.4	"EFFECTIVE COAL CONCENTRATIONS" FOR SOME OF THE MORE HARMFUL TRACE ELEMENTS ASSOCIATED WITH COAL	194
VII.1	ORGANIC/INORGANIC AFFINITIES OF SOME ELEMENTS IN COAL	218

The author of this thesis has granted The University of Western Ontario a non-exclusive license to reproduce and distribute copies of this thesis to users of Western Libraries. Copyright remains with the author.

Electronic theses and dissertations available in The University of Western Ontario's institutional repository (Scholarship@Western) are solely for the purpose of private study and research. They may not be copied or reproduced, except as permitted by copyright laws, without written authority of the copyright owner. Any commercial use or publication is strictly prohibited.

The original copyright license attesting to these terms and signed by the author of this thesis may be found in the original print version of the thesis, held by Western Libraries.

The thesis approval page signed by the examining committee may also be found in the original print version of the thesis held in Western Libraries.

Please contact Western Libraries for further information:

E-mail: libadmin@uwo.ca

Telephone: (519) 661-2111 Ext. 84796

Web site: <http://www.lib.uwo.ca/>

CHAPTER I: INTRODUCTION AND OBJECTIVES

I.1 INTRODUCTION

Coal remains one of the most perplexing of all geologic materials. Anyone pursuing coal studies knows only too well the complicated relationship between the organic and inorganic chemistries responsible for its formation and diagenesis. Furthermore, few geologic resources are so controversial in their use.

Proportionately, coal is one of the most important geologic deposits. Although it accounts for only a small percentage of the sedimentary rocks of the earth's surface it supplies North America with approximately 14% of its energy needs and this figure is on the rise. Unfortunately, the benefits are not without cost. The by-products of coal combustion, particulates, CO₂, SO₂ (and other gases), and organic molecules, may be the single largest polluters of our environment. This author estimates that 6.81x10⁸ metric tons of coal were consumed yearly in North America during the first part of this decade (calculated from figures in the 1982 U.S. Energy Atlas) resulting in the production of 1.02x10⁸ tons/year of ash. If 2% of this escaped emission control devices 2.04x10⁶ tons/year of particulate matter were released into the atmosphere. The form of these particulates (as sub-micron sized fly ash) and the

concentrations of harmful trace elements associated with them has long been a concern to the Health Sciences.. Only after the mode of occurrence of the various trace elements has been determined can steps be taken to deal with the control of their emission. To that end, this work attempts to better define the geochemistries of two large western U.S. coal deposits: the Upper Cretaceous Emery Coal Field, Utah and the Paleocene Powder River Coal Basin, Wyoming.

I.2 OBJECTIVES

The purpose of this study was three-fold:

- (1) Document the overall geochemistry of two large Western U.S. coal deposits; the Cretaceous, Emery Coal Field, southcentral Utah and one of the larger Paleocene, Powder River Basin coals from the Powder River Coal Field, Wyoming.
- (2) Describe the relationships of the elements detected both within and between the two coals.
- (3) Elucidate a number of selected topics pertinent to coal science, e.g., environmental aspects of coal utilization and the question of organic/inorganic affinities of the elements.

One of the major goals in completing the above, (1) and (2), was to preserve the integrity of the original mineral matter in the coal. Therefore, whenever possible, the coal was

subjected to as little pretreatment as possible, e.g., elemental analyses were performed on whole coal (except where noted) to avoid the errors introduced during ashing and/or chemical (acid) and mechanical (heavy liquid) pretreatments.

Special attention was given to some of the more potentially harmful trace elements associated with coal (see Chapter VI): Zn, As, Se, Cd, Sb, Hg and U.

CHAPTER II: GENERAL DESCRIPTION OF FIELD AREAS

II.1 UTAH: EMERY COAL FIELD

II.1.1 INTRODUCTION

The Emery Coal Field is situated in the southern portion of Castle Valley (once called the Castle Valley Field) in east-central Utah (Figure II-1) and includes portions of Sevier and Emery Counties. This NNE trending field covers approximately 540 Km² as an elongate body 55 Km in length and varying in width from 6-13 Km (Affolter, et.al., 1979). It is bordered on the west by the Wasatch Plateau, on the north by the Book Cliffs and on the southeast by the San Rafael Swell.

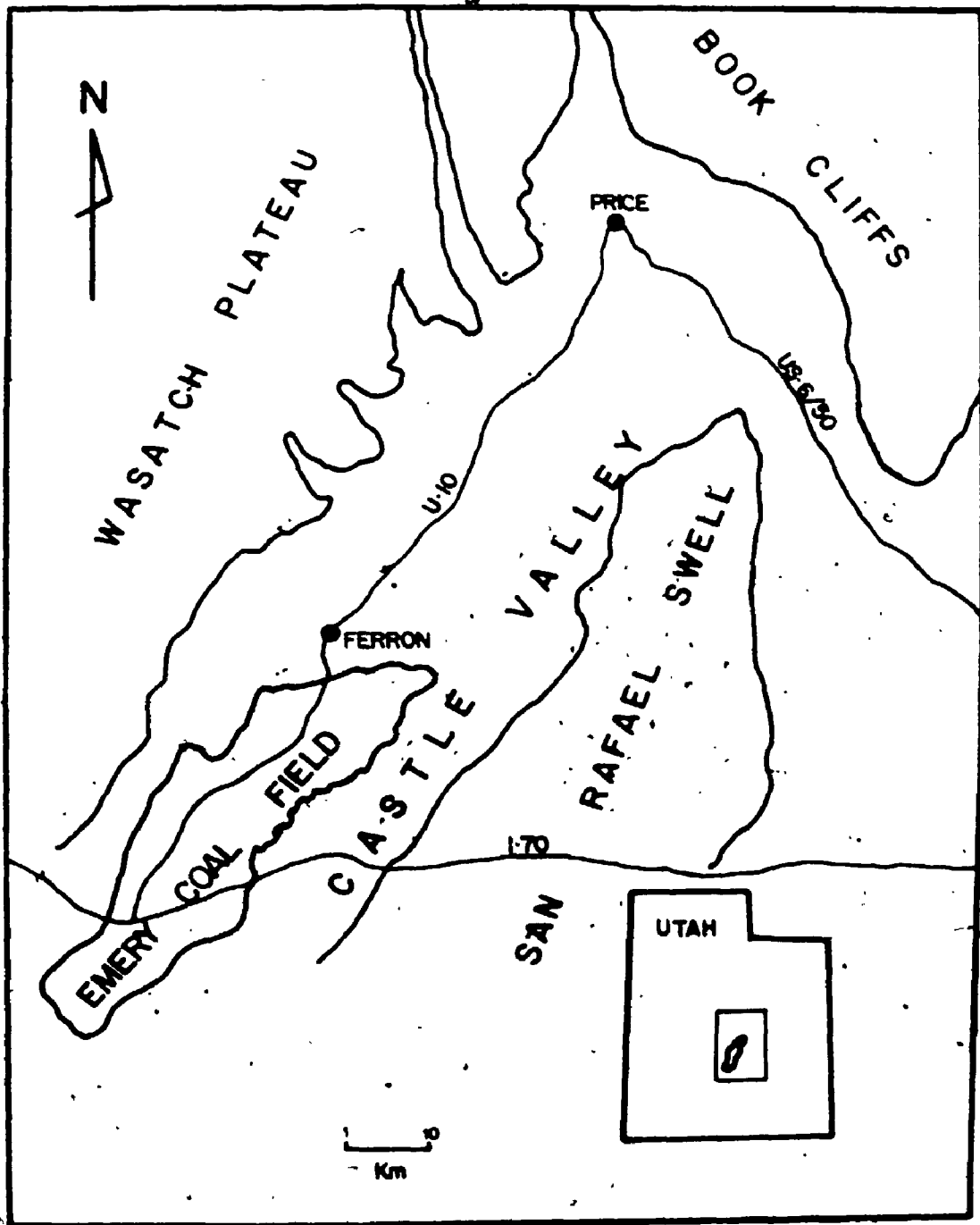
The Emery Field was first described in detail by Lupton in 1916 and later by Doelling in 1972. While the Emery Field represents one of the smaller coal deposits of Utah, Doelling (1971, 1972) has estimated that the field contains approximately 3.9×10^8 metric tons of recoverable, low sulphur (0.99% average), medium ash (8.9% average), high volatility C bituminous coal.

II.1.2 UPPER CRETACEOUS HISTORY

The Upper Cretaceous history of the Rocky Mountain Region is

FIGURE II-1

LOCATION MAP, SHOWING THE POSITION OF THE EMERY
COAL FIELD IN SOUTH-CENTRAL UTAH.
(COMPILED FROM: AFFOLTER, 1979, FIG. 1; COTTER,
1976, FIG. 2)



7

marked by four major transgressive-regressive sequences of the Western Interior Cretaceous Seaway beginning in Late Albian time (110 ma) and culminating at the end of Maastrichtian time (65 ma): Greenhorn Cycle (Albian-Turonian); Niobrara Cycle (Turonian-Campanian); Claggett Cycle (Middle Campanian); Bearpaw Cycle (Campanian-Maastrichtian). During this same period tectonic activity, related to the Sevier Orogeny, was increasing to the west resulting in large scale overthrusting and local vertical uplift (Armstrong, 1968). The proximity of a large epeirogenic sea to an area of active uplift resulted in large quantities of clastic debris being delivered to the foreland of a newly forming Cretaceous basin, the Rocky Mountain Geosyncline (Figure II-2), which began subsiding at approximately the same rate at which sediment was being supplied (McGookey, 1972). This relationship resulted in periodic emergence and submergence of shorelines along the western edge of the seaway. The above scenario produced ideal environments for the formation of peatlands.

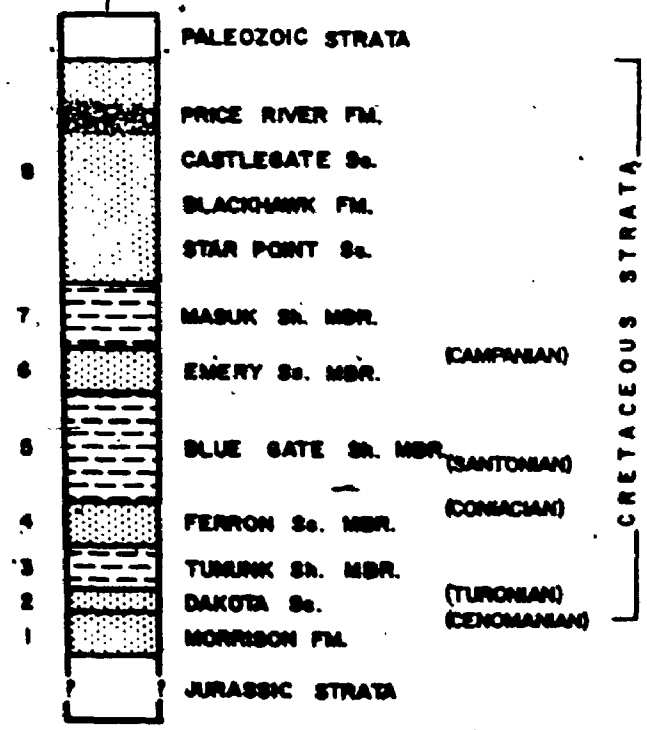
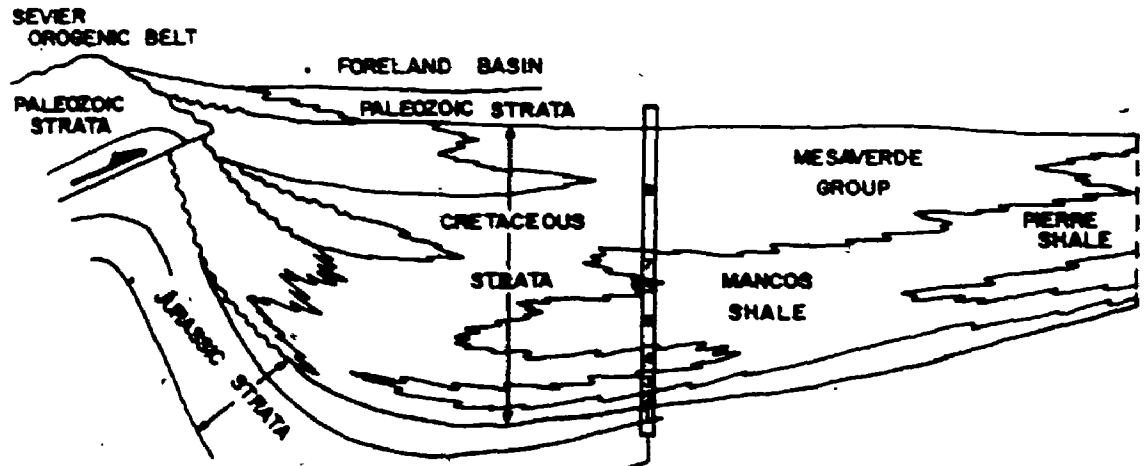
It was during a regressive stage of the Greenhorn Seaway (Turonian) that the Ferron Sandstone, the most important coal bearing strata of the Mancos Shale, was deposited in central Utah at the southwest edge of the foreland basin (Ryer, 1981).

FIGURE II-2

THE X-SECTION (TOP PART OF DIAGRAM) REPRESENTS A GENERALIZED VIEW OF CRETACEOUS STRATA ALONG A NE-SW LINE RUNNING THROUGH THE EMERY COAL FIELD. THE SCHEMATIC SHOWS THE ACCUMULATION OF CRETACEOUS SEDIMENTS IN THE FORELAND BASIN OF THE ROCKY MOUNTAIN GEOSYNCLINE. THE SOURCE OF THE SEDIMENTS IS THE SEVIER OROGENIC BELT TO THE WEST.

THE STRATIGRAPHIC COLUMN (BOTTOM PART OF DIAGRAM) REPRESENTS STRATA IN THE EMERY COAL FIELD. LITHOLOGIC DATA (LEGEND) REPRESENT ONLY THE MAJOR LITHOFACIES PRESENT IN EACH ROCK TYPE. THE APPROXIMATE LOCATIONS OF STAGE BOUNDARIES (TURONIAN, ETC.) ARE INCLUDED.
(COMPILED FROM: ARMSTRONG, 1968, FIG. 5; RYER, 1981, FIG. 4; RYER, 1983, FIG. 1)

W **ROCKY MOUNTIAN GEOSYNCLINE** E



II.1.3 UPPER CRETACEOUS (TURONIAN) STRATIGRAPHY

Economically important coals of the Emery Coal Field occur within the Upper Cretaceous (Turonian) Ferron Sandstone Member of the Mancos Shale. Lupton (1916) named 14 coal beds within the Ferron Sandstone and labeled them from A to M starting with the lowest coal. Doelling (1972) used Lupton's designations but reorganized the coal beds into three zones: lower coal zone, beds A-E; middle coal zone, beds F-G; and upper coal zone, beds H-M (Figure II.3),

While the lower coal zone contains more widespread and extensive coals it is the I and J coals of the upper coal zone that are mined in the southern portion of the Emery Coal Field. Locally, the I bed may reach a thickness of 6-7 m (Cotter, 1976).

II.1.4 PALAEOENVIRONMENT

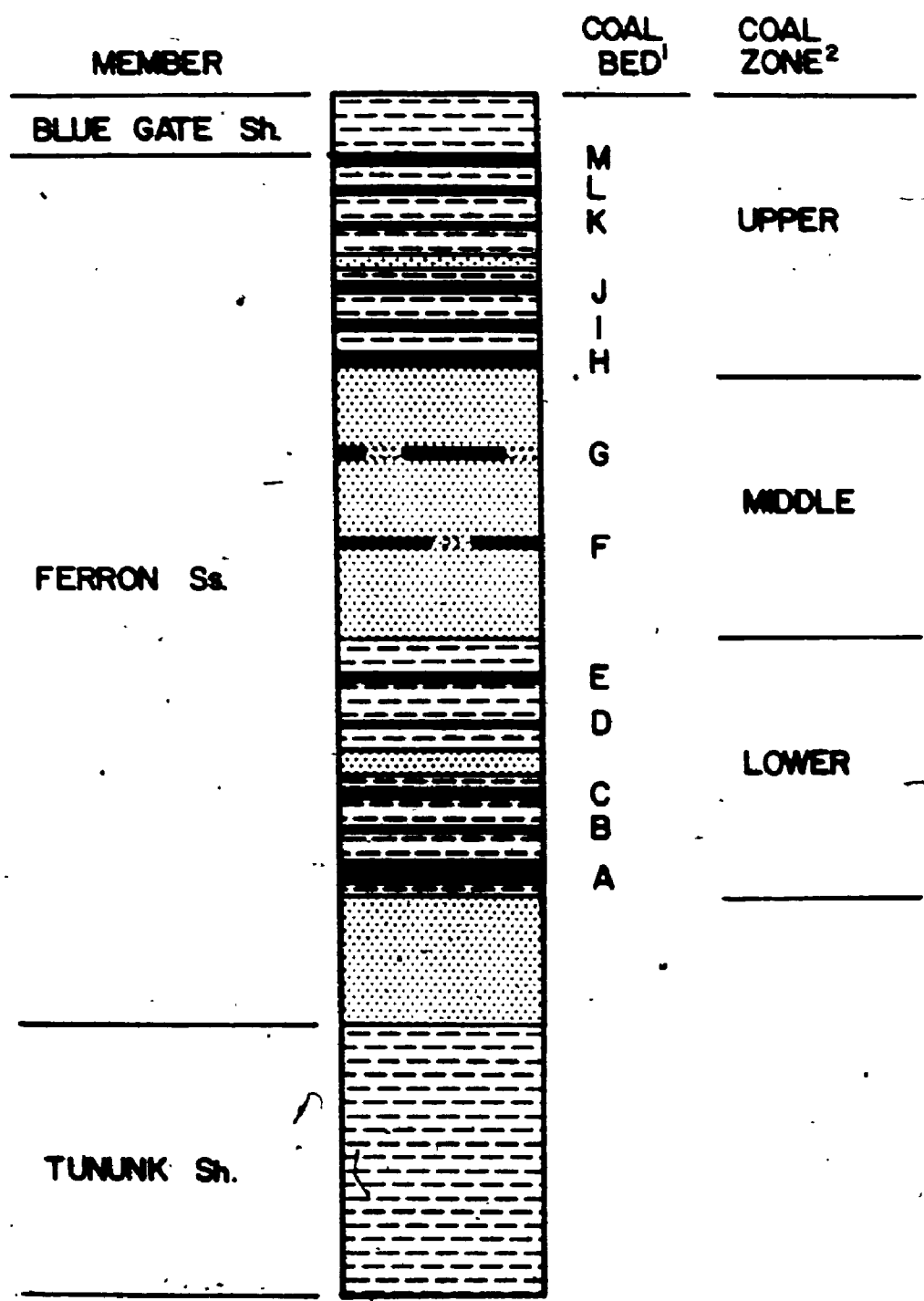
As noted earlier, the clastic debris which would become the Rocky Mountain Geosyncline accumulated on the western shore of the Western Interior Cretaceous Seaway. The origin of these sediments, for the most part, was the Cordilleran Miogeosyncline to the west which was being uplifted by the Sevier Orogeny (Figure II-2) (Armstrong, 1968). Because of the pulsating nature of this orogenic event clastic material was supplied to the foreland basin at varying rates

FIGURE II-3

GENERALIZED STRATIGRAPHIC COLUMN SHOWING THE RELATIVE POSITIONS OF COAL BEDS WITHIN THE FERRON SANDSTONE MEMBER OF THE MANCOS SHALE FORMATION IN THE SOUTHERN PORTION OF THE EMERY COAL FIELD, UTAH. COAL BEDS A-M (1) WERE ORIGINALLY NAMED BY LUPTON IN 1916 AND LATER DIVIDED INTO COAL ZONES (2) BY DOBLLING IN 1972. COALS FOR THIS STUDY WERE COLLECTED FROM THE I/J SEAMS. NO SCALE IS GIVEN DUE TO THE VARIABLE THICKNESSES OF THE COALS THROUGHOUT THE EMERY FIELD. THE I/J SEAMS ARE APPROXIMATELY 5 METERS THICK WHERE SAMPLES WERE COLLECTED FOR THIS STUDY.

(ADAPTED FROM COTTER, 1976)

MANCOS SHALE FORMATION



1

resulting in periodic emergence and submergence of local shorelines. It was during a period of increased sedimentation that the Last Chance Delta formed as part of the Ferron Sandstone.

The Last Chance Delta was a river dominated, high-constructive deltaic system responsible for depositing the coal bearing sequence of the Ferron Sandstone in the southern portion of Castle Valley (Figure II-4,A) (Cotter, 1976). Ryer (1981, 1983) has determined that the various coals of the Ferron Sandstone in the Emery Coal Field are associated with delta plain deposits of a series of individual delta systems, piled one atop the other, which are truncated by transgressive/regressive erosional surfaces.

Coal deposits within the Ferron Sandstone are elongate and arranged perpendicular to the trend of the ancient shoreline (Figure II-4,B). The geometry of these coal deposits and their direction of thickening is related to both the subsidence of the delta during deposition and the orientation of drainage (erosion) immediately after deposition (Flores, 1981).

II.1.6 SAMPLE COLLECTION

Samples of Utah coal were collected in the east-central

FIGURE II-4

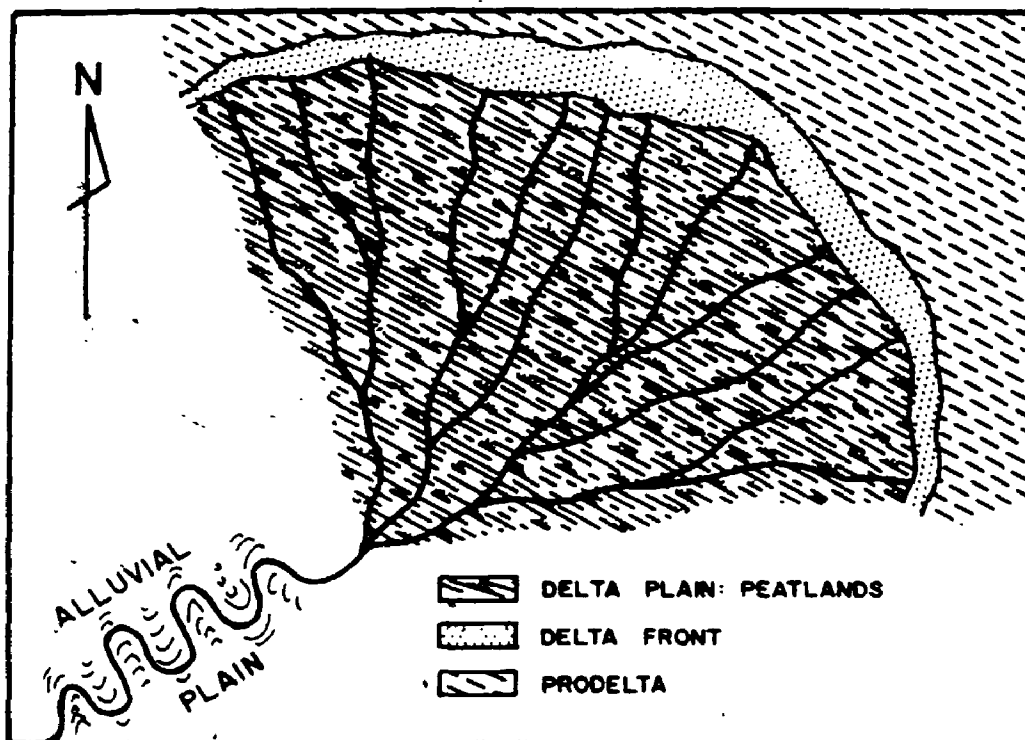
A - SIMPLIFIED SCHEMATIC OF THE TURONIAN LAST CHANCE DELTA OF SOUTHERN UTAH. THIS TYPE OF RIVER DOMINATED, CONSTRUCTIVE DELTA IS THE SOURCE OF THE FERRON SANDSTONE AND ASSOCIATED COALS IN THE EMERY COAL FIELD. PEATS (SUBSEQUENTLY COALS) ACCUMULATED WITHIN DELTA PLAIN SEDIMENTS IN INTERDISTRIBUTARY SWAMPS.

(ADAPTED FROM COTTER, 1976, FIG. 9)

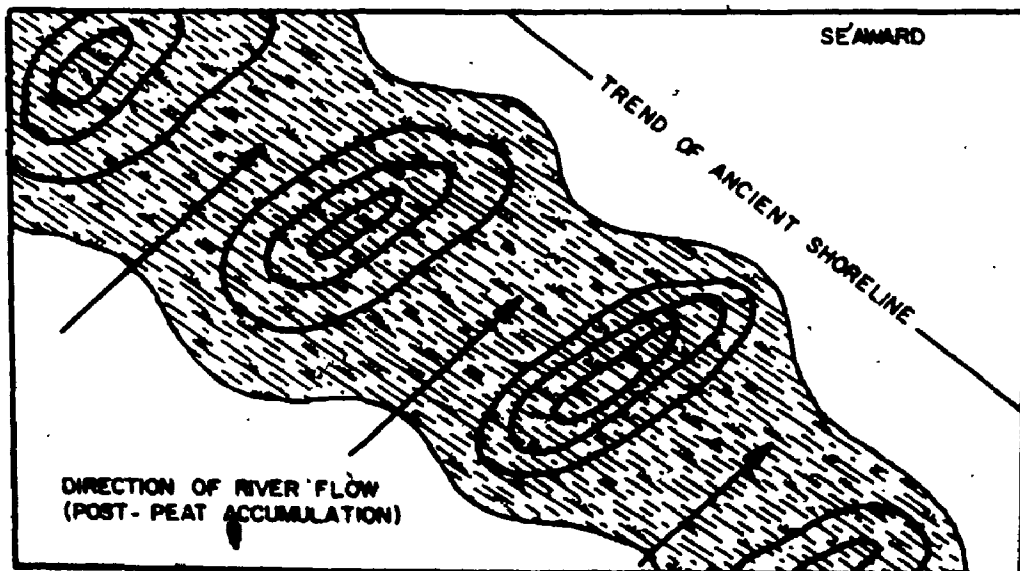
B - PREDICTIVE MODEL FOR THE SHAPE AND ORIENTATION OF FERRON SANDSTONE PEATS (COALS). CLOSED CONTOURS REPRESENT RELATIVE THICKENING OF THE PEAT. PEAT DEPOSITS ARE ELONGATE PERPENDICULAR TO THE TREND OF THE ANCIENT SHORELINE AND DELTA FRONT SEDIMENTS. THIS MODEL HELPS EXPLAIN THE SHAPE AND ORIENTATION OF FERRON COALS AS BEING DEPENDENT ON FLUVIAL EROSION SUBSEQUENT TO PEAT DEPOSITON.

(ADAPTED FROM RYER, 1981; FIG. 23B)

A



B



portion of the Emery Coal Field, Emery and Sevier Counties, Utah (sections 28, 29, 32 and 33, T22S, R6E). The coal is mined from a subsurface room and pillar operation with coal exposed along two intersecting sets of corridors. One set of corridors trends NE-SW for approximately 3 Km, a second shorter set of tunnels runs NW-SE for approximately 1.6 Km (Figure II-5). Per the direction of mine officials, sampling was confined to those corridors presently in use for mine inspection ("access corridors" in Figure II-5).

Samples were collected at 22 locations across the lateral extent of the mine (Figure II-5). Two samples of coal were collected at each site: those designated as "A" were collected from the top of the exposed face of the seam; those designated as "B" were collected from the bottom of the seam (below "A"). It should be noted that the exposed face of the seam typically included only the middle 2-3 m of the 6 m thick seam: This was due to the fact that roughly 1 m of coal was left on both the floor and roof of the tunnel for safety reasons. These two meters of coal would represent the extreme top and bottom of the coal seam. Furthermore, because the corridors are located within the coal seam it was not possible to sample the sediments above or below the seam. Additional samples included efflorescent coatings, partings and Fe-sulfide nodules, when present.

The surfaces of the mine walls were dusted with a fine

51

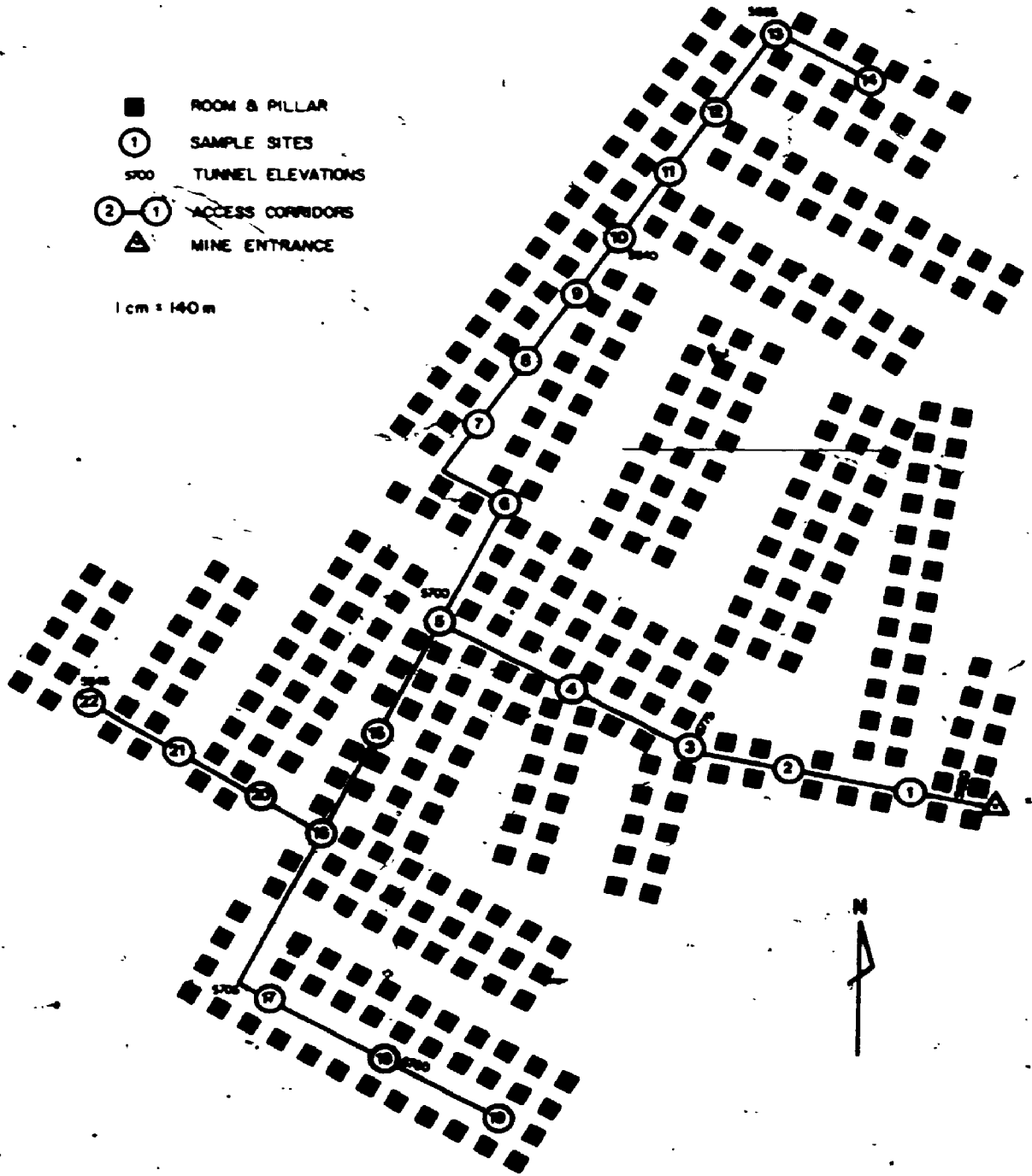


FIGURE II-5
UTAH SAMPLE LOCATION DIAGRAM

SCHEMATIC OF THE SUBSURFACE ROOM AND PILLAR MINE FROM WHICH SAMPLES OF UTAH COAL WERE COLLECTED FOR THIS STUDY. THE MINE ENTRANCE MARKS A POINT WHERE THE I/J COAL OUTCROPS AT THE SURFACE. THE I/J SEAM STRIKES NE-SW AND DIPS 7°-8° NW IN THIS PART OF THE EMERY COAL FIELD. SAMPLE SITE #22 IS APPROXIMATELY 100 M BELOW THE SURFACE.

- ROOM & PILLAR
- ① SAMPLE SITES
- 5700 TUNNEL ELEVATIONS
- ②-① ACCESS CORRIDORS
- ▲ MINE ENTRANCE

1 cm = 140 m



limestone powder used to control coal dust. This material was thoroughly removed (to a depth of approximately 3 cm) prior to sample collection. Subsequently, .5-1 Kg of "fresh" coal was placed in a plastic bag and sealed with tape.

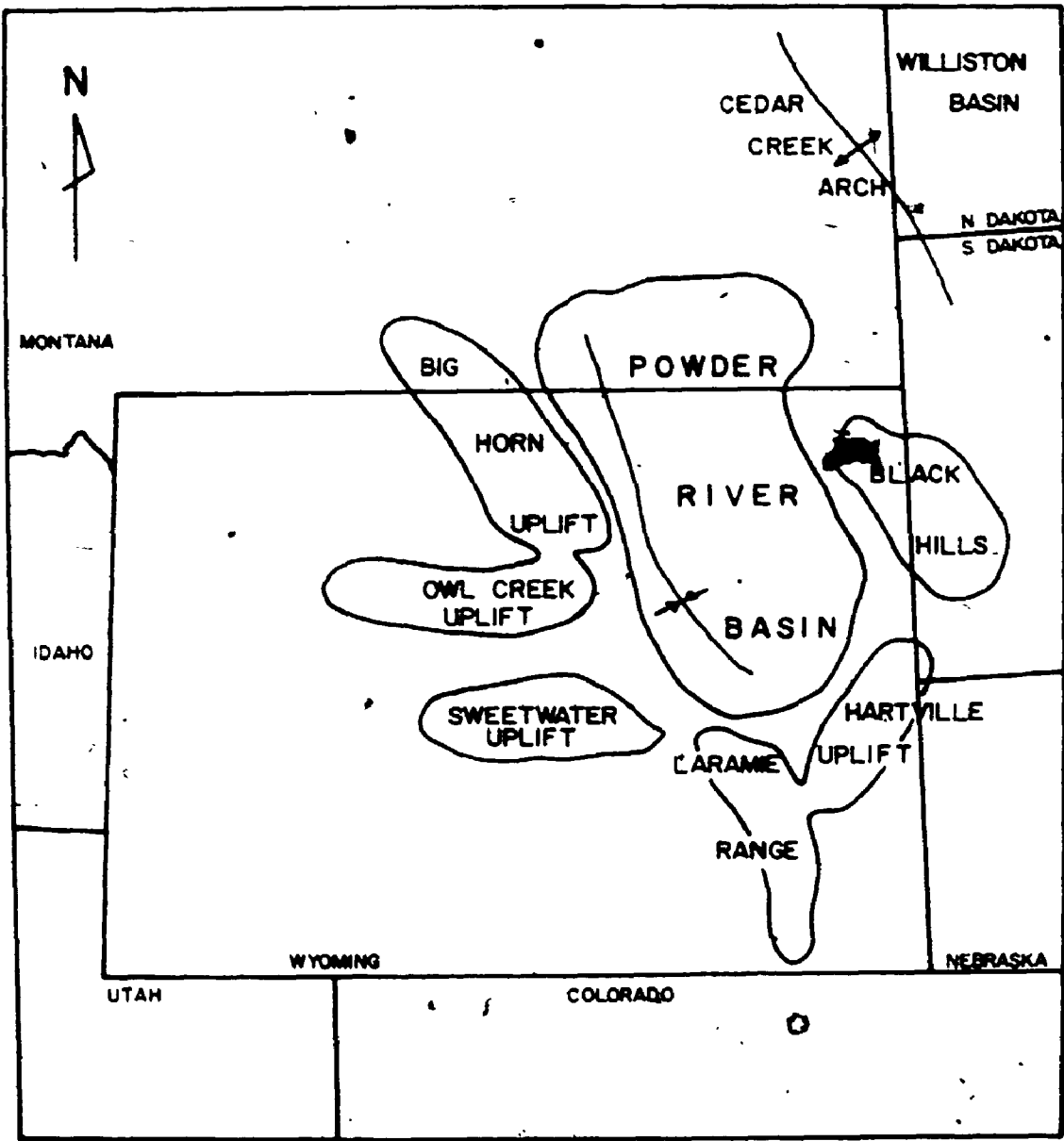
II.2 WYOMING: POWDER RIVER COAL FIELD

II.2.1 INTRODUCTION

The Powder River Coal Basin covers some 31,100 Km² in northeastern Wyoming and southeastern Montana (Glass, 1981) adjacent to the physiographic border between the Northern Great Plains and The Rocky Mountain Provinces (Figure II-6). The basin is separated from the Williston Basin to the north by the Miles City - Cedar Creek Arch and from that point, in a clockwise direction, is rimmed by, The Black Hills, Hartville Uplift, Laramie Range, Sweetwater Uplift, Owl Creek Uplift and the Big Horn Mountains (Glaze and Keller, 1965). Twelve coal fields within the basin contain coals ranging in age from Upper Cretaceous to Eocene. Of these, the two most prolific coal bearing strata include the Upper Paleocene, Tongue River Member of the Fort Union Formation and the Eocene, Wasatch Formation, this work is concerned with the former. The United States Geological Survey has estimated that the Powder River Coal Basin contains 10¹¹ metric tons of identifiable coal resources of which

FIGURE II-6

LOCATION MAP SHOWING THE POSITION OF THE POWDER RIVER COAL/STRUCTURAL BASIN IN NE WYOMING AND SE MONTANA. THE POWDER RIVER COAL BASIN COVERS SOME 7,500 SQUARE KILOMETERS WITHIN WYOMING.



approximately 5×10^{10} metric tons are considered as recoverable reserve base (Glass, 1979). The majority of this (63%) is located in Campbell County (Figure II-7). This one coal reserve alone could provide North America, at the present rate of usage, with its energy needs, allocated to coal, for approximately 100 years. Powder River Basin coals are typically subbituminous - bituminous, medium ash (avg. 7.9%) and low in sulfur (avg. 0.54%) (Glass, 1978).

The Powder River Coal Basin is the same in name and aerial extent as the Powder River Structural Basin. The basin is formed by an asymmetrical syncline bordered on the west by the Big Horn Mountains and on the east by the Black Hills (Figure II-6). The axis of the syncline runs NNW-SSE along the western edge of the basin. In the western limb of the fold Upper Cretaceous and Paleocene rocks dip 15-20° to the east resulting in relatively thin outcrops patterns compared to the same strata which dip gently westwardly (2-5°) in the eastern arm of the fold. The younger Eocene rocks occur as a nearly flat lying cover throughout the central portion of the basin (Figure II-7) (Glass, 1976).

II.2.2 EARLY TERTIARY (PALEOCENE) HISTORY

At the close of the Cretaceous NE Wyoming was essentially a featureless plain, the final remnant of the last regression of the Lewis Sea to the SE (McGrew, 1971; Robinson, 1972).

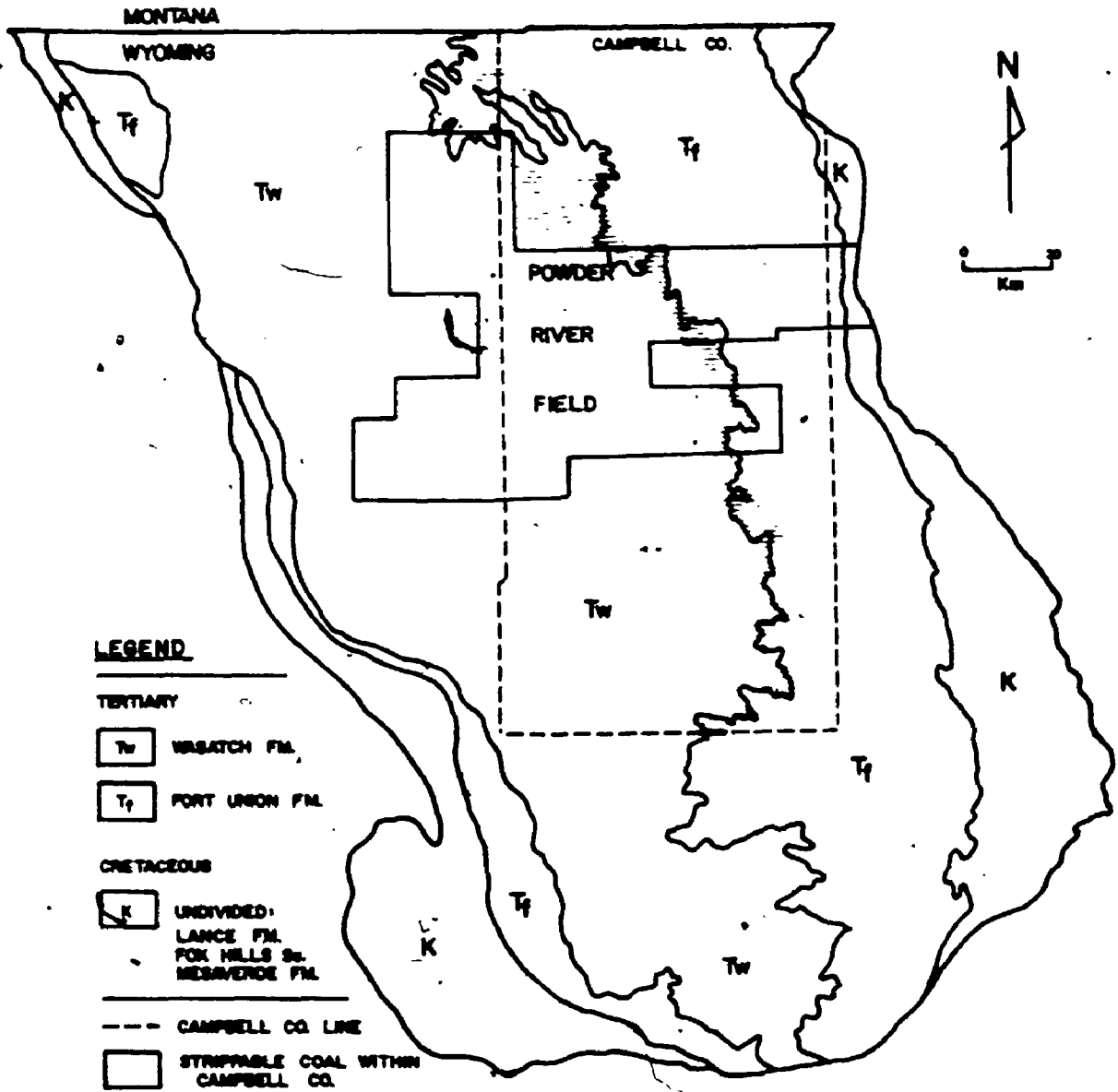
22



FIGURE 11-7

OUTLINE OF THE POWDER RIVER COAL BASIN IN WYOMING SHOWING THE GENERALIZED GEOLOGY OF THE PALEOCENE FORT UNION FORMATION, THE EOCENE WASATCH FORMATION AND OLDER UNDIFFERENTIATED CRETACEOUS STRATA. THE MAJORITY OF THE STRIPPABLE TERTIARY COALS IN NE WYOMING ARE LOCATED IN CAMPBELL COUNTY ALONG THE PALEOCENE/EOCENE CONTACT. COALS FOR THIS STUDY WERE COLLECTED IN THE SE PORTION OF THE POWDER RIVER COAL FIELD.

(COMPILED FROM GLASS, 1976, FIGS. 1, 2 AND 4)



21

The earliest Tertiary marked the onset of the Laramide Orogeny which extended through the Paleocene into the Eocene. During this time mountain building occurred from New Mexico to Canada resulting in the formation of numerous basins separated by local uplifts. The Powder River Basin owes its present day shape to tectonic events that took place during this time (Weichman, 1965).

The configuration of the geology of the basin is a result of its tectonic history. During the Paleocene, western Wyoming and Idaho were undergoing geosynclinal compression. At the same time material was being subducted from the southwest. These two factors resulted in vertical readjustment of crustal material. As the basin formed, intense warping, and eventually faulting, developed near the basin margins, lessening in intensity towards the basin axis. Due to differential uplift, warping on the western flank, adjacent to the Big Horn Uplift, was more intense than on the eastern edge, adjacent to the Black Hills Uplift, resulting in basin asymmetry (Fanshawe, 1971).

In the Powder River Basin, sediment which accumulated during this period formed a part of the coal bearing, Upper Paleocene, Fort Union Formation. Owing to the nature of the tectonic activity which occurred throughout the Rocky Mountain Region, the Fort Union Formation occurs mainly in isolated patches in a NE-SW line of basins which include the

Williston Basin in western North Dakota, northwest South Dakota and eastern Montana, the Powder River Basin in northeastern Wyoming, the Wind River Basin in central Wyoming and the Green River Basin in southwestern Wyoming and northwestern Utah (Robinson, 1972). Coal is found, to some extent, in all of these basins.

II.2.3 UPPER PALEOCENE STRATIGRAPHY

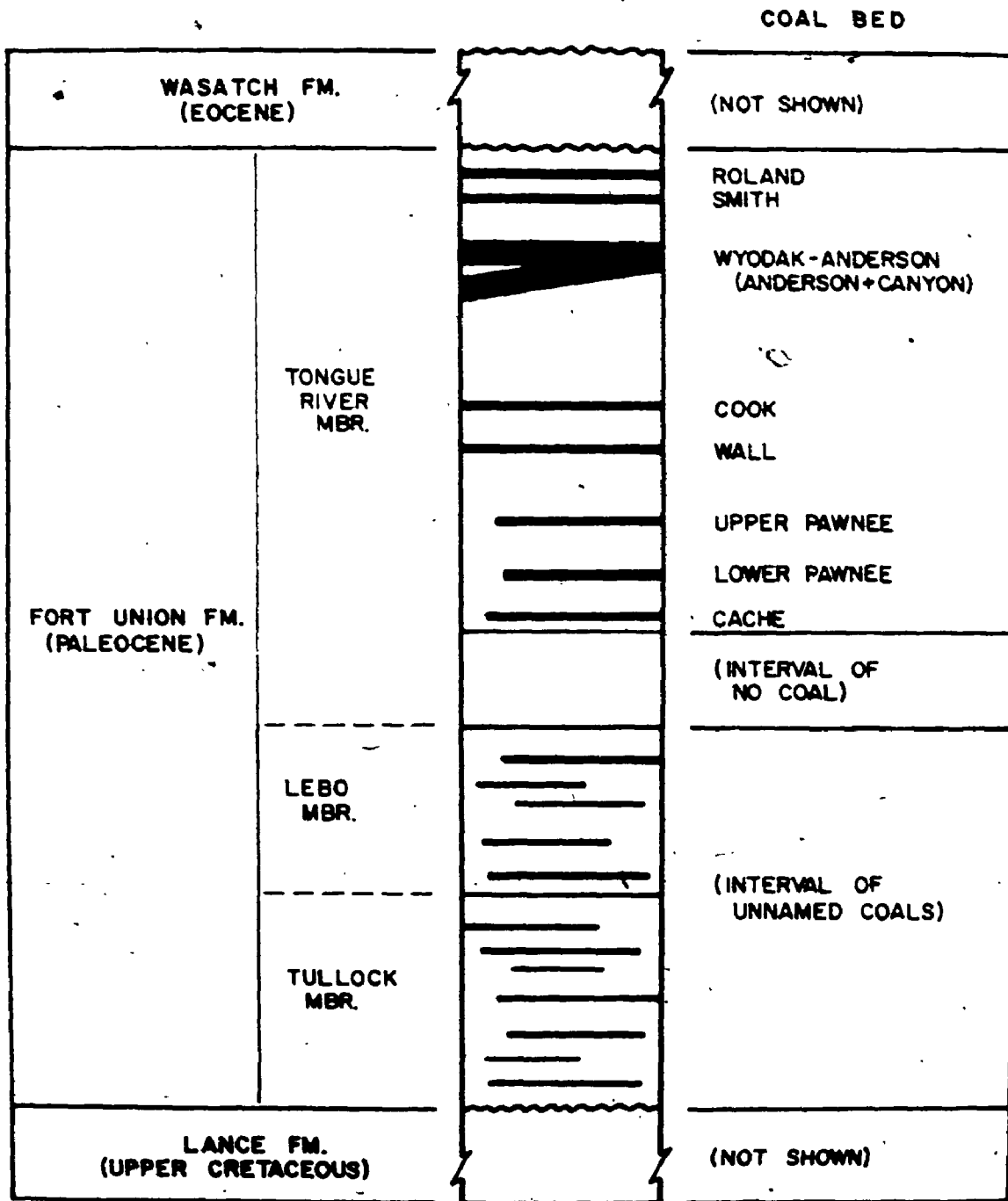
Detailed stratigraphic description of the coal-bearing Paleocene/Eocene rocks in the Powder River Basin can be found in Flores (1981) and Ethridge *et al.* (1981) and many other references cited by these authors. This work attempts only to familiarize the reader with the major rock formation nomenclature and associated coal bed names in the area in an attempt to locate these strata within the geologic time frame.

During the Laramide Orogeny rocks as old as Pre-Cambrian in age were exposed in the cores of uplifted mountains throughout the Wyoming Province (Houston, 1971). These topographic highs shed eroded sediments into adjacent basins across Wyoming. In the Powder River Basin the coal bearing Paleocene stratigraphy is best represented by the 600-900 m Fort Union Formation (Glass, 1976) which is subdivided into the Tullock, Lebo and Tongue River Members (Figure II-8). Each of these strata represent a stage in the development of

FIGURE II-8

GENERALIZED STRATIGRAPHY OF THE PALEOCENE FORT UNION FORMATION IN THE POWDER RIVER COAL BASIN SHOWING THE RELATIVE POSITIONS OF THE MAJOR COAL BEDS WITHIN THE TONGUE RIVER MEMBER. THE FORT UNION FORMATION RANGES FROM 600-900 METERS IN THICKNESS. MAJOR COAL SEAMS ARE FOUND IN THE 450 METER THICK TONGUE RIVER MEMBER. COALS FOR THIS STUDY WERE COLLECTED FROM THE 30 METER THICK WYDOK-ANDERSON SEAM.

(COMPILED FROM GLASS, 1976, FIGS. 2 AND 3)



the Laramide Orogeny. Coals for this study were collected from the Wyodak-Anderson seam in the upper part of the Tongue River Member (Figure II-8).

Deposition of the basal Paleocene, Tullock Member marks the beginning of the Laramide Orogeny prior to the beginning of basin subsidence. Next came the accumulation of Middle Paleocene Lebo sediments signalling the onset of Laramide structural movement. Finally, as the Laramide Orogeny began to peak in the Late Paleocene, deposition of the Tongue River Member marked the close of Paleocene sedimentation in the Powder River Basin (Curry, 1971).

II.2.4 PALEOENVIRONMENT

One aspect of this work is concerned with the variation in geochemistry of coals from different depositional settings. However, the purpose of this section is merely to define the paleoenvironment of the Powder River Basin peatlands during the early Tertiary. The size, economic importance and easy accessibility of Paleocene/Eocene coals throughout the Powder River Basin have led to numerous studies by coal scientists. Interested readers are referred to the various works concerned with the detailed reconstruction of these paleoenvironments using lithofacies data, e.g., Flores (1980, 1981) and Ethridge, et.al., (1981) and the numerous references within.

The Upper Paleocene Tongue River Member of the Fort Union Formation can be divided into two major fluvial facies, each containing economically important coals: a fluvial-channel-dominated facies and a fluvial-lake-dominated facies (Flores, 1981). The lower 335 m of the Tongue River host thick (locally as much as 30m), lenticular coal bodies associated with upper alluvial plain (fluvial-channel-dominated) sediments. Lithofacies data and their relationship to thick channel sands suggests that these coals accumulated in poorly drained swamps on broad floodplains constructed by high-sinuosity streams (Flores, 1976, 1981).

Thinner (usually less than 5 m) and more continuous coals are found in the upper 122 m of the Tongue River. The precursors to these coals formed in lower alluvial plain (fluvial-lake-dominated) sediments. Coals of this origin contain numerous partings, fresh water mollusks and are interbedded with limestone. Deposition of these coals took place in and around lakes that formed in backswamp areas adjacent to linear fluvial channels. Overbank and crevasse splay detritus are the sources of the many partings responsible for bifurcation in these coals (Flores, 1981).

II.2.5 SAMPLE COLLECTION

Wyoming coal samples were collected from an open pit mine

located in the southeast portion of the Powder River Coal Field, Campbell County, Wyoming (SE Section, T48N, R71W). The coal is mined from two benches, each approximately 1600 m long, 30 m wide and 13 m high (Figure II-9). Samples were collected from 6 zones at 4 levels representing vertical and horizontal sequences from top to bottom along the length of the benches (Figure II-9). Additional samples include: "floor" samples, collected across the horizontal length of each bench; one sample of clinker, collected approximately 300 m from the benches; and two samples of overburden collected above either end of the upper bench.

Due to mine safety regulations, sampling of the two vertical walls (levels 1, 2, 3 and 4) was accomplished with the aid of a front end loading tractor. The bucket of the tractor was used to dig out a face sample at the desired level and then lowered so that hand samples could be selected. Approximately .5-1 Kg of sample was collected at each site, placed in a plastic bag and sealed with tape.

FIGURE II-9

SCHEMATIC OF THE OPEN-PIT BENCH MINE FROM WHICH SAMPLES OF WYOMING COAL WERE COLLECTED FOR THIS STUDY. SAMPLES OF COAL (N61WU, ETC.) WERE COLLECTED FROM FOUR LEVELS WITHIN SIX ZONES. OVERBURDEN (OB1 AND OB6) WAS COLLECTED ABOVE EITHER END OF THE UPPER BENCH.

CHAPTER III: DATA PRESENTATION; RESULTS AND DISCUSSION

III.1 ASH

High temperature ash was prepared for 21 samples of coal from the Emery Coal Field, Utah (Table III-1) and 24 samples of coal from the Powder River Coal Field, Wyoming (Table III-2).

III.1.1 UTAH

The ash content of the Utah coals ranged from a high of 23.0% to a low of 3.4% with a mean of 8.2% (Table III-1). It bears noting that the high variability of these data (1 sigma +/-56%) is due to the large ash content of 4 of the samples (U2A, U14A, U18 and U19A). If the other 17 samples are considered separately the mean is 6.3% with a standard deviation (1 sigma) of +/-30%. Three of the "anomalously" high figures come from "A" samples, collected towards the top of the seam. In the case of the 5 sample sites for which "A" and "B" (bottom of the seam) samples were ashed, the average for the "A" samples is 10.5% while the average for the "B" samples is only 7.0%. The top of the seam appears to be slightly "dirtier" than the bottom.

III.1.2 WYOMING

TABLE III-1

=====

% ASH IN 21 SAMPLES OF COAL FROM THE
EMERY COAL FIELD, UTAH.

SAMPLE	% ASH	
U2A	13.2	
U2B	6.2	
U3	8.2	
U5A	7.4	
U5B	9.6	
U6	4.8	
U8	6.2	
U10A	3.8	
U10B	8.6	
U12	4.0	
U13	3.4	
U14A	15.4	
U14B	5.8	
U15	8.8	
U16	7.6	
U17	5.8	
U18	23.0	
U19A	12.8	
U19B	4.8	
U20	8.4	
U22	4.2	
		WITHOUT THE ANOMALOUS VALUES~
MAXIMUM	23.0	9.6
MINIMUM	3.4	3.4
RANGE	6.8	2.8
MEAN	8.2	6.3
STD	4.6	1.9
(N)	21	17

=====

STD - STANDARD DEVIATION
(N) - NUMBER OF SAMPLES
 - (U2A, U14A, U18, U19A)

TABLE III-2

=====

% ASH IN 24 SAMPLES OF COAL FROM THE
POWDER RIVER COAL FIELD, WYOMING.

SAMPLE	LEVEL	% ASH
(ZONE 6)-----		
T62F	1	4.8
N61WU	2	4.6
N61WL	3	0.8
S62WU	4	3.8
S62WL	5	0.2
(ZONE 5)-----		
N51WL	3	3.6
S52WU	4	3.6
S52WL	5	4.2
(ZONE 4)-----		
N41WU	2	5.4
N41WL	3	1.2
S42WU	4	2.2
S42WL	5	4.0
(ZONE 3)-----		
N31WU	2	4.6
N31WL	3	3.8
S32WU	4	3.2
S32WL	5	3.2
(ZONE 2)-----		
N21WL	3	3.8
S22WU	4	15.0
S22WL	5	3.8
(ZONE 1)-----		
T12F	1	7.2
N11WU	2	9.4
N11WL	3	3.8
S12WU	4	5.4
S12WL	5	3.0

WITHOUT
ANOMALOUS
VALUES

MAXIMUM	15.0	9.4
MINIMUM	0.2	1.2
RANGE	75.0	7.8
MEAN	4.4	4.3
STD	2.9	1.6
(N)	24	21

=====

STD - STANDARD DEVIATION
(N) - NUMBER OF SAMPLE
- (N61WL, N62WL, S22WL)

The ash content of the Wyoming samples ranged from 15.0% to 0.2% with a mean of 4.4% (Table III-2). As in the case of the Utah coals, the large variation (1 sigma, +/-66%) results from 2 very low values (N61WL and S62WL) and one anomalously large value (S22WU). If these data are not considered the mean ash content becomes 4.3% with a standard deviation (1 sigma) of +/-37%.

The ash content of the 6 zones and 5 levels are also considered separately (see Sect. II.2.5 for explanations of "zones" and "levels" as they apply to sample sites). Mean values for levels 2, 3, 4 and 5 (2 being the uppermost and 5 being the bottom) are 6.0%, 3.8%, 5.5% and 3.1% respectively. If these levels are considered without the anomalous figures noted above the mean values become 6.0%, 3.2%, 3.6% and 3.6% and the largest ash content is found in the top of the seam. The results for zones 1-6 (representing 6 vertical sections across the seam) are 5.4%, 7.5%, 3.7%, 3.2%, 3.8% and 2.4% respectively. Once again, without the anomalous values, the means become 5.4%, 3.8%, 3.7%, 3.2%, 3.8% and 4.2% respectively.

III.1,3 SUMMARY

The major difference in ash content for both the Utah and Wyoming coals occurs vertically within the seam: Utah - top 10.5%, bottom 7.0%; Wyoming - top 6.0%, bottom 3.1%. This

difference is not surprising when one considers that the accumulation of organic matter in peatlands is typically terminated by increased sedimentation as a result of basin subsidence, hence, more sediment is incorporated in the last organics to accumulate. This material is preserved as the top of the coal seam. This does not preclude that other mechanisms of increasing the ash content at the top of a coal seam are not also operating, e.g., preferential precipitation on mineral matter from groundwater entering from the top of the seam.

There does not appear to be any discernable lateral variation in ash content in either the Utah or Wyoming samples. This is due, presumably, to the fact that the confines of both mines, and therefore the area sampled, are minuscule compared to the total aerial extent of the seams. In fact, these data, considered as a whole for each mine separately, actually represent a single sample site within the seam.

III.2 CHEMICAL AND MINERALOGICAL ANALYSES (BY METHOD)

III.2.1 INTRODUCTION

Representative samples of coal from each location, Emery Coal Field, Utah and Powder River Coal Field, Wyoming, were selected for analysis by a variety of methods. Analyses

were performed at the following laboratory facilities: The University of Western Ontario - X-Ray Fluorescent Spectroscopy (XRF), X-Ray Diffraction (XRD) and Scanning Electron Microscopy (SEM) coupled with Energy Dispersive Spectroscopy (EDS); Becquerel Labs, Ontario - Instrumental Neutron Activation Analysis (INAA); Nuclear Activation Services Ltd., Ontario - multiple-method coal analytical package (includes INAA, XRD, XRF, Direct Current Plasma (DCP), Rabbit (short lived INAA), Prompt Gamma Counting and special wet methods). The data presentation and discussion for each method of analysis are presented separately.

III.2.2 INSTRUMENTAL NEUTRON ACTIVATION ANALYSIS

III.2.2.1 INTRODUCTION

Ten samples of whole coal and 2 samples of Fe-sulfide nodules from Utah and 6 samples of whole coal from Wyoming were analyzed by INAA for the elements Zn, As, Se, Cd, Sb, Hg and U. These elements were chosen because of the potentially harmful environmental impact they pose resulting from coal utilization.

III.2.2.2 UTAH: WHOLE COAL

Five pairs of samples (10 sample total) of whole coal from Utah were analyzed. Each pair included a sample taken from

the top ("A") and bottom ("B") of the seam (e.g., Sample 2A and 2B). Table III-3 shows the results for the Utah samples.

Mean concentrations for 5 of the elements indicate relative abundances of As, 3.45 ppm > Se, 1.65 ppm > Hg, 0.96 ppm > U, 0.79 ppm > Sb, 0.34 ppm. Two of the elements, Zn and Cd, were not present at concentrations above detection limits, a maximum of <9.2 ppm in the case of Zn and <2.0 ppm in the case of Cd. Only Sb and U were detected in all 10 samples. Nine samples contained detectable levels of As, 4 samples contained Se, and Hg was detected in only 2 of the samples. The highest range of concentrations (maximum/minimum) occurs in As, 27.5 times (x) followed by U 8.1x, Sb 4.2x, Se 2.4x and Hg 1.1x. The large variations in concentrations for a given element are also reflected in the relative standard deviations (1-sigma) of (in %) As(123), Se(35), Sb(41), Hg(4) and U(70).

III.2.2.3 UTAH: Fe-SULFIDE NODULES

In addition to the whole coal samples, 2 samples of Fe-sulfide nodules (pyrite/marcasite), from two separate locations in the Utah mine, were analyzed (Table III-3, bottom). Average concentrations of As, 310 ppm, Se, 35 ppm and Hg, 36 ppm were determined in the two samples, U, 0.52 ppm was detected in only one of the samples. Zn, Cd and Sb were not detected above maximum detection limits of Zn

TABLE III-3

INSTRUMENTAL NEUTRON ACTIVATION ANALYSES (INAA) OF 7
ELEMENTS IN WHOLE COAL AND PYRITE NODULES (PYT. NOD.) FROM
THE EMERY COAL FIELD, UTAH (% MST (MOISTURE) INCLUDED).

SAMPLE	ELEMENT CONCENTRATIONS (PPM)							MST (%)
	Zn	As	Se	Cd	Sb	Hg	U*	
WHOLE COAL								
2A	<5.7	5.47	<0.91	<1.40	0.37	<0.35	1.15	2.8
2B	<4.6	0.45	<0.70	<1.10	0.31	<0.28	0.70	3.0
5A	<5.8	0.42	1.20	<1.50	0.34	<0.33	1.17	2.9
5B	<6.3	10.80	2.40	<2.00	0.53	1.00	0.29	2.6
10A	<3.8	0.40	<0.55	<1.20	0.14	<0.31	0.26	2.6
10B	<7.5	11.00	2.00	<1.50	0.20	0.91	0.45	2.5
14A	<7.4	0.53	<1.10	<1.00	0.43	<0.31	1.00	2.6
14B	<4.7	0.78	<0.76	<1.60	0.26	<0.27	0.37	2.8
19A	<9.2	1.20	<0.84	<1.10	0.59	<0.32	2.10	2.8
19B	<7.0	<0.35	1.00	<1.20	0.18	<0.28	0.44	3.0
MAXIMUM	NA	11.00	2.40	NA	0.59	1.00	2.10	3.0
MINIMUM	NA	0.40	1.00	NA	0.14	0.91	0.26	2.5
RANGE	NA	27.5	2.4	NA	4.2	1.1	8.1	1.2
MEAN	NA	3.45	1.65	NA	0.34	0.96	0.79	2.8
STD	NA	4.26	0.57	NA	0.14	0.04	0.55	0.2
(N)	NA	9	4	NA	10	2	10	10
PYT. NOD.								
6CA	<39.0	268	31.2	<3.60	<0.22	33.3	0.52	1.1
13CA	<25.0	333	38.8	<3.80	<0.24	38.3	<0.46	0.7

(N) - NUMBER OF SAMPLES
 NA - NOT APPLICABLE
 STD - STANDARD DEVIATION
 ~ - RANGE = MAXIMUM/MINIMUM

<30.0 ppm, Cd <3.80 ppm and Sb <0.24 ppm. It was also noted by the laboratory doing the analyses that the nodules contained "unusually high" concentrations of Fe, W , Au and Co (no numbers were reported).

The ash content of these 10 Utah coal samples ranged from 15.4% to 3.8% with an average of 9.2%.

III.2.2.4 WYOMING: WHOLE COAL

Six samples of coal from Wyoming were analyzed: 4 wall samples and 2 floor samples. The six samples were chosen to represent 2 vertical sequences of 3 samples each collected from opposite ends of the mine benches. Unfortunately, based on the analyses contained herein and observations made at the mine, there is reason to believe that the floor samples were contaminated at the mine, therefore, wall and floor samples are considered separately. The data are listed in Table III-4.

The elements As, Se, Sb and U were detected in all 4 of the wall samples. Mean concentrations of these elements indicate relative abundances of Se, 3.38 ppm > As, 2.42 ppm > U, 0.71 ppm > Sb, 0.38 ppm. None of the samples contained the elements Zn, Cd or Hg at concentrations above the maximum detection limits of Zn <10.0 ppm Cd <1.4 ppm and Hg <0.74 ppm.

TABLE III-4

=====

INSTRUMENTAL NEUTRON ACTIVATION ANALYSES (INAA) OF 7
ELEMENTS IN WHOLE COAL FROM THE POWDER RIVER COAL FIELD,
POWDER RIVER BASIN, WYOMING (% MST (MOISTURE) INCLUDED).

SAMPLE	ELEMENT CONCENTRATIONS (PPM)							MST %
	Zn	As	Se	Cd	Sb	Hg	U	

WHOLE COAL								

FLOOR SAMP:*								
T62F	14.00	15.80	12.90	<1.20	0.23	1.40	0.39	9.60
T12F	<15.0	17.80	9.48	<1.80	0.75	<0.91	1.09	9.90
WALL SAMP:								
N61WU	<7.70	0.77	1.10	<1.00	0.29	<0.31	0.61	10.00
S62WU	<7.50	1.00	0.71	<1.10	0.24	<0.34	0.37	10.50
N11WU	<8.90	0.64	1.10	<1.20	0.65	<0.34	0.82	9.00
S12WU	<10.0	7.25	10.60	<1.40	0.32	<0.74	1.04	9.40
MAXIMUM	NA	7.25	10.60	NA	0.65	NA	1.04	10.50
MINIMUM	NA	0.64	0.71	NA	0.24	NA	0.37	9.00
RANGE~	NA	11.33	14.93	NA	2.71	NA	2.81	1.17
MEAN	NA	2.42	3.38	NA	0.38	NA	0.71	9.73
STD	NA	2.79	4.17	NA	0.16	NA	0.25	0.57
(N)	NA	4	4	NA	4	NA	4	4

=====

* - FLOOR SAMPLES NOT USED IN STATISTICAL CALCULATIONS
(SEE TEXT FOR EXPLANATION)

(N) - NUMBER OF SAMPLES

NA - NOT APPLICABLE

STD - STANDARD DEVIATION

~ - RANGE = MAXIMUM/MINIMUM

Ash contents of the 4 wall samples range from 9.4% to 3.8% with an average of 5.8%.

One or both of the floor samples contained detectable levels of six of the elements: As, 16.8 ppm > Zn, 14.0 ppm > Se, 11.2 ppm > Hg, 1.40 ppm > U, 0.74 ppm > Sb, 0.49 ppm. Neither sample contained Cd above the detection limit of <1.80 ppm.

Ash contents for the floor samples were 4.8% and 7.2% (avg., 6.0%).

III.2.3 X-RAY FLUORESCENT SPECTROSCOPY

III.2.3.1 INTRODUCTION

The concentrations of 19 elements (Al, S, K, Ca, Fe, Ti, V, Cr, Mn, Co, Ni, Cu, Zn, Ga, Rb, Sr, Zr, Ba, and Pb) in whole coal from the Emery Coal Field, Utah (21 samples) and the Powder River Coal Field, Wyoming (24 samples) were determined using x-ray fluorescent spectroscopy. The elements can be separated into four groups based on mean concentrations as follows: >0.1%, 100 ppm - 0.1%, 10 - 100 ppm and <10 ppm.

III.2.3.2 UTAH: WHOLE COAL

Table III-5 shows the results of the XRF analyses for 21 samples of Utah coal. Five elements were present at mean concentrations >0.1%: S, detected in 20 samples (n=20), was the most abundant element with a mean concentration of 1.4% followed by Ca, 0.65% (n=21), Fe, 0.58% (n=14) and K, 0.10% (n=2). The concentration range (maximum/minimum) for these elements varied from a high of 48x in the case of Fe to Al 35x, S 26x, Ca 9.5x and K 7x.

The elements Ti, Ba and Sr were detected in all 21 samples (n=21) at mean concentrations between 100 ppm - 0.1%: Ti, 688 ppm, Ba, 213 ppm and Sr, 203 ppm. Titanium exhibited the largest concentration range, 9.4x, followed by Sr 3x and Ba 1.8x.

Zirconium, Mn and V were detected in all 21 samples (n=21) at concentrations between 10 - 100 ppm. Zirconium was the most abundant with a mean concentration of 31 ppm followed by Mn, 30 ppm and V, 10 ppm. Vanadium showed the largest concentration range in this group, 20x, followed by Mn 4.5x and Zr 3.5x.

Eight elements were present in the Utah samples at mean concentrations <10 ppm: in order of decreasing abundance they are Cr, 8.8 ppm (n=21), Cu, 7.3 ppm (n=21), Zn, 6.1 ppm (n=5), Pb, 4.7 ppm (n=21), Ni, 3.3 ppm (n=21), Ga, 2.3 ppm

TABLE III-5

X-RAY FLUORESCENT SPECTROSCOPY OF 19 ELEMENTS IN WHOLE COAL FROM THE EMERY COAL FIELD, UTAH.

ELEMENT CONCENTRATIONS

SAMPLE	PPM																		
	Al	S	K	Ca	Fe	Ti	V	Cr	Mn	Co	Ni	Cu	Zn	Ba	Rb	Sr	Zr	Ba	Pb
U2A	0.72	0.70		0.45		1309	8.6	13.1	28	0.9	2.5	7.7		1.9	1.3	204	50	278	6.5
U2B	0.69	0.35		0.43	0.41	794	7.0	8.6	31		6.4	7.0		1.8	0.6	156	29	270	3.2
U3	0.85	0.72		0.58	0.16	666	8.4	3.6	30	0.7	3.6	5.1		1.4	1.3	216	30	248	2.3
USA	0.66	1.64		0.80		553	8.1	8.8	29	4.3	2.3	7.3		2.2	0.7	227	29	215	4.0
USB	0.23	2.49		0.93	1.95	147	5.7	4.1	31		3.2	8.9		3.0	0.5	251	21	216	13.0
U6	0.38	1.53		0.43		522	6.1	4.8	32	2.0	2.7	5.3		3.1	0.7	210	24	245	2.1
U8	0.62	1.90		0.36	0.09	1142	14.4	6.4	32	1.9	2.4	5.0		3.4	0.6	148	35	196	3.9
U10A	0.58	3.25		6.41		219	2.8	1.8	32	2.7	1.8	3.0		0.1	0.6	209	21	212	3.4
U10B	0.28	3.43		0.63	2.90	172	4.6	6.7	31		1.5	6.3	4.9	2.4	1.4	212	21	195	12.6
U12	0.37	1.72		0.49		340	7.9	4.7	32	1.7	3.0	3.5		1.3	0.5	215	20	211	2.5
U13	0.08	0.63		0.58	0.31	201	2.3	1.7	30		3.1	2.5		0.1	0.9	286	18	239	2.5
U14A	0.53	1.51		2.53		737	11.2	13.4	8	2.1	2.3	12.7		3.1	2.1	400	54	224	4.1
U14B	0.65	1.48		0.50	0.29	275	5.9	7.2	30	0.5	2.8	3.9		1.1	1.3	174	21	230	3.8
U15	1.36	0.72	0.03	0.31	0.17	1143	16.9	14.7	35	1.8	3.1	10.1	3.6	3.6	2.6	138	34	161	4.4
U16	0.95	2.53		0.38	0.46	878	12.5	9.0	35	1.8	4.1	8.5		4.0	0.5	142	27	186	4.2
U17	0.51	2.05		0.38	0.27	783	7.1	6.2	33		3.6	6.6	2.8	1.3	0.6	143	28	213	4.0
U18	2.75	0.74	0.18	0.90	0.51	1377	46.2	36.6	15	0.8	6.8	20.5	16.0	9.2	14.3	234	61	176	9.4
U19A	1.29			1.05	0.06	1127	16.4	14.4	28	1.7	3.5	11.4		3.6	2.5	159	49	151	4.0
U19B	0.37	0.13		0.27	0.25	743	7.8	6.2	36		4.2	4.7	3.0	1.3	0.3	134	26	173	2.5
U20	0.87	0.44		0.40		1068	9.9	12.7	32	1.7	3.3	8.8		2.1	0.8	141	35	195	2.9
U22	0.25	0.13		0.76	0.28	247	4.3	1.1	31	1.7	2.7	5.0		0.2	0.9	256	22	239	4.0
D.L. (PPM)	30	0.5	10	3	5	6	0.4	0.5	0.6	0.5	0.5	0.6	0.9	0.2	0.5	3.4	3	1.2	2.1
MAXIMUM	2.75	3.43	0.18	2.53	2.90	1377	46.2	36.6	36.0	4.3	6.8	20.5	16.0	9.2	14.3	400	61.3	228	13.0
MINIMUM	0.08	0.13	0.03	0.27	0.06	147	2.3	1.1	8.0	0.5	1.5	2.5	2.8	0.1	0.3	134	17.7	151	2.1
RANGE	35	26	7.0	9.5	48	9.4	20	33	4.5	8.6	4.5	8.2	5.7	92	45	3	3.5	1.8	6.2
MEAN	0.71	1.40	0.10	0.65	0.58	688	10.4	8.8	29.6	1.7	3.3	7.3	6.1	2.3	1.7	203	31.1	213	4.7
STD	0.56	0.96	0.08	0.47	0.78	392	9.1	7.4	6.3	0.9	1.3	4.0	5.0	1.9	2.9	63	12.2	33	3.0
(N)	21	20	2	21	14	21	21	21	16	21	21	21	5	21	21	21	21	21	21

BLANK SPACES REPRESENT CONCENTRATIONS LESS THAN DETECTION LIMITS (D.L.).

STD - STANDARD DEVIATION

(N) - NUMBER OF SAMPLES

D.L. - DETECTION LIMIT

ND - NO DATA.

~ - RANGE = MAXIMUM/MINIMUM

(n=21), Co, 1.7 ppm (n=16) and Rb, 1.7 ppm (n=21). Gallium showed the widest concentration range, 92x, followed by Rb 45x, Cr 33x, Co 8.6x, Cu 8.2x, Pb 6.2x, Zn 5.7x and Ni 4.5x.

III.2.3.3 WYOMING: WHOLE COAL

Table III-6 lists the results of the XRF analyses for the Wyoming coals (24 samples). Results for two "floor" samples (T62F and T12F) are reported but not considered with the other 22 "wall" samples because of suspected contamination at the mine.

Three elements were present at mean concentrations >0.1%: S, 0.98% (n=12), Ca, 0.98% (n=22) and Al, 0.39% (n=21). Aluminum showed the largest variation in concentration with a range of 41x followed by S 4.1x and Ca 1.3x.

Four elements were found at mean concentrations between 100-1000 ppm: Ti, 767 ppm (n=12), Fe, 500 ppm (n=4), Ba, 461 ppm (n=22) and Sr, 269 ppm (n=22). Titanium showed the largest concentration range, 83x, followed by Fe 6x, Sr 5x and Ba 2.6x.

All 22 wall samples of Wyoming coal contained four elements at mean concentrations between 10²-100 ppm: Mn, 23 ppm, Zr, 22 ppm, V, 12.3 ppm and Cu, 11.5 ppm. Copper exhibited the largest concentration range, 13x, followed by Zr 6.1x, V 6x

TABLE III-6

X-RAY FLUORESCENT SPECTROSCOPY OF 19 ELEMENTS IN WHOLE COAL FROM THE POWDER RIVER COAL FIELD, POWDER RIVER BASIN, WYOMING.

ELEMENT CONCENTRATIONS

SAMP. LEV.	PPM																			
	Al	S	K	Ca	Fe	Ti	V	Cr	Mn	Co	Ni	Cu	Zn	Ga	Rb	Sr	Zr	Ba	Pb	
(ZONE 6)-----																				
N61MU	2	0.14	1.02		1.00	714	20.4	6.3	20	1.2	2.4	14.8		1.7	0.6	158	21	386	2.9	
N61ML	3	0.36			0.94	133	16.2	0.2	27	12.4	4.7	10.4	3.1	1.6	1.9	279	18	578	11.1	
S62MU	4	0.41	0.73		0.87		12.9	2.6	31	2.7	2.1	4.2		2.6	1.8	400	15	670	3.4	
S62ML	5	0.31			0.94	97	15.9	1.0	28	12.6	2.9	9.0		1.3	1.7	352	18	723	8.2	
(ZONE 5)-----																				
N51ML	3	0.50			0.99	182	8.9	3.3	22	2.4	1.4	4.1		0.2	0.6	153	22	390	3.1	
S52MU	4	0.60	0.50		0.92		7.1	3.0	21	2.0	3.1	3.9		3.7	1.2	241	16	528	2.8	
S52ML	5	0.09			0.95	644	9.2	6.1	26	2.7	3.3	9.0		0.7	1.2	198	22	520	3.3	
(ZONE 4)-----																				
N41MU	2	0.31	1.55		1.00	353	20.3	5.2	15	5.0	5.1	9.2	3.2	2.6	0.4	222	25	456	3.9	
N41ML	3	0.04	0.55		1.00		8.1	0.2	8	11.4	3.6	11.6	4.6	0.3	1.3	175	14	510	11.6	
S42MU	4	0.15			0.90		3.6	1.1	26	3.0	2.0	3.7		0.4	0.8	154	13	320	2.7	
S42ML	5	0.72			0.99	0.03	4.5	0.4	23	13.9	4.2	27.0	3.6	1.0	2.8	763	18	843	11.2	
(ZONE 3)-----																				
N31MU	2	0.11	0.78		1.09	458	9.6	10.5	20	2.7	6.2	13.3	6.0	0.8	0.9	190	26	334	3.6	
N31ML	3	0.30	0.59		1.06	51	8.9	6.8	20	2.4	7.6	5.1	3.5	1.4	0.6	182	15	333	3.7	
S32MU	4	0.26	1.01		0.95	0.04	10.1	1.7	34	3.8	2.7	5.3	5.0	1.4	1.5	276	16	439	3.6	
S32ML	5	0.24			1.00		3.7	0.3	34	8.4	3.8	6.1			0.6	165	14	391	8.9	
(ZONE 2)-----																				
N21ML	3	0.50	0.74		1.11	183	11.7	1.8	19	25.4	4.3	10.9	3.7	2.3	1.8	205	18	375	15.7	
S22MU	4	1.65			0.85	4208	27.1	20.6	31	5.8	6.5	34.4	5.2	5.9	3.4	761	76	548	8.1	
S22ML	5				0.91	0.02	4.6	3.4	30	0.9	1.8	3.2		0.3	1.1	154	15	336	2.0	
(ZONE 1)-----																				
N11MU	2	0.24	2.03		1.10	1336	27.5	8.0	6	3.7	2.2	43.1		2.7	0.8	184	32	344	3.1	
N11ML	3	0.29	0.73		1.06		5.7	3.2	11	12.1	4.7	5.9		0.7	0.9	187	16	354	7.3	
S12MU	4	0.87	1.51		0.92	0.12	847	25.0	10.3	22	3.8	7.6	12.2	3.8	3.9	1.5	355	37	418	7.7
S12ML	5	0.10			0.93		9.4	0.2	23	6.8	4.5	6.9	3.2		0.4	163	12	345	7.1	
D.L. (PPM)		30	0.5	10	3	5	6	0.4	0.2	0.6	1.2	0.5	0.6	0.9	0.2	0.5	3.4	3.0	1.2	2.1
MAXIMUM		1.65	2.03	ND	1.11	0.12	4208	27.5	20.6	34	25.4	7.6	43.1	6.0	5.9	3.4	763	75.6	843	15.7
MINIMUM		0.04	0.50	ND	0.85	0.02	51	3.6	0.2	6	0.9	1.4	3.2	3.1	0.2	0.4	153	12.3	320	2.0
RANGE*		41	4.1	ND	1.3	6.0	83	7.6	103	5.7	28	5.4	13	1.9	30	8.5	5	6.1	2.6	7.9
MEAN		0.39	0.98	ND	0.98	0.05	767	12.3	4.4	23	6.6	3.9	11.5	4.1	1.8	1.3	269	21.7	461	6.1
STD		0.35	0.46	ND	0.07	0.04	1099	7.3	4.7	7.5	5.8	1.8	10.1	0.9	1.4	0.7	171	13.2	138	3.7
(N)		21	12	0	22	4	12	22	22	22	22	22	22	11	20	22	22	22	22	22

(CONTINUED)

TABLE III-6 (CONTINUED)

ELEMENT CONCENTRATIONS

SAMP. LEV.	Z										PPM									
	Al	S	K	Ca	Fe	T	V	Cr	Mn	Co	Ni	Cu	Zn	Ga	Rb	Sr	Zr	Ba	Pb	
T6ZF	1	0.29	3.12	0.80	1.05	10.6	10.9	21	3.5	21.0	5.1	11.9	1.6	1.2	207	16	454	13.5		
T1ZF	1	0.56	4.63	0.79	2.11	18	23.0	8.4	18	6.0	40.9	13.3	10.5	4.7	3.2	440	25	446	18.1	
MEAN		0.4	3.9	ERR	0.8	1.6	18	17	9.7	20	4.8	31	9.2	11	3.2	2.2	324	21	450	16

BLANK SPACES REPRESENT CONCENTRATIONS LESS THAN DETECTION LIMITS (D.L.).

(ZONE 1..6) AND LEV. (LEVEL) ARE EXPLAINED IN THE TEXT.

STD - STANDARD DEVIATION (1 SIGMA)

D.L. - DETECTION LIMIT

(N) - NUMBER OF SAMPLE

ND - NO DATA.

- RANGE = MAXIMUM/MINIMUM

and Mn 5.7x.

Seven elements were present at mean concentrations <10 ppm: Co, 6.6 ppm (n=22), Pb, 6.1 ppm (n=22), Cr, 4.4 ppm (n=22), Zn, 4.1 ppm (n=11), Ni, 3.9 ppm (n=22), Ga, 1.8 ppm (n=20), and Rb, 1.3 ppm (n=22). Concentration ranges for this group, in decreasing order, are: Cr 103x, Ga 30x, Co 28x, Rb 8.5x, Pb 7.9x, Ni 5.4x and Zn 1.9x.

Potassium was not detected in any of the Wyoming coal samples. Values for the two "floor" samples (T62F and T12F) are given at the end of Table III-6.

III.2.4 MULTIPLE-TECHNIQUE ANALYSIS

III.2.4.1 INTRODUCTION

Five samples of Utah coal were analyzed for 56 elements using a variety of techniques included in a coal analytical "package" offered by Nuclear Activation Services Ltd., Hamilton, Ontario. The results of these analyses are shown in Table III-7 which includes the analytical method used for each element. Eight samples of coal from Wyoming were run through similar analyses at the same lab for 40 elements. The results of the Wyoming analyses are shown in Table III-8. The data in Tables III-7 and III-8 are sorted relative to two criteria: first, the number of samples (N) in which a

TABLE III-7

ANALYSES OF 56 ELEMENTS (WHOLE COAL BASIS) FROM THE EMERY COAL FIELD, UTAH.

ELEMENT	SAMP. ANAL.			ELEMENT CONCENTRATIONS*										
	D.L.	TYPE	METH.	US	DB	U13	U17	U22	MAX	MIN	RNG	MEAN	STD (ML)	
Ca (Z)	0.1	M	I	0.9	0.6	6.9	1.7	0.6	6.9	0.6	11.5	2.10	2.40	5
Si (Z)	0.001	A	I	2.40	1.50	0.57	0.71	1.30	2.4	0.57	4.2	1.30	0.65	5
Fe (Z)	0.005	M	I	0.20	0.63	0.21	2.82	0.25	2.82	0.195	14.5	0.82	1.01	5
Al (Z)	0.001	A	I	0.79	0.72	0.41	0.57	1.28	1.28	0.41	3.1	0.75	0.29	5
Na (Z)	0.002	M	I	0.17	0.16	0.17	0.13	0.13	0.17	0.13	1.3	0.15	0.02	5
Mg (Z)	0.001	A	I	0.17	0.12	0.18	0.12	0.14	0.18	0.12	1.5	0.15	0.02	5
Ti	10	A	I	670	490	270	200	430	670	200	3.4	412	166	5
P	10	A	I	70	20	10	70	1300	1300	10	130	294	504	5
Sr	5	M	I	220	230	190	120	280	280	120	2.3	208	53	5
Ba	20	M	I	210	160	190	160	210	210	160	1.3	186	22	5
B	0.5	M	P	88	110	100	140	140	88	88	1.6	116	21	5
K	10	A	I	90	80	200	60	140	200	60	3.3	114	50	5
Zr	1	A	I	40	31	22	15	33	40	15	2.7	28	9	5
Mn	0.1	M	R	21.0	14.0	7.8	6.9	5.7	21.0	5.7	3.7	11.1	5.7	5
Ce	0.5	M	I	10.9	7.2	5.0	10.1	15.0	15	5	3.0	9.6	3.4	5
V	0.5	M	R	9.0	10.0	3.9	4.8	4.9	10.0	3.9	2.6	6.5	2.5	5
Pb	0.2	A	D	8.0	8.0	3.6	4.7	8.0	8	3.6	2.2	6.5	1.9	5
La	0.1	M	I	6.4	3.3	1.8	8.4	11.6	11.6	1.8	6.4	6.3	3.5	5
As	0.2	M	I	0.1	4.0	0.6	26.0	0.8	26.0	0.1	520	6.3	10.0	5
Cr	0.2	M	I	6.5	3.9	2.5	2.4	2.4	6.5	2.4	2.7	3.5	1.6	5
Ni	50	M	I	4.5	2.6	3.4	3.6	3.1	4.5	2.6	1.7	3.4	0.6	5
Nd	0.5	M	I	3.7	2.8	1.9	3.2	5.2	5.2	1.9	2.7	3.4	1.1	5
Zn	0.05	A	I	4.0	1.4	1.4	5.4	3.0	5.4	1.4	3.9	3.0	1.5	5
Cu	0.05	A	I	3.8	2.1	0.5	3.6	4.9	4.9	0.5	9.8	3.0	1.5	5
Nb	1	A	I	3	3	1	1	3	3	1	3.0	2.2	1.0	5
Th	0.1	M	I	2.7	2.8	0.7	0.7	1.3	2.8	0.7	4.0	1.6	0.9	5
Sc	0.01	M	I	1.70	1.60	0.52	0.93	0.82	1.7	0.52	3.3	1.11	0.46	5
Co	0.1	M	I	0.9	1.3	1.0	1.2	1.0	1.3	0.9	1.4	1.1	0.1	5
Mo	0.4	M	I	0.5	1.2	0.7	1.4	1.0	1.4	0.5	2.8	1.0	0.3	5
Hf	0.1	M	I	1.3	0.7	0.3	0.2	1.0	1.3	0.2	6.5	0.7	0.4	5
U	0.01	M	R	0.78	1.22	0.18	0.44	0.50	1.22	0.18	6.8	0.62	0.35	5
Sr	0.01	M	I	0.72	0.54	0.33	0.51	0.74	0.74	0.33	2.2	0.57	0.15	5
Dy	0.5	M	R	0.74	0.51	0.33	0.42	0.74	0.74	0.33	2.2	0.53	0.15	5
Yb	0.01	M	I	0.33	0.17	0.12	0.17	0.29	0.33	0.12	2.8	0.22	0.08	5
Sb	0.1	M	I	0.3	0.4	0.1	0.1	0.1	0.4	0.1	4.0	0.2	0.1	5
Eu	0.05	M	I	0.18	0.24	0.05	0.15	0.14	0.24	0.05	4.8	0.15	0.06	5
Lu	0.01	M	I	0.06	0.05	0.02	0.03	0.05	0.06	0.02	3.0	0.04	0.01	5
AU (PPB)	1	M	I	1	1	1	2	1	2	1	2.0	1.20	0.40	5

(CONTINUED)

TABLE IIP-7 (CONTINUED)

ELEMENT	D.L.	SAMP. ANAL.		ELEMENT CONCENTRATIONS*										
		TYPE	METH.	U3	U8	U13	U17	U22	MAX	MIN	RNG	MEAN	STD (N)	
Cl	10	W	R		10	10	90	10	90	10	9.0	30	35	4
Y	1	A	X	5		2	2	2	5	2	2.5	2.8	1.3	4
Rb	1	A	X	3		2	1	3	3	1	3.0	2.3	0.8	4
Br	0.5	W	I		0.6	0.5	1.1	0.8	1.1	0.5	2.2	0.8	0.2	4
S (Z)	0.01	A	X	ND	ND	0.49	3.70	ND	3.7	0.49	7.6	2.10	1.44	3
Se	0.2	W	I	0.6	1.7		2.3		2.3	0.6	3.8	1.5	0.7	3
Cs	0.1	W	I		0.1		0.3	0.2	0.3	0.1	3.0	0.2	0.1	3
I	0.5	W	R		0.6		0.5		0.6	0.5	1.2	0.6	0.0	2
Ag	0.05	A	D	ND	ND	0.35	0.55	ND	0.55	0.35	1.6	0.45	0.10	2
Hg	5	A	S			100			100	100	1.0	100	0.0	1
Ta	0.1	W	I				0.2		0.2	0.2	1.0	0.2	0.0	1
Cd	0.02	A	X						NA	NA	NA	NA	NA	0
Be	1	A	X						NA	NA	NA	NA	NA	0
In	0.1	W	R						NA	NA	NA	NA	NA	0
M	1	W	I						NA	NA	NA	NA	NA	0
Tb	0.05	W	I						NA	NA	NA	NA	NA	0
Ga	10	W	R						NA	NA	NA	NA	NA	0
Bd	0.5	W	P						NA	NA	NA	NA	NA	0

* - CONCENTRATIONS IN PPM UNLESS OTHERWISE NOTED. BLANK SPACES REPRESENT CONCENTRATIONS LESS THAN DETECTION LIMITS.

SAMP.

TYPE - SAMPLE TYPE (W = WHOLE COAL; A = COAL ASHED AT 350 C AND CORRECTED FOR 10% ASH).

ANAL.

METH. - ANALYTICAL METHOD (X = X-RAY FLUORESCENCE; I = INSTRUMENTAL NEUTRON ACTIVATION ANALYSIS (INAA); R = SHORT LIVED INAA; P = PROMPT GAMMA COUNTING; D = DIRECT CURRENT PLASMA; S = SPECIAL WET METHOD).

MAX - MAXIMUM VALUE

MIN - MINIMUM VALUE

STD - STANDARD DEVIATION

D.L. - DETECTION LIMIT

ND - NO DATA

NA - NOT APPLICABLE

(N) - # SAMPLES

RNG - RANGE

5

given element was detected; second, in decreasing order of abundance (mean values) within each value of N.

III.2.4.2 UTAH: WHOLE COAL

All five samples (N=5) of Utah coal contained detectable levels of the first 39 elements (Ca to Au) in Table III-7. Seven of those elements (Ca to Mg) were present at mean concentrations >0.1%, 6 elements (Ti to K) were present at mean concentrations between 100 ppm and 0.1%, 2 elements (Zr and Mn) occur between 10-100 ppm, 15 elements (Ce to Mo) were present in the range 1-10 ppm and 9 of the elements (Hf to Lu) occur at concentrations of <1 ppm.

The elements Cl, Y, Rb and Br were detected in only 4 of the samples (N=4), ranging from a high of 30 ppm for Cl to 0.8 ppm in the case of Br.

Selenium, 1.5 ppm, and Cs, 0.2 ppm, were detected in three of the samples (N=3).

Two samples (N=2) contained detectable levels of I, 0.6 ppm, and Ag, 0.45 ppm.

Mercury, 100 ppm, and Ta, 0.2 ppm, were detected in only one sample each (N=1).

The last seven elements in Table III-7 (Cd to Gd) were not present above the lower limits of detection in any of the Utah samples (N=0).

III.2.4.3 WYOMING: WHOLE COAL

Table III-8 shows that 29 elements (Ca to Au) were detected in all 8 samples (N=8) of Wyoming coal. The first 5 elements (Ca to Mg) were present at mean concentrations >0.1%, 4 elements (Na to Sr) between 100 ppm and 0.1%, 3 elements (Mn to Zn) between 10-100 ppm, 8 elements (V to Br) from 1-10 ppm and 9 of the elements (Sc to Au) were present at mean concentrations of <1 ppm.

Antimony, 0.07 ppm, and Eu, 0.06 ppm, were present in 7 samples (N=7).

Five samples (N=5) contained detectable levels of Se, 0.6 ppm, Cs, 0.3 ppm and Tb, 0.06 ppm.

Molybdenum, 0.7 ppm, was detected in only 4 of the samples (N=4).

None of the Wyoming samples (N=0) contained measurable amounts of the last 5 elements (Ni to K) in Table (wtbl03a).

III.2.4.4 WYOMING OVERBURDEN SEDIMENT AND CLINKER

TABLE III-8

ANALYSES OF 40 ELEMENTS IN COAL FROM THE POWDER RIVER COAL FIELD, POWDER RIVER BASIN, WYOMING

		ELEMENT CONCENTRATIONS*														
ANAL.																
ELEMENT	D.L.	METH.	N61ML	S62ML	N41ML	S42ML	N21ML	S32ML	N11ML	S12ML	MAX	MIN	RNG	MEAN	STB (N)	
Ca (Z)	0.03	I	0.92	0.98	0.94	1.02	1.17	1.03	1.12	0.88	1.17	0.88	1.3	1.01	0.09	8
Al (Z)	0.00	R	0.51	0.66	0.33	0.6	0.39	0.27	0.28	0.32	0.66	0.27	1.8	0.42	0.14	8
S# (Z)	0.01	S	0.21	0.34	0.33	0.32	0.35	0.3	0.39	0.21	0.39	0.21	1.9	0.31	0.06	8
Fe (Z)	0.01	I	0.17	0.18	0.12	0.19	0.14	0.19	0.2	0.16	0.20	0.12	1.7	0.17	0.03	8
Mg (Z)	0.05	I	0.11	0.13	0.15	0.13	0.18	0.13	0.16	0.1	0.18	0.10	1.8	0.14	0.02	8
Na	30	I	710	790	530	590	370	780	510	870	870	370	2.4	644	160	8
Ba	20	I	600	240	240	640	280	290	250	240	640	240	2.7	348	159	8
Tl	20	R	180	320	105	120	300	210	200	180	320	105	3.0	202	71	8
Sr	50	I	320	130	135	470	150	130	150	100	470	100	4.7	198	121	8
Mn	20	R	10.5	17.6	34	19.2	25.8	6.2	41.9	17.8	41.9	6.2	6.8	21.6	11.1	8
Cl	10	R	21	13	14	16	16	12	9	13	21.0	9.0	2.3	14.3	3.3	8
Zn	5	I	11	10	10	14	11	10	8	9	14.0	8.0	1.8	10.4	1.7	8
V	30	R	7.4	20.3	6.6	4.8	10.8	4.4	5.3	6.8	20.3	4.4	4.6	8.3	4.9	8
Co	0.1	I	3.9	6.4	5.7	6.1	5.6	5	4	4	6.4	3.9	1.6	5.1	0.9	8
As	0.5	I	2.2	6	5	5.7	4.7	4.4	3.4	3.2	6.0	2.2	2.7	4.3	1.2	8
Ce	0.5	I	3.3	3.6	2.2	6.7	4.4	2.3	4.2	2.2	6.7	2.2	3.0	3.6	1.4	8
Cr	0.5	I	2.3	3.1	1.9	1.5	3	1.9	2.1	2.1	3.1	1.5	2.1	2.2	0.5	8
La	0.1	I	1.5	1.4	1.1	3.8	2.2	1	1.8	1.1	3.8	1.0	3.8	1.7	0.9	8
Nd	0.5	I	1.2	1.5	1	2.7	1.6	1.2	2	1	2.7	1.0	2.7	1.5	0.5	8
Br	0.5	I	0.8	1.4	1.2	1.2	1.6	1	1.2	1.2	1.6	0.8	2.0	1.2	0.2	8
Sc	0.01	I	0.83	1.2	0.58	0.88	1.3	0.52	0.57	0.64	1.30	0.52	2.5	0.82	0.28	8
Th	0.02	I	0.6	0.7	0.4	0.5	1	0.4	0.6	0.4	1.0	0.4	2.5	0.6	0.2	8
Dy	0.03	R	0.26	0.34	0.2	0.57	0.37	0.34	0.28	0.25	0.57	0.20	2.9	0.33	0.11	8
Sm	0.05	I	0.22	0.33	0.2	0.53	0.32	0.31	0.34	0.21	0.53	0.20	2.7	0.31	0.10	8
Hf	0.1	I	0.3	0.4	0.2	0.3	0.4	0.3	0.3	0.2	0.4	0.2	2.0	0.3	0.1	8
U	0.03	D	0.21	0.31	0.14	0.17	0.26	0.13	0.17	0.13	0.31	0.13	2.4	0.19	0.06	8
Yb	0.05	I	0.11	0.15	0.11	0.16	0.14	0.25	0.19	0.12	0.25	0.11	2.3	0.15	0.04	8
Lu	0.00	I	0.014	0.025	0.018	0.024	0.023	0.041	0.029	0.019	0.041	0.014	2.9	0.024	0.008	8
Au (PPB)	1	I	1	3	1	5	2	23	12	1	23.0	1.0	23.0	6.0	7.3	8
Sb	0.05	I	0.07	0.07	0.11		0.07	0.05	0.05	0.08	0.11	0.05	2.2	0.07	0.02	7
Eu	0.05	I	0.06	0.06	0.05	0.08	0.07	0.06	0.05		0.08	0.05	1.6	0.06	0.01	7
Se	0.5	I		0.6	0.5	0.7		0.5	0.5		0.7	0.5	1.4	0.6	0.1	5
Cs	0.2	I		0.2	0.2	0.2		0.3		0.4	0.4	0.2	2.0	0.3	0.1	5
Tb	0.05	I		0.07	0.05	0.1		0.05	0.05		0.10	0.05	2.0	0.06	0.02	5
Mo	0.5	I		1.2			0.5		0.7	0.5	1.2	0.5	2.4	0.7	0.3	4
Ni	50	I									NA	NA	NA	NA	NA	0
M	1	I									NA	NA	NA	NA	NA	0
Rb	5	I									NA	NA	NA	NA	NA	0
Ta	0.5	I									NA	NA	NA	NA	NA	0
K (Z)	0.02	I									NA	NA	NA	NA	NA	0

* - CONCENTRATIONS IN PPM UNLESS OTHERWISE NOTED. BLANK SPACES REPRESENT CONC. LESS THAN D.L.

† - SULFUR ANALYSIS FROM COAL ASHED AT 350 C AND CORRECTED FOR 10% ASH.

ANAL.

METH. - ANALYTICAL METHOD (I = INSTRUMENTAL NEUTRON ACTIVATION ANALYSIS (INAA); R = SHORT LIVED INAA; P = PROMPT GAMMA COUNTING; D = DELAYED NEUTRON COUNTING; S = SPECIAL NET METHOD)

MAX - MAXIMUM VALUE

MIN - MINIMUM VALUE

STB - STANDARD DEVIATION

(N) - # SAMPLES

D.L. - DETECTION LIMIT

ND - NO DATA

NA - NOT APPLICABLE

RNG - RANGE

III.2.4.4.1 INTRODUCTION

The concentrations of 40 elements in two sediment samples (overburden) and one sample of clinker (see Sect. III.2.4.4.3 for explanation) associated with the Wyoming coals studied here are shown in Table III-9. The two overburden samples were collected above and at either end of the coal seam (bench) from which coal samples for this study were collected. The sample of clinker was taken from a bulk pile which was being excavated (for use as paving stone) from below one corner of the coal bench approximately 0.5 Km from where the coals were collected. In effect, the overburden represents sediments immediately adjacent to the top of the seam while the clinker represents the remains of sediments stratigraphically lower than the coal (seat earths).

Table III-10, columns 1 and 2, lists the average concentrations for 39 elements in the overburden and clinker from this study. Data from Hinkley and Ebens (1977, table 55) and Ebens and McNeal (1977, tables 60 and 61) on the average concentrations of three sediment types that occur as overburden associated with strippable coal deposits in the Fort Union Formation throughout the Northern Great Plains Coal Province, including the Powder River Coal Field, are used for comparison as shown in columns 3, 4 and 5: column

TABLE III-9

ANALYSES OF 40 ELEMENTS IN OVERBURDEN SEDIMENTS (OB) AND CLINKER FROM THE POWDER RIVER COAL FIELD, POWDER RIVER COAL BASIN, WYOMING.

ELEMENT CONCENTRATIONS*							
ELEMENT	D.L.	ANAL. METH.	OVERBURDEN SEDIMENTS				CLINKER
			OB6	OB1	RMS	MEAN	
Na	30	I	920	860	1.1	890	1000
Mg (Z)	0.05	I	0.45	0.72	1.6	0.59	0.28
Al (Z)	0.002	R	6.52	8.39	1.3	7.46	8.49
S (Z)	0.01	S	ND	ND	NA	NA	NA
Cl	10	R	<200	<200	NA	NA	<200
K (Z)	0.02	I	1.20	1.30	1.1	1.25	1
Ca (Z)	0.03	I	0.53	0.48	1.1	0.51	0.46
Sc	0.01	I	15	15	1.0	15.00	13
Ti	20	R	3700	4400	1.2	4050	4700
V	30	R	112	136	1.2	124	115
Cr	0.5	I	87	93	1.1	90	90
Mn	20	R	360	190	1.9	275	1180
Fe (Z)	0.01	I	3.84	2.38	1.6	3.11	1.94
Co	0.1	I	16	18	1.1	17.0	16
Ni	50	I			NA	NA	
Zn	5	I	93	100	1.1	97	93
As	0.5	I	12	17	1.4	14.5	16
Se	0.5	I		1	1.0	1.0	
Br	5	I	0.7	0.9	1.3	0.8	0.7
Rb	5	I	150	170	1.1	160	150
Sr	50	I	130	200	1.5	165	150
Mo	0.5	I	6.6	7.2	1.1	6.9	6
Sb	0.05	I	1.1	1	1.1	1.05	2.8
Cs	0.2	I	8.5	9.5	1.1	9.0	10
Ba	20	I	630	630	1.0	630	750
La	0.1	I	43.1	46.6	1.1	44.9	38.2
Hf	0.1	I	8.8	8.9	1.0	8.9	10
Ta	0.5	I	1.1	1.3	1.2	1.2	1.1
W	1	I	2	3	1.5	2.5	3
Au (PPB)	1	I	6	7	1.2	6.5	6
Ce	0.5	I	83	92	1.1	87.5	71
Nd	0.5	I	31	35	1.1	33.0	27
Sm	0.05	I	5.9	6.4	1.1	6.15	4.9
Eu	0.05	I	1.04	1.3	1.3	1.17	1.04
Tb	0.05	I	0.81	1.04	1.3	0.93	0.76
Dy	0.03	R	4	4.8	1.2	4.4	4.2
Yb	0.05	I	3.13	3.22	1.0	3.18	2.99
Lu	0.005	I	0.511	0.516	1.0	0.514	0.472
Th	0.02	I	16	18	1.1	17.0	14
U	0.03	D	4.91	5.69	1.2	5.30	4.61

* - CONCENTRATIONS IN PPM UNLESS OTHERWISE NOTED. BLANK SPACES REPRESENT CONCENTRATIONS LESS THAN D.L.

ANAL. - ANALYTICAL METHODS ARE THE SAME AS IN FIGURE (UTBLOS3A)

D.L. - DETECTION LIMIT

ND - NO DATA

STD - STD DEVIATION

NA - NOT APPLICABLE

RMS - RANGE

(N) - # SAMPLES

3, fine grained sedimentary rocks; column 4, shale; column 5, sandstone. When comparing element concentrations in the following discussions ratios falling between 0.67 and 1.5 (+/- 50%) are arbitrarily (based on the known variability of coals) considered inconsequential, i.e., the concentrations are close enough as not to represent a substantial enrichment or depletion in one or other of the samples.

III.2.4.4.2 OVERBURDEN SEDIMENT

The concentrations of 37 elements (Ni and Cl were not present above the limits of detection) detected in two overburden samples from this work are listed in decreasing order of abundance in column 1 of Table III-10. These data are compared to average concentrations in similar sediments associated with Powder River Coal Field coals: column 9, comparison with shales; column 10, comparison with sandstones.

Work done by the U.S.G.S. to assess the environmental impact of overburden usage in the Northern Great Plains Coal Province has shown that changes in mineralogy over large areas is responsible for changes in the major and trace element geochemistries of the sediments, depending on the trace elements in question. For example, Mg, Ca, Na, Ba and Ti vary significantly over the largest sampling area and correlate well with the occurrence of dolomite, calcite,

TABLE III-10
 GEOCHEMISTRY (39 ELEMENTS) OF SEDIMENT (SEDS) AND CLINKER (CLINK) ASSOCIATED WITH COAL FROM THE POWDER RIVER COAL FIELD (PRCF), POWDER RIVER BASIN, WYOMING. DATA FOR OTHER NORTHERN GREAT PLAINS (NGP) SEDIMENTS ARE SHOWN FOR COMPARISON. RATIOS ARE EXPLAINED IN THE TEXT. (CONCENTRATIONS IN PPM)

ELEMENT	THIS WORK (PRCF)		OTHER NGP SEDS *			RATIOS				
	COL.1	COL.2	COL.3	COL.4	COL.5	COL.6	COL.7	COL.8	COL.9	COL.10
	SEDS	CLNK	FN RX	SHALE	SANDST	EL. COL1:COL2	EL. COL1:COL4	EL. COL1:COL5	EL. COL2:COL4	EL. COL2:COL5
Al	75000	80000	79400	70000	41000	K 2.3	As 2.8	Se 5.3	Mn 3.7	Mn 4.2
Fe	31000	19000	31000	24000	15000	Mg 2.0	Co 1.9	As 3.3	As 3.1	As 3.6
K	23000	10000	22000	19000	14000	Fe 1.6	Rb 1.5	Co 3.1	Co 1.8	Co 3.0
Mg	6000	3000	14400	14000	11000	Sm 1.3	Th 1.3	Rb 2.8	Ti 1.4	Rb 2.6
Ca	5000	5000	12000	14000	24000	Ce 1.2	Ce 1.3	V 2.7	Rb 1.4	V 2.5
Ti	4050	4700	3800	3400	2300	Tb 1.2	U 1.3	Sc 2.6	Al 1.2	Sc 2.3
Na	1000	1000	6600	4200	4900	Md 1.2	Fe 1.3	Th 2.4	V 1.2	Zn 2.1
Ba	630	750	420	940	700	Th 1.2	V 1.3	Zn 2.2	Zn 1.2	Al 2.1
Mn	275	1180	300	320	280	La 1.2	Sc 1.3	Fe 2.1	U 1.1	Ti 2.0
Sr	185	150	ND	170	160	Au 1.2	Zn 1.2	Cr 2.0	Sc 1.1	Cr 2.0
Rb	160	150	110	110	58	Sc 1.2	K 1.2	U 2.0	Th 1.1	Th 2.0
V	124	115	86	97	46	Mo 1.2	Ti 1.2	Al 1.8	Cr 1.1	U 1.7
Zn	97	93	100	80	44	U 1.1	Cr 1.1	Ti 1.8	Ce 1.1	Yb 1.4
Cr	90	90	72	84	45	Br 1.1	Al 1.1	K 1.6	La 0.9	Ce 1.3
Ce	88	71	65	67	55	Eu 1.1	La 1.1	Ce 1.6	Sr 0.9	Fe 1.3
La	45	38	33	42	35	Sr 1.1	Sr 1.0	Yb 1.5	Yb 0.8	Mo 1.2
Md	33	27	ND	ND	ND	Ta 1.1	Yb 0.9	Mo 1.4	Ba 0.8	La 1.1
Co	17	16	8.7	9.1	5.4	Lu 1.1	Mn 0.9	La 1.3	Fe 0.8	Ba 1.1
Th	17	14	13	13	7.1	V 1.1	Mo 0.9	Sr 1.0	Mo 0.7	Sr 0.9
Sc	15	13	11	12	5.7	Rb 1.1	Ba 0.7	Mn 1.0	K 0.5	K 0.7
As	14.5	16	3.6	5.1	4.4	Yb 1.1	Mg 0.4	Ba 0.9	Ca 0.4	Mg 0.3
Hf	10	10	ND	ND	ND	Co 1.1	Ca 0.4	Mg 0.5	Na 0.2	Ca 0.2
Cs	9	10	ND	ND	ND	Dy 1.0	Na 0.2	Ca 0.2	Mg 0.2	Na 0.2
Mo	6.9	6	6.1	8.1	5	Zn 1.0	Eu ERR	Na 0.2	Sb ERR	Sb ERR
Sm	6.2	4.9	ND	ND	ND	Na 1.0	Ta ERR	Eu ERR	Cl ERR	Sm ERR
U	5.3	4.6	3.7	4.1	2.7	Ca 1.0	Sm ERR	Cs ERR	Sm ERR	Cs ERR
Dy	4.4	4.2	ND	ND	ND	Cr 1.0	Cl ERR	Md ERR	Eu ERR	Ni ERR
Yb	3.2	3.0	2.9	3.7	2.1	Hf 1.0	Ni ERR	Cl ERR	Au ERR	Hf ERR
W	2.5	3	ND	ND	ND	As 0.9	Au ERR	Au ERR	Ta ERR	Lu ERR
Ta	1.2	1.1	ND	ND	ND	Cs 0.9	Hf ERR	Hf ERR	Ni ERR	Eu ERR
Eu	1.2	1.0	ND	ND	ND	Al 0.9	Cs ERR	Br ERR	Hf ERR	Tb ERR
Sb	1.1	2.8	ND	ND	ND	Ti 0.9	Tb ERR	Ta ERR	Tb ERR	Ta ERR
Se	1	<0.5	0.2	ND	0.19	Ba 0.8	Br ERR	Sb ERR	Se ERR	Cl ERR
Tb	0.9	0.8	ND	ND	ND	M 0.8	Sb ERR	Sm ERR	Md ERR	Md ERR
Br	0.8	0.7	ND	ND	ND	Sb 0.4	Lu ERR	M ERR	Lu ERR	M ERR
Lu	0.51	0.47	ND	ND	ND	Mn 0.2	Md ERR	Lu ERR	Cs ERR	Br ERR
Au	0.007	0.006	ND	ND	ND	Cl ERR	Dy ERR	Ni ERR	Dy ERR	Au ERR
Ni	<50	<50	30	31	16	Ni ERR	Se ERR	Tb ERR	M ERR	Se ERR
Cl	<200	<200	ND	ND	ND	Se ERR	M ERR	Dy ERR	Br ERR	Dy ERR

* OTHER NGP SEDIMENTS: FN RX (FINE GRAINED SEDS), DATA FROM HINKLEY AND EBENS, 1977, TABLE 55;
 SHALE AND SANDST (SANDSTONE), DATA FROM EBENS AND MCNEAL, 1977, TBLS. 60 & 61
 ND - NO DATA
 ERR - DATA NOT AVAILABLE FOR CALCULATION

plagioclase and chlorite. Other elements (B, Co, Cr, Cu, Ge, Ni, Sc, Th, V, Y, Zr and Yb) were found to vary on a regional basis, probably as a function of the type of clays present in the overburden. The trace elements As, Hg and Se did not vary significantly on a regional scale (Hinkley, et al., 1980; Ebens and McNeal, 1977).

In addition, these studies showed that the mineralogy, and related geochemistry of the overburden did not vary significantly over the area of a typical strip mine (1-5 Km separation). Furthermore, the largest variations occurred vertically within single cores taken and were related to variations in lithology, i.e., fine grained rocks or sandstones (Hinkley and Ebens, 1976 and 1977).

The results of this study are in excellent agreement with the above mentioned works. The comparisons are presented in Table III-10. The concentrations of 23 elements (As - Ya) in overburden sediments from this work are compared to mean values for shales collected throughout the Northern Great Plains Coal Province in Table III-10, column 7. Eighteen of the elements (Rb - Ba) are present at similar concentrations (+/- 50%) in both sample sets. Two elements (As and Co) are present at slightly higher concentrations in the samples from this study while 3 elements (Mg, Ca and Na) occur at significantly lower concentrations. Column 8 (Table III-10) compares data from this study with sandstones from

throughout the Northern Great Plains Coal Province. These data do not correlate as well as those for the shales. Of the 24 elements compared in column 8, 15 (Se - Ce) are enriched in the Powder River Coal overburden relative to the sandstones, only 6 elements (Yb - Ba) are present at similar concentrations and 3 elements (Mg, Ca and Na) are relatively depleted.

In both cases mentioned above Mg, Ca and Na are the only elements appreciably depleted in the Powder River Coal Field overburden relative to either the shales or sandstones. As shown by Hinkley and Ebens (1977) this difference can be explained by the absence of the minerals calcite, dolomite, and plagioclase. Likewise, seven of the elements reported by Hinkley, et. al., (1980) and Hinkley and Ebens (1977) as being correlatable with clays throughout the area they studied are among the 13 elements found enriched by this study relative to the other sandstones. Conversely, only Co was enriched in the Powder River Coal Field overburden relative to the other shales. It appears from these data that the geochemistry of the overburden in the Powder River Coal Field is dominated, at least where samples for this study were collected, by the presence of clays in the sediments.

When traveling through the Powder River Basin in NE Wyoming one cannot help but notice that the majority of the topographic highs consist of gently westward dipping mesas capped with a reddish-orange hue and that the same colour scheme highlights the berms of paved highways and the tops of secondary (gravel) roads (it only makes sense to look for the most accessible and the "strongest" paving materials on the erosionally resistant topographic highs). The material in question is "clinker", a rock formed when the in situ combustion of coal beds bake the surrounding strata, typically sandy to shaley siltstones in the case of the Powder River Basin. In some cases clinker is produced by temperatures approaching 2000°C resulting in fusing or melting of the parent material and the formation of high temperature mineral phases such as beta cristobalite (Herring, 1980). Metamorphism of the parent rock under these conditions makes it more resistant to erosion than the adjacent rocks, hence, inversion of topography results during erosion and the clinker becomes the resistant cap rock. Detailed accounts of how burns (in situ coal fires) are caused, sustained and the results can be found in Herring (1980) and Coates (1980) and references within.

Direct observation of a 100 year old burn at Bowman, North Dakota sets the rate of burning at approximately 3 m/yr (Herring, 1980). Coates and Naeser (1980) have determined the rate of burning to be approximately 10 m/1000 yr at

Little Thunder Creek, Wyoming (Rochelle Hills, Southern Campbell County). They base their findings on fission track dating of zircons annealed during burning. In addition they have predicted that a single burn in the Powder River Basin, that has lasted for the past 750,000 years, has released a mass of carbon approximately equal to the amount contained in the present atmosphere!

A natural result of the formation of clinker is mobilization of the elements contained in both the parent material and the coal. Some elements, or compounds (e.g., Se, Hg, F, CS₂, CO₂) are volatilized and escape to the atmosphere via chimneys created in the overlying strata by fracturing due to heating and warping (Herring, 1980). Other elements (e.g., S, As, Sb) enter into recombination by condensing onto overlying material as combustion gases cool, and others are left behind as refractory compounds (e.g., Al, Si). This fractionation process is not unlike the formation of ash and slag in the furnace of a coal burning plant. The result is that the clinker should be different, chemically, from the material from which it formed. The following discussion shows that this is not the case for the clinker analyzed in this study.

The concentrations of 36 elements (Se, Ni and Cl were not detected above detection limits) in the clinker analyzed in this work are listed in column 2 of Table III-10. These

data are compared to typical Northern Great Plains Coal Province shales and sandstones in columns 9 and 10 respectively in the same manner as the overburden discussed in the previous section.

As in the case of the overburden samples, the geochemistry of the clinker is very similar to the shales (col. 9). Sixteen of the 23 elements (Ti - Mo) detected in both sample sets occur at similar concentrations (+/- 50%). Three elements (Mn, As, and Co) are enriched in the clinker and 4 elements (Ca, Na, Mg and K) are depleted. Conversely, when the clinker is compared to the sandstones (col. 10) only 8 elements (Yb - K) are present at similar concentrations while 12 elements (Mn - U) are present at higher concentrations and 3 elements (Mg, Ca and Na) at lower concentrations than the sandstones. These data show that the clinker is more similar, geochemically, to the shales of the Northern Great Plains than to the sandstones from the same area.

III.2.4.4.4 COMPARISON OF CLINKER VS OVERBURDEN

A most striking geochemical similarity exists between the clinker and overburden analyzed in this work. Of the 36 elements these samples have in common the ratios of 31 (Sm - W) fall between 1.3 and 0.8 (col. 6, Table IIF-10) and 20 of those (U - Ti) vary by less than 10%. Only K, Mg and Fe

were found at substantially higher concentrations and Sb and Mn at lower concentrations in the overburden relative to the clinker. Many of the elements expected to be enriched in the clinker due to their refractory nature (e.g., Al, Ti, V, U, W) as well as those one would predict as being volatilized during burning (e.g., As, Zn) exist at nearly identical concentrations in both the overburden and the clinker. Explanations for these observations are speculative. The temperature of the burn, exact mineral phases hosting trace elements and the geochemistry of the post-burn environment (groundwater) as well as depth to the water table might all play a part in the observed geochemistries.

The main assumptions to be drawn from the geochemical data is that the precursor to the clinker was a shaley rock similar in composition to the present overburden and that little geochemical change took place during its formation.

III.3 SCANNING ELECTRON MICROSCOPY / ENERGY DISPERSIVE SPECTROSCOPY (SEM/EDS)..

III.3.1 INTRODUCTION

Scanning Electron Microscopy (SEM) coupled with Energy dispersive Spectroscopy (EDS) has long been a useful tool in examining the in situ occurrence and distribution of minute mineral phases in coal. Typically, SEM/EDS analyses are

60

performed on cut and polished sections or broken fragments. Sample preparation, in these cases, requires a minimum of mechanical (polishing) and chemical (lubricants) pretreatment. A disadvantage to this technique is that the analyst is limited to a two dimensional surface through the coal. In many cases this surface is selected on the basis of macroscopic identification of unusual structures or discoloration, and is therefore biased. This technique is useful, however, a technique is needed which more readily allows analysis of the finely disseminated mineral matter in coals with a better probability of finding those constituents which may be "hiding" under polished surfaces, but without subjecting the coal to methods of preconcentration such as density separations (heavy liquids), thermal ashing (low or high temperature) or chemical methods such as wet oxidation (acids). All of these can affect the mineralogy or the coal and, therefore, the distribution and combinations of the constituent elements.

The method used in this study involved crushing the sample (150 mesh) and forming a pellet in the same manner as for XRF analysis but without adding any type of binder. In effect, the sample is homogenized such that the surface of any pellet should contain a representative amount of each mineral constituent in the coal. The trick then is to find those particles. Only after one has peered into the CRT of the SEM for long periods does it become apparent that this

task is impossible (within a normal time frame). Figure III-1 (pellet) shows that the backscatter electron image (BEI) (for atomic number contrast) of a pellet resembles an aerial view of New York City at night with each individual mineral particle shining brightly on the dark background of the coal matrix. Obviously, there is little chance of finding all of the different mineral phases represented in the surface of a given sample. However, this method is very useful for observing the more prevalent minerals and hence in identifying discrete element assemblages.

The above technique was employed for a number of pellets from both the Utah and Wyoming coals. The samples were selected on the basis of chemical anomalies as reported from other methods (XRF/INAA) as well as high ash contents. In the following discussions each spectrum and/or list of elements applies to an individual grain identified in the pellet.

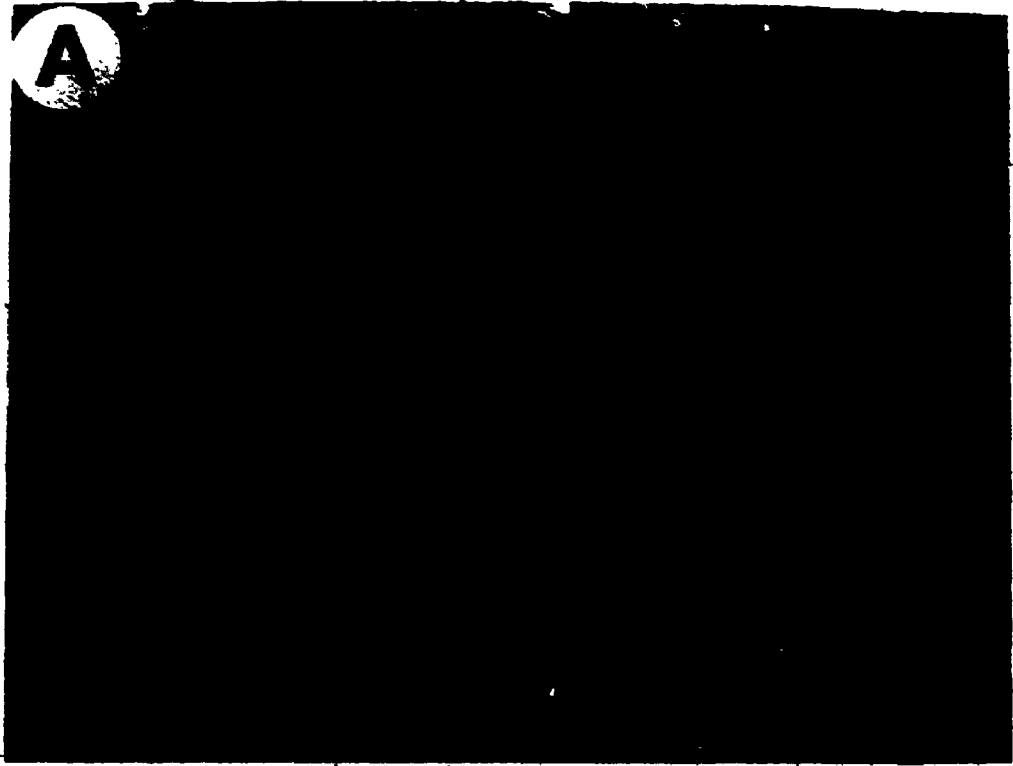
SEM/EDS analyses of pyrite nodules from the Utah coals are presented in a separate sections.

Conclusions regarding the probable/possible presence of a given mineral phase based solely on the element assemblages listed here are speculative. However, it is not uncommon in the literature to find such evidence used to support other types of analyses, e.g., XRD, when common mineral phases are

FIGURE III-1

A - PHOTOMICROGRAPH (BACKSCATTER ELECTRON IMAGE) OF A TYPICAL PELLET OF WHOLE COAL FROM WHICH EDS ANALYSES WERE COLLECTED. BRIGHT SPECKS REPRESENT MINERAL PHASES IN THE SURFACE OF THE PELLET. THE DARKER MATRIX IS COAL."

B - PHOTOMICROGRAPH OF ONE OF THE GRAINS SHOWN IN "A" ABOVE.



present. In as much as the data from this study correlate well with other work and since the mineral phases suggested here are common in other coals studied, the following conclusions are deemed valid.

The relative peak heights for the elements represented in the spectra discussed here are used as a semiquantitative means of determining whether or not the element is a major or trace constituent of the grain.

Furthermore, as with the TEM work of Allen and VanderSande (1983) many of the elements contained in the following spectra were also detected when the apparently clean coal (matrix) was analyzed. It must be assumed that these elements exist on an atomic scale bound in inorganic combinations as well as in larger visible minerals and that this occurrence has affected the EDS spectra accordingly.

The following spectra are discussed on the basis of their most probable mineralogy. By no means is this considered to be a definitive statement as to the true mineralogy. On the contrary, the majority of the element assemblages found in these individual particles can be attributed to many more than one mineral and in most cases to a mixture of two or more phases. However, a compromise in avoiding chemical pretreatment to insure the integrity of the minerals seems favorable in light of the fact that the main purpose of this

71

part of the study was to identify mineral assemblages which are probably inseparable by most mechanical methods.

As noted above the majority of the element assemblages represented by the following spectra can be explained in more than one way. In fact it is almost impossible to discuss the spectra individually, i.e., without reference from one to another. Therefore, some of the more plausible reasons for the complexity of the following spectra are listed below. One or the other of these are applicable, in some part, to the discussions concerning the origins of the following spectra (except for the simplest).

EDS is not efficient in detecting elements below atomic number 11 (Na) and so these light elements are not included in the following discussions. This is not to say that they are not present (e.g., the C in carbonate or the O in oxides). In addition, many of the small peaks (perturbations) are not labeled for one of two reasons: they are too small to resolve and therefore no identification was possible; they are sum or escape (artifact) peaks of existing elements.

Some of the common complications arising when trying to assign mineral names to EDS spectra include:

1. Spectra which can be attributed to more than one mineral, e.g., a spectrum containing the

elements Al, Si and K might belong to either a clay such as Illite ($K_0.5Al_2(Al, Si)_4O_{10}(OH)_2$) or to potassium feldspar ($KAlSi_3O_8$). Both could yield the same spectrum and the choice is often contingent on the presence of accessory peaks of other elements.

2. Spectra from a single mineral which contains the elements found in two or more other separate minerals and vice versa. This problem typically involves a clay mineral. For example, a spectrum containing the elements Mg, Al, Si, Ca, Ti and Fe could indicate the presence of clays such as chlorite or a mixed layer clay of the type illite-montmorillonite. Alternatively, an aggregate of kaolinite ($Al_2Si_2O_5(OH)_4$), which included adsorbed Ti, and a mixed carbonate ($(Mg, Ca, Fe)CO_3$) would produce virtually the same spectrum. To further complicate matters, the same spectrum could result if the aggregate contained the minerals kaolinite (Al, Si), ilmenite (Fe, Ti) and carbonate (Ca, Mg, Fe), obviously, other combinations are also possible.

This group can be expanded to include

7

discrete minerals which contain some amount of surface coatings of another mineral. If the coating is elementally different than the host the spectrum becomes more complicated. If, on the other hand, the coating contains one or more of the same elements as the host the peaks for those elements become disproportionately larger than would be expected.

3. Spectra produced when the spectral resolution of the incident electron beam (approximately 5 microns) is larger than the grain being analyzed, the resulting spectrum would contain peaks for those elements present in the matrix adjacent to the target grain. These matrix-elements may be present either as metal-organics or inorganically combined on an atomic scale within the matrix (Allen and VanderSande, 1983). In either case, they will appear as belonging to the target grain and therefore complicate identification. Typically these spectra also have large brehmstrallungs (backgrounds) indicative of the organic carbon in the coal matrix (Goldstein and Yakowitz, 1975).
4. Spectra from minerals in which extensive diadochy, ion exchange or solid solution are

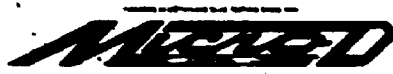
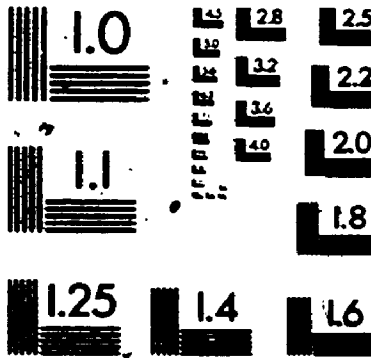
74

common will invariably yield peaks which make identification, based on expected stoichiometry, more difficult. These problems are inherent in mineralogy.

The electronics of EDS can affect the relative peak heights of the elements making it more difficult to determine whether a given element is a major or minor (trace) constituent of the particle. A few of the problems which are a function of the equipment include:

1. Preferential absorption by the Be window employed on most EDS detectors. Absorption of the characteristic x-rays of elements lighter than atomic number 11 (Na) is virtually quantitative, making detection of those elements impossible by conventional EDS methods. Furthermore, adsorption of x-rays emitted by those elements slightly heavier than Na also occurs, decreasing with increasing atomic number. Peaks for those elements are usually smaller than their actual concentrations would predict.
2. Non-counting of signal in the pile-up rejecter is a problem brought about by using too high of a count rate, usually due to an excessive excitation energy for the element in question. When this occurs signals cannot

2



be assigned to a given energy level and so are rejected (not counted), resulting in decreased peak heights for those elements. Unfortunately, it would be impractical to use an optimum excitation energy (1.5-3 times the characteristic energy) for each element as that would mean collecting only the peaks for a given element, or two, in a given spectrum, or analysis.

3. As can be seen by the x-ray continuum (white radiation) there is preferential absorption by the system of x-rays towards the higher end of the spectrum. This translates into smaller peaks than might be expected for some elements.

All of the above electronic aberrations produce peaks which are not representative of the relative abundance of the elements affected. Other problems which affect peak heights of the constituent elements have to do with detector geometry (the spatial relationship of the detector and the sample), degree of polish on the sample surface, cleanliness of the detector window, and etc., these are adequately covered in textbooks dedicated to the subject of SEM/EDS (Goldstein and Yakowitz, 1975).

Suffice to say, there are many problems associated with

identifying minerals based solely on EDS spectra, i.e., EDS is not a tool for determinative mineralogy and that is not ~~let's~~ purpose here. Rather, this work is concerned with the types and assemblages of the elements which can be identified in minute (discrete) particles in coal, leading to a better understanding of the relationships of the elements in the coals.

III.3.2 UTAH: WHOLE COAL

III.3.2.1 INTRODUCTION

The elements detected in discrete mineral particles in pellets of Utah coal using EDS include Mg, Al, Si, S, K, Ca, Ti, Mn, Fe, Sr, Zn, Sn and Ba. The various combinations in which these elements were found are listed in Table III-11, according to mineral designations. Letter designations in Table III-11 (e.g., a, b, etc.) correspond to the letters of the spectra in Figure III-2. All of the elements detected using EDS (excluding Sn for which no independent analysis was attempted) were also found by one of the other analytical techniques discussed in other sections in this work.

The spectra are discussed according to their probable representation of one of the major mineral groups: clays, carbonate, silicate, oxide, sulfide and sulfate.

TABLE III-11

=====

LIST OF ELEMENT ASSEMBLAGES DETECTED BY EDS IN DISCRETE MINERAL PHASES IN PELLETS OF UTAH COAL. THE SAMPLES ARE LISTED ACCORDING TO MINERAL GROUPS. LETTER DESIGNATIONS ("A", ETC.) CORRESPOND TO THE SPECTRA IN FIGURE III-2.

=====

CLAYS

-
- A) Al-Si
 - B) Al-Si-K
 - C) Mg-Al-Si-K-Ti-Fe
 - D) Mg-Al-Si-K-Ti-Mn-Fe
 - E) Mg-Al-Si-Ca-Ti-Fe

SILICATES (OTHER THAN CLAYS)

-
- F) Si
 - G) Si-Zr
 - H) Al-Si-Ga
 - B) Al-Si-K (SAME AS ABOVE)
 - I) Si-Ca-Ti-Fe

CARBONATES

-
- J) Mg-Si-Ca-Fe

OXIDES

-
- K) Ti-Fe
 - L) Al-Si-Ti-Fe
 - M) Al-Si-Sn-Fe

SULFIDES

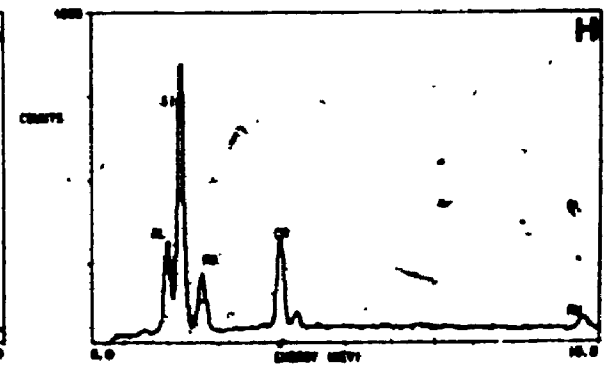
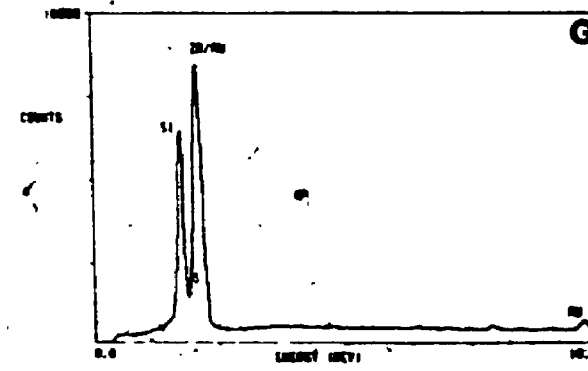
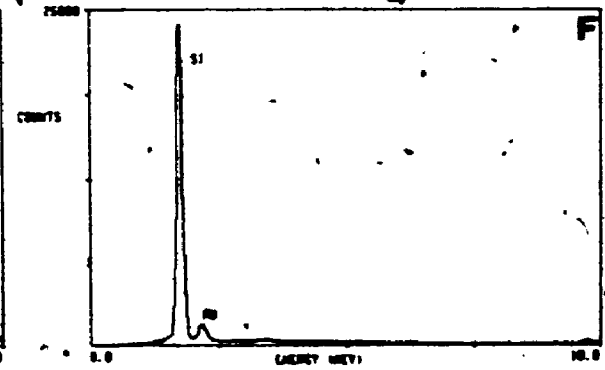
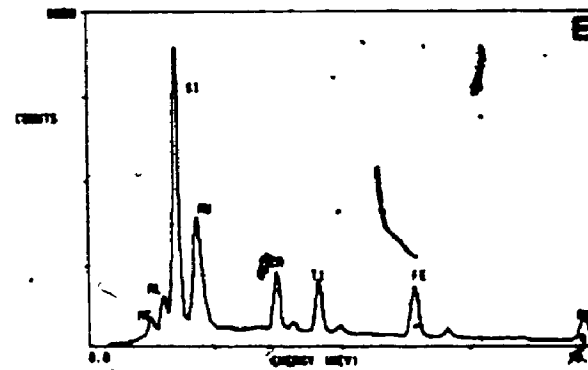
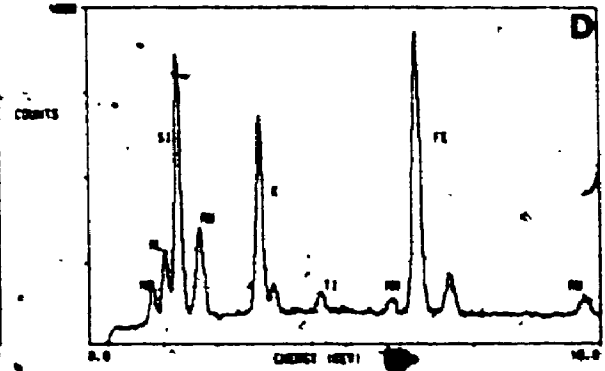
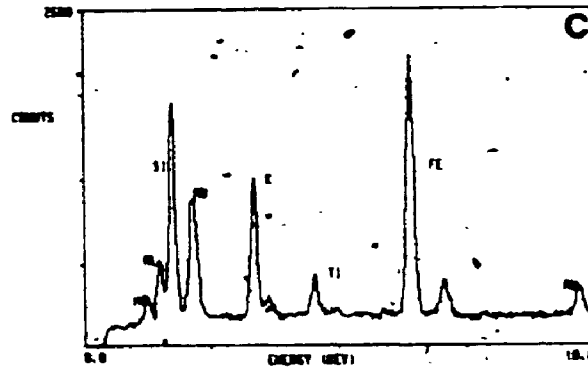
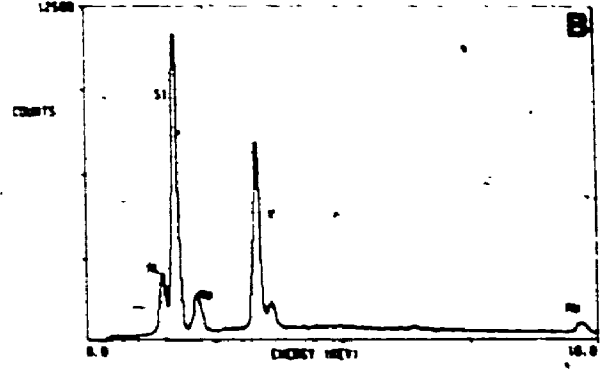
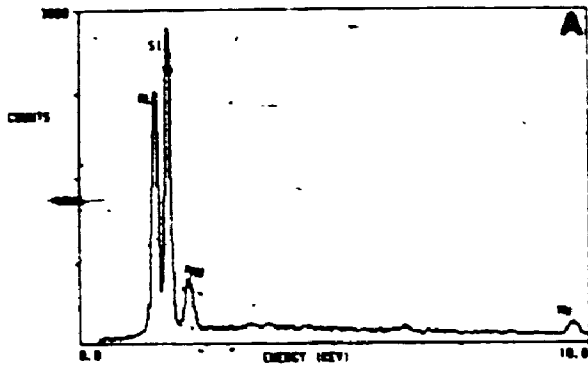
-
- N) S-Fe

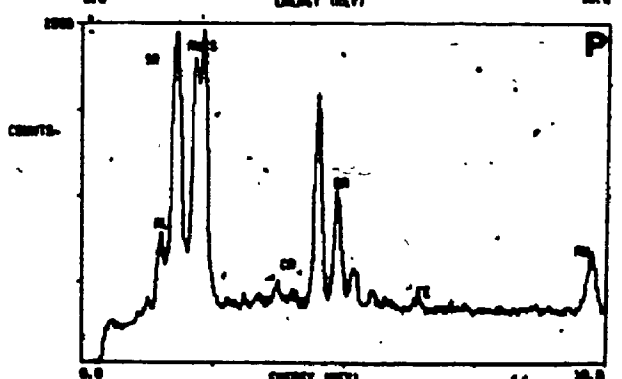
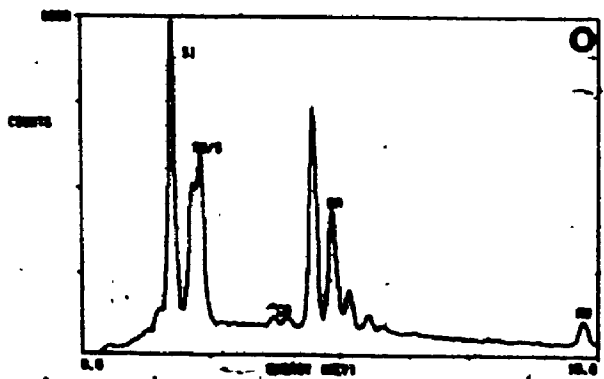
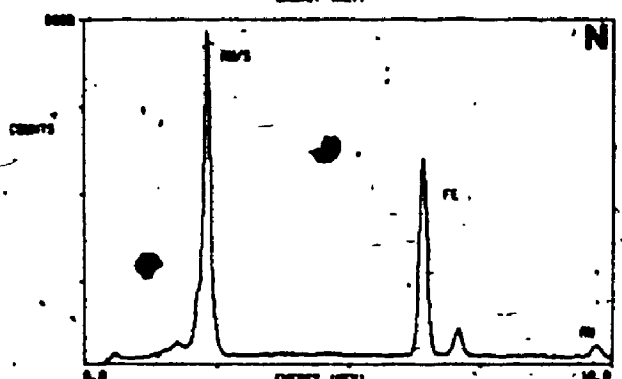
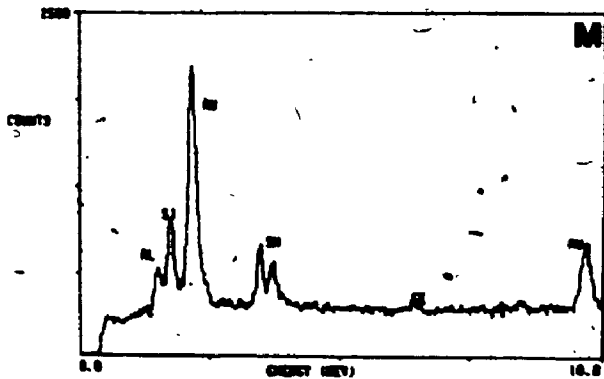
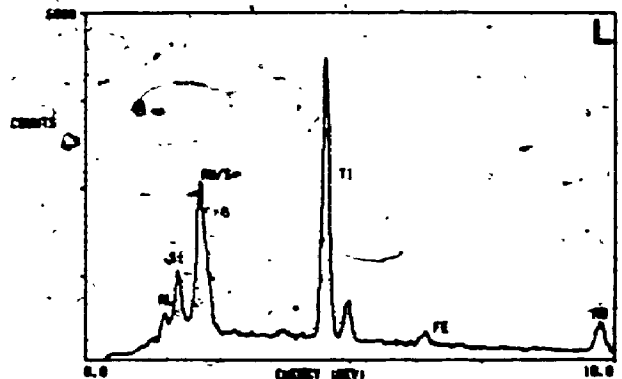
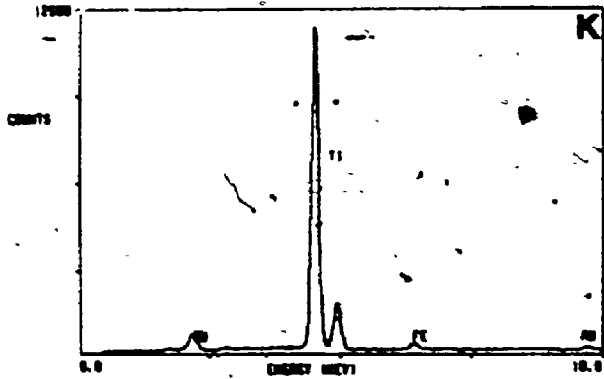
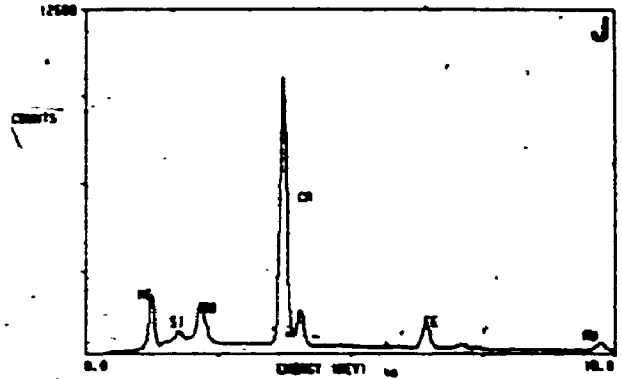
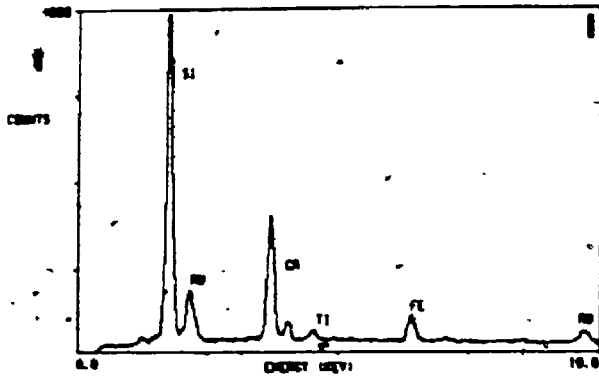
SULFATE

-
- O) Si-S-Ca-Ba
 - P) Al-Sr-S-Ca-Ba-Fe

FIGURE III-2

A TO P - REPRESENTATIVE EDS SPECTRA OF INDIVIDUAL
GRAINS CONTAINED IN WHOLE COAL PELLETS OF UTAH
COAL.





III.3.2.2 CLAYS

Clays are ubiquitous in coals. Typically they are the main inorganic constituent of a coal and may comprise 50% or more of the total mineral matter (Gluskoter, 1975). The formation of clays both from the hydrolysis of aluminosilicates as well as reactions between dissolved alumina and colloidal silica in solutions are well known. Owing to these different origins, clays may be considered as either allogenic or authigenic to the depositional basin. Furthermore, the authigenic fraction may be either syngenetic or epigenetic with regard to both the peatification and coalification processes.

Those spectra interpreted as representing clays are among the most complicated as far as the number of elements are concerned. This is not surprising, considering the wide compositional range of most clays and their high ion-exchange capacity. Data compiled by Kuhn, et al., (1980) on the geochemistry of clays associated with coals from Illinois, The Eastern United States and the Western United States show that for the clays kaolinite, illite, montmorillonite, chlorite and mixed layer clays the major elements included Mg, Al, Si, K, Mn and Fe and the minor constituents numbered 27 and "etc." in varying combinations.

KAOLINITE: The mineral kaolinite is represented in

Figure III-2, A. Kaolinite is the common weathering product of feldspars from acidic (granitic) rocks (Krauskopf, 1967; Brownlow, 1979) and is reported in virtually all mineralogic studies of coals. Figure III-2, A shows the peaks for Al and Si at approximately the same heights which is consistent with the 1:1 ratio of these elements in this mineral. The absence of peaks for other elements is expected given that the composition of kaolinite is normally very close to the ideal formula (Krauskopf, 1967) and its ion-exchange capacity is low (1-10 mEq/100 g) (Brownlow, 1979).

ILLITE: Figure, III-2, B contains the elements Al, Si and K. While these elements make-up the mineral illite they are also constituents in other silicates commonly found in coals (e.g., feldspars). It is unlikely that illite would produce such a "clean" spectrum. The structure of illite is transitional between muscovite and montmorillonite (Krauskopf, 1967) and substitution of Fe^{2+} and Mg^{2+} for Al^{3+} in the octahedral layer can be as high as 33%, however, peaks for these elements are absent in Figure III-2, B. Also, ion-exchange in illite ranges from 10-40 mEq/100g (Brownlow, 1979). These two characteristics would lend themselves to a more complicated element assemblage than shown in Figure III-2, B. However, under the proper conditions of high $[K^+]$ and high $[H^+]$ and lacking the availability of Mg

and Fe, formation of a "pure" illite is possible (this spectrum is also included in the section on Silicates).

MIXED LAYER CLAYS: The spectra in Figures III-2, C and D are believed to represent mixed layer clays of the type illite-montmorillonite. Both spectra have similar ratios of Al:Si (0.18 for C and 0.16 for D), Mg:Al (0.75 for C and 0.67 for D) and K:Fe (0.53 for C and 0.68 for D). Both also contain lesser amounts of Ti and Figure III-2, D contains a small Mn peak. The ratios of illite:montmorillonite in these types of clays can extend from 1:9 to 9:1. Owing to the large K peak in these spectra and the lack of Ca, this clay is probably closer to the 9:1 end with illite predominating over montmorillonite. The peak for Fe is large in both cases. The relatively large concentration of Si relative to Al probably stems from a limited substitution of Al^{3+} for Si^{4+} in the tetrahedral layers and is further enhanced by extensive substitution of Fe^{3+} for Al^{3+} in the octahedral layer. Substitutions of these types can reach 33% and 100% respectively in illite and montmorillonite (Krauskopf, 1967) and could result in spectra as shown. The Ti and Mn in the two spectra probably exist absorbed into the clay lattice. Both illite and montmorillonite allow extensive ion-exchange (Brownlow, 1979).

GLAUCONITE (MONTMORILLONITE): The Spectrum in Figure III-2, E is interpreted as representing glauconite/montmorillonite. The ratio for Al:Si (0.08) is much lower than the other clays and the ratio for Mg:Al (0.50) is slightly lower. The major difference is the presence of Ca. In as much as Fe and Ca are major elements in montmorillonite and because glauconite forms from illite by extensive replacement of Al^{3+} for Fe^{2+} in the octahedral layer accompanied by Ca^{2+} replacing K^+ in the inter layer spaces (Krauskopf, 1967), both interpretations are possible. As with the other clays, the Ti is probably absorbed into the inter layer areas.

III.3.2.3 SILICATES (OTHER THAN CLAYS)

As with the clays the interpretation of EDS spectra for even the more simple silicates is much more tenuous than for some of the other mineral phases. This stems from the extensive variety of silicate minerals, many of which contain the same elements but in varying amounts and structures, two characteristics undetectable by EDS. Once again, the following inferences are based on data collected here as well as in the literature and offer the best explanation possible.

QUARTZ (SILICA): The spectrum in Figure III-2, F

83

contains only the peak for Si and represents one of the members of the silica group, probably quartz. Quartz is ubiquitous in detritus in coals but an authigenic origin cannot be ruled out.

ZIRCON: The spectrum in Figure III-2, G contains peaks for Si and Zr. Zircon is common in many coals as detritus owing to its resistance to mechanical and chemical weathering. In some cases zircon is abundant enough that when annealed during in situ coal fires (burns) they can be used to fix the rate of burning (Herring, 1980).

FELDSPARS: Two types of feldspars, plagioclase and K-feldspar, are represented by the spectra in Figures III-2, H and III-2, B respectively (note: an alternative interpretation for B is given in the section on clays). Feldspars have been reported in coals from varied locations (Kuhn, 1980). They are among the most common of the silicate minerals in both igneous and sedimentary rocks of the earth's crust and therefore are present as detritus in coals. In addition, authigenic feldspars were reported as early as the 1860's by both Rose (1865) and Drain (1861) (as cited in Kastner, 1971) and this origin is also possible in coals. Assuming that these two spectra belong to feldspars is complicated by a number of

things. The ratios of Al:Si (0.24 for H and 0.13 for B), for example, are very different than would be expected, 1:1 in the case of plagioclase and 1:3 in the case of potassium feldspar, even with considerable preferential absorption (by the Be window of the detector) of Al relative to Si. An alternative explanation for the spectrum in Figure III-2, B is given in the section on clays but considering the "clean" nature of the spectrum it is most likely a simple K-aluminosilicate. An alternative for the spectrum in Figure III-2, H might be a Ca member of the garnet group, e.g., grossularite ($\text{Ca}_3\text{Al}_2(\text{SiO}_4)_3$). Garnets are resistant to weathering and are common detrital constituents in sediments.

Si-Ca-Ti-Fe: The spectrum in Figure III-2, I shows peaks for Si, Ca, Ti and Fe, a common assemblage in the silicate minerals. The field is narrowed somewhat by the absence of an Al peak. This mineral could be a member of a number of different silicate groups, e.g., pyroxene (augite, $\text{CaFe}(\text{Al},\text{Si})_2\text{O}_6$), garnet (andradite, $\text{Ca}_3\text{Fe}_2(\text{SiO}_4)_3$) or sphene (CaTiSiO_5), and there are others.

III.3.2.4 CARBONATES (FE/MG-CALCITE)

Carbonates are a common mineral phase associated with coals

(Rao and Gluskoter, 1976). The large crustal abundance of the metals Ca, Mg and Fe and their complete diadochy in the carbonate phase (solid solution) accounts for the extreme variability of carbonate minerals in coals from different areas. Gluskoter (1975, and references within) notes that the most common carbonates associated with coals are dolomite and ankerite but that the occurrence of pure calcite and siderite are not unusual. Furthermore, the predominance of one carbonate over another is often a function of location.

The spectrum representing carbonates is shown in Figures III-2, J. Typically Ca is the major element present and is usually accompanied, in varying degrees, by Mg and/or Fe. The peaks for C and O (from the CO₂) are not detectable by EDS. This, and the fact that no other peaks for anions (e.g., S or P) are present are evidence for assigning these spectra to the carbonates, probably calcite with minor Mg and Fe. However, Ca-oxalate (and other oxides of Ca) has been reported in modern peats (Bardin and Bish, 1983). There is a possibility that some of the Mg and Fe in these spectra are present as oxides (goethite, or brucite). Goethite (FeOOH), for example, is a common constituent in some coals as the end product of pyrite weathering (Huggins, et al, 1983). However, the fact that the peaks for Mg and Fe are almost always present in minor amounts with the Ca, and in such varying amounts, leads to the conclusion that they are

part of the carbonate fraction.

III.3.2.5 OXIDES

Oxides and hydroxides are common constituents in both fresh and weathered coals (Kuhn, et.al., 1980; Huggins, et.al., 1983). The three spectra in Figures III-2, K, L and M, and are believed to represent, at least in part, the presence of rutile group minerals of Ti and Sn.

Ti-DIOXIDE (RUTILE): Titanium is the major constituent of spectra in Figures III-2, K and L. In the case of Figure III-2, L no other peaks (save a small Fe peak) are present, and so it probably represents one of the TiO_2 minerals, e.g., rutile. The Fe is probably bound in the rutile which is known to incorporate as much as 11% Fe_2O_3 (Berry and Mason, 1959). The spectrum in Figure III-2, L is slightly more complicated, containing peaks for Al and Si in addition to those for Ti and Fe. While Ti is commonly associated with clays (absorbed) it is unlikely that Ti would yield such a large peak under these conditions and hence, this spectrum also represents a TiO_2 mineral and the Al and Si are most likely present as clay. This does not preclude that some of the Ti is not also present in the clay.

CASSITERITE: The spectrum in Figure III-2, M contains peaks for the element Sn along with those for Al, Si and Fe. This was the only spectra to yield a Sn peak. Nonetheless, Sn was reported as early as 1935 by V.M. Goldschmidt (1935) in coal ashes at concentrations 10 times that of crustal abundance. Most probably this spectra represents the mineral cassiterite which is a common detrital resistate. Alternatively, it may represent a clay with abundant adsorbed Sn, both are common in the sedimentary environment (Rankama and Sahama, 1950).

III.3.2.6 SULFIDES (PYRITE/MARCASITE)

Sulfides are a common constituent of the mineral matter in coal and, mainly for environmental reasons, are the most studied. While the dimorphs of Fe-sulfide, pyrite and marcasite, are the most common sulfides found in coals, galena (PbS), and sphalerite (ZnS) have also been found in substantial amounts (Gluskoter, 1975; Kuhn, 1980). Sulfides in coal owe their existence to both chemical (by the decay of organic matter) and microbial reduction of sulfate in the presence of chalcophile elements.

Pyrite/marcasite was the only sulfide mineral detected in these coals and is represented by the spectrum in Figure III-2, N. Of the many particles which yielded spectra

identical to that shown, none contained spectral lines for any of the other elements which are typically found in sulfides (e.g., Pb, Zn, Cd, etc.). Presumably, these elements were either absent during the time of formation of these sulfides or are present at concentrations too small to be detected by EDS (approximately 0.1%).

III.3.2.7 SULFATES

Sulfates are the common product of the oxidation of sulfides in coals exposed to weathering but also have been reported in fresh (unweathered) coals (Allen and VanderSande, 1983). Discussion of the formation of the more common Fe-sulfates (not detected in the coal pellets) and related secondary minerals in pyrite nodules associated with these coals is covered in Chapter IV. The sulfates detected in pellets of whole coal contained the elements Ba and Sr. Barium and Sr are a geochemically coherent pair and are among the more abundant trace elements found in sedimentary rocks. Typically they are transported as sulfate in the weathering solutions of igneous rocks and readily form the sulfates barite (BaSO₄) and celestite (SrSO₄).

BARITE: Figure III-2, O contains the peaks for Si, S, Ca and Ba. Owing to the predominance of Ba over Ca and the substantial S peak, this spectrum probably represents the mineral barite, a common constituent in

coals (Kuhn, 1980). The Ca in this spectrum is probably contained in the barite (Berry and Mason, 1959). The size of the Si peak implies that a grain of silica was contacted by the x-ray beam (possibly below or adjacent to the barite). This would seem the only source for the Si considering that there are no Ba-silicates which could produce this pattern.

BARITE/CELESTITE: The spectrum in Figure III-2, P is interpreted as a Ba/Sr-sulfate. In as much as a solid solution series exists between Ba and Sr in the sulfate phase and because both are represented by major peaks it is difficult to assign a name. It should be noted that there may be an appreciable amount of Si represented in the Sr peak as these elements overlap in EDS analyses. If this is the case the Si is likely to be combined with the Al as clay which also incorporates the tiny bit of Fe shown. The Ca of this spectrum is probably replacing Sr in the sulfate.

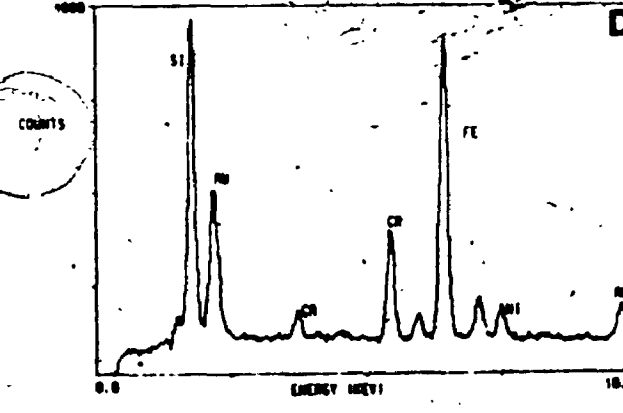
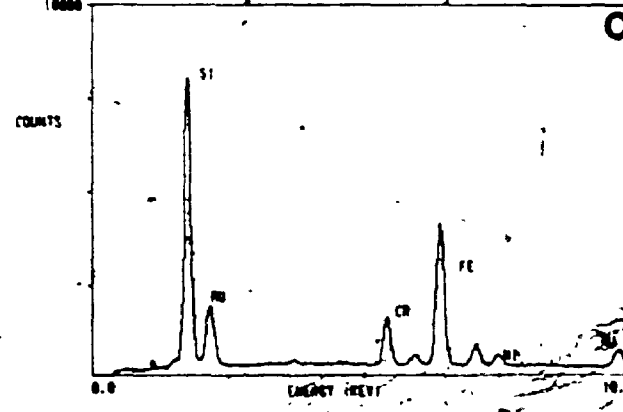
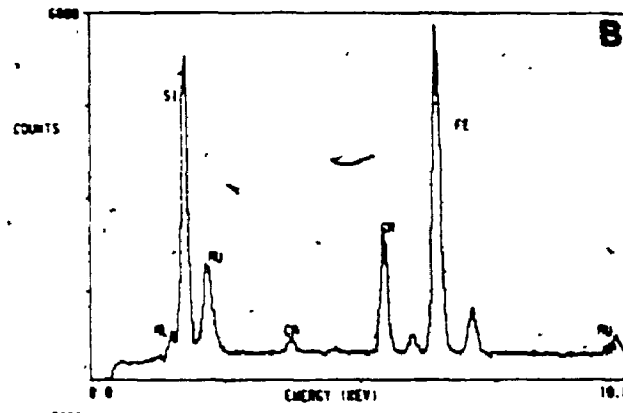
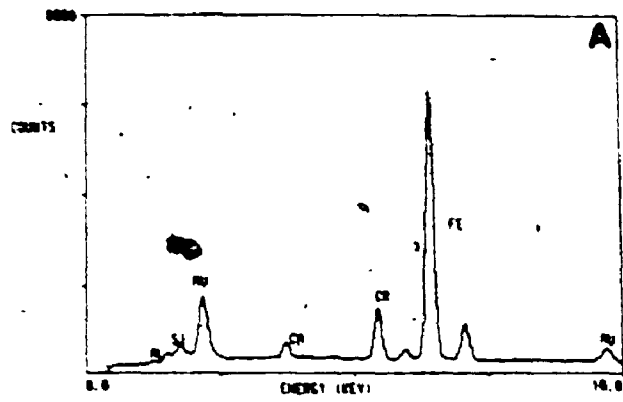
III.3.3 WYOMING: WHOLE COAL

III.3.3.1 INTRODUCTION

Spectra identified as quartz, pyrite/marcasite, Ba-sulfate and Ti-oxide were noted in the Wyoming coal pellets. The interpretation of these spectra are the same as for the Utah

FIGURE III-3

A TO D - REPRESENTATIVE EDS SPECTRA OF INDIVIDUAL
GRAINS CONTAINED IN WHOLE COAL PELLETS OF WYOMING COALS.



samples and so are not repeated here. Spectra unique to the Wyoming samples are shown in Figure III-3, A-D: "A" and "B" are similar in their elemental assemblages, as are "C" and "D", but within each set there are noticeable differences.

Virtually all of the EDS analyses of the Wyoming coal share in common the presence of Al, Si and Ca. Furthermore, the relative abundances (peak heights) for these three elements appear to be related. However, no spectrum contained only those elements, i.e., they are always present with other elements but in lesser amounts. This would suggest that they are present either in the matrix (atomically and/or organically bound) or as coatings attached to the surfaces of mineral grains. Evidence for the former was noted during analyses of "clean" coal matrix, all of those spectra contained Al, Si and Ca. The fact that the amounts of these elements vary in the spectra shown in Figure III-3 is probably a function of the amount of the incident electron beam that contacted the matrix adjacent to the target grain. Where Si is represented as a major peak it is due to the presence of a Si mineral rather than the above explanation.

III.3.3.2 INTERPRETATION

The spectra in Figure III-3, A and B contain the elements Al, Si, Ca, Cr and Fe. The probable origin of the Al, Si and Ca in these analyses is discussed above. However, the major

difference between these two spectra is the large Si peak in Figure III-3, B. Assuming that the Al, Si and Ca in Figure III-3, A are contained in the matrix, only Cr and Fe result from the target grain. This would indicate the presence of an Fe/Cr-oxide (e.g., chromite).

The Si in Figure III-3, B is present either as quartz, intimately related with the Fe/Cr-oxide, or as Fe/Cr-silicate. In the later case, an Fe-silicate with Cr^{3+} replacing Fe^{3+} (a common diadochy) offers the best explanation.

The Spectra in Figure III-3, C and D contain the elements Al, Si, Ca, Cr, Fe and Ni (the Al is not labeled in "D" and the Ca is not labeled in "C", both are very small). Unlike the spectra in Figure III-3, A and B, Si was always present as a major constituent with Cr, Fe and Ni, indicating that the presence of Ni is tied to the presence of Si. Rankama and Sahama (1950) note that Ni-silicates are common in some peats. Considering this source, the formation of Cr/Fe/Ni-silicates is likely. Chrome, Fe and Ni were never observed alone but the presence of Cr/Fe/Ni-oxide plus quartz cannot be ruled out.

III.3.3.3 SUMMARY

The Wyoming coal studied here contains approximately half as

such ash as the Utah coal. Accordingly, the number of mineral particles observed in the surfaces of the pellets of Wyoming coal was substantially lower. It follows that there is much less chance of finding particles which are truly representative of the mineral constituents within the Wyoming coal. One example which illustrates this problem is that no Mg was detected in any of the discrete grains analyzed in the Wyoming samples even though the concentration of Mg in the Utah coal (avg. 0.15%) and the Wyoming coal (avg. 0.14%) is similar. Magnesium (along with Al, Si and Ca) was, however, detected as a constituent in analyses of the matrix, i.e., "clean" coal. Possible explanations for this include (1) no Mg-clays (or other silicates, carbonates, etc.) are present (2) if Mg-minerals are present they are too small and evenly distributed within the matrix to be detected (imaged) (3) the Mg is contained predominately in metal-organic complexes within the matrix (highly unlikely) (4) other pellets, not analyzed, contain the majority of the Mg-minerals suggesting localized concentrations. This last possibility, (4), is consistent with other observations, e.g., spectra containing Cr and Fe were not detected in the same samples as those containing Cr, Fe and Ni. The Cr and Fe are obviously more widespread in the Wyoming coals while the Ni is more locally concentrated. This may also be the case for Mg. Unfortunately, all the samples could not be analyzed by this method and so this question remains unanswered based on EDS

analyses.

The ubiquitous nature of Al, Si, and Ca (Mg to a lesser degree) in the Wyoming coals, but never as discrete particles, leads one to believe that clays are present but that they are too small to be imaged. The fact that no physical separation (partings or lenses) of detritus was noted anywhere within the seam from where the Wyoming samples were collected would support this observation, indicating that the clays are probably authigenic in origin.

Other common mineral phases detected in the Utah coal (e.g., carbonates, simple silicates, etc.) were not found in the Wyoming samples. One major reason for this could be the difference in depositional settings between the coals. The Utah coal received periodic incursions of marine water alternating with deltaic detritus in a near shore environment. The Wyoming coal accumulated in a more quiescent fluvio-lacustrine setting where sediment (e.g., overbank splay, etc.) may have been excluded by vegetation which "protected" the peatlands.

III.3.4 UTAH: FE-SULFIDE NODULES

III.3.4.1 INTRODUCTION

Iron sulfide nodules associated with the Utah coals were

28

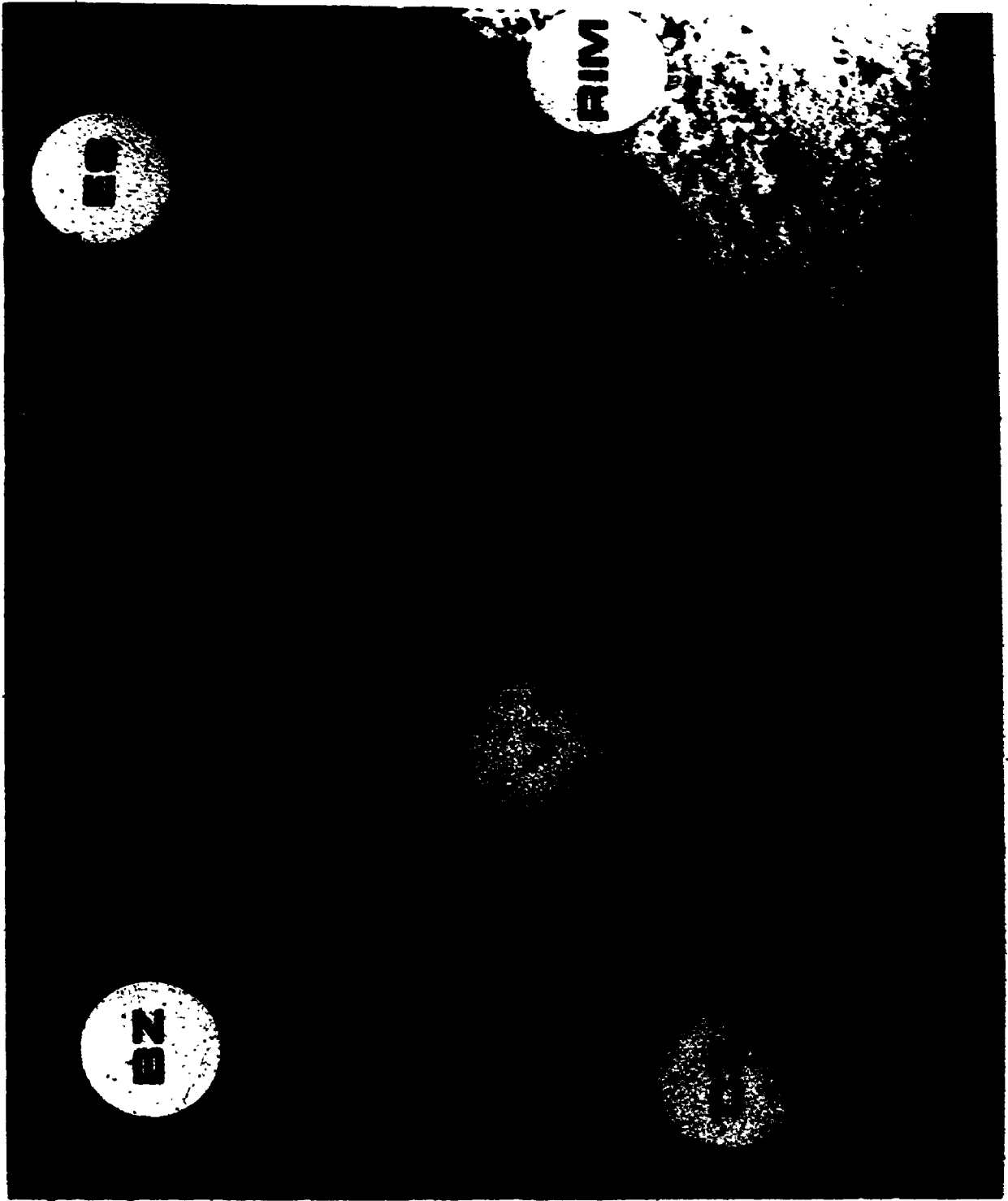
FIGURE III-4

PHOTOMICROGRAPH OF THE EDGE OF ONE OF THE FE-SULFIDE NODULES FOUND IN THE UTAH COAL. THREE DISTINCT AREAS ARE SHOWN.

LOWER RIGHT - SHOWS THE EDGE (RIM) OF THE NODULE.

LOWER LEFT TO UPPER RIGHT - SHOWS THE "COALY" ZONE (CZ) WITH VEINLETS (V).

UPPER LEFT - SHOWS THE BEGINNING OF THE BANDED ZONE (BZ) WHICH IS SEPARATED FROM THE "COALY" ZONE BY WHAT APPEARS TO BE AN EROSIONAL SURFACE (ES).



collected at various locations from within the mine. The nodules were present throughout the extent of the mine and did not appear to be related, i.e., in zones (layers) or adjacent to other types of structures, e.g., partings or lenses of detritus. The nodules varied in size and were generally tear-drop shaped. Those nodules collected ranged in size from 1-5 cm in length and 1-3 cm in width but much larger and smaller nodules were noted. The nodules were cut (water lubricated saw) and flat ground (9 micron hard diamond lap with water lubricant). Scanning Electron Microscopy (SEM) and Energy Dispersive Spectroscopy (EDS) were used to observe the structure of the nodules and adjacent areas and to characterize the chemical and spatial relationships of the constituent minerals. Three different areas were observed based on textural relationships and mineralogy. These relationships give evidence for origin and time of emplacement. Figure III-4 shows the three areas in question which consist of the nodule (lower right), a "coaly" zone including veinlets radiating away from the surface of the nodule (lower left to upper right) and a finely banded zone (upper left).

III.3.4.2 MINERALOGY AND GEOCHEMISTRY

The internal structure of the nodules is shown in Figures III-5, A and B. The parallel and arcuate arrangement of cells in the nodule (Figure III-5, A) are indicative of a

FIGURE III-5

A - PHOTOMICROGRAPH OF THE INTERNAL AREA OF THE FE-SULFIDE NODULES FROM THE UTAH COALS. THE PARALLEL AND ARCUATE NATURE OF THE CELLULAR STRUCTURES INDICATES A BIOLOGIC PRECURSOR.

B - PHOTOMICROGRAPH OF SOME OF THE CELLS IN "A". CELLS APPEAR OVATE OWING TO THE ORIENTATION OF THE SECTION. CELL INFILLING IS FE-SULFIDE. NOTE THAT CELL WALLS ARE NOT DISTORTED IMPLYING THAT THE CELL FILLINGS WERE EMPLACED PRIOR TO COMPACTION (COALIFICATION).

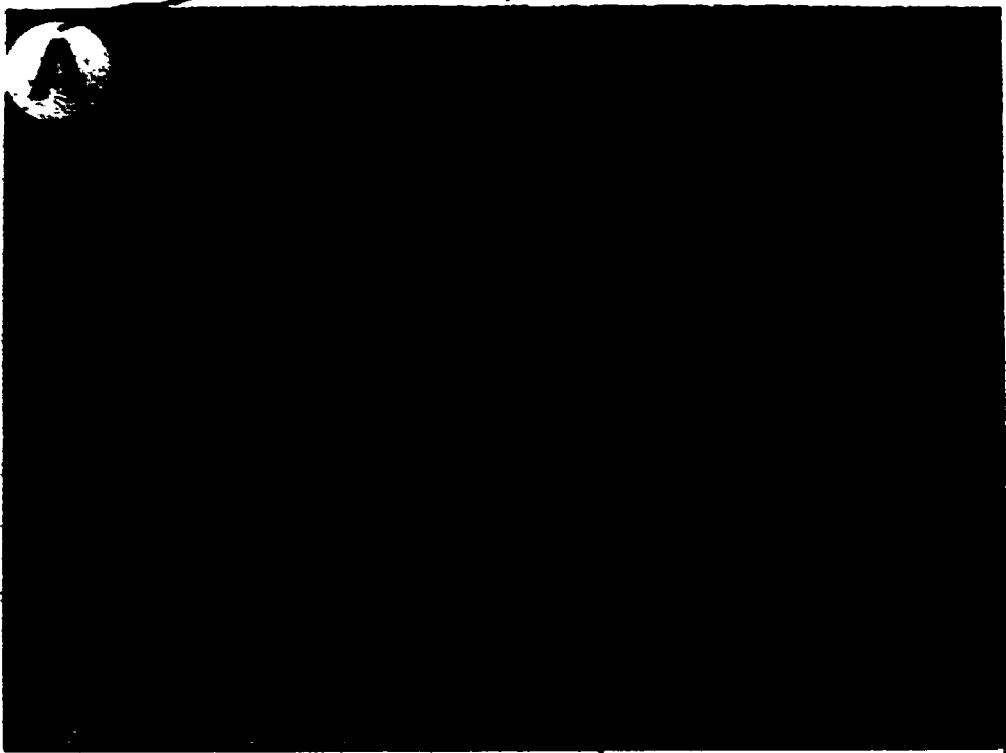


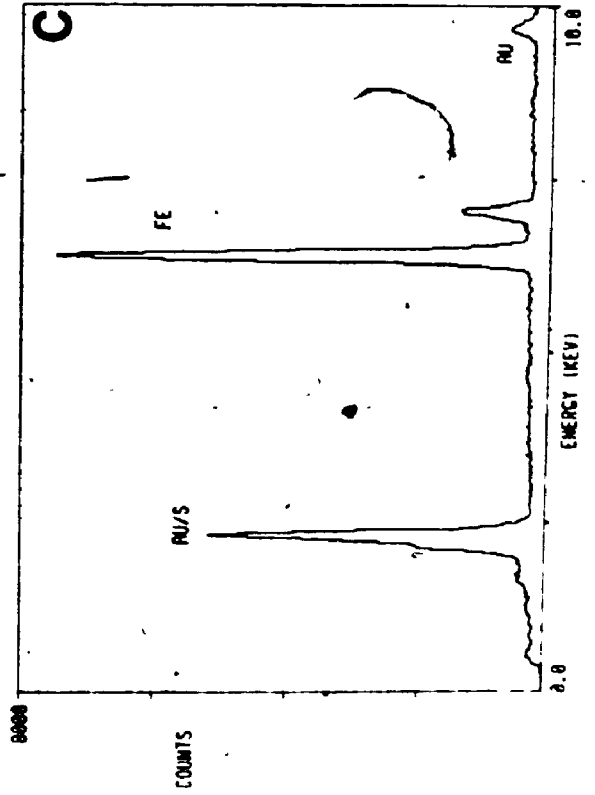
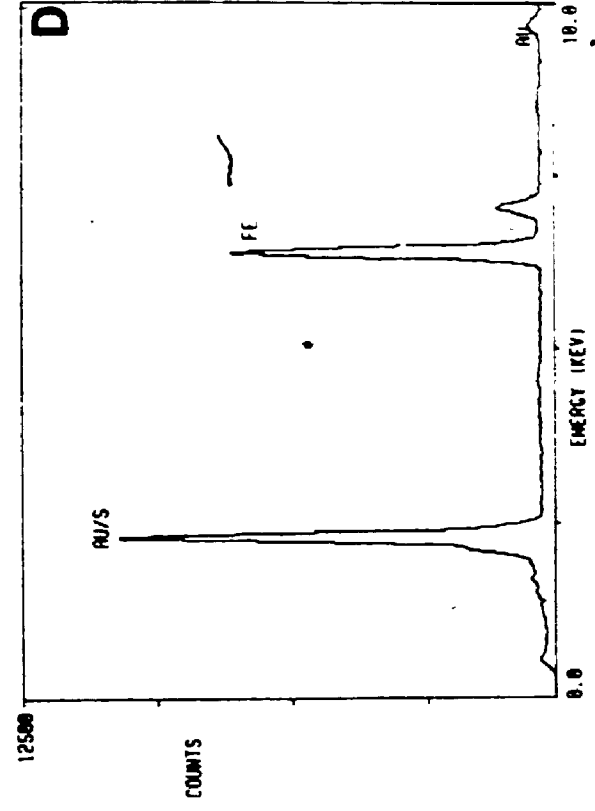
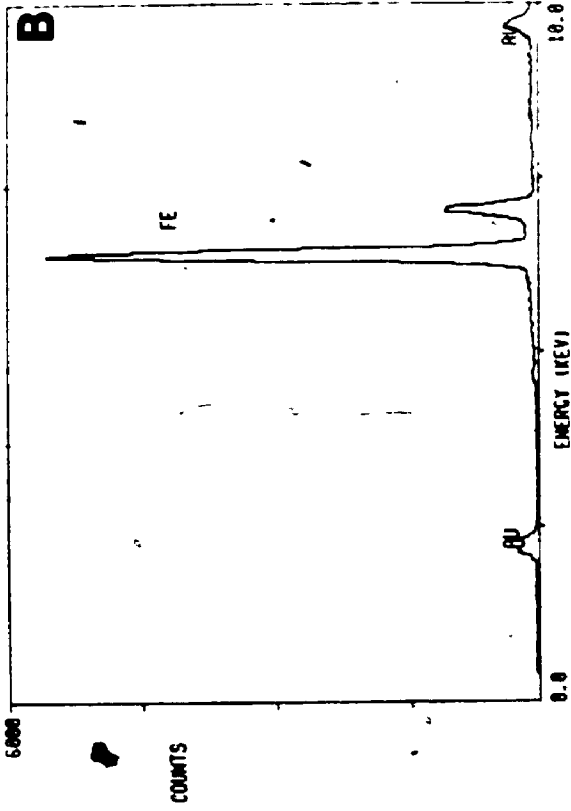
FIGURE III-6

A - PHOTOMICROGRAPH OF A BRECCIATED VEINLET FROM WITHIN THE "COALY" ZONE OF THE FE-SULFIDE NODULES IN THE UTAH COALS.

B - EDS SPECTRUM FROM THE GRAIN AT THE FAR RIGHT OF THE PHOTOMICROGRAPH (b'). ONLY FE IS SHOWN, INDICATING AN OXIDE OR CARBONATE PHASE.

C - EDS SPECTRUM FROM THE GRAIN IN THE CENTRAL PART OF THE PHOTOMICROGRAPH (c'). THE PREDOMINANCE OF S RELATIVE TO FE INDICATES FE-SULFIDE.

D - EDS OF THE MATRIX (CEMENT) ADJACENT TO THE CENTRAL GRAIN (d'). THE PREDOMINANCE OF FE OVER S INDICATES FE-SULFATE.



biologic precursor. Close examination of the cells (Figure III-5, B) shows there has been little distortion of the cell walls. This would indicate that the cell infillings were emplaced prior to coalification (compaction). As shown by EDS the cell infilling is Fe-sulfide (pyrite/marcasite). Some isolated occurrences of Ca-Sulfate (gypsum) and Ca-carbonate (calcite) were also noted within the interior of the nodules.

The area immediately adjacent to the nodules consists mainly of coal which has been cut (fractured) by veinlets. The larger veinlets radiate away from the nodule while smaller veinlets can be seen running parallel the surface of the nodule. In some places the veinlets appear brecciated as shown by the angular shapes of the grains in Figure III-6, A. The chemistries of the individual fragments vary. EDS (Figure III-6, B) of the large grain at the far right of the photomicrograph in Figure III-6, A shows only the presence of Fe. The unusually flat nature of the left side of the spectrum collected on this grain (0-4 Kev range) is suspicious and appears to have been artificially suppressed (possibly by the electronics). However, multiple analyses from within this grain and at varying detector geometries yielded essentially identical results and this phenomenon was not experienced in the spectra collected on adjacent grains, therefore, the analysis shown is considered real. This grain is interpreted as being either an Fe-

oxide/hydroxide or Fe-carbonate, the oxide seems most likely. The ratio of Fe:S in the spectrum (Figure III-6, C) collected from the grain in the central part of the photomicrograph in Figure III-6, A indicates that it is an Fe-sulfate while analyses of the matrix (cement ?) between the grains (Figure III-6, D) shows S predominating over Fe, indicating the presence of Fe-sulfide. Close proximity of these phases has also been reported on an atomic scale from Transmission Electron Microscopy of coals (Allen and VanderSande, 1983). Furthermore, this relationship is common when sulfides begin to oxidize to sulfates (Huggins, et.al, 1983). It is believed that the veinlets represent precipitation of Fe-sulfide in shrinkage cracks formed during coalification.

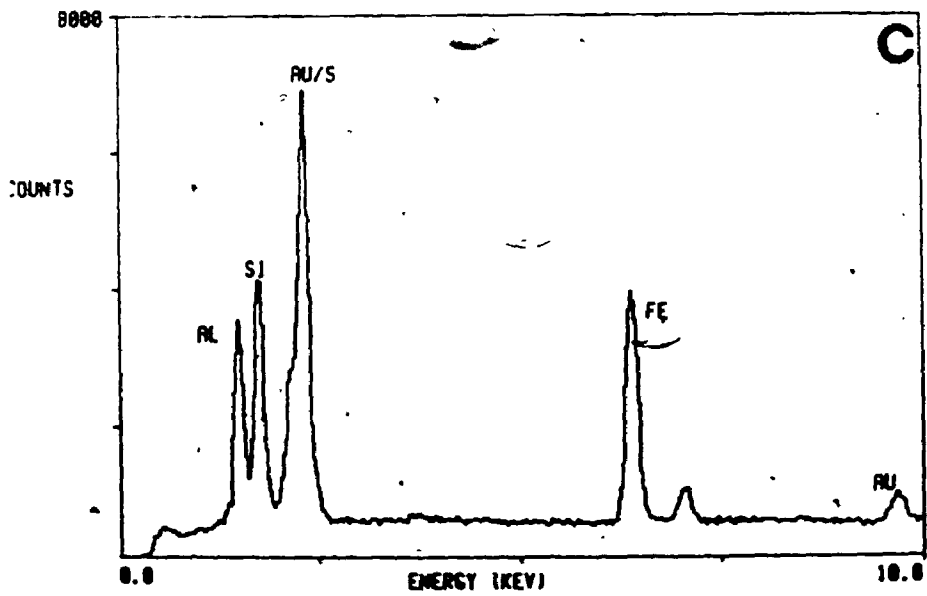
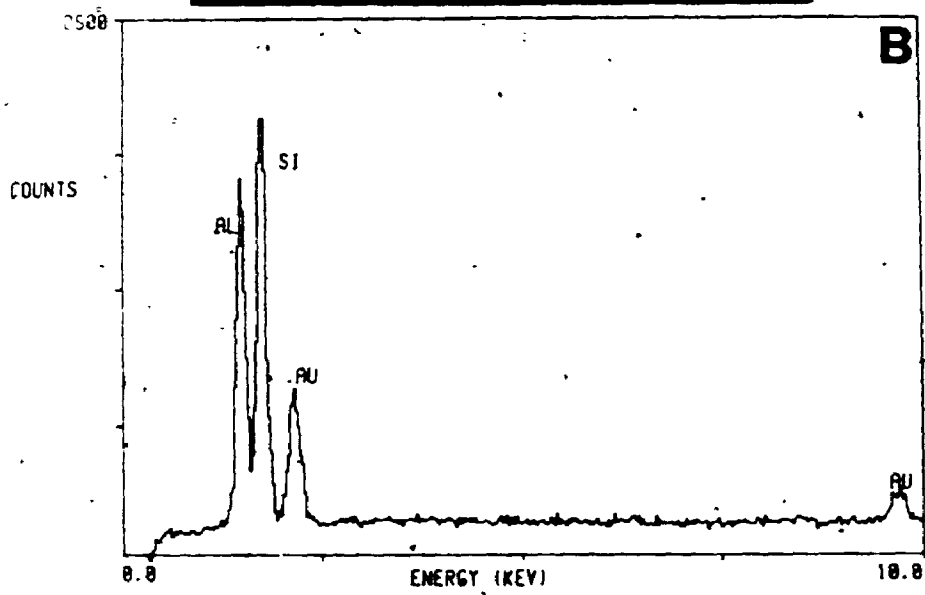
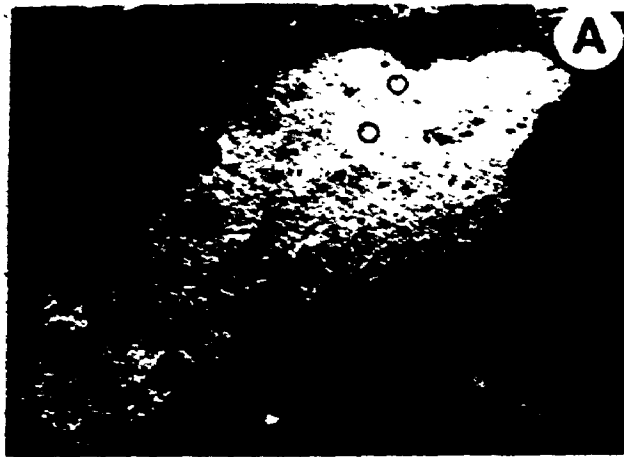
Within this "coaly" area, Fe-sulfide also occurs as isolated spherical masses confined mainly to the periphery of the nodules. These masses appear to be aggregates and presumably represent coalescing crystallites, indicating that precipitation of this material was less vigorous than for the more massive cellular fillings within the nodule. The spherical form suggests emplacement while the matrix (humus) was still soft enough for growth to occur, possibly penecontemporaneous with the cell infillings. The distribution of these isolated spheres around the edge of the nodule are evidence for the simultaneous development of separate but similar microchemical environments.

FIGURE III-7

A - PHOTOMICROGRAPH OF A CLAY BLEB FROM WITHIN THE "COALY" ZONE ADJACENT TO THE FE-SULFIDE NODULES. CIRCLES ENCLOSE FE-SULFIDE GRAINS WITHIN THE CLAY.

B - EDS SPECTRUM FROM THE CLAY BLEB SHOWN IN "A". THE PEAKS FOR AL AND SI INDICATE THE PRESENCE OF KAOLINITE.

C - EDS SPECTRUM FROM THE FE-SULFIDE CRYSTALS CONTAINED IN THE CLAY BLEB (CIRCLES IN "A"). THE PEAKS FOR S AND FE ARE FROM THE FE-SULFIDE, WHILE THE PEAKS FOR AL, AND SI ARE FROM THE CLAY MATRIX.



Clays observed in the "coaly" zone are shown in Figure III-7, A. The clays occur as isolated, shapeless blebs and are not related to the veinlets of Fe-sulfide. As indicated by EDS (Figure III-7, B) the clay is kaolinite. Small subhedra of Fe-sulfide were detected within the clay blebs (arrows in Figure III-7, A and accompanying spectrum in Figure III-7, C). There is no textural relationship (e.g., within banding or partings) between the clay and surrounding coal matrix to indicate the time of emplacement, however, the irregular shape of the clays may indicate an authigenic origin, i.e., while the humus was still soft. The subhedral form of the included Fe-sulfides would also favour this time of emplacement.

The "coaly" zone and veinlets end abruptly at what appears to be an erosional surface (Figure III-4): there is no other evidence to support the idea that the surface is erosional in nature. Across this boundary the coal becomes more or less regularly banded with carbonate (Figure III-8, A) but within a few mm of the contact the bands become crenulated (Figure III-8, B) and the mineralogy changes.

The relatively smooth banding adjacent to the contact consists mostly of alternating layers of Ca-carbonate (calcite) and coal with the occasional occurrence of clay and Fe-sulfide confined to the edges of the carbonate. The

011

FIGURE III-8

A - PHOTOMICROGRAPH OF THE BANDED ZONE CLOSEST TO THE FE-SULFIDE NODULE. LIGHT AREAS ARE PREDOMINATELY CALCITE (CAL), DARK AREAS ARE THE COAL MATRIX.

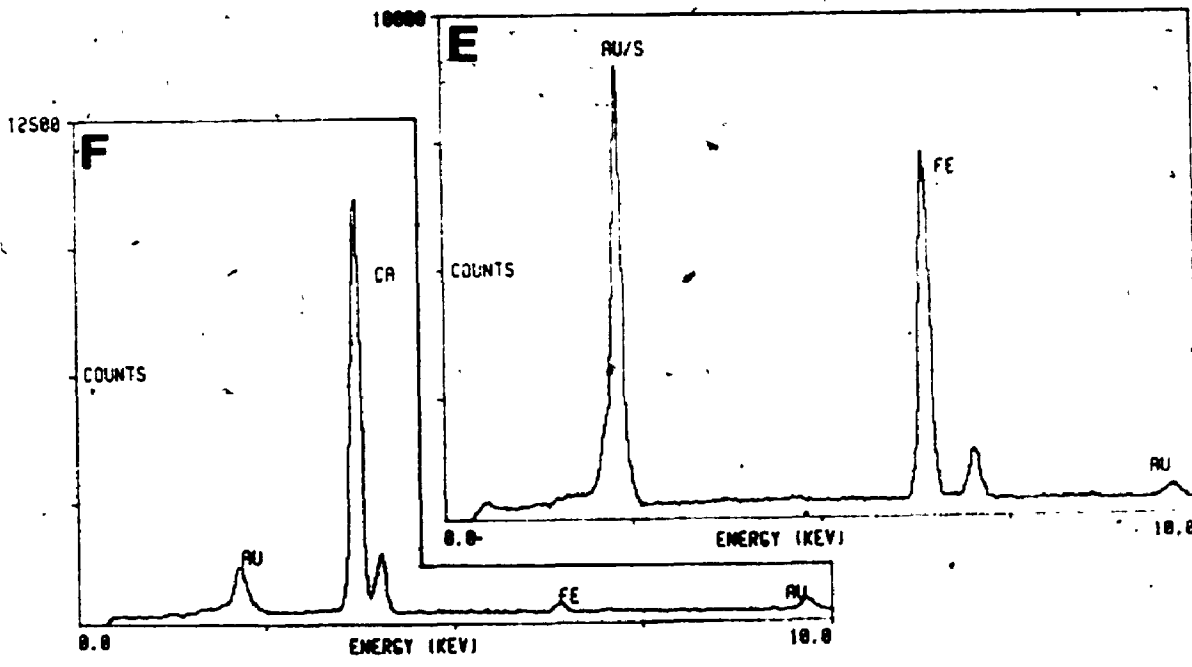
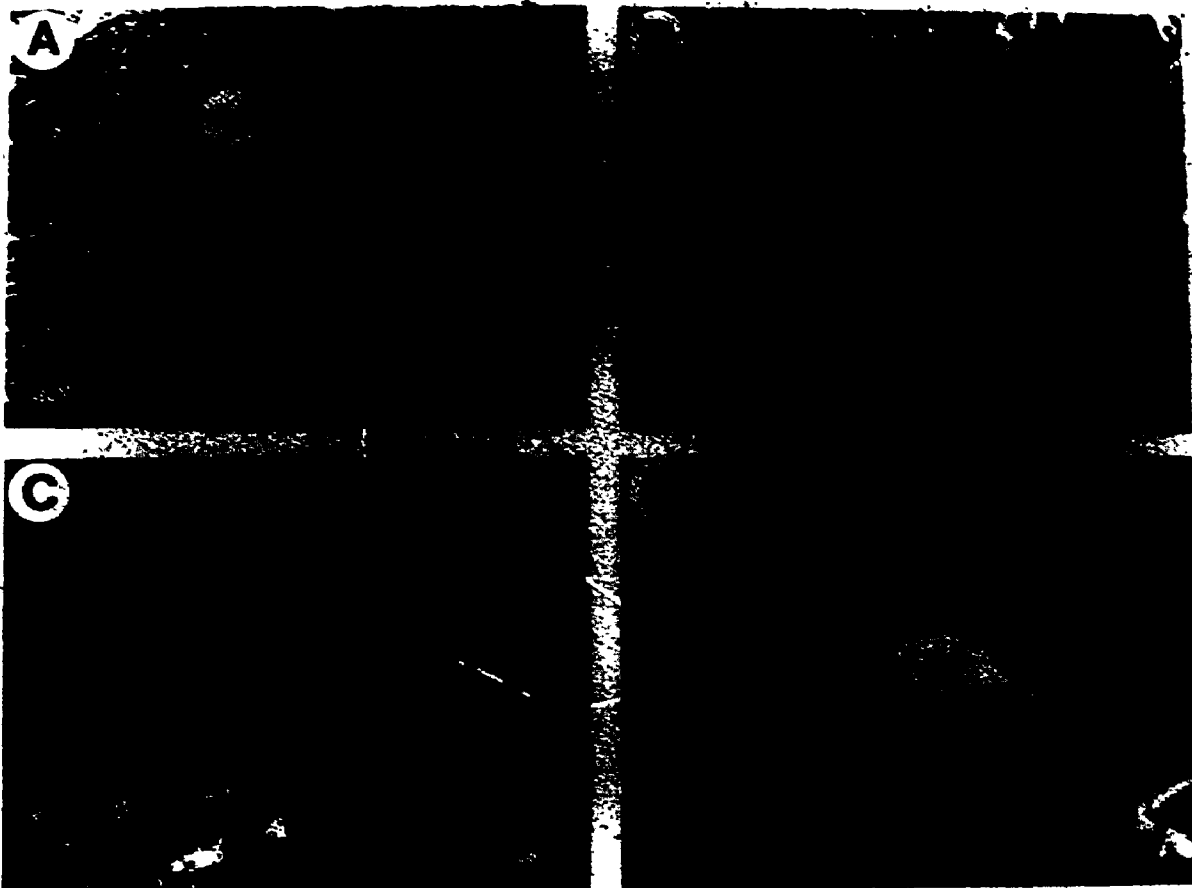
B - PHOTOMICROGRAPH OF THE BANDED ZONE FARTHER FROM THE FE-SULFIDE NODULE THAN THE BANDING SHOWN IN "A". THE LIGHTEST AREAS ARE FE-SULFIDE (PYT), THE LESS LIGHT AREAS ARE CALCITE (CAL) AND THE DARK AREAS ARE COAL.

C - PHOTOMICROGRAPH SHOWING THE MICRO-FAULTS DEVELOPED IN THE COAL BANDS (DARK AREAS) WITHIN THE BANDED ZONE ("A" AND "B"). THE MICRO-FAULT IS FILLED WITH CALCITE (CAL), FE-SULFIDE (PYT) IS ALSO SHOWN IN ADJACENT FRACTURES.

D - PHOTOMICROGRAPH OF A CALCITE RHOMBUS (CAL) WITHIN ONE OF THE CALCITE LAYERS FROM THE BANDED ZONE ("A"). THE DARK AREA IS COAL.

E - TYPICAL EDS SPECTRUM FROM ANY OF THE FE-SULFIDE SHOWN IN "B" AND "C".

F - TYPICAL EDS SPECTRUM FROM ANY OF THE CALCITE SHOWN IN "A", "B", "C" AND "D".



porous nature of the carbonate in this area suggests that precipitation was incomplete during the time of emplacement and/or that subsequent dissolution has occurred. In places micro-faults in the coal layers are filled with Ca-carbonate indicating that the coal was brittle at the time of deposition (Figure III-8, C). The material within these breaks may have originated in the pores that now exist in the adjacent layers. In other places discrete rhombuses of calcite were observed within pores in the carbonate layers (Figure III-8, D). One would not think that the supersaturation needed to initiate precipitation of a new crystal in the presence of a host mineral of the same chemistry could be attained and this might very well be a cleavage fragment trapped in the pore during grinding. A representative spectrum of the various forms of calcite discussed is shown in Figure III-8, F.

As the banding becomes more distorted (Figure III-8, B) the presence of Fe-sulfide increases. Since Fe-sulfide is competent enough to preserve plant morphology (as casts) in coals (Kronberg et al., 1987), its presence in the distorted bands is considered as evidence for precipitation after the banding became crenulated, possibly while the carbonate was being dissolved. The form of the Fe-sulfide in this area, as irregular masses rather than thin distorted bands, would also indicate precipitation after distortion. The spectrum in Figure III-8, E is representative of the

sulfides throughout this area.

III.3.4.3 SUMMARY

The foregoing textural relationships taken together indicate, in some ways, the relative times of emplacement of the mineral phases associated with the nodules and more precisely, individual events:

- (1) Infilling of the cellular structure with Fe-sulfide during the early stages of peatification/coalification (prior to compaction) resulting in their preservation: simultaneous growth of the spherical masses of Fe-sulfide and clays in the soft humus adjacent to the nodules.
- (2) The "erosional" surface probably represents small scale slumping, due to differential compaction, around the more competent nodule
- (3) Precipitation of Fe-sulfide in shrinkage cracks (veinlets) adjacent to the nodules during coalification. Movements within the coal during this period (compaction) resulted in brecciated zones within the veinlets.
- (4) The bands of calcite were presumably precipitated along with humus during peatification. The alternating relationship of calcite and humus might reflect small changes in the chemistry of the pore waters, i.e., fluctuations between

saturation and under saturation with respect to the carbonate phase.

- (5) Distortion of the banding seems to have occurred after the coal became brittle as evidenced by the angular nature of some of the coal bands and the emplacement of calcite within micro-faults.
- (6) Precipitation of Fe-sulfide within the distorted bands probably accompanied by dissolution of the calcite, sometime after the banding was distorted.

CHAPTER IV: SPONTANEOUS OXIDATION OF Fe-SULFIDE TO Fe-SULFATE

IV.1 INTRODUCTION

The spontaneous oxidation of Fe-sulfide to various forms of hydrated Fe/Al-sulfate was observed occurring on the surfaces of the nodules described in the previous Chapter. Similar observations have been reported from numerous natural environments (Bol'shakov and Plushko, 1971; Cody and Biggs, 1973; Raymond, et.al., 1983; Zodrow and Moandlish, 1978; Zodrow, et.al., 1979) as well as the laboratory (Huggins, et.al., 1983; Weise, et.al., 1986).

Basically, this reaction creates relatively soluble salts from the relatively insoluble sulfides and is of importance for a number of reasons. Oxidation of Fe-sulfide in coal mines contributes considerably to the problem of acid drainage waters in areas of active mining as well as coal refuse piles, and storage sites. The reaction is exothermic ($\Delta H = -1465.49 \text{ KJ}$ in the case of pyrite \rightarrow melanterite) and is believed to be responsible for in situ coal fires (burns) and spontaneous combustion in coal storage piles. The large volume increase associated with the transformation of sulfide to hydrated sulfate contributes to the instability of roofs and pillars in mines and to increased mechanical erosion in road cuts (Zodrow and Moandlish, 1978).

The types of hydrated sulfates formed appears to be a function of environment (moisture) as well as the availability of elements necessary to the formation of the secondary minerals. If, for example, the reaction is one involving redistribution of the elements inherent in the original mineral along with the addition of water then hydration/dehydration is the important mechanism. Reactions of this type were reported by Zodrow, et.al., (1979) who noted fibroferrite ($\text{FeSO}_4(\text{OH})\cdot 5\text{H}_2\text{O}$) growing from melanterite ($\text{FeSO}_4\cdot 7\text{H}_2\text{O}$) on laboratory stored samples and also replacing melanterite on mine walls. Many other secondary mineral phases were also noted and their presence/absence seemed to be a function of humidity as they changed diurnally and with increased distance from the mine adit. In a similar study Zodrow and Mcandlish (1979) noted the alteration of melanterite to rozenite ($\text{FeSO}_4\cdot 4\text{H}_2\text{O}$). Apparently the laboratory controlled reactions in these studies were not in contact with other minerals, such as clays, and so ambient conditions (humidity and temperature) were the controlling factors.

The formation of other hydrated sulfates such as epsomite ($\text{MgSO}_4\cdot 7\text{H}_2\text{O}$) and halotrichite ($\text{FeAl}_2(\text{SO}_4)_4\cdot 22\text{H}_2\text{O}$) requires not only addition of water but also the introduction of Mg or Al and so are dependent of the presence of other mineral phases, e.g., carbonate (for the Ca) and clays (for the Al). Of course many other mineral phases, as well as the pore

solutions, could provide these elements. Huggins, et.al., (1983) point out the importance of the spacial arrangement of the constituent mineral matter in coals for the above types of reactions to occur, noting as many as 6 different iron phases including sulfide, sulfate and hydroxide intimately related (<1 mm separation).

IV.2 GEOCHEMISTRY OF SECONDARY MINERAL PHASES

The major hydrated sulfates described here were identified as szomolnokite and halotrichite based on EDS analyses and confirmed by limited single crystal XRD. Other phases were detected (XRD) but not identified owing to their scarcity (Weise, et.al., 1986). For that reason, in the following discussion those secondary minerals containing S and Fe will be collectively referred to as szomolnokite and those containing Al, S and Fe will be referred to as halotrichite. Other phases are certainly present as the reactions involved in their formation are transitional (stepwise) (Huggins, et.al., 1983). The distribution of the secondary minerals on samples studied here correlated well with the occurrence of original mineral phases.

IV.2.1 SZOMOLNOKITE

Szomolnokite was the predominant secondary mineral associated with (distributed throughout) the internal area

of the nodules where initial SEM/EDS analyses had detected only Fe-sulfide with limited clay, Ca-carbonate and Ca-sulfate. The szomolnokite occurs as equant euhedral to subhedral crystals covering the majority of the interior of the nodules (Figure IV-1, A) and masks the cellular structures which were observed on freshly cut surfaces. Szomolnokite was also observed growing on the Fe-sulfide spheres adjacent to the exterior of the nodules and in places well developed rosettes similar to the one shown in Figure IV-1, B were developed. A representative EDS spectrum for the szomolnokite is shown in Figure IV-1, C. Generally, szomolnokite was the only secondary mineral to develop on "clean" surfaces of Fe-sulfide, i.e., where other elements were not available from sources such as clays or carbonate. The progressive alteration of Fe-sulfide to szomolnokite is shown in Figures IV-2, A to F. The physical changes in this sequence demonstrate the volume change which results from the oxidation of sulfides in coal and hence contribute to the mechanical erosion associated with the process. During the first stages of alteration the surface of the sulfides become fractured (Figure IV-2, A) and as the process proceeds anhedral grains develop (Figure IV-2, B). Subsequent grains take on a subhedral appearance (Figures IV-2, C, D and E) and finally euhedral crystals are formed (Figure IV-2, F).

IV-2.2 HALOTRICHITE

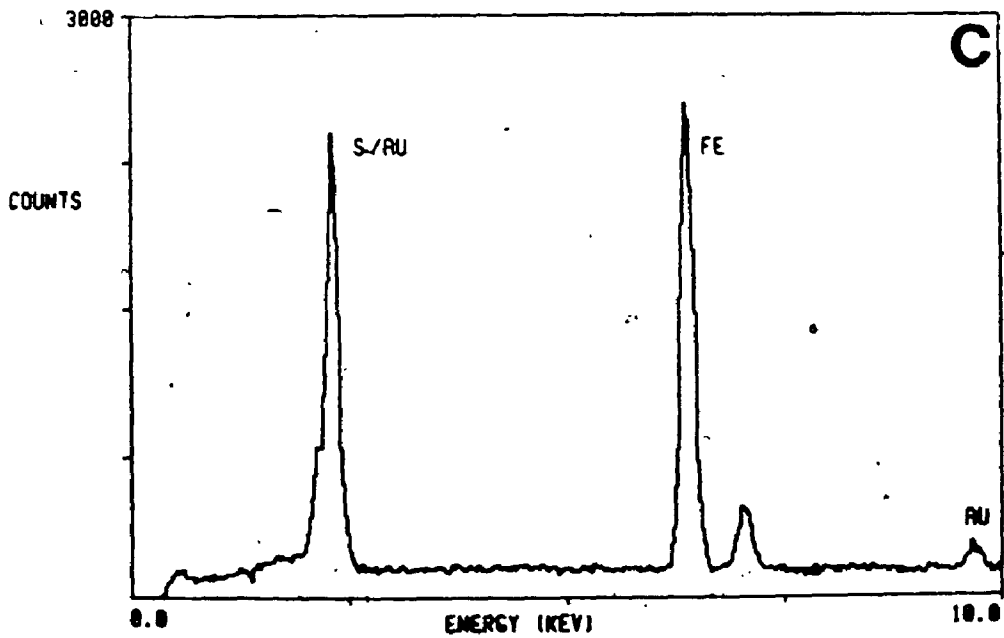
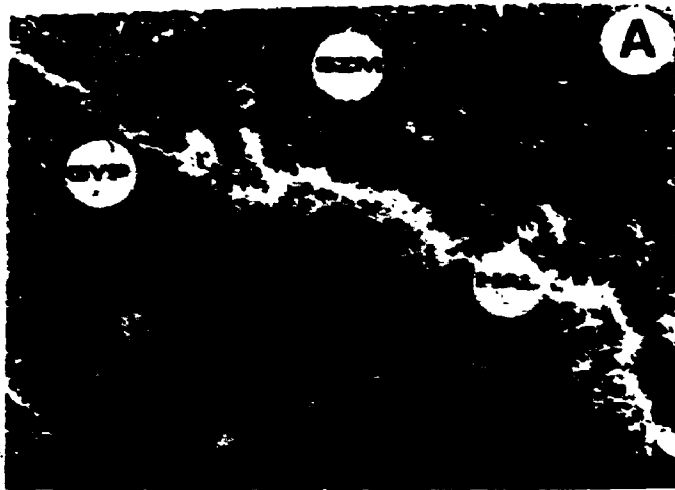
011

FIGURE IV-1

A - PHOTOMICROGRAPH OF THE INTERIOR OF AN FE-SULFIDE NODULE AFTER OXIDATION OF THE FE-SULFIDE TO FE-SULFATE. THE SMALLER EUHEDRAL, EQUANT GRAINS ARE SZOMOLNOKITE (SZM) WHICH COVERS THE INTERIOR OF THE NODULE AND MASKS THE CELLULAR STRUCTURES NOTED ON FRESHLY CUT SURFACES (SHOWN IN FIGURE III-4). A "RIBBON" OF ACICULAR HALOTRICHITE (HAL) CAN BE SEEN GROWING ALONG THE SURFACE OF A VEINLET OF GYPSUM (GYP). BUNDLES OF HALOTRICHITE ARE ALSO PRESENT IN THE LOWER PORTION OF THE PHOTOMICROGRAPH.

B - PHOTOMICROGRAPH OF A EUHEDRAL ROSETTE OF SZOMOLNOKITE OBSERVED GROWING ON THE SURFACE OF ONE OF THE ISOLATED SPHERES OF FE-SULFIDE AT THE PERIFERY OF THE NODULE.

C - TYPICAL EDS SPECTRUM FROM THE SZOMOLNOKITE SHOWN IN "A" AND "B". NOTE THE RATIO (PEAK HEIGHTS) OF S TO FE IS CLOSE TO 1:1.



191

FIGURE IV-2

A TO F - A SERIES OF PHOTOMICROGRAPHS SHOWING THE PROGRESSIVE ALTERATION OF FE-SULFIDE TO FE-SULFATE AND THE ATTENDED VOLUME CHANGE. IN "A", THE FRESH FE-SULFIDE IS JUST BEGINNING TO BREAK-UP AS SHOWN BY THE CRACKS FORMED. A "POPCORN" TEXTURE IS DEVELOPED IN "B" AS ANHEDRAL MASSES FORM. "C" SHOWS THE DEVELOPEMENT OF SUBHEDRAL GRAINS. IN "D" AND "E" THE CRYSTALS BECOME MORE DEVELOPED, TENDING TOWARDS EUHEDRA IN "E". THE END PRODUCT, A EUHEDRAL ROSETTE, IS SHOWN IN "F". NOTE THE CHANGE IN VOLUME IN THE SEQUENCE: THE GRAIN IN "A" IS NEARLY FLUSH WITH THE SURFACE OF THE SAMPLE WHILE IN "F" THE ROSETTE HAS ERUPTED OUT OF THE SURFACE AND NOW SITS ON TOP OF THE SAMPLE (MAGNIFICATION VARIES AS SHOWN AT THE BOTTON OF EACH PHOTOMICROGRAPH).



The formation of halotrichite results from the oxidation of Fe-sulfide in the presence of clays and is evidence for the degradation of clays in the process. The majority of the halotrichite observed occurs at the rims of the nodules where there are abundant clays and gives the appearance of a "forest" of acicular crystals (Figure IV-3, A). In places acicular bundles of halotrichite were associated with szomolnokite on the surfaces of isolated spheres of Fe-sulfide (Figure IV-3, B, upper left) while on adjacent spheres only platy crystals of halotrichite had developed (Figure IV-3, B, lower right). The isolated spheres of Fe-sulfide are composed of aggregates of crystals as can be seen in the granular nature of the one shown in Figure 3-B (lower right). The clays necessary for the formation of the halotrichite are probably hosted within grain boundaries.

Halotrichite also occurs in the interior of the nodules as isolated bundles and "ribbons". The bundles are composed of more or less parallel acicular crystals capped by anhedral material (Figure IV-4, A). The material on top of the bundle yields EDS spectra characteristic of those for szomolnokite and halotrichite (Figures IV-4, B and C) and also include the peak for Si. This material appears to have been carried along as the halotrichite grew. The Si is likely present as residual silica (from the degradation of the clays) or as clay combined with a portion of the Al. The minerals in this

FIGURE IV-3

A - PHOTOMICROGRAPH OF THE "FOREST" OF ACICULAR HALOTRICHITE (HAL) WHICH FORMED AT THE RIM OF THE NODULE. THE LOWER RIGHT OF THE PHOTOMICROGRAPH IS THE INTERIOR OF THE NODULE WHILE THE UPPER LEFT IS THE "COALY" ZONE.

B - PHOTOMICROGRAPH OF HALOTRICHITE (HAL) WHICH FORMED ON THE ISOLATED SPHERES OF FE-SULFIDE ADJACENT TO THE RIM OF THE NODULE. IN THE UPPER LEFT HALOTRICHITE (HAL) IS SHOWN ASSOCIATED WITH SZOMOLNOKITE (SZM) WHICH HAS DEVELOPED ON THE SURFACE OF THE FE-SULFIDE SPHERE. IN THE LOWER RIGHT, PLATEY CRYSTALS OF HALOTRICHITE (HAL) HAVE DEVELOPED ON A SPHERE OF FE-SULFIDE WHICH HAS NOT YET OXIDIZED TO FE-SULFATE.

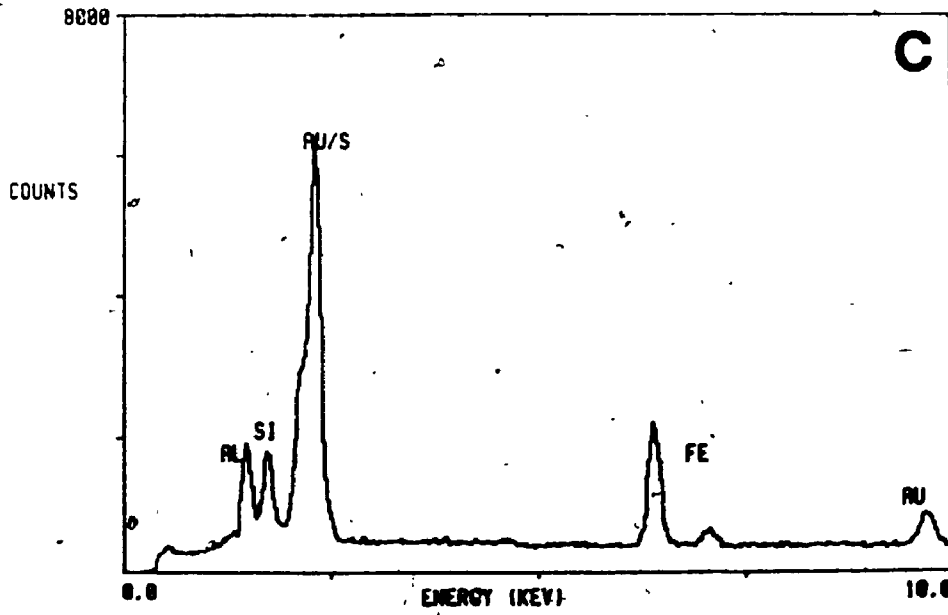
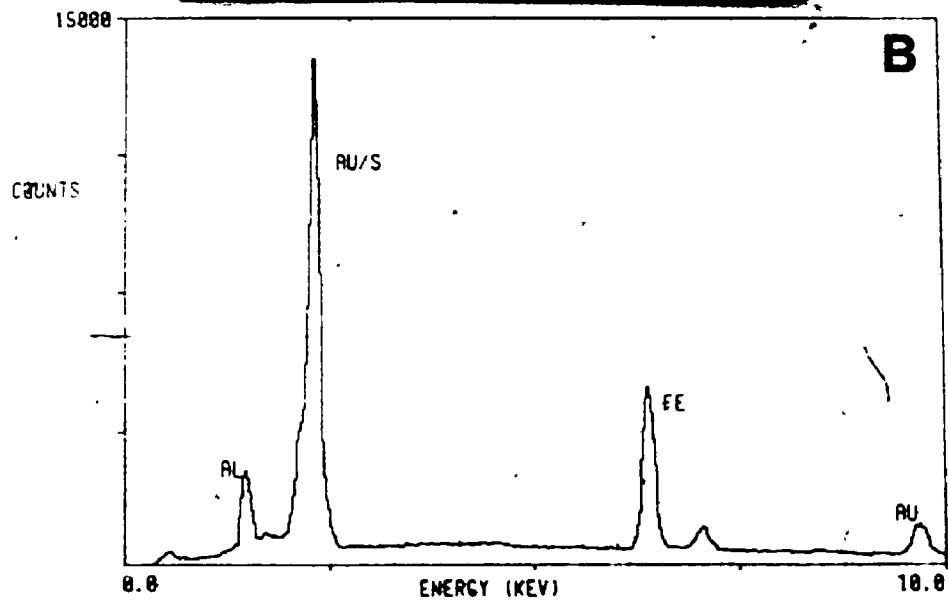
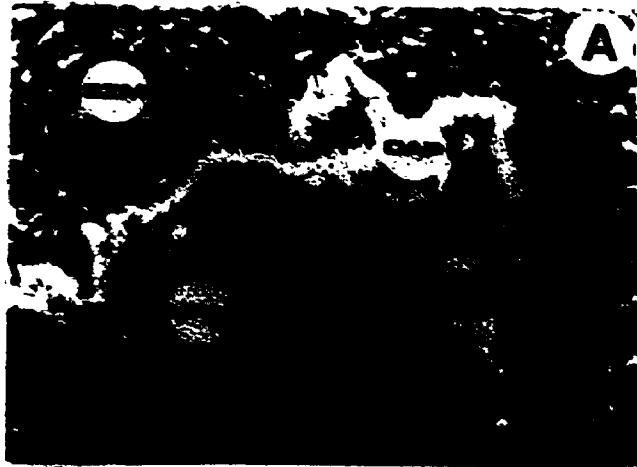


FIGURE IV-4

A - PHOTOMICROGRAPH OF ONE OF THE BUNDLES OF ACICULAR HALOTRICHITE (HAL) FROM WITHIN THE INTERIOR OF THE NODULE. NOTE EQUANT CRYSTALS OF SZOMOLNOKITE (SZM) SURROUNDING THE HALOTRICHITE.

B - EDS SPECTRUM OF THE ACICULAR HALOTRICHITE

C - EDS SPECTRUM OF THE MATERIAL "CAPPING" (CAP) THE HALOTRICHITE. THIS MATERIAL IS BELIEVED TO BE A MIXTURE OF HALOTRICHITE, FE-SULFIDE, FE-SULFATE AND SILICA WHICH WAS CARRIED ATOP THE BUNDLE AS IT GREW UP FROM THE SURFACE OF THE SAMPLE.



material are too intimately related to allow for individual EDS analyses and consequently the resulting spectra are a composite of more than one phase.

Closer examination of the base of one of the bundles shows further evidence that the halotrichite grew from the surface of the sample. Figure IV-5, A shows the needles of halotrichite emerging from cracks in the coal substrate as well as from within an area of Fe-sulfate. Obviously, the chemical reactions between the clay and sulfide are taking place at some distance below the surface and the cracks are providing pathways through which the secondary minerals and/or solutions are forced, this a function of the volume increase which accompanies the addition of oxygen and water to the secondary mineral structures (oxidation and hydration). As pointed out by Weise, et.al., (1986) the partial pressure of oxygen required for the oxidation of Fe-sulfide to hydrated Fe-sulfate will not be favored below the surface owing to the exothermic nature of the reaction. Therefore, it is possible that this reaction takes place at, or near, the surface. A first step in the process involves the oxidation of Fe-sulfide to Fe-sulfate with excess H^+ as one product. If the heptahydrate melanterite is considered as the sulfate product and pyrite the reactant, ΔG (-1196.91 KJ) and ΔH (-1465.49 KJ) for the reaction are large and the formation of the sulfate is spontaneous (Weise, et.al., 1986). This reaction requires only airborne moisture to

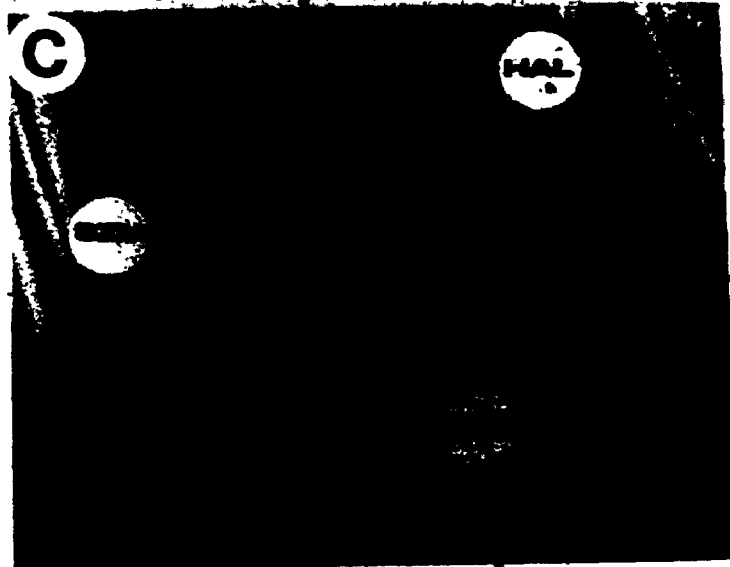
051

FIGURE IV-5

A - PHOTOMICROGRAPH OF ACICULAR HALOTRICHITE (HAL) GROWING FROM CRACKS IN THE SURFACE OF THE COAL (C) IN THE INTERIOR OF THE NODULE. SZOMOLNOKITE (SZM) IS SHOWN SURROUNDING THE HALOTRICHITE.

B - PHOTOMICROGRAPH OF HALOTRICHITE (HAL) GROWING THROUGH/AROUND/FROM A CRYSTAL OF SZOMOLNOKITE (SZM). NOTE THE GROWTH LINES IN THE HALOTRICHITE, CONVERGING FROM THE SURFACE OF THE SZOMOLNOKITE.

C - PHOTOMICROGRAPH OF A BUNDLE OF ACICULAR HALOTRICHITE (HAL) AS SHOWN IN FIGURE IV-4. NOTE THE GRAINS OF SZOMOLNOKITE (SZM) ATTACHED TO THE HALOTRICHITE. THE SZOMOLNOKITE HAS BEEN CARRIED ALONG AS THE HALOTRICHITE GREW, AFTER IT ATTACHED AS SHOWN IN "B".



no doubt that some of the needles of halotrichite, as shown in Figure IV-5, A, are emerging from the cracks in the coal surface but possibly this initial stage of extrusion is followed by precipitation of material carried in capillary solutions, i.e., delivered to the base of the reaction area from the subsurface. That the process continues is shown in Figure IV-5, C which shows how grains of szomolnokite attached to the halotrichite needles are lifted from the surface as growth continues. Certainly, both processes, extrusion and growth at the surface, are important.

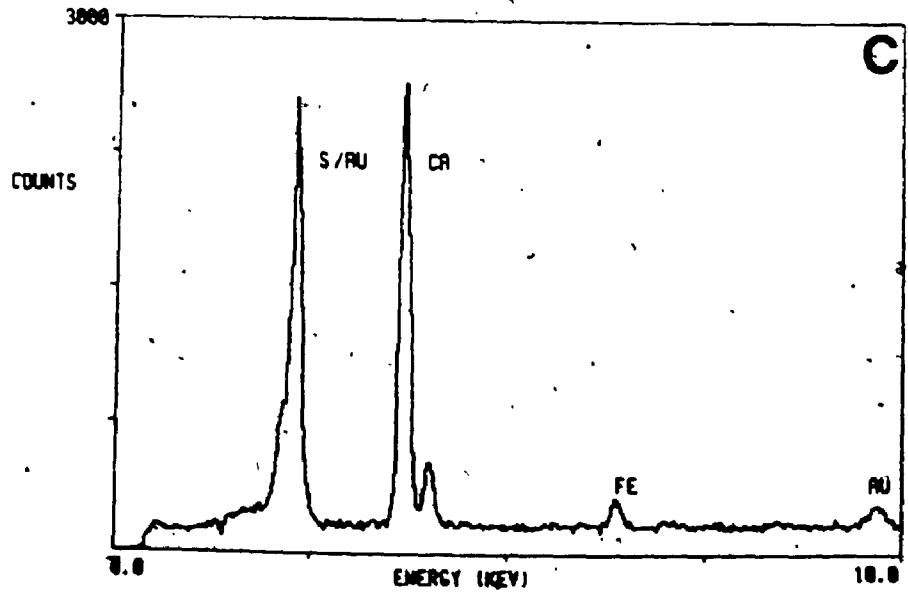
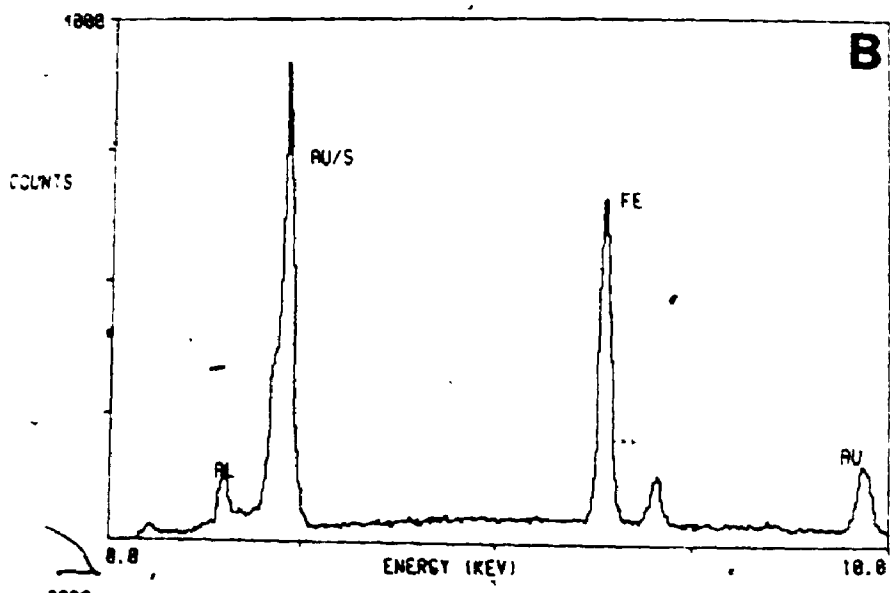
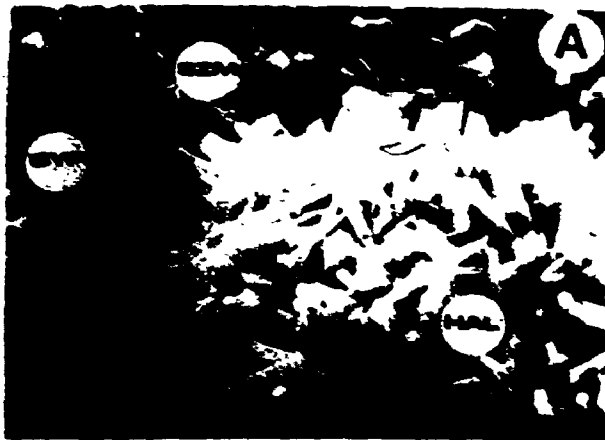
Unlike the bundles, "ribbons" of halotrichite (Figures IV-1, A and IV-6, A) do not give any evidence of being extruded from the subsurface and do not incorporate other material (szomolnokite or silica) during formation. This form of halotrichite consists of randomly oriented acicular crystals which yield spectra similar to the one shown in Figure IV-6, B. These "ribbons" were only observed in the interior of the nodules and associated with (growing on) Ca-sulfate (Figures IV-6, A and IV-1, A and the spectrum in Figure IV-6, C) which occurs as wavy veinlets in the surface of the nodules. It is presumed that growth occurred at the surface and that initially formed crystals were pushed up as subsequent growth continued, resulting in the random orientation noted. The exact relationship of the gypsum and halotrichite is not clear. It is possible that the gypsum is secondary, formed by the reaction between pre-existing calcite and pyrite as

FIGURE IV-6

A - PHOTOMICROGRAPH OF THE END OF THE HALOTRICHITE (HAL) "RIBBON" SHOWN IN FIGURE IV-1, A. NOTE THE "CLEAN" APPEARANCE OF THE HALOTRICHITE, I.E., IT DOES NOT CONTAIN THE "CAP" OF MATERIAL AS OBSERVED ON THE BUNDLES OF HALOTRICHITE (FIGURE IV-4, A), NOR DOES ANY MATERIAL APPEAR TO BE TRAPPED WITHIN THE RANDOMLY ORIENTED ACICULAR CRYSTALS. THE "RIBBON" APPEARS TO BE FOLLOWING A VEINLET OF GYPSUM (GYP). THE EQUANT CRYSTALS SURROUNDING THE HALOTRICHITE ARE SZOMOLNOKITE (SZM).

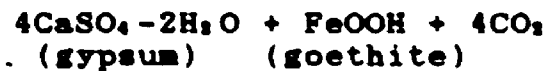
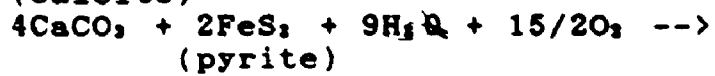
B - TYPICAL EDS SPECTRUM FROM THE HALOTRICHITE SHOWN IN "A"

C - EDS SPECTRUM OF THE GYPSUM SUBSTRATE ON WHICH THE HALOTRICHITE IS GROWING.



proposed by Huggins, et.al., (1983),

(calcite)



This type of coupled reaction could produce halotrichite rather than goethite if kaolinite is added as a reactant.

CHAPTER V: DATA COMPARISONS (OVERALL GEOCHEMISTRY)

V.1 INTRODUCTION

Here the geochemistries of Utah and Wyoming Coals are compared to other works on the same coals and to other coals from geographically similar areas. The Utah and Wyoming coals are also compared to each other in an attempt to understand the mechanisms of emplacement of the elements in the two coals.

V.2 UTAH

Table V-1 shows the concentrations of 49 elements in coals from the Emery Coal Field, Utah as determined from this study (Col.1) compared to other analyses of Emery Coal Field coals (Col.2) (Affolter, et al., 1979) and data from other coal fields in Utah (Col.3) (Dakota and Straight Cliffs Fm., Affolter and Hatch, 1980; Wasatch Plateau Coal Field, Blackhawk Fm., Hatch, et al., 1980; Muddy Creek Coal, Smith, 1981). The data in the first three columns of Table V-1 are listed in order of decreasing abundance relative to this work (Col.1). Columns 4 and 5 show the ratios for the results from this study (Col.1) compared to the other two data sets (Cols. 2 & 3). Ratios of <2 or >0.67 represent differences of $\pm 50\%$ relative to the this study, within these limits the data are in good enough agreement as not to

TABLE V-1

COMPARISON OF THE GEOCHEMISTRY (49 ELEMENTS) OF EMERY COAL FIELD COALS FROM THIS STUDY WITH OTHER EMERY COALS AND OTHER UTAH COALS (PPM).

ELEM.	COL. 1		COL. 2		COL. 3		COL. 4		COL. 5	
	THIS WORK	(N)	OTHER *	(N)	OTHER *	(N)	COL.1:COL.2	ELEM. RATIO	COL.1:COL.3	ELEM. RATIO
Si	13000	5	38000	20	29000	78	Hg	4.8	Hg	13.7
S	12900	25	14000	20	7700	78	Ba	3.0	P	4.0
Ca	9300	26	5000	20	5000	78	Sr	2.9	Ba	2.6
Al	7200	26	18000	20	11000	78	B	2.3	As	2.4
Fe	6400	19	10000	20	3500	78	Ca	1.9	Nd	2.3
Mg	1500	5	1000	20	1000	78	Na	1.5	Ca	1.9
Na	1500	5	1000	20	2200	78	Hg	1.5	Fe	1.8
Ti	635	26	1100	20	657	78	Mn	1.3	Sr	1.7
K	400	7	1000	20	800	78	As	1.2	S	1.7
P	294	5	ND	20	73	78	S	0.9	Mn	1.6
Ba	208	26	70	20	80	78	La	0.9	Hg	1.5
Sr	204	26	70	20	117	78	Se	0.8	Co	1.5
B	116	5	50	20	109	78	Cr	0.8	Hf	1.4
Zr	30	26	50	20	27	78	Nb	0.7	B	1.2
Mn	26	26	20	20	16	78	V	0.6	Cr	1.1
V	9.7	26	15	20	15	78	Fe	0.6	Zr	1.1
Ce	9.6	5	ND	20	13.7	6	Pb	0.6	La	1.1
Cr	7.8	26	10	20	7	78	Zr	0.6	Se	1.1
Cu	6.5	26	14	20	9	78	Ti	0.6	Mo	1.0
La	6.3	5	7	20	5.7	78	Co	0.5	Ti	1.0
Pb	5	26	8.2	20	5.6	78	Mo	0.5	Pb	0.9
Zn	4.6	10	15	20	12	78	Ni	0.5	Nb	0.8
As	4.5	14	4	20	1.9	78	Cu	0.5	Ni	0.8
Nd	3.4	5	ND	20	1.5	7	Ba	0.5	Eu	0.7
Ni	3.3	26	7	20	4.3	78	K	0.4	Sb	0.7
Y	2.8	4	7	20	7	78	Al	0.4	Cu	0.7
Ga	2.3	21	5	20	5	78	Y	0.4	Ce	0.7
Nb	2.2	5	3	20	2.7	78	Th	0.4	Na	0.7
Rb	1.8	25	ND	20	7	7	Sc	0.4	Th	0.7
Se	1.6	7	2	20	1.5	78	Si	0.3	Al	0.7
Th	1.6	5	4.3	20	2.4	78	Sb	0.3	V	0.6
Co	1.6	21	3	20	1.1	78	Yb	0.3	I	0.6
Sc	1.11	5	3	20	2	78	Zn	0.3	Sc	0.6
Mo	1	5	2	20	0.97	78	U	0.2	K	0.5
Hg	0.96	2	0.2	20	0.07	78	Rb	ND	Ba	0.5
B	0.8	4	ND	20	6.3	7	Ce	ND	Si	0.4
	0.7	5	ND	20	0.5	1	Tb	ND	U	0.4
	0.62	15	3.4	20	1.5	78	Cs	ND	Y	0.4
I	0.6	2	ND	20	0.98	5	Se	ND	Zn	0.4

(CONTINUED)

TABLE V-1 (CONTINUED)

COL. 1 : COL. 2 : COL. 3 : COL. 4 : COL. 5										

ELEM.	THIS WORK	(N)	OTHER * EMERY (N)	(N)	OTHER ^ UTAH (N)	(N)	COL.1:COL.2 ELEM. RATIO	COL.1:COL.3 ELEM. RATIO		

Sm	0.57	5	ND	20	3.2	6	Lu	ND	Yb	0.3
Sb	0.29	15	0.9	20	0.4	78	Nd	ND	Cs	0.3
Yb	0.22	5	0.7	20	0.7	78	Be	ND	Rb	0.3
Cs	0.2	3	ND	20	0.76	5	Br	ND	Se	0.2
Eu	0.15	5	ND	20	0.2	2	I	ND	Br	0.1
Lu	0.04	5	ND	20	1	1	Gd	ND	Lu	0.0
Cd	<2	15	ND	20	0.06	52	Cd	ND	Be	ND
Be	<1.0	5	2.0	20	1.3	78	Eu	ND	Cd	ND
Gd	<0.5	5	ND	20	0.45	2	P	ND	Gd	ND
Tb	<0.05	5	ND	20	0.1	1	Hf	ND	Tb	ND

* OTHER EMERY COALS. DATA FROM AFFOLTER, HATCH AND RYER, 1979.

^ OTHER UTAH COALS OUTSIDE THE EMERY COAL FIELD. DATA FROM AFFOLTER AND HATCH, 1980; HATCH, AFFOLTER AND DAVIS, 1980; AND SMITH, 1981

be considered as significantly more or less concentrated in either coal.

The list of ratios in Col. 4 represent relative enrichment/depletion of the elements determined from this study as compared to previous data on coals from the Emery Coal Field. Overall, the first 9 elements in Col. 4 (Hg to As) were found at higher concentrations than previous work while the next 25 elements (S to U) were detected in lesser amounts. The last 15 elements (Rb to Hf) were not detected in one or the other of the two sample groups, and so cannot be compared.

Only 4 elements (Hg to B) were detected at significantly higher concentrations than previously reported (ratios >2). Nine of the elements (B to Nb) were found at similar concentrations (ratios <2 or >0.67). The last 20 elements in Col. 4 (V to U) were detected at substantially lower concentrations (ratios <0.67).

Column 5 of Table V-1 compares data from this work with data on other Utah coals from outside the Emery Coal Field. The Emery coals appear to contain higher concentrations of 18 elements (Hg to Se) than the other Utah coals, two elements (Mo and Ti) were found at identical concentrations, and 25 elements (Pb to Lu) were detected in lesser amounts. Four elements (Be to Tb) were not detected in one or the other of

the coals.

Ratios for twentyfive of the elements in column 5 (Ca to Al) fall in the range <2 to >0.67 ($\pm 50\%$). Five elements (Hg to Nd) are appreciably higher in the Emery coals (ratios >2) and 15 of the elements (V to Lu) are significantly lower in abundance (ratios <0.67).

V.3 WYOMING

Data on the abundance of 36 elements in coals from the Powder River Coal Field (PRCF), Wyoming, as determined from this study, (Col.1), other work on the PRCF (Col.2) (Hatch and Swanson, 1977) and other Wyoming coals from outside the PRCF (Col.3) (Glass, 1978; Swanson et al., 1976) are shown in Table V-2. The data in Cols. 1, 2 and 3 are arranged in order of decreasing abundance relative to this work (Col.1). Columns 4 and 5 are the ratios between this work (Col.1) and the other two data sets (Cols. 2 and 3).

As shown in Col. 4 of Table V-2 this study found higher concentrations of 7 elements (Co to As), lower concentrations of 17 elements (Ca to Th) and identical concentrations of two elements (Cu and Pb) as compared to other work on PRCF coals.

Only 1 element (Co) was detected at appreciably higher

TABLE V-2

COMPARISON OF THE GEOCHEMISTRY (36 ELEMENTS) OF POWDER RIVER BASIN COALS (PRBC) FROM THIS STUDY WITH OTHER PRBC AND OTHER WYO. COALS (PPM).

ELEM.	COL. 1		COL. 2		COL. 3		COL. 4		COL. 5	
	THIS WORK	(N)	OTHER PRBC	(N)	OTHER WYO.	(N)	COL. 1:COL. 2 ELEM. RATIO	COL. 1:COL. 3 ELEM. RATIO		
Ca	9900	20	11000	410	7500	48	Co	3.1	Ti	6.8
S	7200	20	ND	410	4000	48	Se	1.8	Co	3.1
Al	4000	29	7800	410	7200	48	Zr	1.5	Sr	2.5
Hg	1400	8	2100	410	1700	48	Ba	1.4	S	1.8
Fe	1300	12	5400	410	5100	48	Ti	1.3	Na	1.5
Na	600	8	1100	410	400	48	Sr	1.3	Zr	1.5
Ti	541	20	410	410	80	48	As	1.2	Cu	1.4
Ba	431	30	300	410	300	48	Cu	1.0	Ba	1.4
Sr	250	30	200	410	100	48	Pb	1.0	Ca	1.3
Mn	23	30	51	410	40	48	Ca	0.9	Hg	0.8
Zr	22	22	15	410	15	48	Ni	0.8	Ni	0.8
Cl	14	8	ND	410	100	48	V	0.7	V	0.7
Cu	12	22	11.1	410	8	48	Hg	0.7	Mo	0.7
V	11	30	15	410	15	48	Ga	0.6	Ga	0.6
Zn	6.8	19	20	410	18	48	Na	0.5	Mn	0.6
Co	6.2	30	2	410	2	48	Cr	0.5	Al	0.6
Pb	6.1	22	6.4	410	<3.0	48	Al	0.5	Sc	0.5
Ni	3.9	22	5	410	5	48	Mn	0.4	Cr	0.5
Cr	3.8	30	7	410	7	48	Sc	0.4	Zn	0.4
As	3.7	12	3	410	<3.0	48	Mo	0.4	Yb	0.3
Ce	3.6	8	ND	410	<20	48	Zn	0.3	Fe	0.3
Se	1.8	9	1	410	<0.8	48	Yb	0.3	Th	0.2
Ga	1.8	20	3	410	3	48	Sb	0.3	Cl	0.1
La	1.7	8	ND	410	<7.0	48	Fe	0.2	Sb	ND
Nd	1.5	8	ND	410	<15	48	U	0.2	As	ND
Sc	0.82	8	2	410	1.5	48	Th	0.1	Nd	ND
Mo	0.7	4	2	410	1	48	S	ND	Y	ND
Th	0.6	8	4.3	410	2.7	48	Y	ND	Ce	ND
U	0.19	8	0.9	410	<0.9	48	Nb	ND	Nb	ND
Sb	0.18	11	0.6	410	<0.4	48	Ce	ND	U	ND
Yb	0.15	8	0.5	410	0.5	48	K	ND	K	ND
Y	<2.0	22	5	410	5	48	Cl	ND	La	ND
Nb	<2.0	22	1.5	410	1.5	48	La	ND	Se	ND
K	<200	30	500	410	600	48	Nd	ND	Pb	ND
Cd	<1.5	4	0.09	410	<1.5	48	Cd	ND	Cd	ND
Hg	<0.75	4	0.11	410	0.1	48	Hg	ND	Hg	ND

(N) - NUMBER OF SAMPLES

* - OTHER POWDER RIVER BASIN COALS. DATA FROM HATCH & SWANSON, 1976.

* - OTHER WYOMING COALS OUTSIDE THE POWDER RIVER BASIN. DATA FROM GLASS, 1975 AND SWANSON, 1976.

ND - NO DATA

concentrations (ratios >2) while 13 elements (Ga to Th) were determined at significantly lower concentrations (ratios <0.67). Twelve elements (Se to Mg) were present at concentrations similar to those found in other studies ($\pm 50\%$). Ten elements (S to Hg) were not detected in one or the other of the studies.

The ratios in Col. 5 of Table V-2 compare data from this study with data from Wyoming coals outside the PRCF. This work found that PRCF coals contain higher concentrations of 9 elements (Ti to Ca) and lower concentrations of 14 elements (Mg to Cl) than other Wyoming coals. Three elements (Ti to Sr) were present in significantly higher concentrations (ratios >2), 10 elements (S to Mo) at about the same concentrations ($\pm 50\%$) and 10 elements (Ga to Cl) at much lower concentrations (ratios <0.67). The last 13 elements in Col. 5 (Sb to Hg) were not detected in one or the other of the coals.

V.4 UTAH VS WYOMING

Table V-3 compares the overall geochemistries of the Utah and Wyoming coals studied here. Mean concentrations of the elements are listed in decreasing order of abundance relative to the Utah coals. Utah:Wyoming ratios are also listed in decreasing order.

TABLE V-3

COMPARISON OF THE GEOCHEMISTRIES OF COAL FROM THE EMERY COAL FIELD, UTAH (56 ELEMENTS) AND THE POWDER RIVER COAL FIELD, WYOMING (48 ELEMENTS).

(PPM)		UTAH:WYOMING		(PPM)		UTAH:WYOMING			
UTAH	WYO.	ELEM.	RATIOS > 1.0	UTAH	WYO.	ELEM.	RATIOS < 1.0		
ELEM.	MEAN	MEAN	RATIO	ELEM.	MEAN	MEAN	RATIO		
Si	13000	ND	Fe	4.9	Ga	2.3	1.8	Ca	0.9
S	12900	2200	La	3.7	Nb	2.2	<2.0	Se	0.9
Ca	9300	9900	U	3.3	Rb	1.8	1.3	V	0.9
Al	7200	4000	Th	2.7	Co	1.6	6.2	Mn	0.8
Fe	6400	1300	Ce	2.7	Se	1.6	1.8	Pb	0.8
Na	1500	600	Na	2.5	Th	1.6	0.6	Sr	0.8
Mg	1500	1400	Eu	2.5	Sc	4.11	0.82	Zn	0.7
Ti	635	541	Hf	2.3	Mo	1	0.7	Cs	0.7
K	400	<200	Nd	2.3	Hg	0.96	<0.75	Br	0.7
P	294	ND	Cl	2.1	Br	0.8	1.2	Cu	0.6
Ba	208	431	Cr	2.1	Hf	0.7	0.3	Ba	0.5
Sr	204	250	Se	1.8	U	0.62	0.19	Cd	0.3
B	116	ND	Al	1.8	I	0.6	ND	Au	0.2
Zr	30	22	S	1.8	Sa	0.57	0.31	Be	ND
Cl	30	14.3	Lu	1.7	Dy	0.53	0.33	K	ND
Mn	26	22.7	Sb	1.6	Ag	0.45	ND	Cd	ND
V	9.7	11.2	Dy	1.6	Sb	0.29	0.18	Y	ND
Ce	9.6	3.6	Yb	1.5	Yb	0.22	0.15	Tb	ND
Cr	7.8	3.8	Mo	1.4	Cs	0.2	0.3	Ag	ND
Cu	6.5	11.5	Rb	1.4	Ta	0.2	<0.5	I	ND
La	6.3	1.7	Zr	1.4	Eu	0.15	0.06	Hg	ND
Pb	5	6.1	Sc	1.4	Lu	0.04	0.024	P	ND
Zn	4.6	6.8	Ga	1.3	Au	0.001	0.006	Ta	ND
As	4.5	3.7	As	1.2	Cd	<2	<1.5	Nb	ND
Nd	3.4	1.5	Ti	1.2	Be	<1.0	ND	In	ND
Mn	3.3	3.9	Mn	1.1	W	<1	<1.0	W	ND
Y	2.8	62.0	Mg	1.1	Gd	<0.5	ND	Gd	ND
					In	<0.1	ND	Si	ND
					Tb	<0.05	0.06	B	ND

Twenty seven elements (Fe to Mg) were found to be more abundant in the Utah coals than in the Wyoming coals (ratios >1.0) and 13 elements (Ca to Au) were less abundant in the Utah coals (ratios <1.0). Over half of the elements detected in both coals (Sm to Br) were present at differences of less than +/- 50%. Approximately 1/4 of the elements (Fe to Cr) were present at significantly higher concentrations in the Utah coals (ratios >2) while only 4 elements (Cu and Au) were detected at appreciably lower levels (ratios <0.67).

The 39 elements detected in both coals can be conveniently separated into 5 groups on the basis of their mean concentrations as follows: group I, >0.5%; group II, 0.01-0.5%; group III, 10-100 ppm; group IV, 1-10 ppm; group V, <1.0 ppm. An element was placed into a given group if the largest concentration for either the Utah or Wyoming samples fell into that category. Table V-4 shows the 5 groups, each arranged relative to the ratio Utah:Wyoming in decreasing order.

The concentrations of the elements in the five groups are graphed in Figure V-1. A to E. Correlation coefficients for the data in each graph are shown at the top of each graph. The solid line in each graph represents parity for the two coals (X=Y), i.e., ratios Utah:Wyoming of 1. The dashed lines represent the ratios Utah:Wyoming = 0.67 and

TABLE V-4

=====

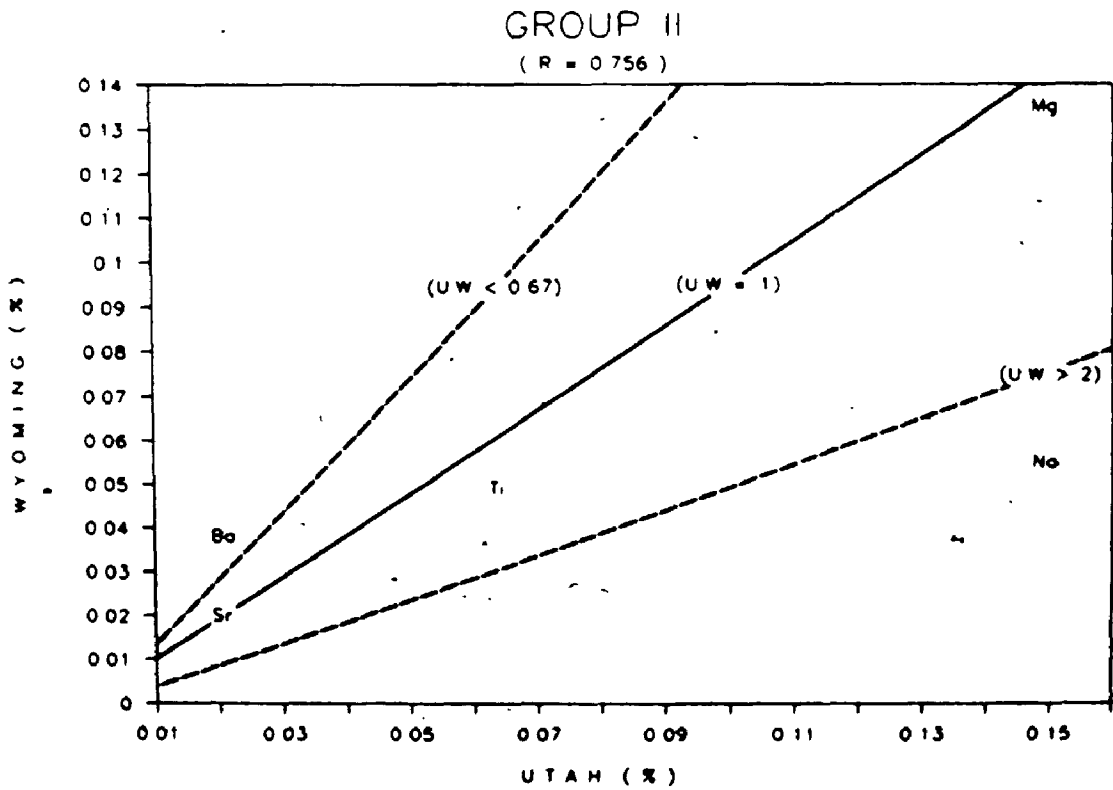
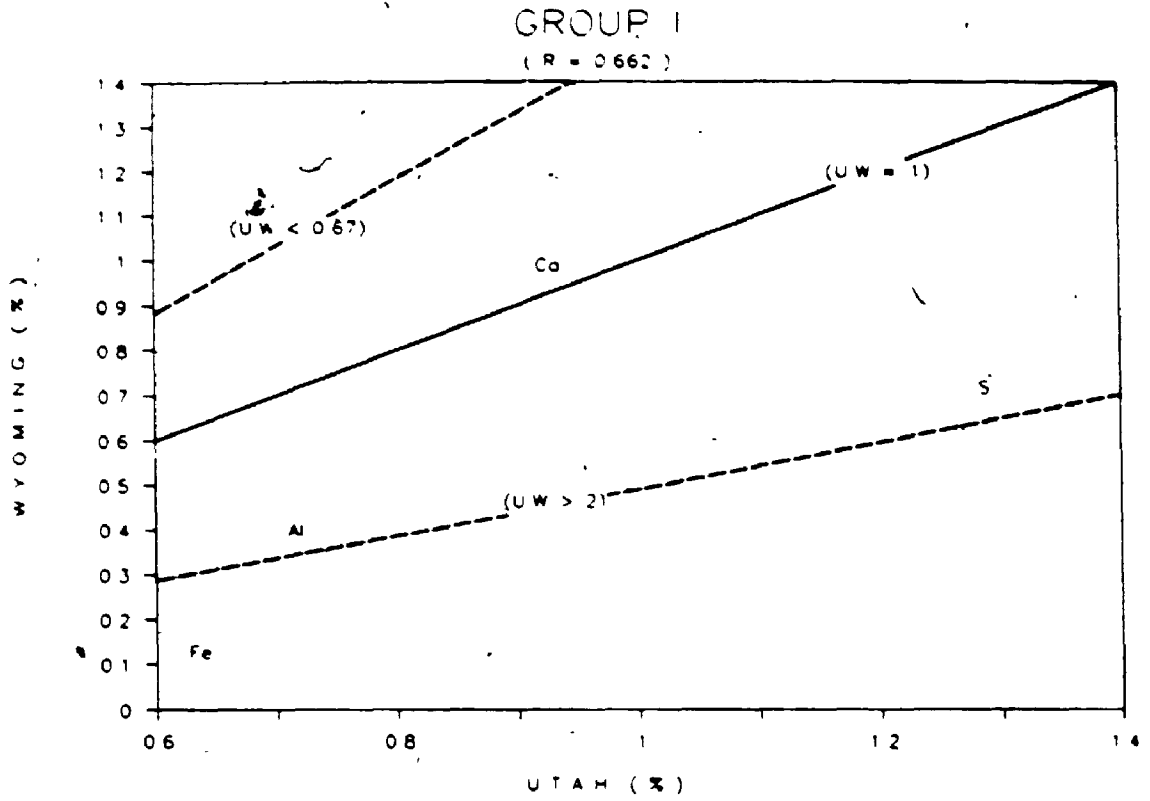
COMPARISON OF THE GEOCHEMISTRIES (39 ELEMENTS)
OF UTAH AND WYOMING COALS FROM THIS STUDY.

	ELEM	UTAH MEAN	WYOMING MEAN	RATIO UTA. : WYO.
GROUP I: (>0.5%)	Fe	0.64	0.13	4.9
	Al	0.72	0.40	1.8
	S	1.29	0.72	1.8
	Ca	0.93	0.99	0.9
GROUP II: (0.01-0.5%)	Na	0.150	0.060	2.5
	Ti	0.064	0.054	1.2
	Mg	0.150	0.140	1.1
	Sr	0.020	0.025	0.8
	Ba	0.021	0.043	0.5
GROUP III: (10-100 PPM)	Cl	30.0	14.3	2.1
	Br	30.0	22.0	1.4
	Mn	26.0	22.7	1.1
	V	9.7	11.2	0.9
	Cu	6.5	11.5	0.6
GROUP IV: 1-10 PPM)	La	6.3	1.7	3.7
	Ce	9.6	3.8	2.7
	Nd	3.4	1.5	2.3
	Cr	7.8	3.8	2.1
	Rb	1.8	1.3	1.4
	Ga	2.3	1.8	1.3
	As	4.5	3.7	1.2
	Se	1.6	1.8	0.9
	Ni	3.3	3.9	0.8
	Pb	5.0	6.1	0.8
	Zn	4.6	6.8	0.7
	Co	1.6	6.2	0.3
	GROUP V: (<1.0 PPM)	U	0.62	0.19
Th		1.60	0.60	2.7
Eu		0.15	0.08	2.5
Hf		0.70	0.30	2.3
Sm		0.57	0.31	1.8
Lu		0.04	0.02	1.7
Sb		0.29	0.18	1.6
Dy		0.53	0.33	1.6
Yb		0.22	0.15	1.5
Mo		1.00	0.70	1.4
Sc		1.11	0.82	1.4
Br		0.80	1.20	0.7
Cs		0.20	0.30	0.7

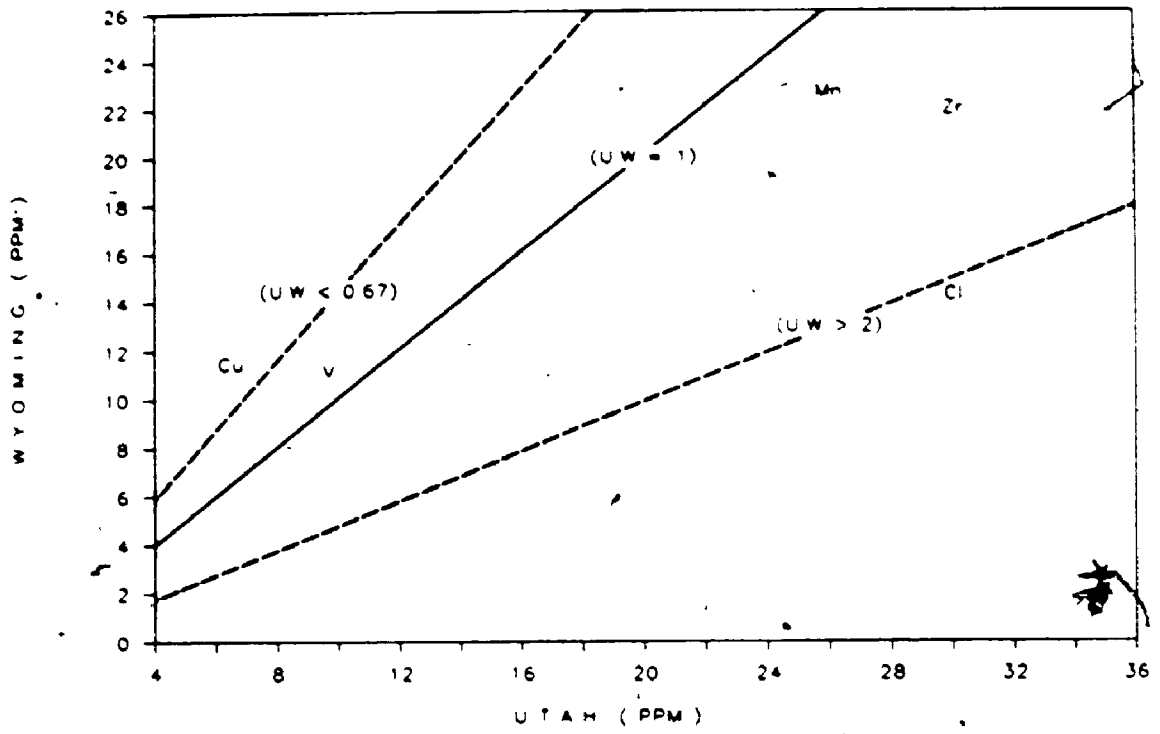
FIGURE V-1

GRAPHS OF THE FIVE GROUPS OF ELEMENTS COMPARED IN THE UTAH AND WYOMING COALS. DASHED LINES REPRESENT ENRICHMENT OR DEPLETION OF GREATER THAN $\pm 50\%$ RELATIVE TO THE UTAH SAMPLES. THE SOLID LINE IN EACH GRAPH DESCRIBES UNITY BETWEEN THE TWO COALS (1:1 RATIO FOR THE ELEMENT).

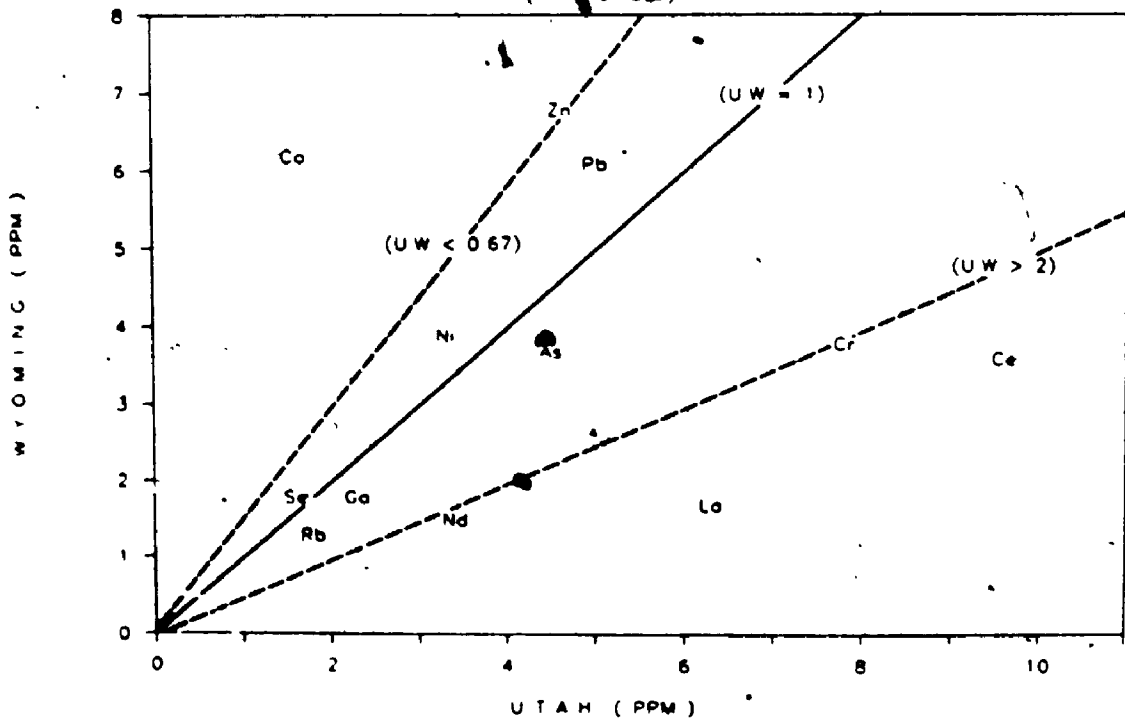
- A - GROUP I ELEMENTS, CONCENTRATIONS $>0.5\%$
- B - GROUP II ELEMENTS, CONCENTRATIONS 0.01-0.5%
- C - GROUP III ELEMENTS, CONCENTRATIONS 10-100 PPM
- D - GROUP IV ELEMENTS, CONCENTRATIONS 1-10 PPM
- E - GROUP V ELEMENTS, CONCENTRATIONS <1 PPM



GROUP III
(R = 0.746)

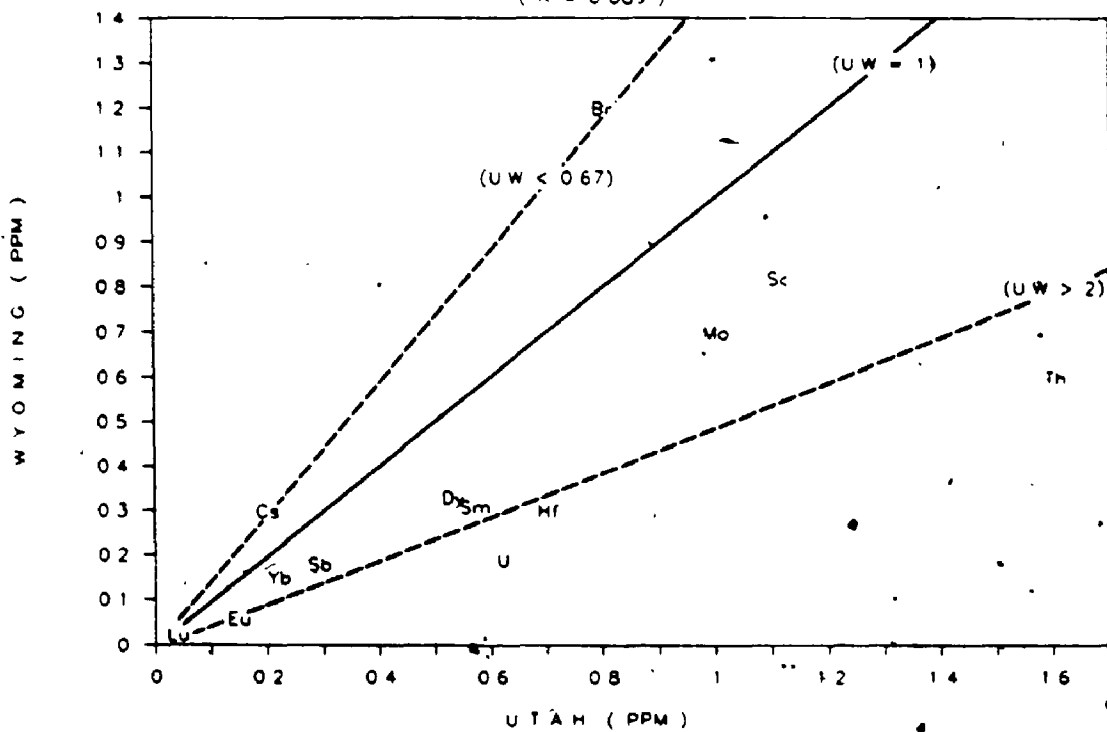


GROUP IV
(R = 0.15)



GROUP V

(R = 0.689)



Utah:Wyoming = 2.0 (+/- 50% relative to the Utah coals), within this zone neither coal is considered as enriched or depleted relative to the other.

The major elements (Group I) detected in both coals include Al, S, Ca and Fe. There is a positive correlation for these elements in the two sample sets ($R=0.662$). Of these only Fe is appreciably more concentrated in the Utah coal while Ca, Al and S are present at similar concentrations in both coals. Iron shows the largest concentration difference of any of the elements ($U:W = 4.9$).

Group II elements show the highest positive correlation ($R=0.758$) for the five groups. Sodium is present at significantly higher concentrations in the Utah coal. Magnesium, Ti and Sr are present at similar concentrations. Only Ba is present at appreciably higher concentrations in the Wyoming coal.

Group III elements also show a good positive correlation ($R=0.748$). In this group only Cl exhibits a notable enrichment in the Utah coal. Three elements, V, Mn, and Zr, are present at fairly similar concentrations and Cu is more concentrated in the Wyoming samples.

There is virtually no correlation ($R=0.152$) between the Utah and Wyoming coals for the elements in Group IV. Of the 12

elements in this group, Cr, Rb, Ga, As, Se, Ni, Pb and Zn exhibit similar concentrations in both coals. Lanthanum, Ce, Nd and Cr are appreciably more concentrated in the Utah coal and Zn and Co are relatively enriched in the Wyoming coal.

Group V is the largest of the five groups (13 elements) and shows positive correlation ($R=0.668$) between the two coals. As a group, these elements exhibit the greatest tendency to be enriched in the Utah coal. Four of the elements, U, Th, Eu and Hf are significantly more concentrated in the Utah samples.

V.4.1 CORRELATION DATA

Correlation data for 16 elements (not all elements the same for each coal) plus ash (AH) for the Utah and Wyoming coals are shown in Tables V-5 and V-6, respectively. The "Top" portion of each table shows the correlation coefficients for the variables listed in alphabetic order. The "Bottom" of each table lists the correlation coefficients for each element in decreasing order of magnitude relative to the other elements, i.e., The first value in each column shows the correlation of an element with itself and, therefore, is 1.0. The Other values decrease down the column and the last value in each column represents the largest negative correlation.

The correlation data from the "Bottom" of each table are graphed in Figure V-2, A to Q. In each case the ordinate represents the correlation coefficients of the element in question with the other elements for Wyoming coal, the abscissa those for the Utah coal. Zero correlation lines are shown where applicable. These plots show whether or not an element correlates with the other elements in positive or negative way between the two coals or not at all.

The 16 elements in Figure V-2, ~~A to P~~ are listed in decreasing order of correlation (R) between the two data sets: Al (R=0.89), Ga (R=0.83), Cr (R=0.67), V (R=0.58), Ti (R=0.55), Ni (R=0.55), Zr (R=0.53), Cu (R=0.48), Ca (R=0.24), Rb (R=0.21), Ba (R=0.18), Mn (R=0.01), Co (R=-0.01), Pb (R=-0.12), Sr (R=-0.34) and S (R=-0.58). Ash (AH) is included at the end, Figure V-2, Q, and shows a correlation of 0.58.

Correlations of >0.50 and <-0.50 between the two data sets are considered significant. Those elements exhibiting correlations >0.50 include Al, Ga, Cr, AH, V, Ti, Ni, Zr and Cu. Sulfur is the only element which shows a large negative correlation (<-0.50). The remaining elements, Ca, Rb, Ba, Pb, and Sr, show relatively insignificant correlations ranging from 0.24 (Ca) to -0.34 (Sr).

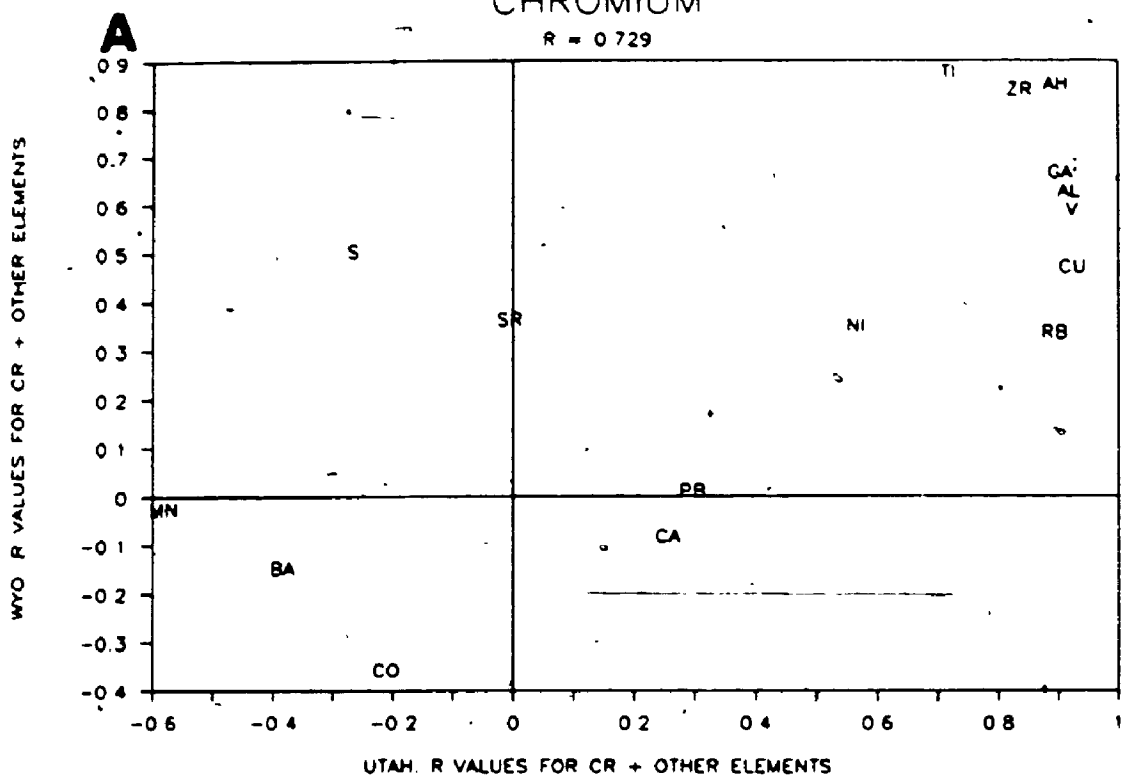
188

FIGURE V-2

A TO Q - GRAPHS OF THE CORRELATION COEFFICIENTS OF INDIVIDUAL ELEMENTS FOR THE UTAH AND WYOMING COALS TAKEN TOGETHER (SEE TEXT FOR EXPLANATION). CORRELATION COEFFICIENTS FOR THE TWO DATA SETS ARE SHOWN AT THE TOP OF EACH GRAPH. THE SOLID VERTICAL AND/OR HORIZONTAL LINES REPRESENT ZERO CORRELATION, WHERE APPLICABLE.

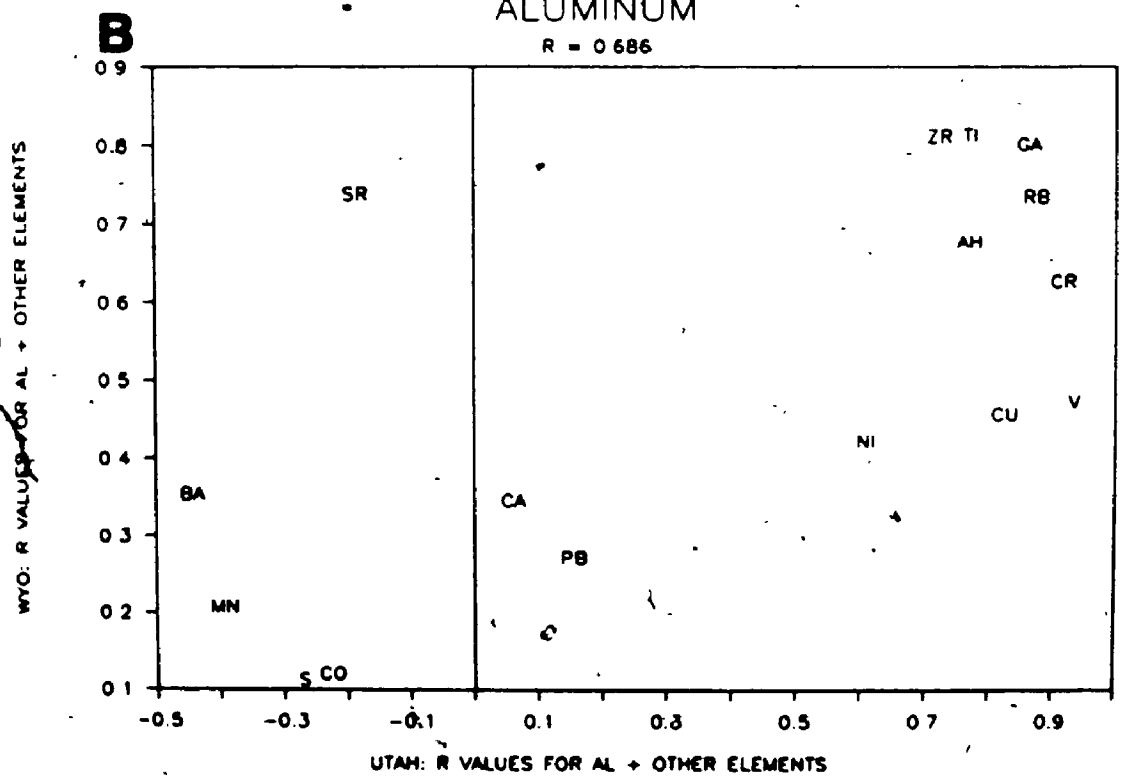
CHROMIUM

R = 0.729



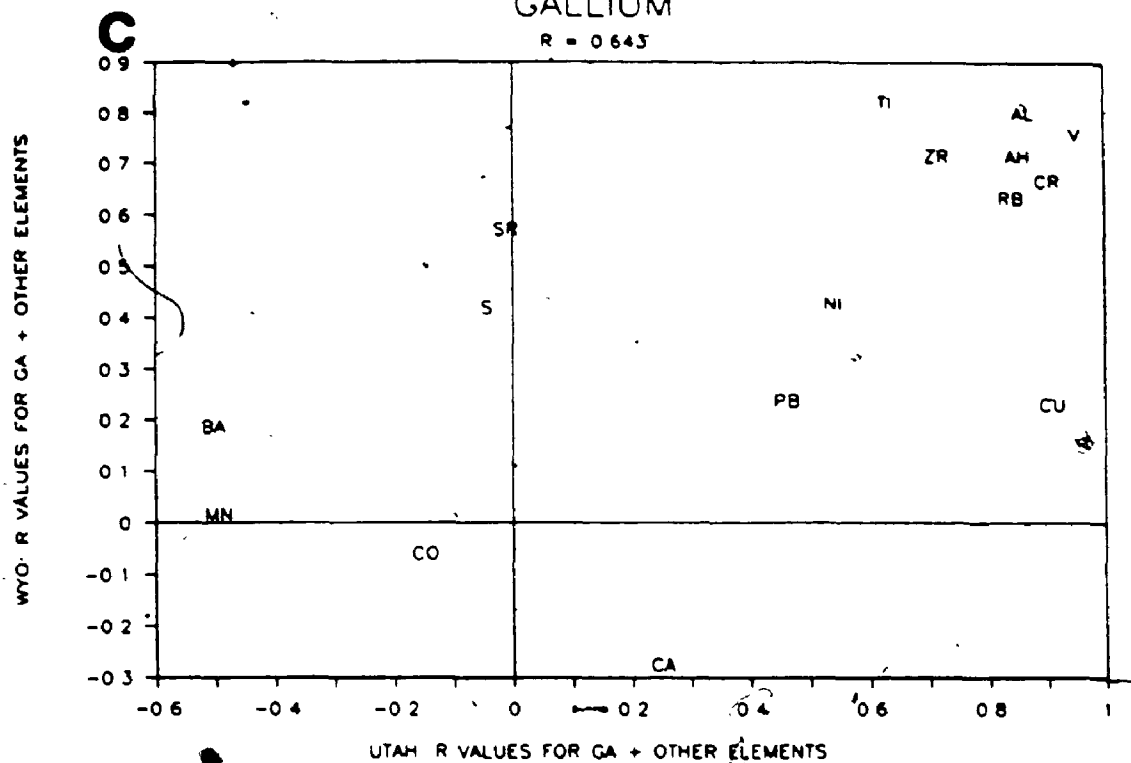
ALUMINUM

R = 0.686



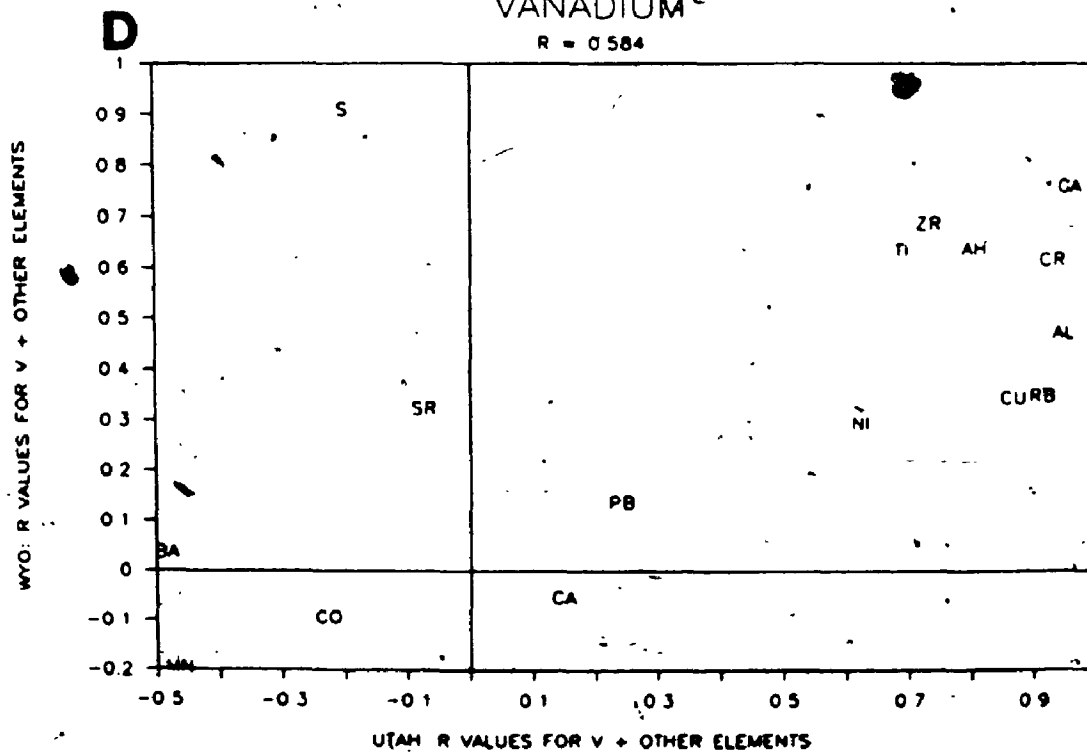
GALLIUM

R = 0.643



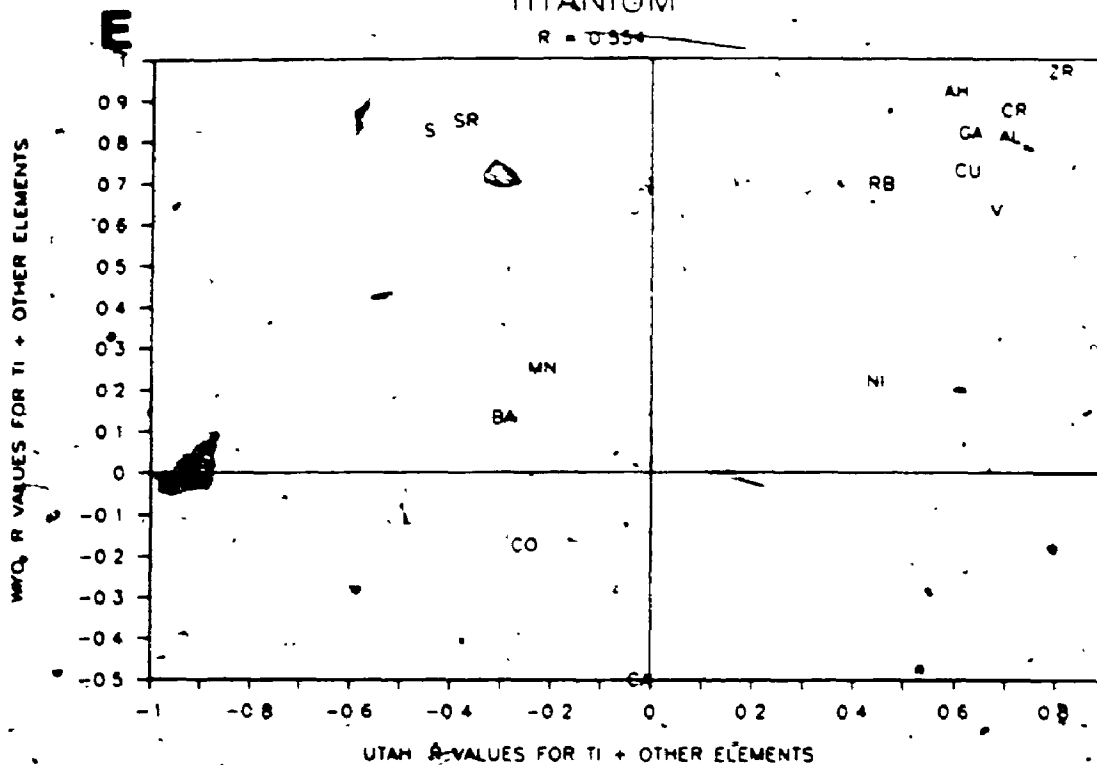
VANADIUM

R = 0.584



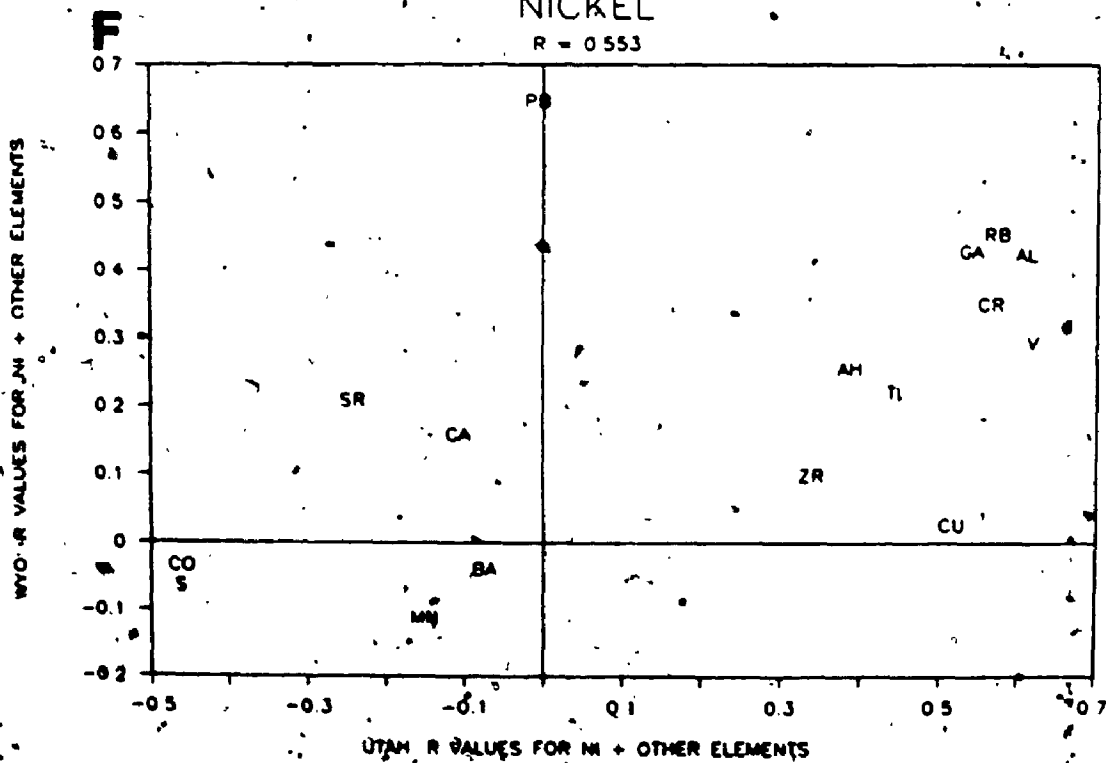
TITANIUM

R = 0.554



NICKEL

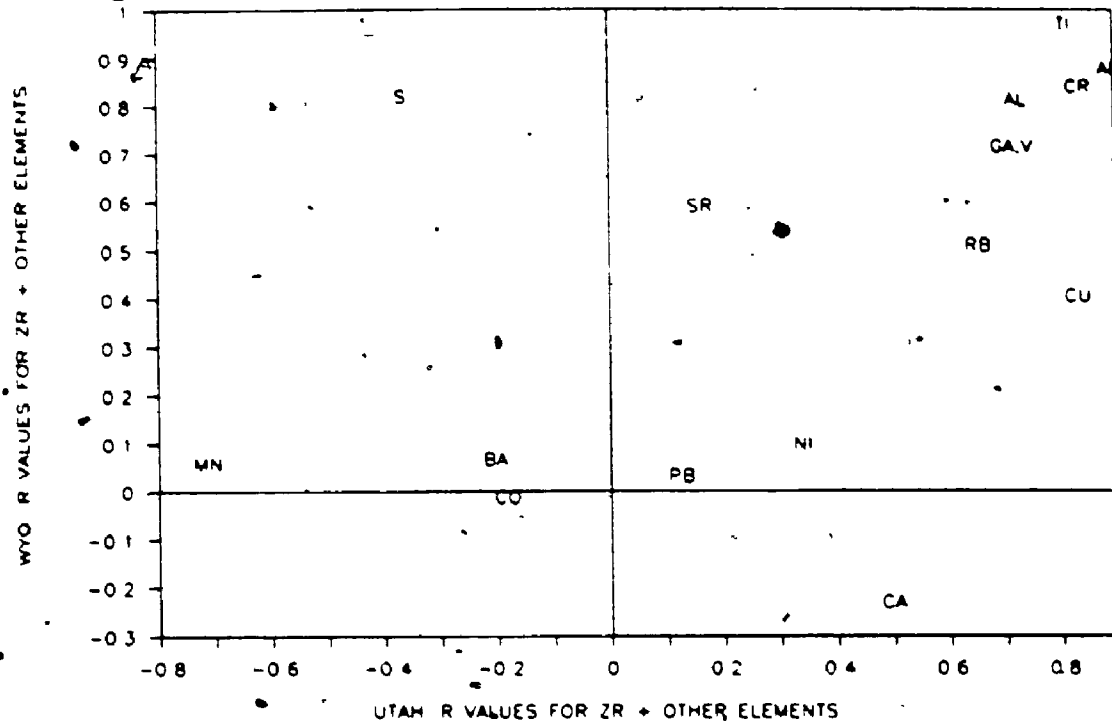
R = 0.553



G

ZIRCONIUM

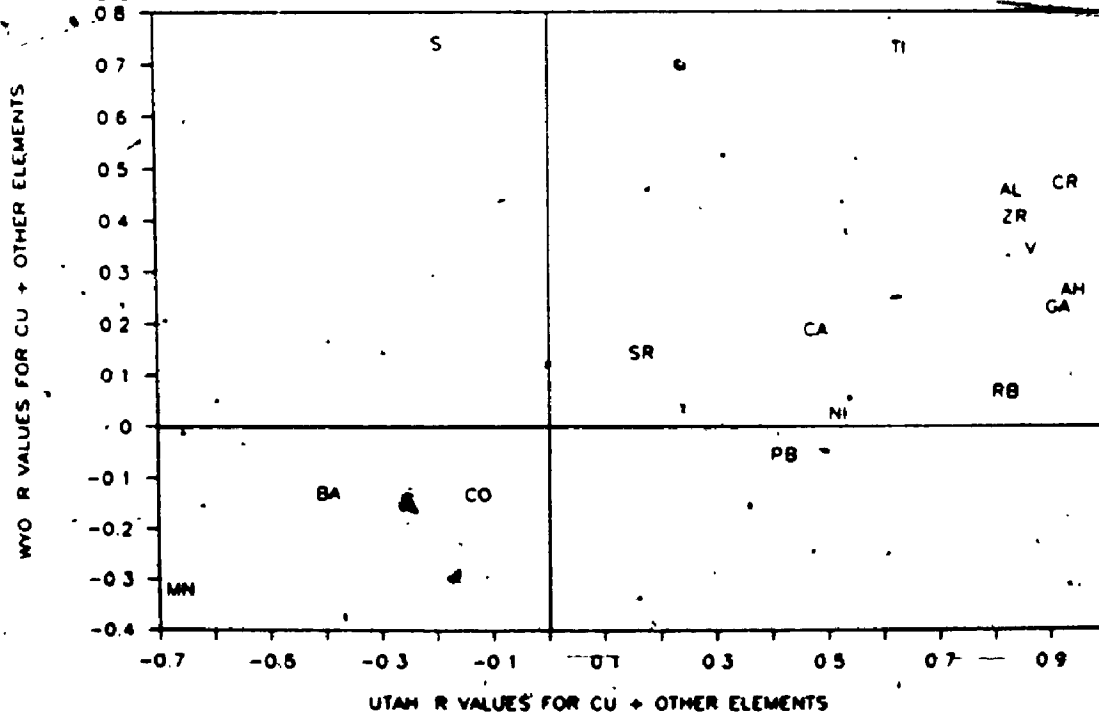
R = 0.526



H

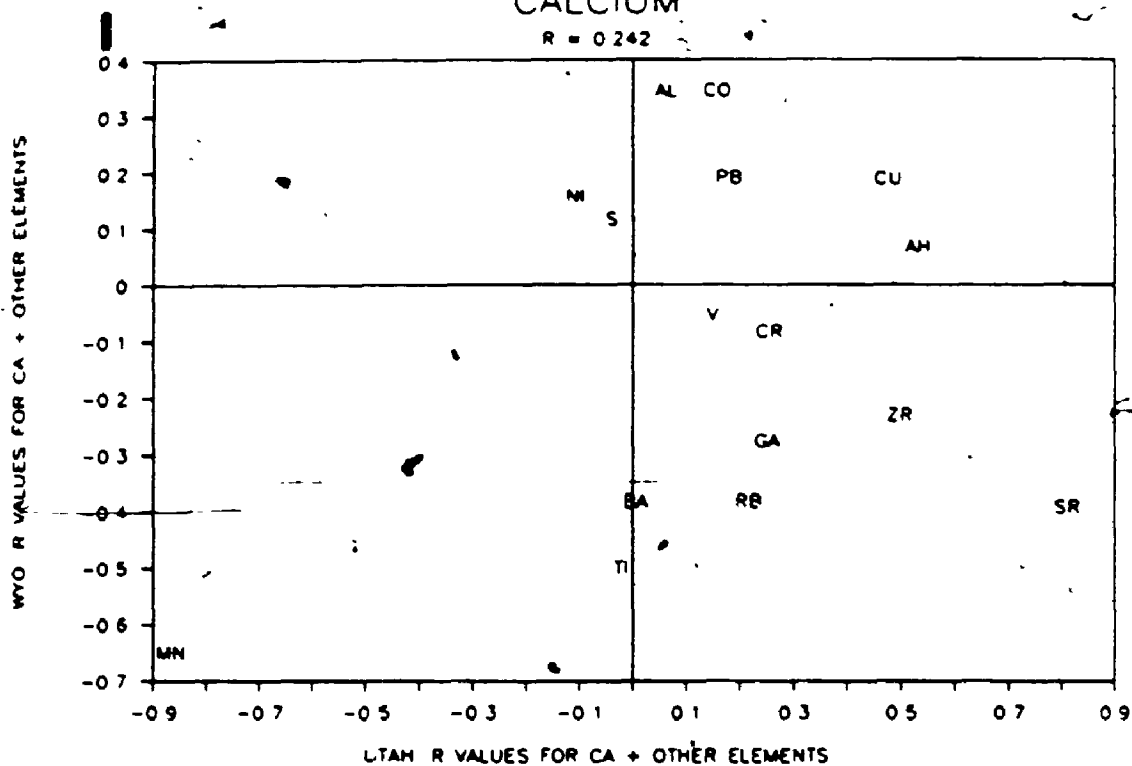
COPPER

R = 0.494



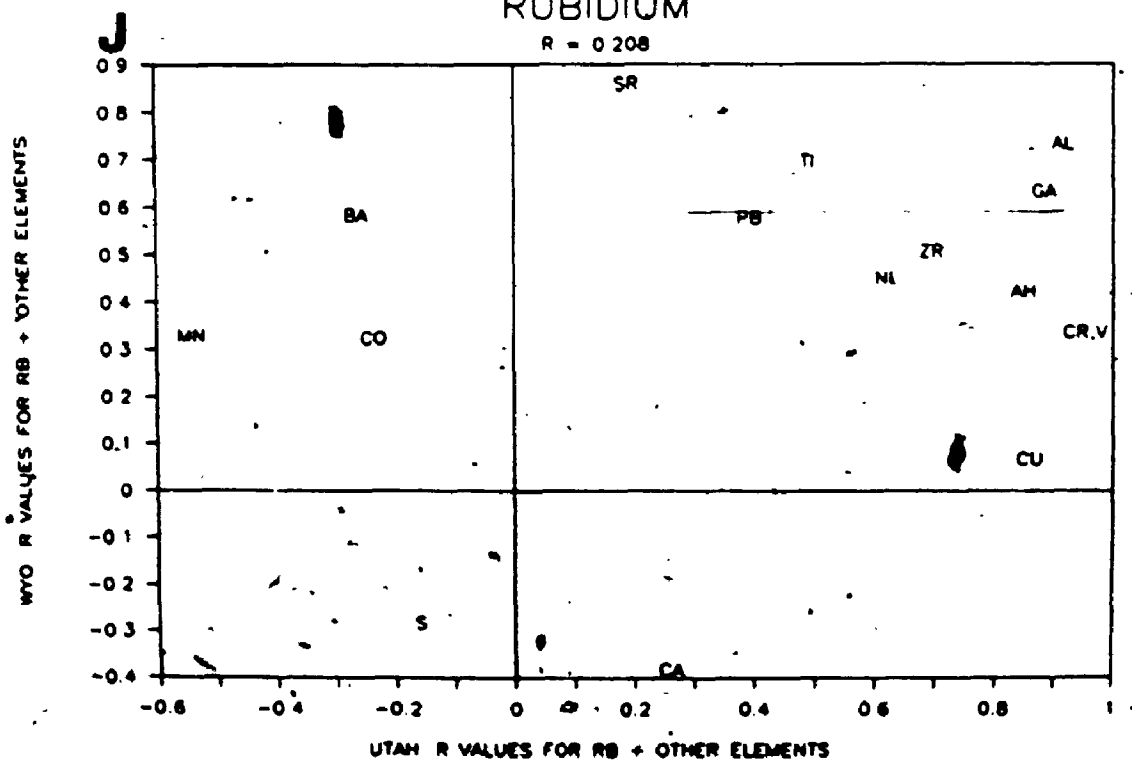
CALCIUM

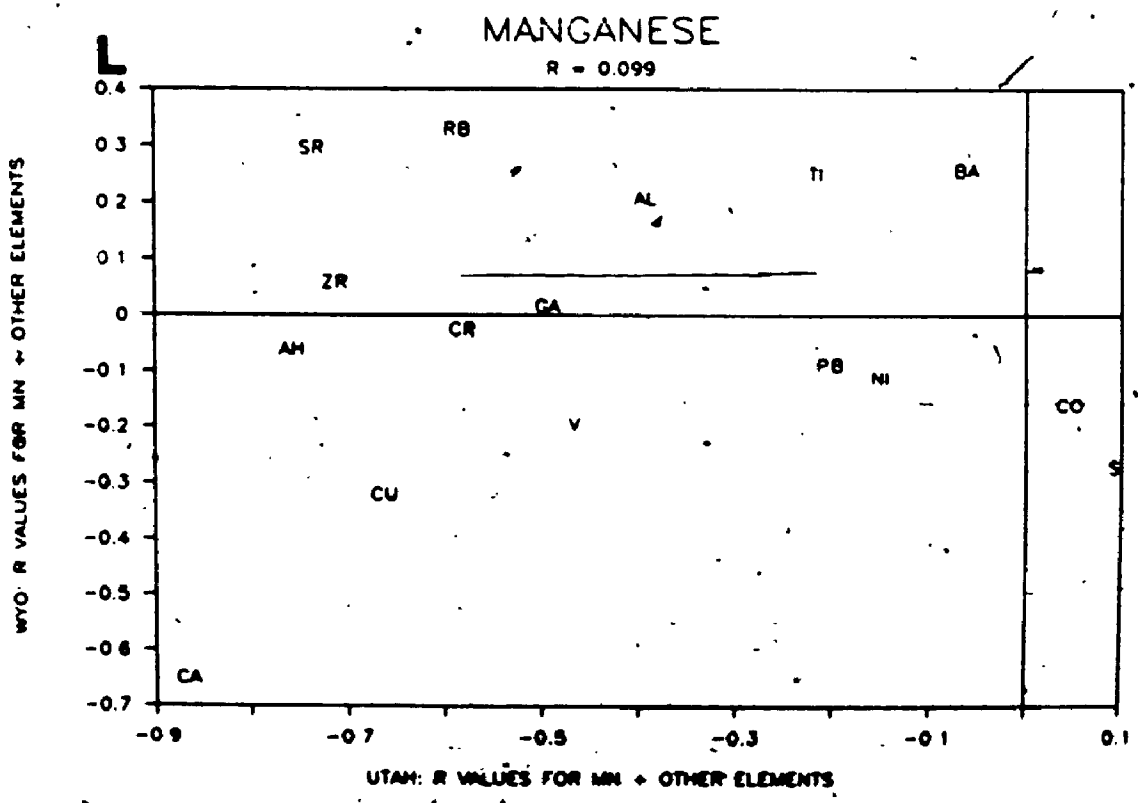
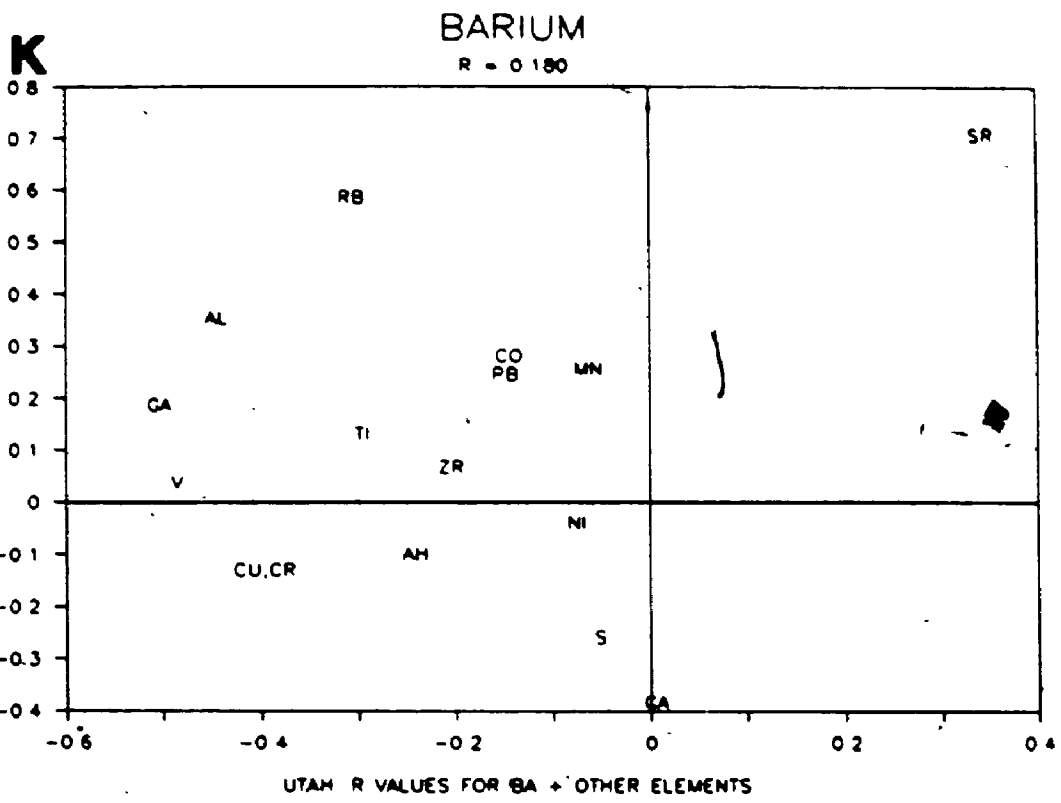
R = 0.242



RUBIDIUM

R = 0.208



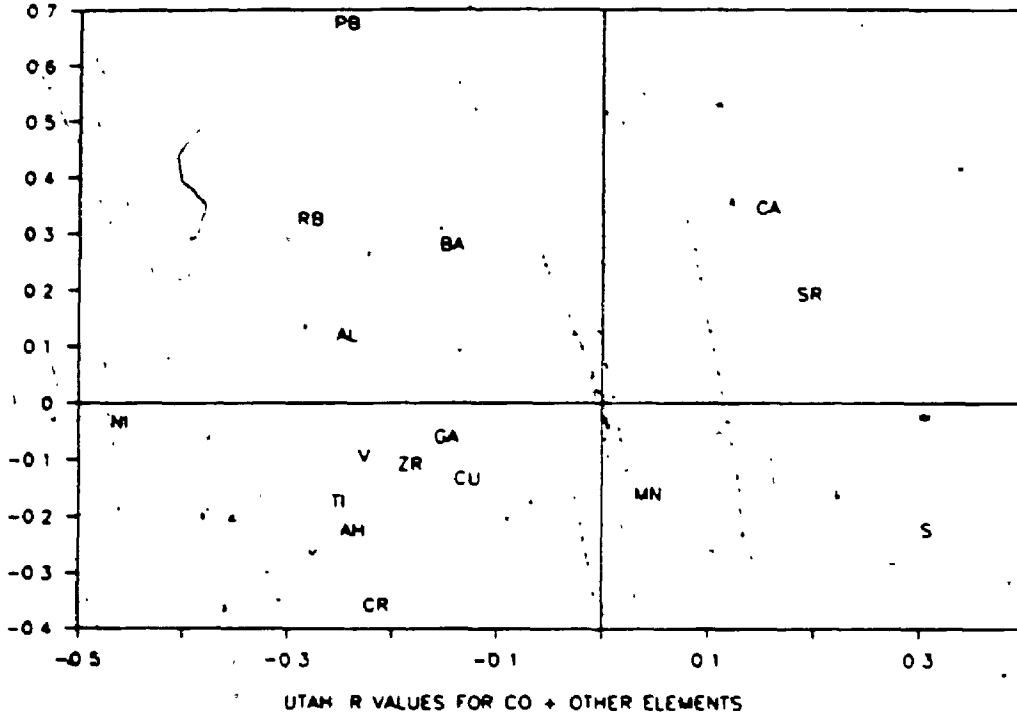


COBALT

R = -0.011

M

WYO: R VALUES FOR CO + OTHER ELEMENTS

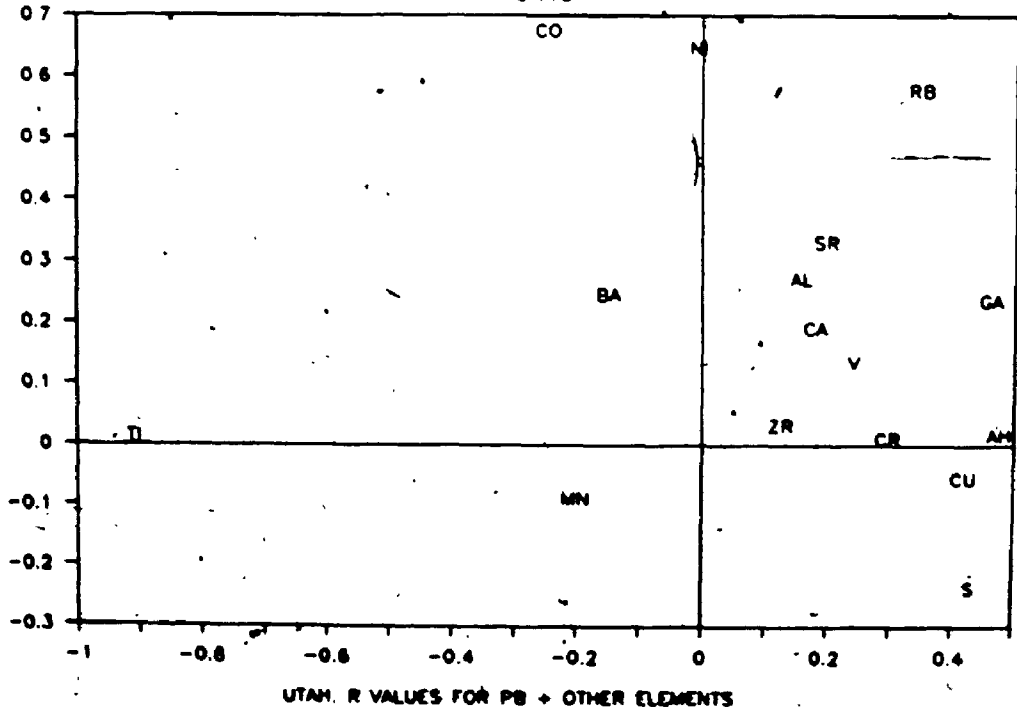


LEAD

R = -0.118

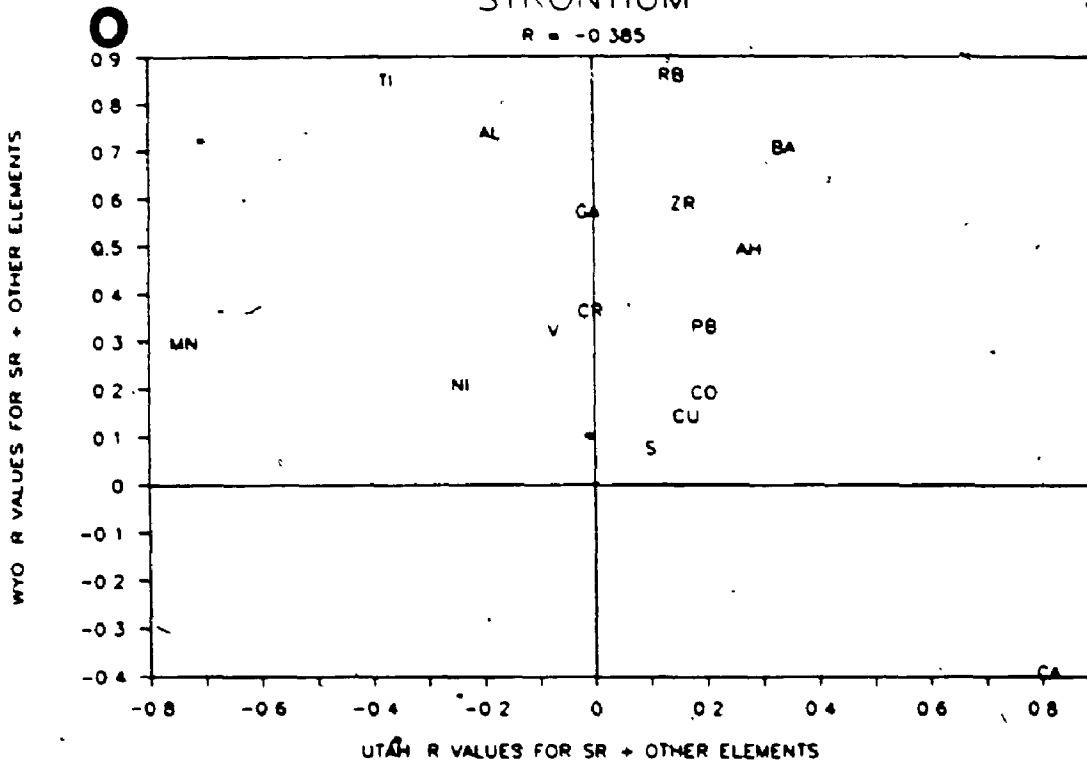
N

WYO: R VALUES FOR PB + OTHER ELEMENTS



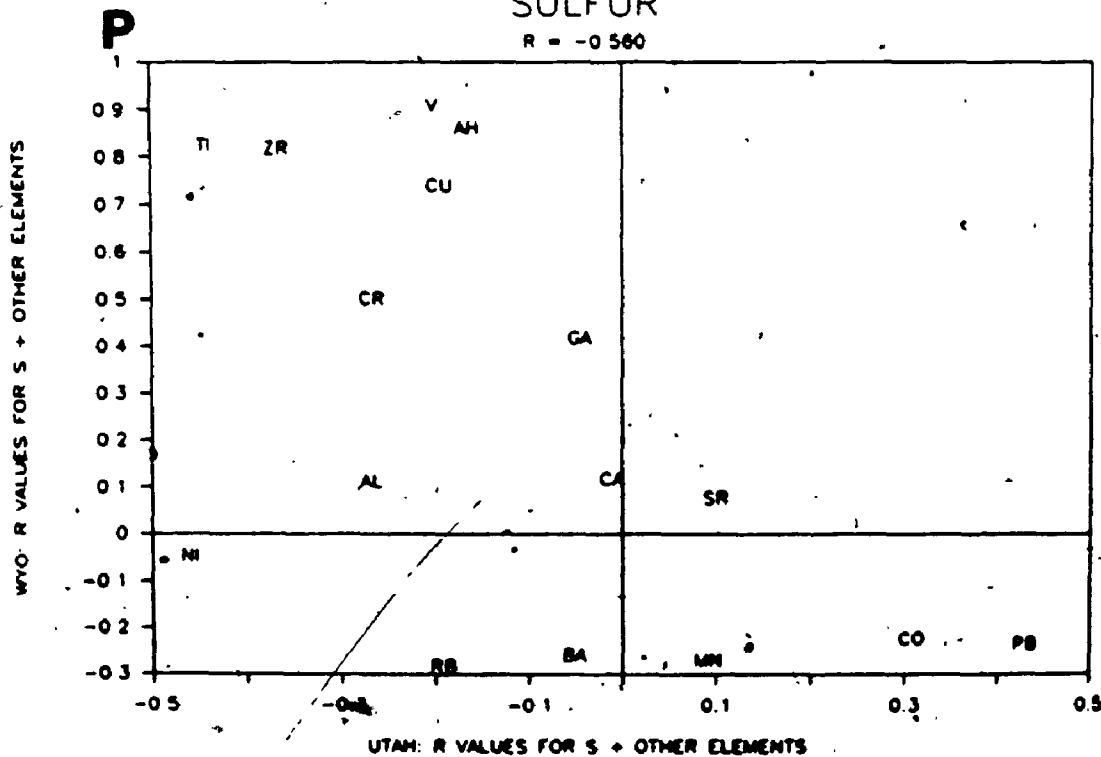
STRONTIUM

R = -0.385



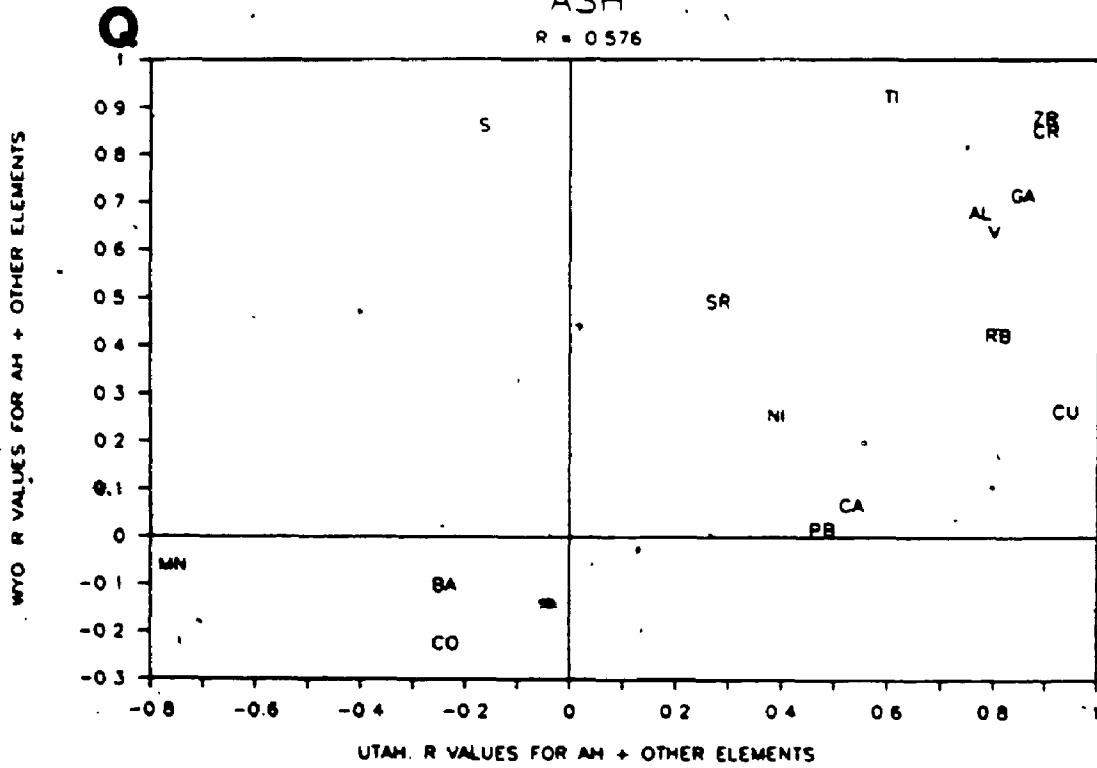
SULFUR

R = -0.560



ASH

R = 0.576



It should be noted that some of these correlation data are misleading owing to outliers (data points a considerable distance from the regression line, not shown in the plots). In fact, in some cases one or two data points have actually resulted in changing the sign (+ or -) of the correlation and/or significantly moving the value. For example, the relatively large negative correlations of Mn with most of the other elements in the Utah samples is responsible for a number of such problems. The Ca-plot would show a slight negative correlation if it were not for the position of Mn in the two data sets but instead the correlation is slightly positive. Calcium in the Mn-plot and Ti in the Pb-plot have similar effects. The reader will observe similar problems in other plots as well. Keep in mind that the correlation data are not being used to predict trends (as in regression analyses). The individual points, taken alone, are used to predict whether or not the elements have similar modes of occurrence in both coals. This type of graphic presentation makes comparisons easier than hunting through tables of data. Look, for example, at the V-plot which shows that V has the highest positive correlation with S in the Wyoming coal but a negative correlation with S in the Utah coal. This might imply that V in the Wyoming coal is contained in a sulfide phase but that it is either organically bound or in hydrolysates in the Utah coal. The latter is corroborated by the high V-Al correlation in the Utah samples.

CHAPTER VI: COAL UTILIZATION / FLY ASH; ENVIRONMENTAL CONSIDERATIONS

VI.1 INTRODUCTION

Concerns over the possible environmental impact resulting from increased coal usage have stimulated interest on the subject of coal geochemistry. Recent works invariably contain, somewhere in their introductory remarks, reference to the environmental risks associated with coal combustion as a function of increased usage. These opening remarks are typically followed by results of work aimed at characterizing the geochemistry of a given coal or coals but with little else but some references, if that, as to why/how coal utilization is environmentally harmful. However, this issue is central to the field of coal geochemistry and so, included here is a section discussing the fate of some of the more volatile and potentially harmful trace elements found in coal as well as the mechanisms by which they escape to the atmosphere during coal combustion. While this work does not take into account other types of harmful emissions, e.g., organic species, gases (SO_2 , CO_2), etc., associated with coal combustion, they are not forgotten. Many references on this subject can be found in a review article by Roy *et al.*, (1981), the results of some of these are summarized below and a new term is proposed to better describe the environmental hazards associated with coal utilization.

VI.2 THE PROBLEM

Given the present public opinion in North America against the use of nuclear power, it appears as though coal offers the only alternative to our ever growing energy demands. This is not to say, however, that coal is the best alternative. Obviously, the rate at which we use coal affects both the amount of waste produced as well as predictions of how long our resources will last. Klein, et al, (1975) estimated that the world coal consumption approached 3×10^9 metric tons in 1975. The National Coal Association predicted that the U.S. would double its utility (power) coal usage (from 4.4×10^8 to 8.5×10^8 metric tons/year) in the ten year period from 1976 to 1985 (Ondov, et al, 1979a). Furthermore, the President's National Energy Plan predicted that U.S. coal consumption would more than double again (to approximately 1.9×10^9 metric tons/year) between 1985 and the year 2000 (Adriano, et al, 1980). While some of this prognostication is a bit top heavy, the trend is definitely towards increased coal usage. As calculated here (from data in the U.N. Energy Yearbook, 1984), and shown in Table VI-1, world coal consumption approached 3.87×10^9 metric tons/year at the beginning of this decade and 6.81×10^9 metric tons of this (17.6%) was consumed in North America (U.S. and Canada). How will this rate of consumption affect the future of the environment and

TABLE VI-1

=====

COAL CONSUMPTION (1982) FOR THE U.S., CANADA AND THE WORLD
(CONSUMPTION=PRODUCTION+IMPORTS-BUNKERS-EXPORTS-CHANGES + STOCKPILES)

TYPE (MILLIONS OF METRIC TONS)

	TYPE (MILLIONS OF METRIC TONS)		TOTAL
	HARD COAL (>5700 CAL/GR)	SOFT COAL (<5700 CAL/GR)	
WORLD	2,763	1,104	3,868
U.S.	591	48	639
CANADA	21	20	41
U.S.+ CANADA (TOTAL)	612	68	681
% OF WORLD	22.2%	6.2%	17.6%

(COMPILED FROM DATA IN THE U.N. ENERGY YEARBOOK, 1984)

=====

TABLE VI-2

=====

COAL RESOURCES FOR THE U.S., CANADA AND THE WORLD

COAL TYPE (MILLIONS OF METRIC TONS)

	COAL TYPE (MILLIONS OF METRIC TONS)						TOTAL	
	PROVEN		RECOVERABLE*		ADDITIONAL		RESOURCES+	
	H	S	H	S	H	S	H	S
WORLD (1981)	920000	600000	515000	431000				
U.S. (1979)	223725	205113	125353	131750	472103	669321	361405	466411
CANADA (1981)			1607	4292	25687	35035	14451	21810
U.S.+ CANADA (TOTAL)								864077

* TOTAL CALCULATED AS, (RECOVERABLE)+0.5(ADDITIONAL).

+ RECOVERABLE ACCOUNTS FOR APPROX. 52% AND 68% OF THE PROVEN RESOURCES
IN THE CASE OF HARD (H) AND SOFT (S) COALS RESPECTIVELY.

(COMPILED FROM DATA IN THE U.N. ENERGY YEARBOOK, 1984)

when will the coal be gone?

VI.3 RESOURCES - CONSUMPTION - WASTE

Coal is a non-renewable resource, ergo the rate of usage and the amount of existing supply are intimately related when trying to determine how long it will last. Table VI-2 gives estimates of the coal resources remaining in the U.S., Canada, and the World (as compiled from data in the U.N. Energy Yearbook, 1984). From Table VI-2: "PROVEN" resources are known to exist; "RECOVERABLE" resources represent the amount of "PROVEN" resources which can be produced under current economic conditions; and "ADDITIONAL" resources are suspected to exist with a high degree of confidence. The recoverable resources account for approximately 52% and 68% of the proven resources for hard (H) and soft (S) coals respectively. Accordingly, it is assumed here that a conservatively proportionate amount (50%) of the additional resources are also recoverable. Based on these figures "TOTAL RESOURCES" are calculated as, $(\text{RECOVERABLE}) + 0.5(\text{ADDITIONAL})$. This figure amounts to 8.64×10^{11} metric tons of coal resources for North America.

Dividing the total resources (8.64×10^{11} metric tons) by the total yearly consumption (6.81×10^9 metric tons) we can predict that coal in North America should last for some 1,269 years at the present rate of consumption. As already

pointed out, coal usage is rising dramatically and this estimate is, at best, only an order of magnitude calculation. A better estimate (taking into account approximately doubling usage every 30 years) lies somewhere in the 200-300 year range.

Given the above estimates on resources and rate of consumption we can calculate the amount of waste that will be produced at the current rate of usage. These calculations are based on average values compiled from numerous studies of existing coal burning facilities, as follows:

1. Approximately 15% (World average) of all coal consumed is ash (this figure will undoubtedly increase as economic restraints force industry to use "dirtier" coals).
2. Approximately 98% (this ranges from 85% to 99.5%, see for example: Bertine and Goldberg, 1971; Lee, et al, 1975; Bolton, et al, 1975; and Ondov, et al, 1979b) of all ash is removed via cleaning devices of one type or another. The remaining 2% is emitted to the atmosphere.
3. Approximately 5% of the potentially harmful trace elements associated with coal penetrate emission control devices (see following discussion). This figure is much higher for elements such as Se

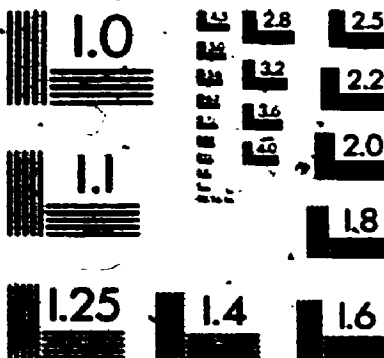
(30%) and Hg (90%) (see for example: Anderson and Smith, 1980; Andren and Klein, 1975; and Billings and Matson, 1972).

Applying the above to North America: 1.02×10^6 metric tons of ash are produced yearly and 2.04×10^6 metric tons are emitted to the atmosphere. Considering that 5.7x more coal is consumed worldwide than in North America: 5.11×10^6 metric tons/year of ash are produced worldwide and 1.16×10^7 metric tons/year of particulate matter is released to the atmosphere. Finally, by the time all the coal in North America (calculated total resources, Table VI-2) has been used up: 1.3×10^{11} metric tons of ash will have been produced and 2.59×10^9 metric tons of particulates will have been emitted to the atmosphere. Other predictions on particulate emissions (Campbell, et al, 1978) and ash produced (Adriano, et al, 1980) as a result of coal combustion are consistent with this study if differences in time and the type of coal usage are considered. These figures are probably quite conservative when one considers that in a country like China, which relies even more heavily on coal for energy, there are virtually no emission control standards! (W.S.Fyfe, personal communication). In one form or another, all of this ash must be dealt with as waste.

3

of/de

3



VI.4 MODE OF OCCURRENCE OF POTENTIALLY HARMFUL TRACE ELEMENTS IN COAL

The elements discussed here (Zn, As, Se, Cd, Sb, Hg and Pb) are potentially some of the most harmful trace elements associated with coal for two reasons: the way they react during coal combustion (their fate); and the fact that they are either known or highly suspected carcinogens and/or mutagens. The subject of toxicity is covered briefly in a later section. Natusch and Wallace (1974), Natusch (1978), Davison, et al, (1974) and Piperno (1975) and references within, cover the subject in detail. Presently we will examine some of the characteristics of the common compounds of these elements which determine their mode of occurrence in coal and ultimately their fate during combustion, there are a number of similarities.

First, the elements in question characteristically occur in the inorganic fraction of coal, i.e., they are part of the mineral matter (Gluskoter, et al, 1977; Gluskoter, 1975; Ruch, et al, 1973). Gluskoter (1975) presented data showing that Zn, As, Cd, Hg and Pb were among the elements with the highest inorganic affinities in four sets of coals from geographically, and depositionally, different settings (Se and Sb to a lesser degree).

Second (and the reason for "First", above), these elements occur mainly as sulfides in coal (chalcophile, Goldschmidt,

1937). This similarity stems mainly from the availability of reacting ligands in the peatland environment and the stability of the compounds formed. All swamp environments contain abundant organic ligands and are conducive to the growth of sulfate reducing bacteria which ultimately result in the production of sulfide ($H_2S \rightarrow HS^- \rightarrow S^{--}$). The organic ligands and the sulfide compete for the chalcophile elements. Partitioning of the element depends, to a large degree, on the concentrations of the two ligands. The stabilities of the compounds which form are a function of the affinities of the two ligands for the metals. Zubovic (1976) uses the example of the affinity of a certain amino acid and sulfide for Cu. He points out that the dissociation constant (K_{sp}) for the Cu-sulfide is 10^{-44} while that of the Cu-amino acid is 10^{-17} , therefore Cu-sulfide is by far the dominant species and Cu-amino acid should only form (appreciable amounts) after the majority of the sulfide has been removed.

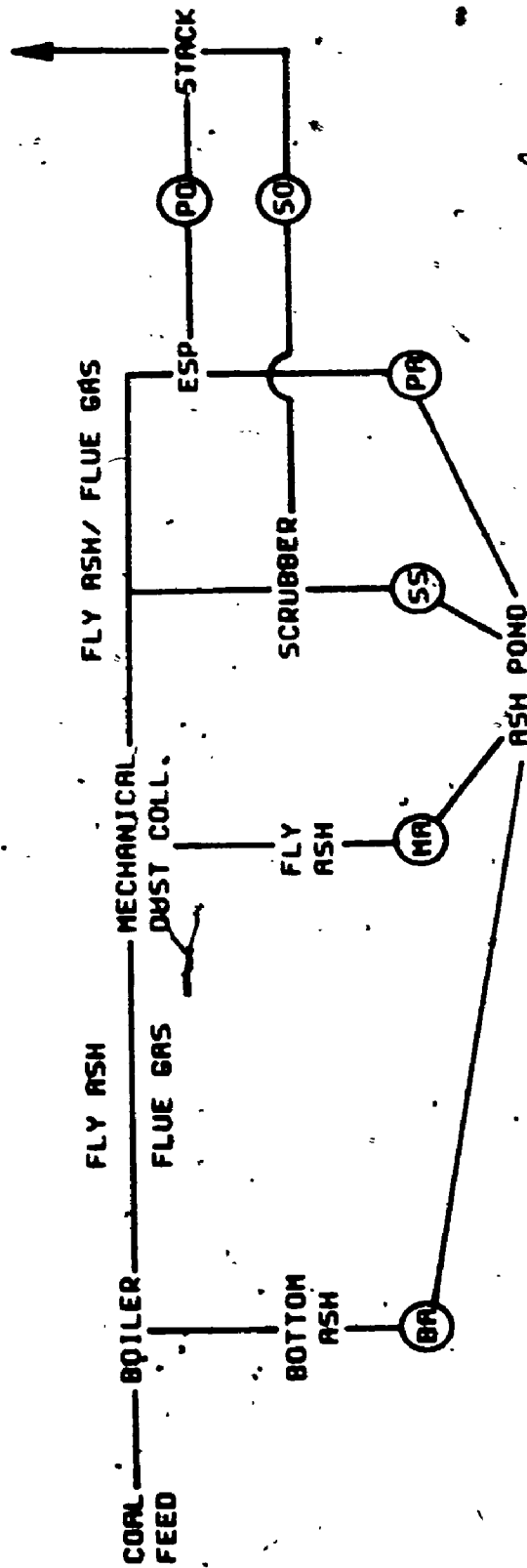
Third, the common compounds of the metals in question, as oxides and sulfides, are volatilized well below the temperatures of coal combustion (Davison, et al, 1974). The result being that the metals are released into the flue gases during combustion, i.e., separated from the coal.

VI.5 ELEMENT PARTITIONING: THE COAL COMBUSTION FACILITY

FIGURE VI-1

SCHEMATIC OF A COAL COMBUSTION FACILITY. PARTITIONING OF ELEMENTS CONTAINED IN THE COAL TAKES PLACE IN THE BOILER (BA), MECHANICAL DUST COLLECTOR (MA), SCRUBBER (SS), AND ELECTROSTATIC PRECIPITATOR (PA) (SEE TEXT). PARTICULATES REACHING THE PRECIPITATOR OUTLET (PO) AND SLURRY OUTLET (SO) ARE EMITTED TO THE ATMOSPHERE. ADAPTED FROM KAAKINEN, 1975)

SCHEMATIC OF A COAL COMBUSTION FACILITY



(ADAPTED FROM KARKINEN, 1975)

Coal combustion facilities (e.g., power plants) act as point sources for redistributing and concentrating the trace elements in coal. Figure VI-1 (adapted from Kaakinen, et al, including abbreviations, 1975) is a schematic of a coal combustion facility which illustrates the locations where trace elements in coal are partitioned during the combustion process.

The first partitioning takes place in the boiler where those elements not volatilized during combustion are converted to bottom ash (BA), or slag, and subsequently separated from the volatilized elements which move downstream along with the fly ash and flue gases. The mixture of fly ash and flue gases then go through a second partitioning in the various emission control devices. Material retained here as mechanical dust collector ash (MA), scrubber slurry (SS) and precipitator ash (PA) is separated from that fraction which passes all emission control devices and is emitted to the atmosphere at the precipitator outlet (PO) and the slurry outlet (SO). Kaakinen, et al, (1975) determined the concentration of Zn, As, Se, Sb, Hg and Pb in fly ash collected at the various partitioning sites. The sequence, BA -> MA -> PA -> PO/SO in Figure VI-1 represents increased distance from the boiler, i.e., downstream direction. The concentrations of the elements in the sequence (BA -> SO) increases from 58 -> 600 ppm for Zn, 15 -> 280 ppm for As, 7.7 -> 440 ppm for Se, 2.8 -> 22 ppm for Sb and 5 -> 340 ppm

for Pb. Only Hg did not increase because it was not detected in either the PO or SO, presumably because it escaped in the gas phase (see for example, Billings and Matson, 1972; Kalb, 1975; Bolton, et al, 1975). This phenomenon is discussed in the next section.

Klein, et al, (1975) noted that the elements could be separated into three groups according to the way they react, or are partitioned, during coal combustion (using the work of Goldschmidt, 1937, but being specific for the materials found in coal burning plants). Group I includes the lithophile elements (e.g., Al, Ca, Fe, Mg, Si, etc.) which are not volatilized below the temperatures of coal combustion (approximately 1550°C) and therefore are retained, for the most part, in the boiler as slag, or bottom ash (BA). Group I elements are enriched in the slag over the coal, but are not appreciably partitioned between slag and fly ash nor between outlet and inlet ash (ash collected prior to and just after scrubbers and electrostatic precipitators, Fig. VI-1). Group II elements (e.g., As, Cd, Sb and Pb) are composed mainly of the chalcophile elements which are volatilized during combustion. These elements are not enriched in the boiler slag relative to the coal but are preferentially concentrated in the inlet ash relative to the slag and in the outlet ash relative to the inlet ash. Group III elements (e.g., Hg and Se) are almost completely converted to the gas

phase and therefore are not partitioned, nor removed, by any of the emission control systems.

VI.6 MECHANISMS OF FLY ASH FORMATION

The change in trace element chemistry of fly ash with increased distance from the combustion chamber, as discussed above, is partially a function of the ways in which fly ash forms. Smith, et al., (1979) proposed three different mechanisms of formation, noting that each contributes some component to the end product. Two of these methods include: homogeneous nucleation of volatilized compounds (0.01 microns) followed by coagulation into larger particles of homogeneous chemistry; and condensation of volatilized compounds onto entrained particles originally in the coal, e.g., soot and sub-micron sized mineral matter. Neither of these appears to be a major contributor to the bulk of the fly ash. Fisher et al., (1976) and Page et al., (1979) have shown that fly ash is not homogeneous chemically, ruling out the process of homogeneous nucleation as a major contributor to the bulk of the fly ash. As for the second case above, its importance lies in the amount of sub-micron sized mineral matter in a given coal, hence this method of formation will vary in importance from one coal to another. A third mechanism of fly ash formation proposed by Smith et al., (1979) appears to offer the most plausible explanation of formation considering the observed chemistry of fly ash.

This method involves the coagulation and condensation of volatilized compounds on the surfaces of particles which have formed by the bursting of initial grains due to rapid gas release in the high heat of combustion. This method explains how/why ash cores are chemically similar to slag (mainly lithophile) while the rims are composed mostly of volatile compounds (chalcophile).

Figure VI-2 schematically summarizes the process of fly ash formation and shows how the trace elements in coal are partitioned into slag, fly ash and vapour. In the combustion chamber temperatures are such (1550°C) that volatile compounds are released as gases, simultaneously fly ash is formed. Compounds meta-stable at these temperatures (lithophile elements) remain as slag. Flue gases begin to cool with increased distance from the boilers until some of the volatilized compounds (chalcophile) oxidize to more stable forms. These compounds condense (coagulate) on the surfaces of entrained fly ash. Finally, the most volatile of the compounds remain in the vapour phase, never reaching the conditions necessary for condensation. What does all this mean to the overall concentration and distribution of trace elements on fly ash?

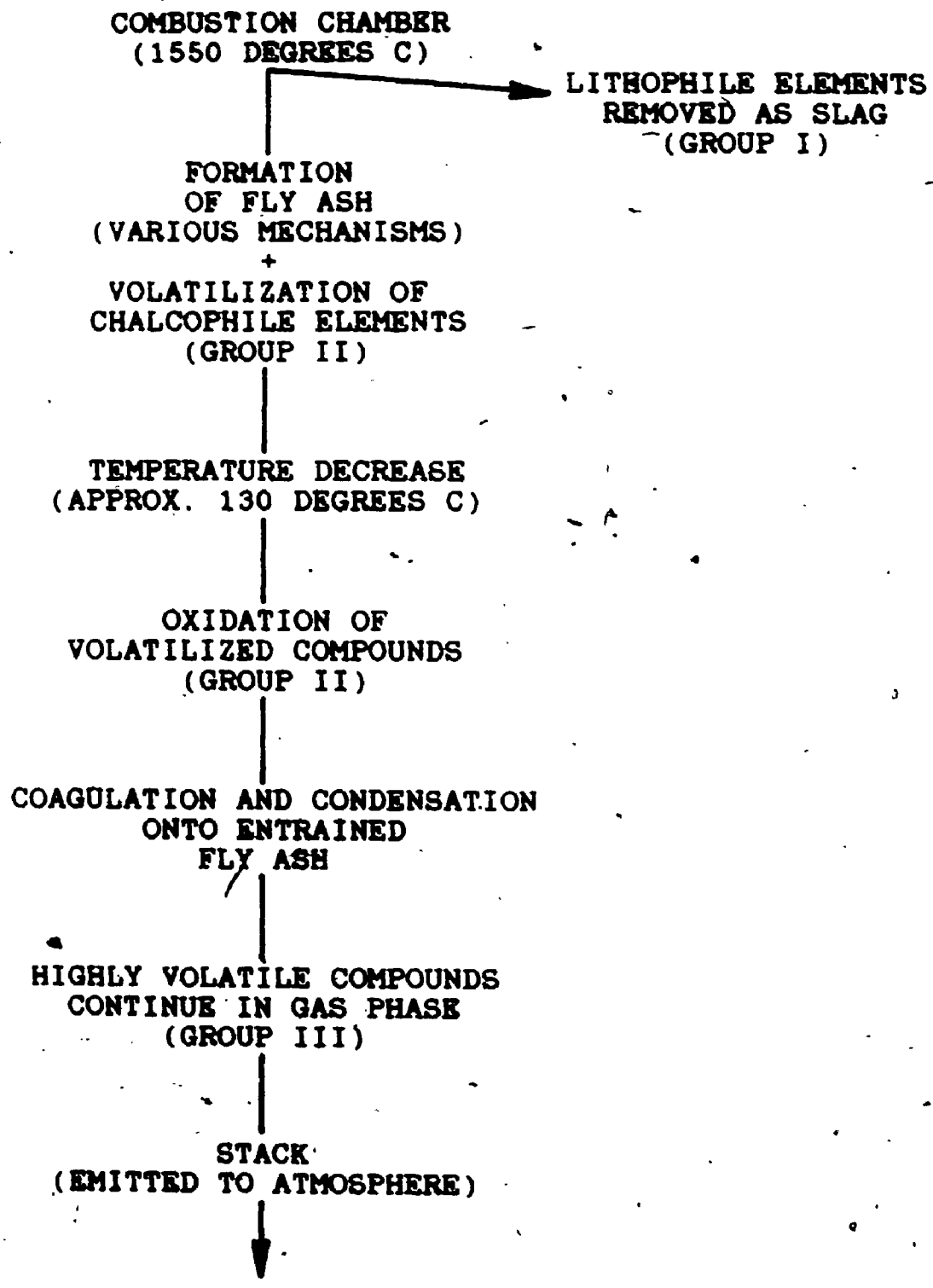
VI.7 "DANGEROUS" CHARACTERISTICS OF FLY ASH

Mechanisms of fly ash formation and the fact that the

FIGURE VI-2

SCHEMATIC SHOWING PARTITIONING OF THE ELEMENTS AND
DEVELOPMENT OF FLY ASH IN A COAL BURNING FACILITY
(ADAPTED FROM SMITH, 1979).

SCHEMATIC SHOWING PARTITIONING OF THE ELEMENTS AND DEVELOPMENT OF FLY ASH IN COAL BURNING FACILITIES.



potentially harmful trace elements associated with coal are volatilized under the conditions of coal combustion combine to impart a "dangerous" character to fly ash, to wit, potentially harmful elements are preferentially concentrated on the surface of the smallest sized fly ash. Simply, volatilized compounds will condense on the surfaces of particles with the highest surface area to volume ratios, i.e., the smallest particles (a fact of particle physics). This is best illustrated by looking at the concentrations of the various elements of size classified (sorted) fly ash as well as concentrations changes from the surface towards the center of the particles, i.e., distribution within the sample.

Natusch et al. (1974) determined the concentrations of a number of elements on size classified fly ash. They found that for particles of 74 microns and greater, those easily retained in the plant by cleaning devices, the concentrations of the elements (in ppm) were Zn (500), As (180), Se (<12), Cd (<10), Sb (1.5) and Pb (140) while the concentrations of the same elements on particles 1-2 microns in size, those escaping to the atmosphere, were Zn (13000), As (1700), Se (59), Cd (35), Sb (53) and Pb (1600). Coles, et al., (1979) examined trace element enrichment ratios (relative to Ce, which remained constant in all size fractions) for Zn, As, Se, Cd, Sb, and Pb in size classified fly ash and found that the larger particles (18.5 microns)

had trace element concentrations consistent with the immobile elements (approximately 1:1). Smaller particles (2.4 microns), however, had enrichment ratios ranging from a low of 4.7x for Cd to a high of 25x in the case of Se.

The relationship between particle size and element concentrations as a function of location within a power plant was shown by Kaakinen, et al, (1975). He plotted enrichment ratios (relative to Al) as a function of distance from the combustion source, i.e., BA -> MA -> PA -> PO -> SO (see Fig. VI-1 for sample locations). This sequence would also represent decreasing particle size. Enrichment ratios for Pb, As, Zn and Sb were <1 for the BA and MA but increased rapidly (>1) for PA, PO and SO with the largest ratios, >4, in the SO.

While overall trace element concentrations increase with decreasing particle size there appears to be a limiting size, above and below which there is relatively little variation. This relationship is illustrated diagrammatically in Figure VI-3. The limiting size lies somewhere between 1 and 10 microns (Campbell, et al, 1978; Smith, et al, 1979). Smith, et al, (1979) places this critical size at approximately 3.0 microns noting that virtually no change in chemistry is observed in particles with diameters below 1 micron and only slight changes are detected on particles greater than 10 microns in diameter.

FIGURE VI-3

SCHEMATIC SHOWING THE RELATIONSHIP BETWEEN PARTICLE SIZE AND TRACE ELEMENT CONCENTRATION FOR PARTICULATE MATTER COLLECTED FROM A COAL BURNING FACILITY (FLY ASH). CONCENTRATIONS OF THE TRACE ELEMENTS INCREASES DRAMATICALLY ON PARTICLES <10 MICRONS IN DIAMETER. BELOW .1 MICRON THERE IS LITTLE CHANGE.

(ADAPTED FROM SMITH, ET AL, 1975)

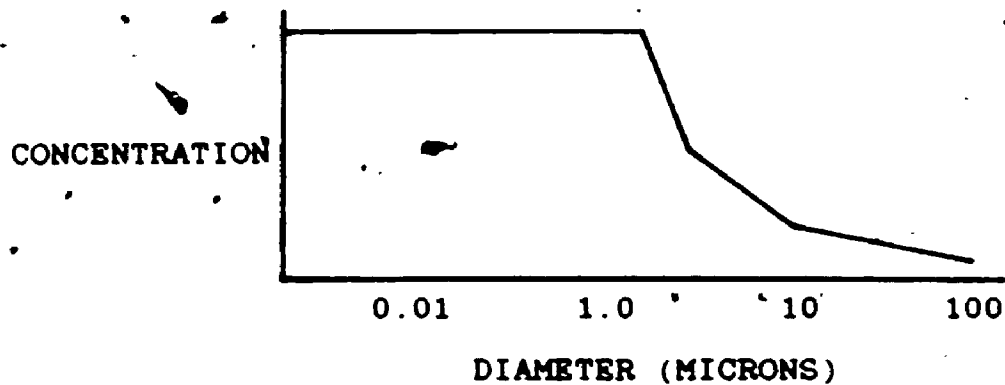
FIGURE VI-4

SCHEMATIC SHOWING THE CONCENTRATION OF TRACE ELEMENTS AS A FUNCTION OF DEPTH BELOW THE SURFACE FOR PARTICULATE MATTER (FLY ASH) FROM A COAL BURNING POWER PLANT. THE MAJORITY OF THE TRACE ELEMENTS ARE CONCENTRATED IN THE UPPER 500 ANGSTROMS OF THE PARTICLE.

(ADAPTED FROM LINTON, ET AL, 1976)

FIGURE VI-3

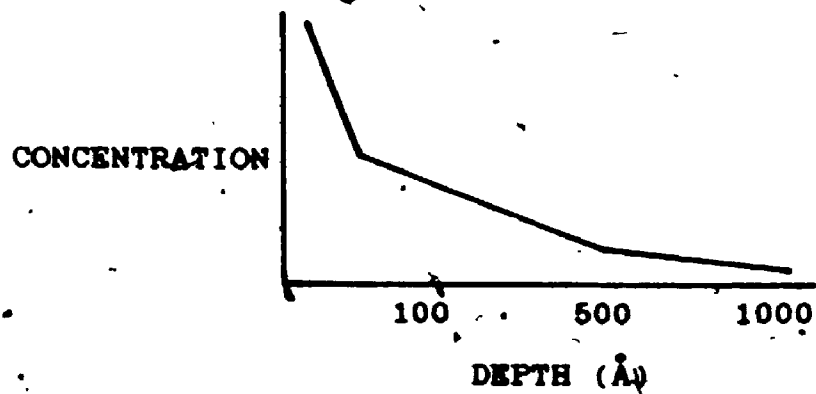
(ADAPTED FROM SMITH, 1975)



=====

FIGURE VI-4

(ADAPTED FROM LINTON, 1976)



The concentrations of various elements as a function of depth below the surface of the fly ash was investigated by Linton, et al., (1976). They found a dramatic decrease in the concentrations of surface predominant elements with depth (Figure VI-4). In fact, the bulk of most of the elements discussed was contained in the outer 500 Angstroms of the surface and as much as 80% of some of the elements were concentrated in the upper 1000 Angstroms.

Further evidence of increased concentrations of trace elements with decreasing size comes from enrichment ratios as a function of specific surface area (surface area to volume ratio). Kaakinen, et al., (1975) found that enrichment ratios for the elements Zn, As, Sb and Pb increased as the specific surface area of the particles increased (i.e., with decreasing size) from <1 to >5 m²/g. The larger particles, for example material collected in the BA and MA had ratios of 0.38x and 1.27x respectively and represented the largest particles (lowest specific surface area) while PA, 3.07x and PO, 4.8x had the largest enrichment ratios and represented the smallest particles (largest specific surface area).

The bottom line particles which are emitted from coal combustion facilities (<3 microns) carry with them unusually high concentrations of potentially harmful trace elements as

surface coatings. The high specific surface area of the particles provide an immense potentially reactive surface area once the particles have found their way into the environment.

VI.8 HEALTH CONSIDERATIONS

The same particles which penetrate emission control devices also penetrate the farthest into the human respiratory system when inhaled. The amount of inhaled material retained in the various areas of the respiratory system is determined by the size of the particles.

Figure VI-5 (adapted from Natusch, et al, 1974) shows the depositional efficiencies (% deposited) as a function of particle diameter for the three major areas of the respiratory system: pulmonary (P); tracheobronchial (T); and nasopharyngeal (N). The nasopharyngeal area is very efficient at removing particles larger than 10 microns and will even filter, from inhaled air, the majority of particulates in the 3 micron range. The tracheobronchial region can remove a maximum of 35% of the particulates as small as 0.01 micron. Material deposited in these two areas is passed quickly (within hours) to the pharynx via cilia action and then to the stomach (by swallowing). Only 5%-15% of the trace elements associated with the inhaled particles is absorbed into the blood through the stomach wall

81

FIGURE VI-5

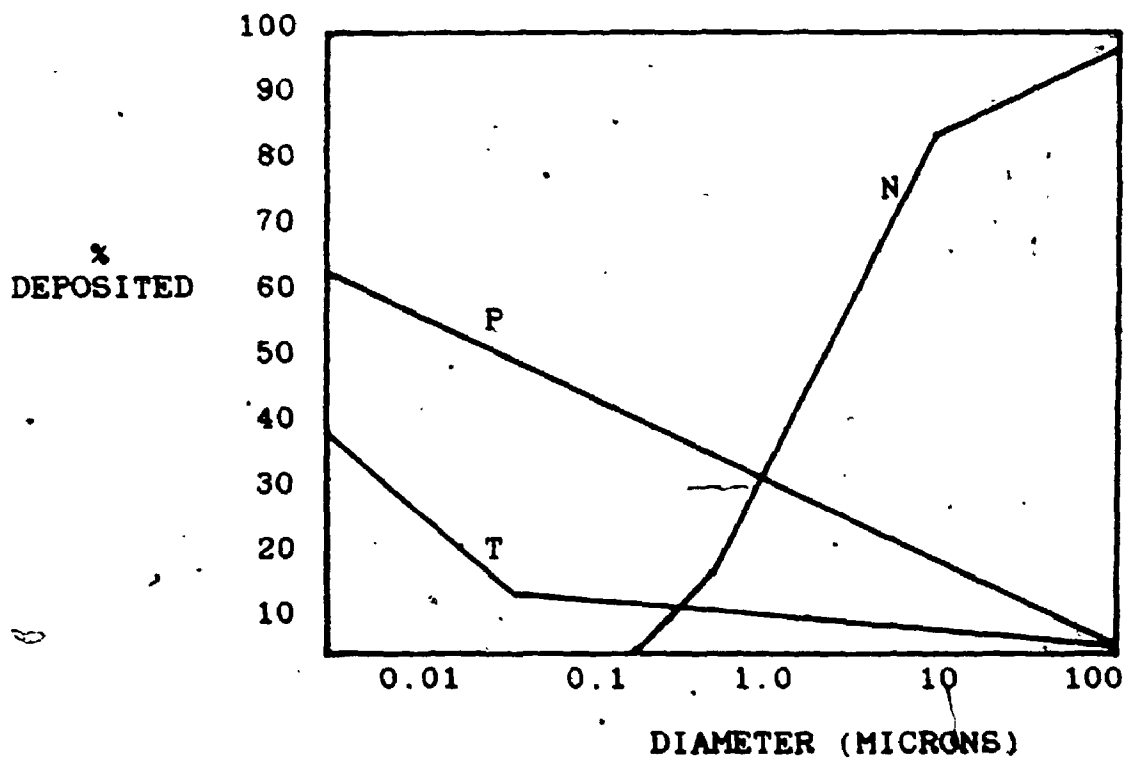
GRAPH SHOWING THE PERCENT OF INHALED PARTICULATES RETAINED (DEPOSITIONAL EFFICIENCIES) IN THE VARIOUS AREAS OF THE RESPIRATORY SYSTEM AS A FUNCTION OF PARTICLE SIZE:

N - NASOPHARYNGEAL,
T - TRACHEOBRONCHIAL,
P - PULMONARY.

(ADAPTED FROM NATUSCH, 1974)

DEPOSITIONAL EFFICIENCIES

(ADAPTED FROM NATUSCH, 1974)



(Natusch, et al., 1974; Piperno, 1975).

The pulmonary region, however, is capable of retaining between 30% and 60% of the sub-micron sized particulates which are inhaled. Residence times in this region range from weeks to years, during which time particulates are in direct contact with the alveolar membrane which separates the inhaled air from the blood. Here, as much as 80% (in the case of Pb) of the harmful trace elements associated with the particulates can be absorbed into the blood. In addition, many of the elements are also cytotoxic to the alveolar macrophage which is responsible for detoxification of the lungs against inhaled particles, i.e., the danger is twofold (Natusch, et al., 1974; Piperno, 1975; Aranyi, 1979).

VI.9 SUMMARY: A NEW TERM

It would appear from the above discussion that assessing the bulk geochemistry of coal and/or fly ash collected in coal burning facilities only in part identify the environmental hazards associated with coal utilization for the following reasons (Natusch, et al., 1974):

1. Bulk analyses of fly ash collected by emission control devices underestimates the amounts of the most toxic trace elements being emitted to the

19

Atmosphere.

2. The preferential concentration and surface predominance of toxic trace elements on submicron sized fly ash increases their potential environmental danger.

In addition, 100% of the potentially harmful elements found in coal are released into the environment in one form or another (e.g., slag or fly ash) and all of this material is potentially dangerous if not managed properly.

Given the above, it is time to coin a new term which more correctly identifies the environmental hazards associated with coal utilization. The "Effective Coal Concentration (ECC)" of an element is herein defined as "The total amount of a given element contained in all the coal consumed in a given year". This is, in effect, the amount of the element which must be dealt with as waste due to coal utilization.

Obviously, this term has little meaning on a local scale, i.e., World averages of trace elements in coal are much different than for local and/or regional coal deposits. For that reason it would be convenient to assign an ECC value to each large coal deposit now being mined as a major source of fuel coal. These figures could be used to anticipate environmental problems of waste disposal as well as to

predict the effects of increased coal usage in a given area, e.g., on a regional basis (I'm sure the Medical Sociologists and Geographers could find some interesting correlations between diseases, deaths and coal usage). Once these figures were compiled, not an awesome task in this age of computers, individual coal burning facilities could easily assess their contribution to the waste problem by calculating their own ECC output based on tonnages of coal burned from various deposits. This index would change with time as a function of the types of coal burned.

For the U.S + Canada and the World, ECC values have been calculated for the elements Zn, As, Se, Cd, Sb, Hg and Pb. Necessary variables are shown in Table VI-3. The top of Table VI-3 lists the average concentrations of the elements covered here and the average penetration of each through emission control devices (Bolton, et.al., 1975). Shown at the bottom of Table VI-3 are figures for yearly consumption, average ash content and total efficiency of ash removal, as discussed earlier in this chapter.

Calculations based on the above figures are shown in Table VI-4. Approximately 1.02×10^9 metric tons of ash are produced yearly in the U.S.+Canada. Of this, $>2.04 \times 10^8$ metric tons are emitted to the atmosphere. The Zn+As+Se+Cd+Sb+Hg+Pb (Total ECC) mobilized yearly as a result of coal utilization in the U.S.+Canada amounts to $>47,000$ metric tons. Over

TABLE VI-3

(SEE TEXT FOR EXPLANATION)

ELEMENT	AVERAGE CONCENTRATION (PPM)	AVERAGE PENETRATION (%)
Zn	35	5
As	10	5
Se	3	30
Cd	1	5
Sb	1	5
Hg	0.2	90
Pb	20	5

U.S.+CANADA, YEARLY CONSUMPTION ... 6.808E+08 MET. TON.

WORLD, YEARLY CONSUMPTION 3.868E+09 MET. TON.

AVERAGE ASH CONTENT 15%

TOTAL EFFICIENCY OF ASH REMOVAL ... 98%

TABLE VI-4

=====
 (SEE TEXT FOR EXPLANATION)

	U.S. + CANADA (METRIC TONNES)	WORLD
ASH PRODUCED, YEARLY	1.021E+08	5.801E+08
ASH EMITTED, YEARLY	2.042E+06	1.160E+07

 EFFECTIVE COAL CONCENTRATION (ECC)

Zn	23,828	135,800
As	6,808	38,810
Se	2,042	11,642
Cd	681	3,881
Sb	681	3,881
Hg	136	776
Pb	13,616	77,610
TOTAL	47,792	272,411

 AMOUNT EMITTED TO THE ATMOSPHERE

Zn	1,191	6,791
As	340	1,940
Se	613	3,492
Cd	34	194
Sb	34	194
Hg	123	699
Pb	681	3,881
TOTAL	3,016	17,188

3,000 metric tons of these same elements penetrate emission control devices.

It bears pointing out that while these figures are important to North America, and the World, as a whole, they are devastating to the local industrial areas where the majority of the coal is consumed. One study of Hg concentration in the near surface atmosphere has shown that approximately 100 times as much Hg is detected in the atmosphere near industrial centers in comparison with rural areas (Billings and Matson, 1972).

CHAPTER VII: OBSERVATIONS ON THE GEOCHEMISTRY OF COAL

VII.1 INTRODUCTION

This chapter is concerned with two different, but related, subjects. The first of these deals with the relative abundance of some of the elements in coal as compared to other rock types as a function of the geochemical nature of the elements. The second topic addresses the problem of the organic/inorganic affinities of the elements. Some of the present available data on organic/inorganic affinities is here interpreted on the basis of the physico-chemical characteristics of the elements in some detail, and some new conclusions are presented. This is not intended to be a definitive statement as to the organic/inorganic affinities of the elements, but rather offers some food for thought.

The ideas that some elements are enriched in coals and that there are some elements which "prefer" the organic or inorganic fractions of coals are hardly new. The fact that some elements are enriched in coal ash relative to the crust of the Earth and that certain elements show a preference for the organic/inorganic fraction in coal was postulated by V.M.Goldschmidt some 50 years ago (Goldschmidt, 1935). In his work on "Rare Elements in Coal Ashes" Goldschmidt cites similar works from some 50 years prior to his own. These original works sparked renewed interest in the subject of

coal geochemistry as the "organic rock" became increasingly important as a source of fuel. Recent works in coal geochemistry have attempted to characterize the occurrence and distribution of the elements in coals from various standpoints.

Naeval (1981) points out the extreme variability of elements in coal, noting that characterization is difficult within seams from a single deposit, let alone between deposits from different areas. Nicholls (1968) determined organic/inorganic affinities (from float/sink data) for a number of elements and concluded that the mechanisms responsible for concentrating an element vary with location. Zubovic (1961, 1966a) found (1) that the distribution of some elements, at the edges of or towards the interior of a given deposit, was a function of proximity to the source area, (2) that the lithology of the source area (igneous vs second order sedimentary) was a contributing factor in the availability of certain elements to the coal swamp (Zubovic, 1961) and (3) that the physical and chemical character (ionic potential) of the elements in question were instrumental in their organic/inorganic affinities (Zubovic, 1966b). Sawyer and Griffith (1983) also noted the importance of source area in controlling the distribution of mineral matter in peats. Kuhn, et al., (1980) and Gluskoter (1975) have also compiled data on organic/inorganic affinities of some elements in coals from different localities. Rao and Gluskoter (1976)

determined quantitatively the major and trace minerals associated with Illinoisan coals. Gluskoter et al., (1977) determined that those elements associated with the organic fraction of coals exhibit less variability while the inorganically combined elements showed the largest ranges in concentrations. Ruch, et al., (1974) conducted a similar study as that of Gluskoter et al., (1977) with similar results. Qualitative and quantitative identification of the mineral matter in low temperature (radio frequency, <150°C) coal ash has been reported by Gluskoter (1965), Estep et al., (1968), O'Gorman and Walker (1971), Frazer and Belcher (1972), Painter et al., (1978) and Miller et al., (1979). The effects of high temperature ashing (150°-1400° C) on the mineral matter in coals was reported by Mitchell and Gluskoter (1976) and Gluskoter (1975). Kuhn (1980), Rao and Gluskoter (1976) and Gluskoter et al., (1977) have correlated trace element data with individual mineral phases in coal.

Probably the most common single premise shared by all of the above works is that the geochemistry of coal is extremely variable!

VII.2 THE RELATIVE ABUNDANCE OF THE GEOCHEMICAL ELEMENTS IN COAL VS OTHER ROCK TYPES.

VII.2.1 INTRODUCTION

In this section data on the relative abundance of 38 elements (those for which data was available in all sample types compared) in the Utah and Wyoming coals, and typical crustal and basaltic rocks are compared. When the various combinations of these data sets are graphed some interesting trends are noted. Surprisingly enough, the resulting graphs do not appear significantly different than if the absolute abundances of the elements were plotted. The geochemical nature of the elements in question, i.e., the class of the element, e.g., lithophile, chalcophile, etc., determines, to a large extent, the position of the element in the following plots. There is a rough separation of the elements when presented in this manner.

It should be emphasized that in the following graphs only the relative abundance of the same 38 elements are plotted so that comparisons, i.e., changes, are easily recognizable. The most abundant element in each data set is assigned the value of #38 and the least abundant element is given the value of #1. For example, in Figure VII-1,A (basalt vs crust) Al is the most abundant element in each rock type (i.e., #38) and Se is the least abundant (i.e., #1). The

segmented line represents the ratio 1:1, correlation coefficients (R) are given at the top of each graph. Figures VII-1, A and B present data for like lithologies: basalt vs crust (A) and Wyoming coal vs Utah coal (B). Figures VII-2, A and B and VII-3, A and B show data for "mixed" lithologies, coal vs crust/basalt.

The following elements, shown in each graph, are here listed according to their most likely geochemical class roughly in order of decreasing relative abundance as shown in Figure VII-1, A:

Chalcophile; S, Cu, Zn, Ga, Pb, As, Sb, Se

Siderophile; Fe, Ni, Co, Mo

Lithophile; Al, Ca, Mg, Na, Ti, Mn, Sr, Ba, V,
Cr, Zr, Ce, Rb, Sc, Nd, La, Sm, Th,
Yb, Br, Hf, Cs, U, Eu, Tb, Lu

Many of the above elements fit into more than one category, e.g., Mo has a strong chalcophile tendency even though it is listed as a siderophile elements. These types of overlap will be useful in describing the anomalies in the following graphs.

VII.2.2 COMPARISONS OF LIKE LITHOLOGIES

Figure VII-1, A shows the plot of the relative abundance of the elements in typical crust and typical basalt (data from

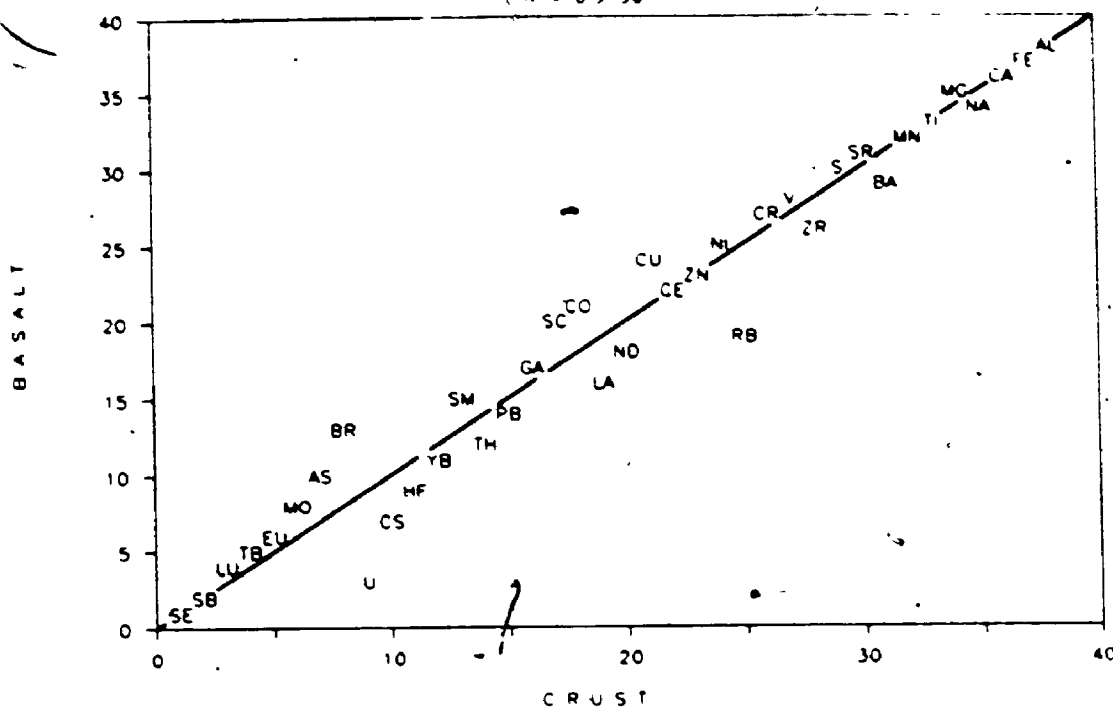
FIGURE VII-1

GRAPHS SHOWING THE RELATIVE ABUNDANCES OF 38 ELEMENTS IN TYPICAL BASALTIC AND CRUSTAL MATERIAL (A) (DATA FROM KRAUSKOPF, 1967) AND BOTH THE COALS FROM THIS STUDY (B) (FOR EXAMPLE, AL IS THE MOST ABUNDANT ELEMENT IN BOTH BASALT AND CRUST, THEREFORE IT IS #38 WHILE SE IS THE LEAST ABUNDANT AND IS #1). CORRELATION COEFFICIENTS ARE SHOWN AT THE TOP OF EACH GRAPH. THE DIAGONAL LINE REPRESENTS THE RELATIONSHIP 1:1, I.E., THE SAME RELATIVE ABUNDANCE IN BOTH DATA SETS.

A

BASALT VS CRUST: RELATIVE ABUNDANCE

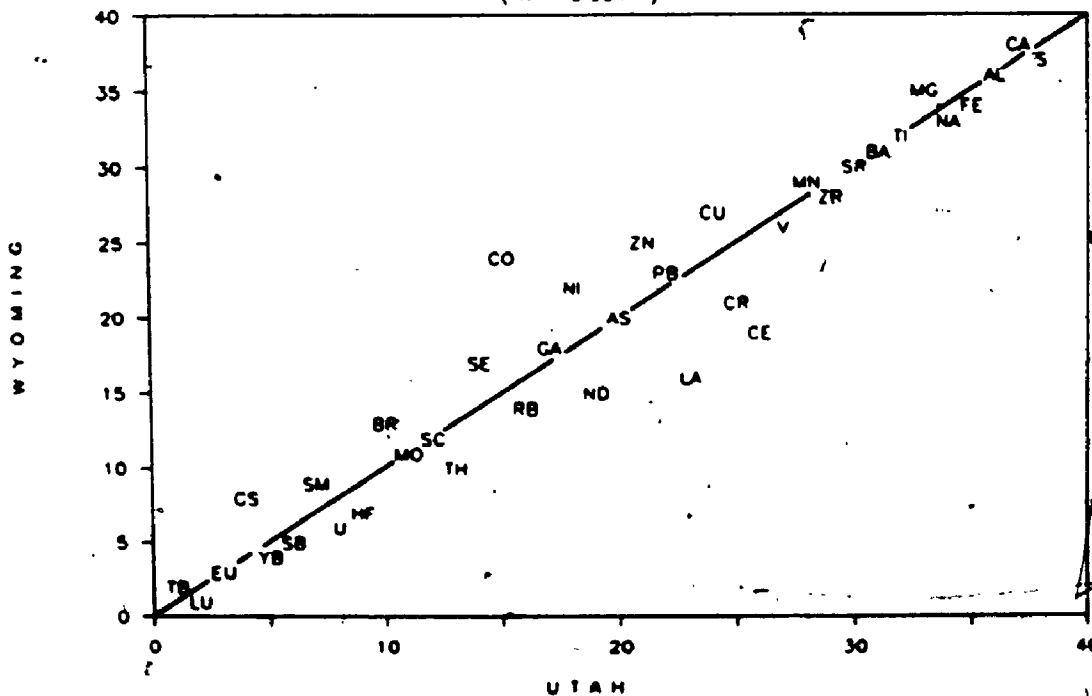
(R = 0.9790)



B

UTAH VS WYO COAL: RELATIVE ABUNDANCE

(R = 0.9641)



Krauskopf, 1967). Agreement between the data sets is very good ($R=0.979$) indicating that the relative abundance of these elements is very similar in the two rock types. Furthermore, the positions of the elements in the graph do not appear to be a function of their geochemical class. That is, the chalcophile elements are distributed throughout the data points ranging from a high position for S to Se, the least abundant in either rock type. The same is true for the siderophile and lithophile elements.

As might be expected, similar good correlation ($R=0.964$) is observed when comparing the two coals (Figure VII-1, B). Correlation for the coal data is better towards the high and low ends of the graph and less so towards the middle (more scatter). Interestingly enough, the scatter of data points in the central part of the graph is due to geochemically similar elements. Cobalt and Ni (siderophile) and Cu, Zn and Se (chalcophile) have shifted towards the Wyoming coal axis while Cr, Ce, La and Nd (lithophile) are more prominent in the Utah coal (note: Ce, La and Nd form a geochemically coherent trio).

The most obvious difference, based on the geochemical nature of the elements, between basalt vs crust and coal vs coal is the shift in the positions of the chalcophile elements (Figure VII-1, A and B). Sulfur moves from approximately position #28 in both rocks to #38 and #37 in the Utah and

Wyoming Coals, respectively. Selenium makes a similarly large move from position #1 in both rocks to approximately #15 in both coals and As goes from around #10 to near #20. The majority of the other chalcophile elements show similar, but lesser, shifts with one exception, Ga. Gallium makes no move at all, possibly a function of the tendency of this metal to follow Al in the sedimentary cycle.

Other shifts are due, in part, to elements being displaced by the chalcophile elements. Some, however, are real. For example, Mo moves up the order considerably in the coals vs crust and basalt and this is likely due to the partial chalcophile nature of this element. conversely, Rb drops in the order when going from rock to coal. This change would probably mimic a similar shift in K, unfortunately data on K is not available for comparison.

VII.2.3 COAL VS ROCK

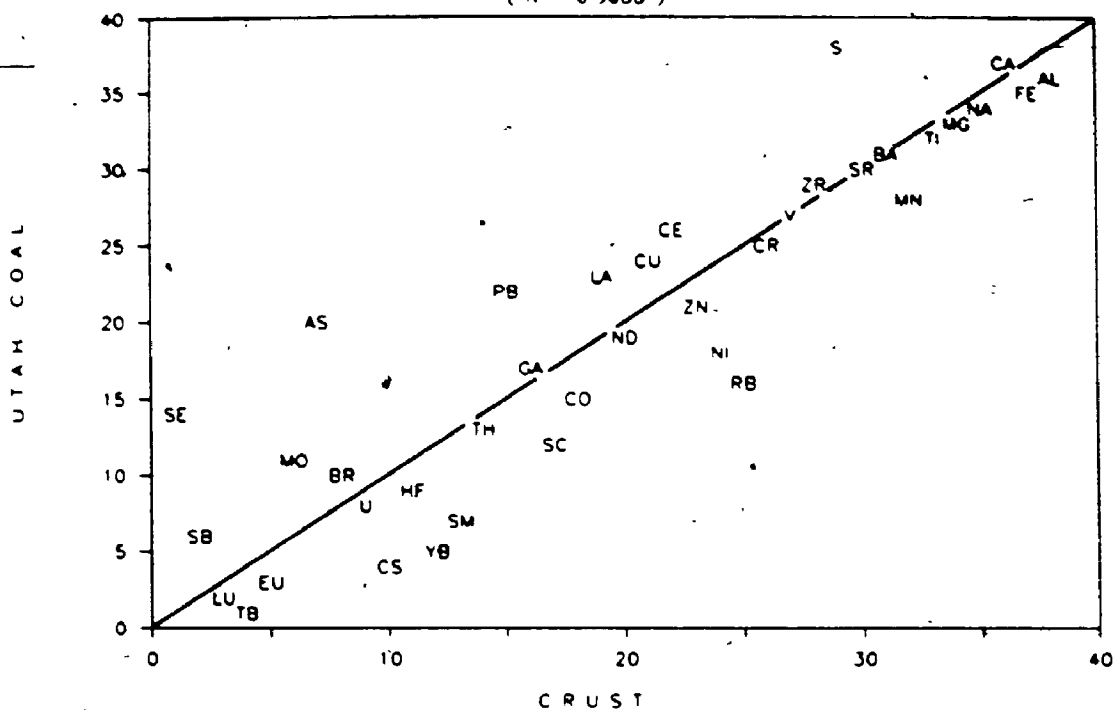
Plots of the relative abundance of the elements for the Utah coal vs basalt/crust are shown in Figure VII-2, A and B and for the Wyoming coal vs basalt/crust in Figure VII-3; A and B. In addition to an overall drop in correlation between the various data sets (R values) there are some similarities which logically result from comparing data sets which have shown high correlation with each other.

FIGURE VII-2

GRAPHS SHOWING THE RELATIVE ABUNDANCE OF 38 ELEMENTS IN UTAH COAL FROM THIS STUDY COMPARED TO TYPICAL CRUSTAL (A) AND BASALTIC (B) MATERIAL (ROCK DATA FROM KRAUSKOPF, 1967). CORRELATION COEFFICIENTS ARE SHOWN AT THE TOP OF EACH GRAPH. THE DIAGONAL LINE REPRESENTS THE RELATIONSHIP 1:1, I.E., THE SAME RELATIVE ABUNDANCE IN BOTH DATA SETS.

A

UTAH COAL VS CRUST: RELATIVE ABUNDANCE

 $(R = 0.9035)$ 

B

UTAH COAL VS BASALT: RELATIVE ABUNDANCE

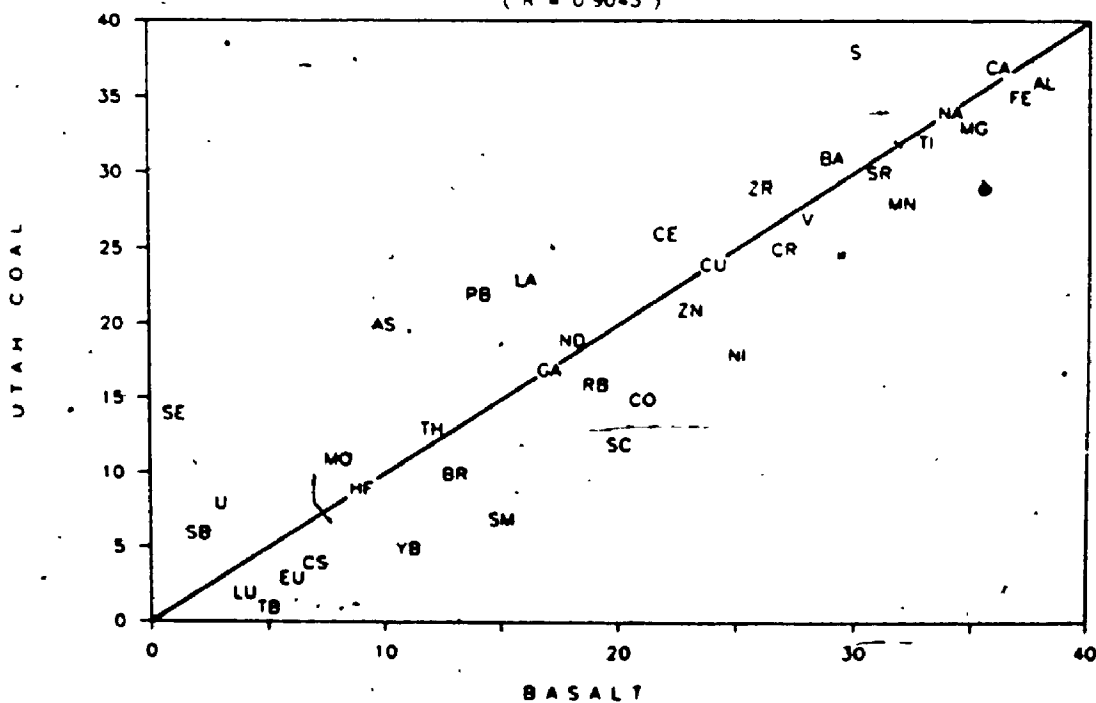
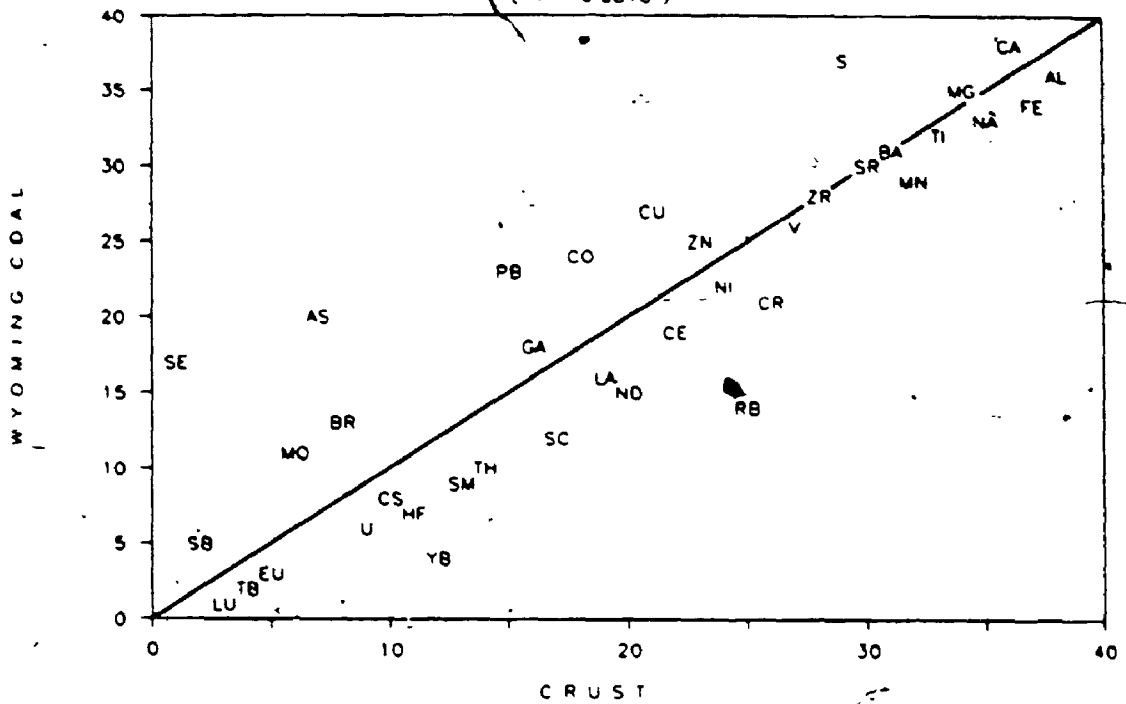
 $(R = 0.9045)$ 

FIGURE VII-3

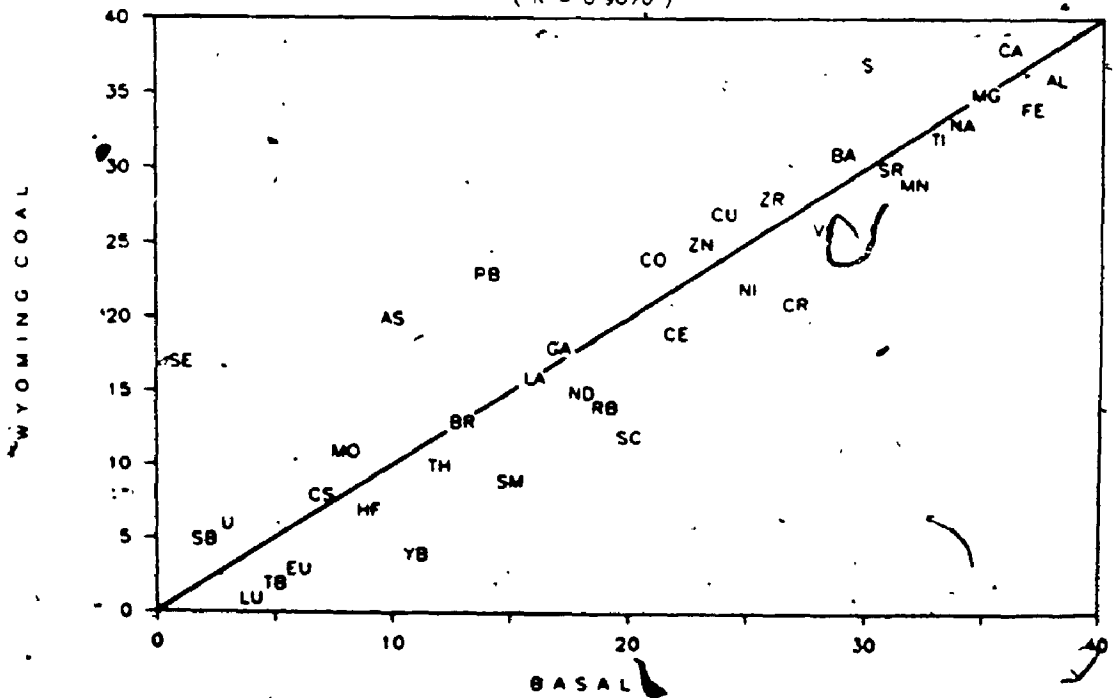
GRAPHS SHOWING THE RELATIVE ABUNDANCE OF 38 ELEMENTS IN WYOMING COAL FROM THIS STUDY COMPARED TO TYPICAL CRUSTAL (A) AND BASALTIC (B) MATERIAL (ROCK DATA FROM KRAUSKOPF, 1967). CORRELATION COEFFICIENTS ARE SHOWN AT THE TOP OF EACH GRAPH. THE DIAGONAL LINE REPRESENTS THE RELATIONSHIP 1:1, I.E., THE SAME RELATIVE ABUNDANCE IN BOTH DATA SETS.

A

WYO COAL VS CRUST: RELATIVE ABUNDANCE

 $(R = 0.8818)$ **B**

WYO COAL VS BASALT: RELATIVE ABUNDANCE

 $(R = 0.9070)$ 

The scatter of the points for the Utah coal vs crust and the Wyoming coal vs crust are virtually identical, as are those for either coal vs basalt. For that matter all 4 of the graphs in Figures VII-2 and VII-3 are very similar.

The most obvious difference when comparing either coal to either rock and/or similarity when comparing both coals to both rocks is the shift of the chalcophile elements towards the coal axis of the graph. A more subtle difference involves a shift of the majority of the lithophile elements towards the rock axis. Neither of these patterns is noticed when comparing rock to rock or coal to coal. In effect, these patterns represent a separation of the elements according to their geochemical character.

VII.2.4 SUMMARY

The above descriptions show that the relative abundances of the elements in two different rock types as well as between two different coals are very similar. In addition, the elements shown do not show a preference for one or the other of the data sets when like materials are compared. However, obvious separation of the elements results when comparing coal to rock. In addition, many trends in the plots can be explained on the basis of geochemical similarities, as between pairs of elements.

VII.3 ORGANIC/INORGANIC AFFINITIES OF THE ELEMENTS IN COAL

VII.3.1 INTRODUCTION

Where/how the various metals reside in coal has long been a question of major importance to the chemist, geochemist and process engineer. It remains largely unanswered, or at best highly speculative. This is owing, mainly, to the difficulty involved in isolating and examining metal-organic complexes found in coals. In this section existing data regarding organic/inorganic affinities of the elements will be used to predict the conditions under which a given metal might show a marked preference for one phase or the other. The following predictions are based on limited observations but many of the conclusions drawn here appear valid. In many cases the present postulate is born out with a high degree of certainty, to wit, the organic/inorganic affinity of a metal is largely predictable based on the oxidation state of the metal at the time it is introduced into the peat/coal environment. In other words, a given metal cannot be considered as having a high organic or inorganic affinity throughout a range of different oxidation states, rather, each oxidation state of the metal must be looked at separately. This has not been the case in the recent literature.

The oxidation state of the metal controls the Ionic

Potential ($IP = \text{charge}/\text{radius}$), which is the parameter used here to describe the physico-chemical nature of the element at the time of emplacement. This view is oversimplified, as other characteristics, e.g., anion affinity (and/or electronegativity in the case of some of the nonmetals, discussed) are obviously important.

By way of introduction, Figures VII-4 and VII-5, A and B are shown to describe the relationships between oxidation state (CHG) and ionic radius (RAD) (data from Greenwood and Earnshaw, 1984). Figure VII-4 shows RAD and CHG values for all the elements detected in coals from this study. Each "point" on the graph represents an element with that combination of RAD and CHG. The columns of points show all the elements with the same CHG. The "N" values at the top of each column indicate the number of individual points in the column and the symbol "<>" shows the average for each column. The segmented line describes the relationship of $IP = \text{CHG}/\text{RAD} = 0.05$ (the significance of which is forthcoming). As shown, 45 points have $IP < 0.05$ and 45 have $IP > 0.05$. Numerous observations can be made from Figure VII-4:

- (1) +3 is the most common oxidation state for the elements shown (the mode).
- (2) No element in the +1 or +2 oxidation state has an $IP > 0.05$.
- (3) No element in the +5, +6 or +7 oxidation state has an $IP < 0.05$.

518

FIGURE VII-4

GRAPH OF THE IONIC POTENTIALS (CHARGE/RADIUS) OF THE ELEMENTS DETECTED IN BOTH COALS FROM THIS STUDY. EACH "DOT" REPRESENTS AN ELEMENT WITH THAT COMBINATION OF CHARGE AND RADIUS. "N" VALUES SHOW THE NUMBER OF INDIVIDUALS IN EACH COLUMN; I.E., OXIDATION STATE. "<>" SHOWS THE MEAN RADII FOR EACH COLUMN. THE SOLID LINE REPRESENTS THE RELATIONSHIP $IP=0.05$, 45 INDIVIDUALS HAVE $IP<0.05$ AND 45 HAVE $IP>0.05$.

IONIC RADIUS VS OXIDATION STATE

(THIS WORK)

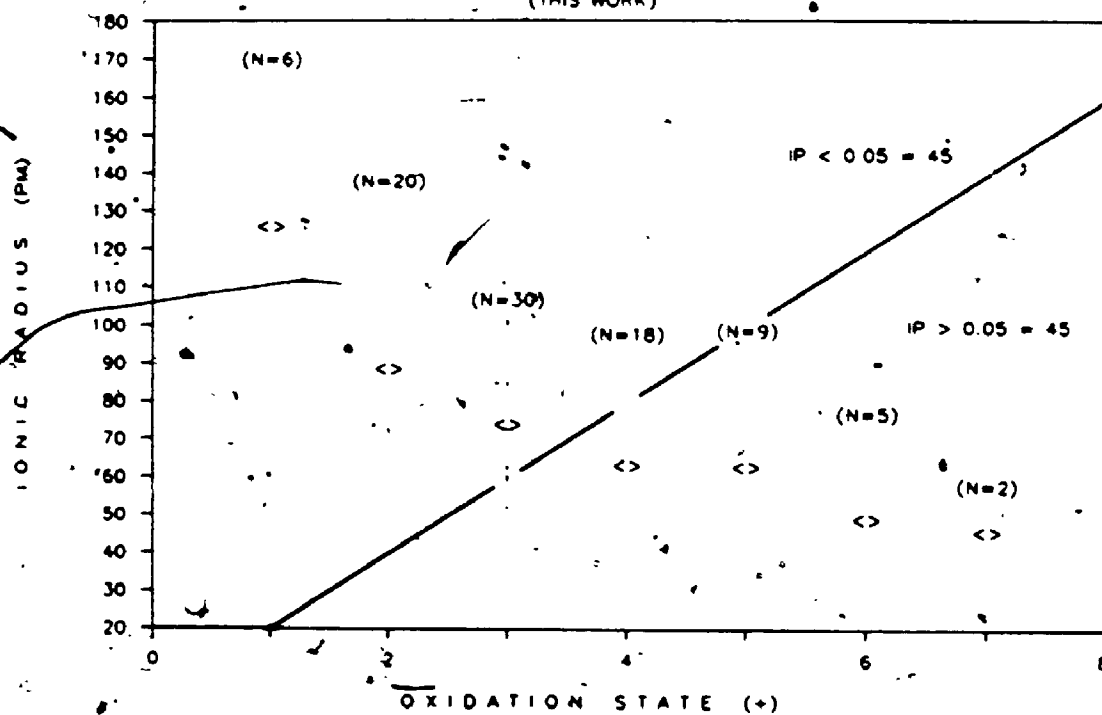


FIGURE VII-5

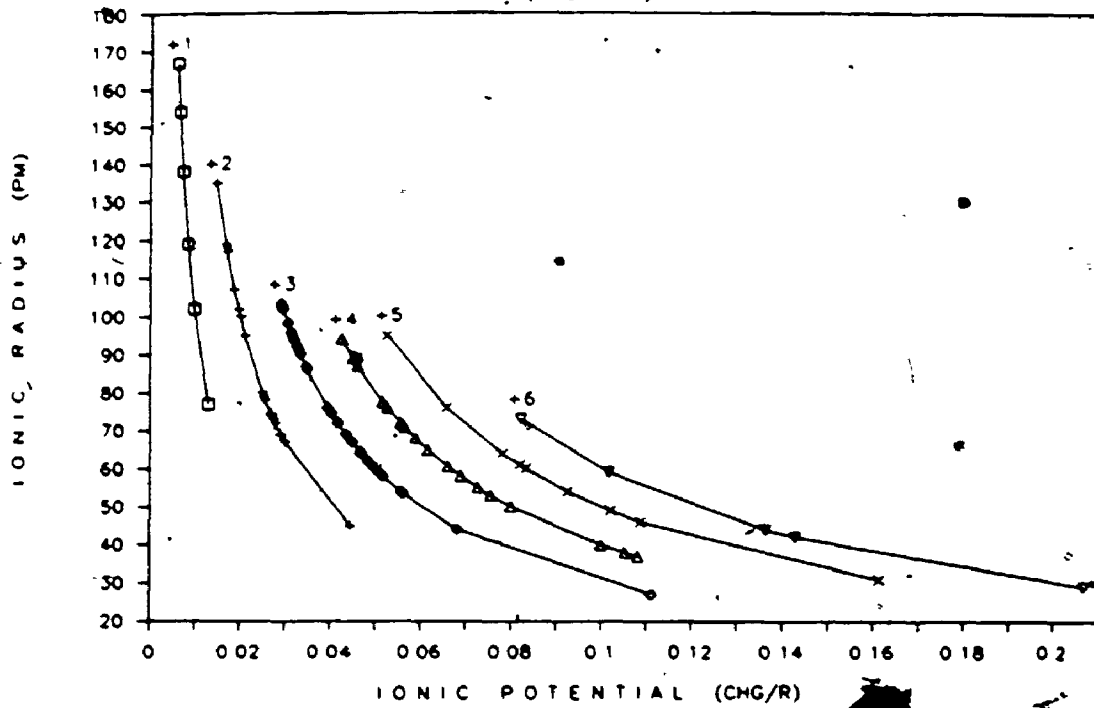
A - GRAPH OF THE IONIC RADII VS IONIC POTENTIALS OF THE ELEMENTS DETECTED IN BOTH COALS FROM THIS WORK. THE VARIOUS SYMBOLS CONNECT ELEMENTS OF LIKE CHARGE, E.G., THE "BOXES" CONNECT THOSE ELEMENTS WITH AN OXIDATION STATE OF +1, ETC.

B - GRAPH OF THE OXIDATION STATES VS IONIC POTENTIALS OF THE ELEMENTS DETECTED IN BOTH COALS FROM THIS WORK. SYMBOLS ARE THE SAME AS FOR FIGURE VII-4.

A

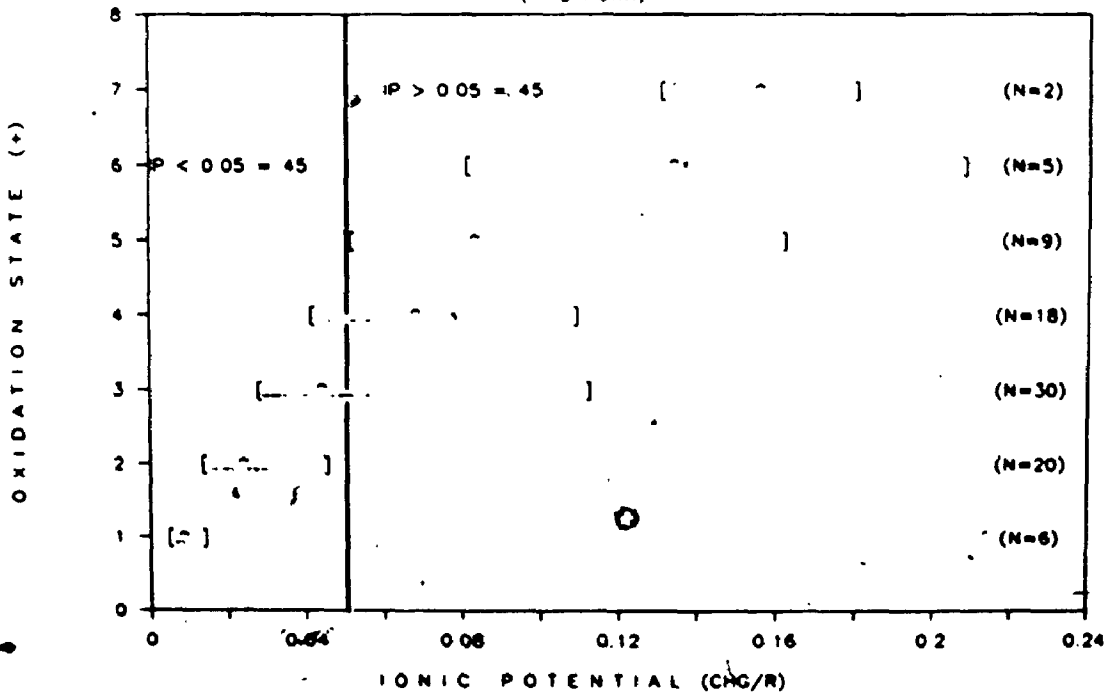
IONIC RADIUS VS IONIC POTENTIAL

(THIS WORK)

**B**

OXIDATION STATE VS IONIC POTENTIAL

(THIS WORK)



- (4) Elements in the +3 and +4 oxidation state straddle the $IP=0.05$ line.
- (5) There is an obvious exponential relationship between the mean values of each oxidation state (an obvious result of the way the ionic radius decreases with increasing charge crossing the periodic table).

The graphs in Figure VII-5, A and B will further illustrate the relationships between IP, CHG and RAD. Figure VII-5, A shows how IP changes as a function of RAD for given values of CHG (points of like charge are labeled at the top of each graph and are represented by like symbols, e.g., data points for +1 oxidation states are shown as "boxes" and are all connected. This plot shows that the IP of the elements increases with decreasing RAD. The reverse is true when CHG is plotted against IP, as the CHG increases so does the IP, as shown in Figure VII-5, B (symbols in Figure VII-5, B are the same as for Figure VII-4). Both these graphs merely describe the relationship $IP=CHG/RAD$.

One premise shared by the majority of the literature is that the geochemistry of coal is extremely variable. The concentrations of some elements vary by orders of magnitude within a given seam and comparisons between various coals show even larger variations. These differences are not surprising considering the complex nature of coal formation and the vastly different mineral contents (ash). It is,

however, disturbing to find that so many of the elements studied are evidently contained in the organic fraction of one coal but the inorganic fraction of another coal. That is, while the lists of relative organic/inorganic affinities show rough correlation between different coals from different studies there are always major discrepancies. Furthermore, the elements exhibiting the largest variabilities are the same in many studies while others are surprisingly consistent. For example, As and Zn are virtually always found in the inorganic fraction of a coal while Ge, Ga and Be are typically associated with the organic fraction, regardless of the coal studied. Conversely, elements like V and Mo range from 100% organic to 100% inorganic affinity within a single coal seam depending on the sample being analyzed, other elements exhibit lesser variabilities. Table VII-1 shows the results of studies of organic/inorganic affinity for 7 different coals.

Obviously, one major factor in the organic/inorganic affinity of any element is the stability of the organic complex vs the common mineral phase(s) it forms. Virtually all of the elements show some organic affinity but this does not necessarily imply that the metal is complexed in an organic molecule. Many elements are merely absorbed on the surface of the organic substrate while others are contained in inorganic phases too small and/or finely disseminated to

TABLE VII-1

TABLE OF ORGANIC/INORGANIC AFFINITIES OF SOME ELEMENTS IN COAL.

GLUSKOTER				ZUBOVIC	HORTON & AUBREY	NICHOLLS		
1	2	3	4	(% ORG.)	(% ORG.)			
B / O	Ge / O	Ge / O	Ge / O	Ge (87) / O	Ge (100) / O			I N T E R I E D I A T E
Ge / O	Ga / MO	B / O	B / O	Be (82) / O	V (100) / MO	B -	ORGANIC	
Be / O	Be / O	P / MO	Be / O	Ga (79) / MO	B (75-100) / O	Ga } Ge } Mo }	USUALLY ORGANIC	
Ti / MO	Ti / MO	Be / O	Sb / MO	Ti (78) / MO	Be (75-100) / O			
Ga / MO	Sb / MO	Sb / MO	V / MO	B (77) / O	Ga (75-100) / MO			
P / MO	Co / MI	Ti / MO	Mo / I	V (76) / MO	Ti (75-100) / MO			
V / MO	P / MO	Co / MI	Ga / MO	Ni (59) / MI	Mo (50-75) / I	Cu } Ni } As }	USUALLY INORGANIC	
Cr / MI	Ni / MI	Se / MI	P / MO	Cr (55) / MI	Ni (0-75) / MI			
Sb / MO	Cu / MI	Ga / MO	Se / MI	Co (53) / MI	Cr (0-100) / MI			
Se / MI	Se / MI	V / MO	Ni / MI	Y (53) / *	Zn (50) / I			
Co / MI	Cr / MI	Ni / MI	Cr / MI	Mo (40) / I	Co (25-50) / MI			
Cu / MI	Mn / I	Pb / I	Co / MI	Cu (34) / MI	Cu (25-50) / MI			
Ni / MI	Zn / I	Cu / MI	Cu / MI	Sr (27) / *	Sn (0) / *	Mn } Zn } Li } Pb } Co } Cr } V } Ba } Sr }	MAINLY INORGANIC	
Mn / I	Zr / I	Hg / I	Ti / MO	La (3) / *				
Zr / I	V / MO	Zr / I	Zr / I	Zn (0) / I				
Mo / I	Mo / I	Cr / MI	Pb / I					
Cd / I	Pb / I	Mn / I	Mo / I					
Hg / I	Hg / I	As / I	As / I					
Pb / I	As / I	Mo / I	Cd / I					
Zn / I		Cd / I	Zn / I					
As / I		Zn / I	Hg / I					

GLUSKOTER: DATA FROM FOUR DIFFERENT COALS;

- "O" - ORGANIC
- "MO" - MOSTLY ORGANIC
- "MI" - MOSTLY INORGANIC
- "I" - INORGANIC

DESIGNATIONS PROPOSED BY
GLUSKOTER (1975)

ZUBOVIC (1960, 1961): % ORGANIC AFFINITY COMPILED FROM DATA ON 13 EASTERN INTERIOR REGION COALS.

HORTON AND AUBREY (1950): DATA FROM THREE VITRAIN SAMPLES.

NICHOLLS (1968): DATA ON COALS FROM VARIOUS LOCATIONS.

* - ELEMENTS NOT DETERMINED BY GLUSKOTER.

be removed by common separation techniques (i.e., float sink). In addition, the density of the inorganic phase, e.g., sulfide vs clay, will affect calculations of organic/inorganic affinity for finely disseminated material.

Other elements are structurally bound within organic complexes, and stability series for metal chelates have been determined for univalent, divalent and trivalent metals (Basolo and Pearson, 1958). These trends roughly parallel the organic affinities observed in coals (Zubovic, 1966b). Apparently, the type of organic ligand (e.g., bidentate/quadridentate) does not significantly change the stability series for a given set of metals (Mellor and Maley, 1948).

Whether or not a given metal resides in a mineral phase or an organic complex in the coal is a function of the difference in the stability (dissociation constant) between the two. Elements with large IP (large charge and small ionic radii) are favored in the organic complexes. As shown by Zubovic (1966b), there is agreement between the relative organic affinity and IP for the specific oxidation states of the 13 elements he considered.

Ionic potential (here calculated in unit charge (+)/radius in pm) can be used as a measure of the organic affinity, i.e., organic chelates favor the smaller, highly charged

metals. This is similar to the way the IP of an element is used to predict whether the element will form soluble cations ($IP < 0.03$), insoluble anions ($IP > 0.10$) or be taken up by the hydrolysates ($0.03 < IP < 0.10$). The key variable is the oxidation state of the metal. As shown in Figures VII-4 and VII-5 the IP increases substantially with increasing charge. Based on the work of Zubovic (1966b and 1976) and calculations made here it appears that $IP = 0.05$ is an approximate boundary between elements exhibiting high organic affinity ($IP > 0.05$) and lower organic affinity ($IP < 0.05$). That is, the higher the IP the larger the organic affinity and the lower the IP the larger the inorganic affinity.

The importance of IP in determining organic/inorganic affinities is a function of the number of oxidation states common to a given element in near surface conditions (and within the conditions of diagenesis, coalification). For purposes of discussion, this work assumes that all the common oxidation states of the elements in question are possible at some time in the peat --> coal --> post-coal depositional environments. This is not an unreasonable assumption, Allen and VanderSande (1983) have identified oxides, sulfates and sulfides of Fe within <100 microns separation in fresh coal, hardly an equilibrium condition.

The data in the following section is presented with the

elements grouped in two ways: according to geochemical nature (chalcophile, etc.); and according to the number of common oxidation states (1, 2, etc.). In each of the following graphs the two dashed lines represent the boundaries $IP=0.03$ and $IP=0.10$, elements with $IP<0.03$ form soluble cations those with $IP>0.10$ form insoluble anions and elements with IP falling between these limits are commonly associated with the hydrolysates. The solid line in each graph represents $IP=0.05$, the "imaginary" boundary separating elements with high organic affinity ($IP>0.05$) from those with low organic affinity ($IP<0.05$). Data in the graphs marked "(literature)" are taken from column 1 of Table VII-1 which lists the results of numerous authors on the organic/inorganic affinities of various elements.

VII.3.2 THE ROLE OF IONIC POTENTIAL (IP) IN DETERMINING THE ORGANIC/INORGANIC AFFINITY OF THE ELEMENTS

The calculated IP for the elements in Table VII-1, column 1 are plotted in Figures VII-6, A, B and C according to the number of common oxidation states. The data in Table VII-1, column 1 are from Gluskoter (1975) and are representative of the other data shown, with obvious exceptions. The data in Figure VII-6 will be used to examine the validity of the premise that IP , and therefore oxidation state, is a controlling factor in determining the organic/inorganic affinity of the elements. The elements will be discussed on the basis of (1) those "always" showing high organic

552

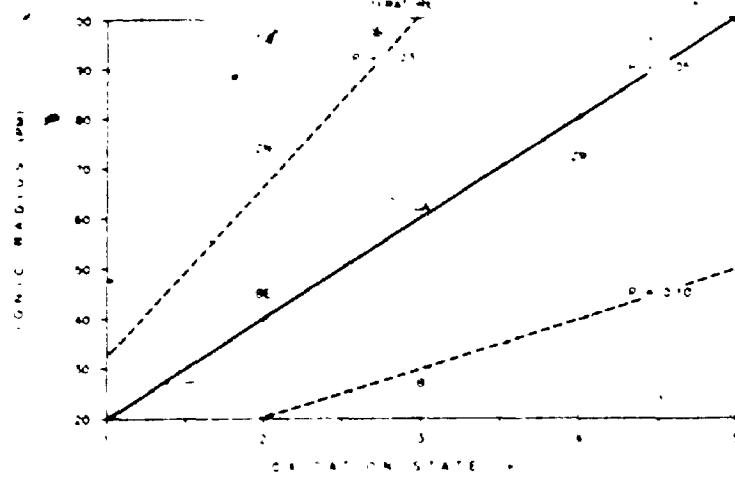
FIGURE VII-6

GRAPHS OF THE IONIC POTENTIALS (CHARGE/RADIUS) OF SOME ELEMENTS FOR WHICH THERE ARE DATA ON ORGANIC/INORGANIC AFFINITIES.

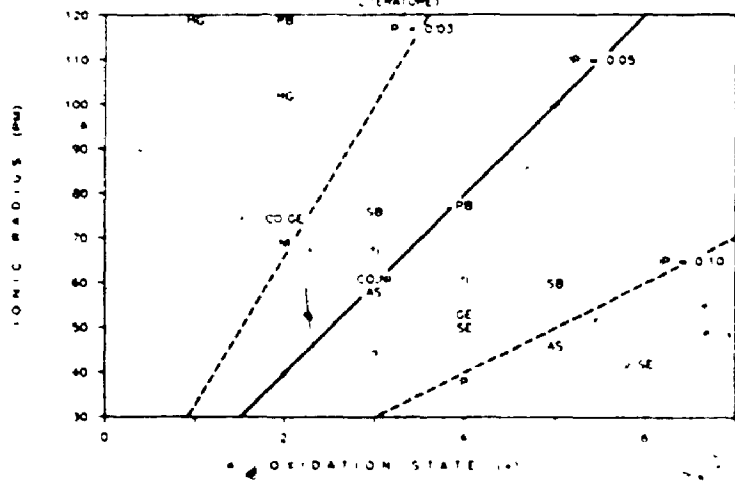
THE ELEMENTS ARE SEPARATED ACCORDING TO THE NUMBER OF COMMON OXIDATION STATES: (A), THOSE OCCURRING IN ONLY ONE OXIDATION STATE; (B) THOSE WITH TWO COMMON OXIDATION STATES; (C) THOSE WHICH COMMONLY EXHIBIT >2 OXIDATION STATES. THE ELEMENTS SHOWN ARE TAKEN FROM COLUMN 1 OF TABLE VII-1 (DATA FROM GLUSKOTER, 1975).

DASHED LINES REPRESENT THE RELATIONSHIPS $IP=0.03$, BELOW WHICH ELEMENTS TEND TO FORM SOLUBLE CATIONS, AND $IP=0.10$, ABOVE WHICH ELEMENTS TEND TO FORM INSOLUBLE ANIONS. THE SOLID LINE DESCRIBES THE RELATIONSHIP $IP=0.05$. ELEMENTS WITH $IP>0.05$ TEND TO OCCUR IN THE ORGANIC FRACTION OF COAL WHILE THOSE WITH $IP<0.05$ SHOW A HIGHER INORGANIC AFFINITY.

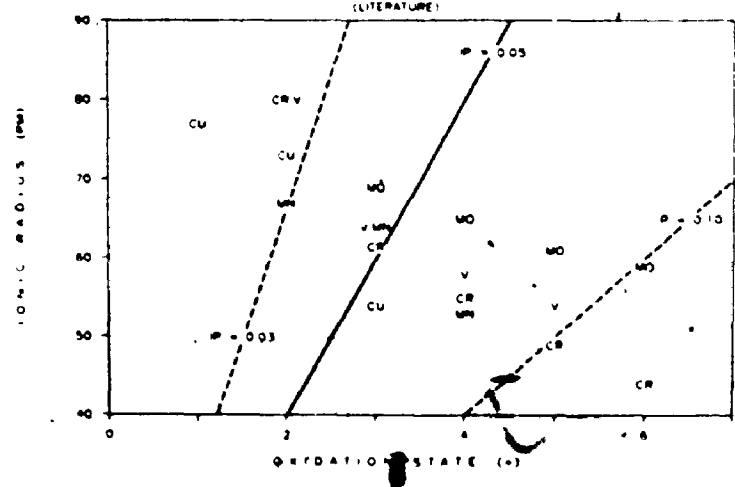
ELEMENTS WITH 1 OXIDATION STATE
(LITERATURE)



ELEMENTS WITH 2 OXIDATION STATES
(LITERATURE)



ELEMENTS WITH >2 OXIDATION STATES
(LITERATURE)



affinities (B, Ge and Be), (2) those that are "always" associated with the inorganic fraction (Mn, Zr, Mo, Cd, Hg, Pb, Zn and As) and (3) those exhibiting large variations between the two phases (Ti, Ga, P, V, Cr, Sb, Se, Co, Cu and Ni). This later group can further be subdivided into those elements "usually" in organic combination (Ti, Ga, P, V and Sb) and those "usually" found with the inorganic fraction (Cr, Se, Co, Cu and Ni). In the following discussion, the IP's will be shown in parentheses following the symbol of the element.

The elements B, Ge and Be generally exhibit the highest organic affinities. Of these, B and Be occur in only one oxidation state. The IP of B^{3+} (0.11) is consistent with a high organic affinity while Be^{2+} (0.04) should favor an inorganic association. The two oxidation states of Ge straddle the IP=0.05 line, but Ge^{4+} (0.08) is the common oxidation state and would tend towards organic affinity.

For the elements which are commonly associated with the inorganic fraction of coals the amount of observed relative organic affinity, in decreasing order, is, Mn, Zr, Mo, Cd, Hg, Pb, Zn and As (this order varies considerably from one data set to another). For the most part the predicted inorganic affinity of these elements, based on IP, correlates well with the observed inorganic affinities. Two of these elements that occur in only one oxidation state,

Cd^{2+} (0.02) and Zn^{4+} (0.03), are consistent with a high inorganic affinity. Based on IP Zr^{4+} (0.06) should exhibit a higher organic affinity than observed. The fact that Zr is normally present in the resistates (zircon) in the sedimentary environment (i.e., not in soluble form) may account for the unusually high inorganic affinity. The other elements in this group exist in more than one oxidation state. The IP for both common oxidation states of Hg, Hg^{1+} (0.01) and Hg^{2+} (0.02), lie well within the area of high inorganic affinity. Lead $^{2+}$ (0.02) should show higher inorganic affinity than Pb^{4+} (0.05) and both are common, explaining why Pb generally shows higher organic affinity than Hg. Manganese $^{2+}$ (0.03), Mn^{3+} (0.05) and Mn^{4+} (0.08) straddle the IP=0.05 line and, as expected, Mn is quite variable within the highly inorganic group. Molybdenum appears anomalous at first glance, of its 4 common oxidation states, Mo^{3+} (0.04), Mo^{4+} (0.06), Mo^{5+} (0.08) and Mo^{6+} (0.10), three are well within the organic field. The typically high inorganic affinity of Mo probably stems from the fact that Mo^{6+} (the most common oxidation state) forms the oxyanion molybdenate and so is not free to complex with the organics. However, the relatively high position of Mo in column 4 of Table VII-1, as well as its variability throughout the data sets, suggest that Mo^{5+} and Mo^{4+} are available to form organic complexes. Arsenic poses another exception for this group. Even though As consistently shows one of the highest inorganic affinities its two common

oxidation states, As^{3+} (0.05) and As^{5+} (0.11), fall at and well within the organic field. Obviously, the strong electronegative nature of As, especially in a reducing (coal) environment, results in As^{3+} being complexed in an inorganic phase.

The middle group of elements in column 1 of Table VII-1 exhibit large variabilities in organic/inorganic affinities. This is not surprising considering that they all, except Ga, exist in multiple oxidation states which straddle (or impinge on), to some extent, the $\text{IP}=0.05$ boundary. As predicted, these elements should vary substantially in their organic/inorganic affinities depending on their oxidation state at the time of being introduced into the peat/coal setting. Unpredicted trends occur for Sb^{3+} and Se^{2+} , as for As above, with Se^{4+} (0.08) favoring an organic affiliation. The strong electropositive nature of Cr^{6+} , V^{5+} and P^{5+} would lead to formation of the inorganic oxyanions chromate, vanadate and phosphate, respectively, while the lower oxidation states of each, Cr^{3+} (0.07), Cr^{4+} (0.10), V^{3+} (0.05), V^{4+} (0.07) and P^{3+} (0.07) would favor organic complexes. The highest oxidation states of Cu^{2+} (0.06), Co^{2+} (0.05) and Ni^{2+} (0.05) lie close to the $\text{IP}=0.05$ boundary but their lower oxidation states, Cu^{1+} (0.03), Cu^{0} (0.01), Co^{0} (0.03) and Ni^{0} (0.03) are all within the inorganic field, thus the observed tendency of these metals to occur in the inorganic phase. Conversely, the lower oxidation state of

Ti³⁺ (0.04) is close to the boundary while Ti⁴⁺ (0.07) lies in the inorganic field and this element favors the organic phase. Finally, Ga³⁺ (0.05) lies directly on the IP=0.05 line and so it exhibits a variable nature.

Ionic potentials for the elements detected in both coals from this study are shown in Figure VII-7, A-F. The elements discussed above are also included in these graphs so it is not necessary to discuss these data, again. It is interesting, however, to see the data grouped according to their geochemical natures, i.e., chalcophile, etc. The lithophile elements are further subdivided on the basis of the number of oxidation states only for convenience/clarity (there were too many lithophile elements for one graph).

Ionic potentials for most of the chalcophile elements lie near or below the IP=0.05 value. Only Se, Sb, As and S lie within the organic field of the graph (IP>0.05) and, as discussed above, these elements generally form anions and so are not available to complex with organic ligands. Therefore, it is not surprising that, as a group, the chalcophile elements show relatively low affinity for the organic fraction of coal (except organic S).

Of the siderophile elements, Mo shows a large variation in organic/inorganic affinity owing to its many oxidation states and the fact that it also has a strong chalcophile

FIGURE VII-7

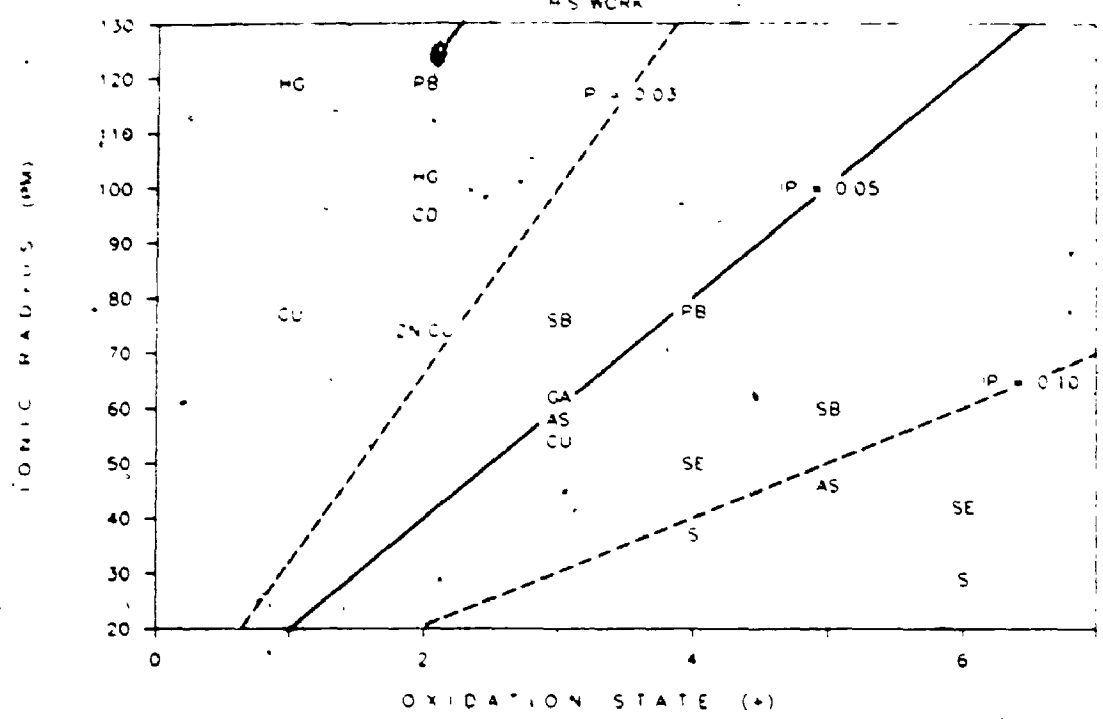
GRAPHS OF THE IONIC POTENTIALS (CHARGE/RADIUS) OF THE ELEMENTS DETECTED IN BOTH COALS FROM THIS STUDY. THE DASHED AND SOLID LINES ARE THE SAME AS IN FIGURE VII-6.

THE ELEMENTS ARE SEPARATED ACCORDING TO THEIR GEOCHEMICAL NATURE: (A), CHALCOPHILE; (B), SIDEROPHILE; (C), (D), (E) AND (F), LITHOPHILE, FURTHER SUBDIVIDED BY NUMBER OF COMMON OXIDATION STATES.

A

CHALCOPHILE ELEMENTS

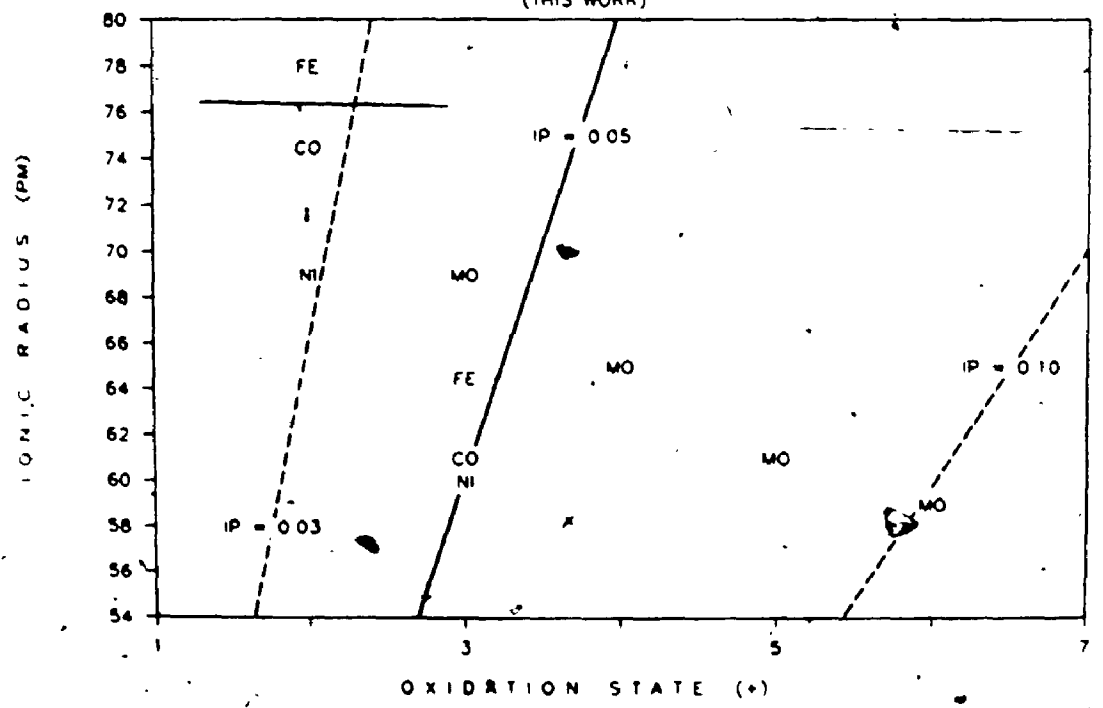
(THIS WORK)



B

SIDEROPHILE ELEMENTS

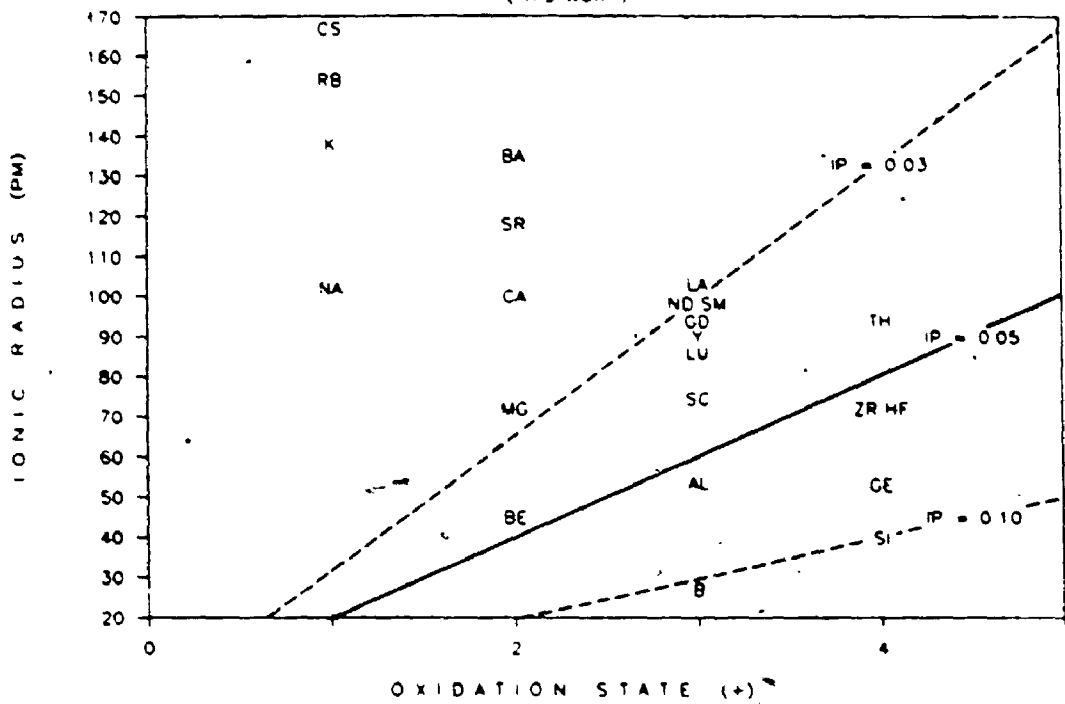
(THIS WORK)



C

LITHOPHILE ELEMENTS: 1 OXIDATION STATE

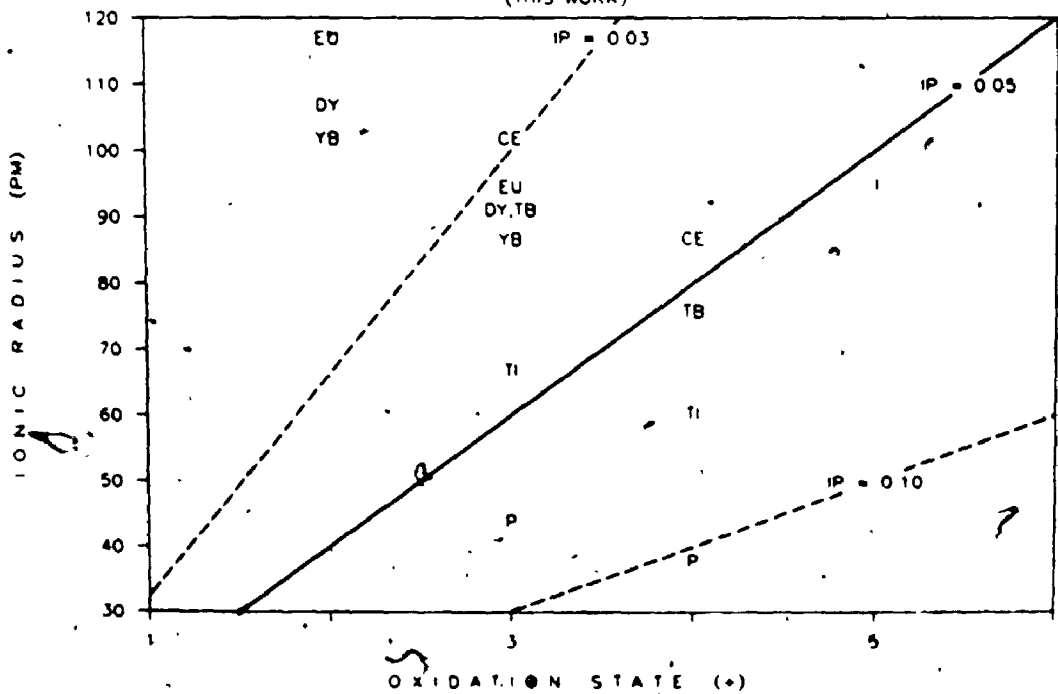
(THIS WORK)



D

LITHOPHILE ELEMENTS: 2 OXIDATION STATES

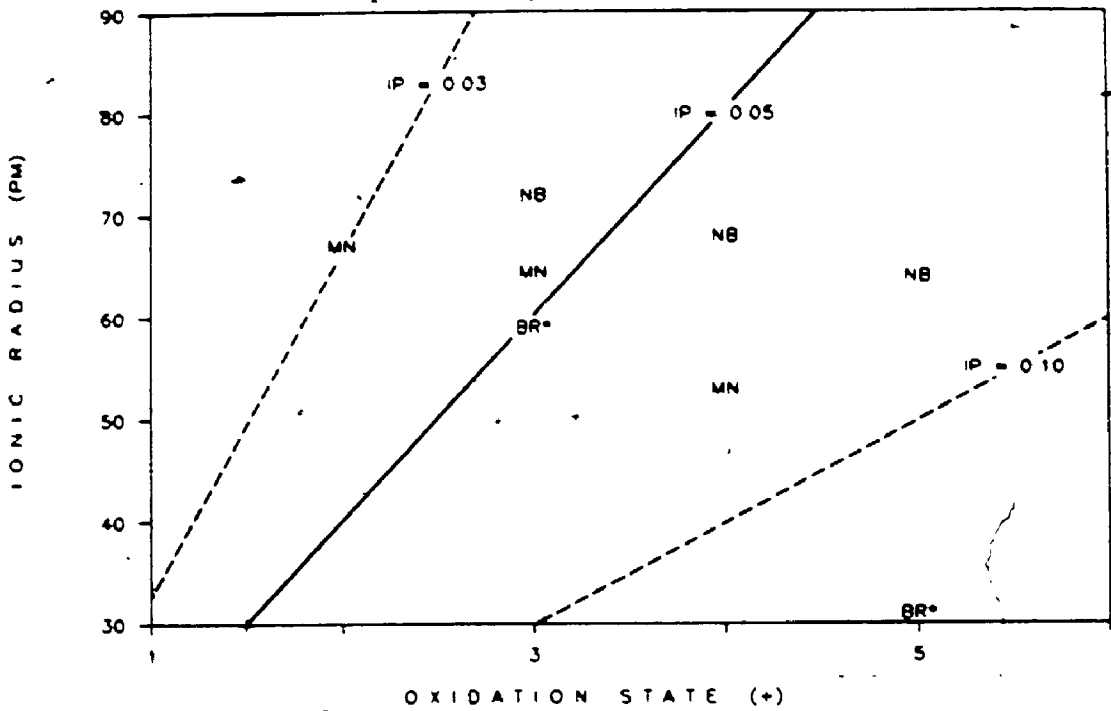
(THIS WORK)



E

LITHOPHILE ELEMENTS: 3 OXIDATION STATES

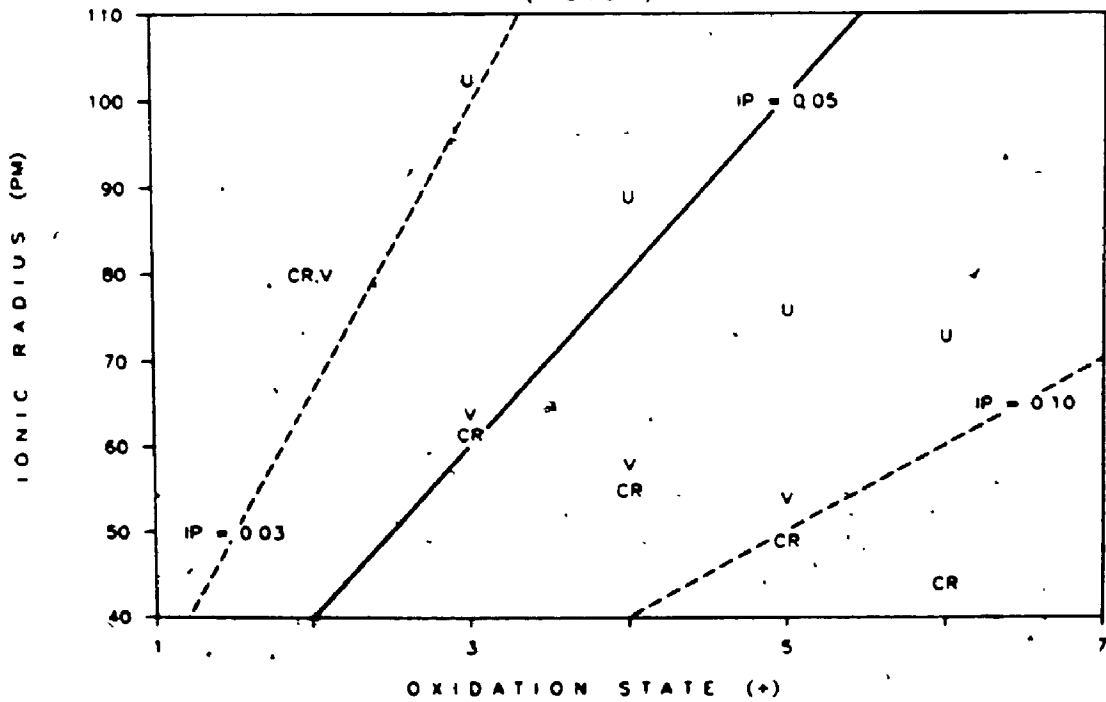
(THIS WORK)



F

LITHOPHILE ELEMENTS: 4 & 5 OXID. STATES

(THIS WORK)



character. The other siderophile elements are distinctly inorganic, as expected, based on their IP values. Some inorganic tendencies are noted because Fe, Co and Ni each have one oxidation state which lies close to the IP=0.05 line.

Data on the organic/inorganic affinities of the majority of the lithophile elements are not available. The elements in Figure VII-7, C-F, for which multiple data are available, are discussed above, with the following exceptions.

Horton and Aubrey (1950) determined that Sn has a 0% organic affinity while Zubovic et al., (1961) found Sn associated with the organic fraction of coal 27% of the time. Tin is similar to elements such as Co and Ni, with Sn^{2+} (0.02) falling well within the inorganic field and Sn^{4+} (0.06) lying close to the IP=0.05 line. This would account for the mostly inorganic nature of Sn.

Nicholls (1968) observed that Ba^{2+} (0.01), Sr^{2+} (0.02) and Li^{1+} (0.01) were "mainly inorganic" in nature, as would be indicated by the fact that each element exists in only one oxidation state which lies well within the inorganic field.

Breger et al., (1955) determined that U has an 85% organic affinity. Uranium occurs in 4 oxidation states that straddle the IP=0.05 boundary, as with Cr, Mo and V, additional work

will probably show large variations in its organic/inorganic affinity.

Some generalizations can be made regarding the organic/inorganic affinities of the other lithophile elements. The Alkali and Alkaline-earth elements, except Be, have IP values which would predict a large inorganic affinity. These elements typically form large soluble cations ($IP < 0.03$). Recent data by Miller and Givens (1987) show that large amounts of Ca, Mg, Sr, Ba and Na, when associated with organic matter in coal, are extractable with 1.0 N ammonium acetate and are, therefore, probably present as carboxylate salts. They also found that some of the Ti and Al associated with organic matter was extractable by 1.0 N HCl. The majority of the Rare Earth elements (those with only one oxidation state, +3) should show little affinity for the organic fraction of coal based on IP values. Not only are the IP's of these elements too small but they are also taken-up by hydrolysates.



VII.4 SUMMARY

The organic/inorganic affinity of an element cannot be examined without first qualifying the oxidation state of the element. Elements with large values of $IP > 0.05$ tend towards a higher organic affinity but other considerations, e.g., whether or not the element forms oxyanions, if the element

is only present in resistates (i.e., not as an aqueous species) and what other mineral phases (e.g., hydrolysates) are competing with the organic ligands, must be considered. In most cases the above factors are controlled by the oxidation state of the element and as this variable changes so will the organic/inorganic affinity of the element. In general, the smaller the IP of an element, the less it's organic affinity.

The following general rules appear to apply:

- (1) For elements with only one oxidation state;
 - (A) If the IP of the element is substantially larger than 0.05 it will exhibit high organic affinity.
 - (B) If the IP of the element is substantially smaller than 0.05 it will exhibit a high inorganic affinity.
 - (C) If the IP of the element lies close to 0.05 it will exhibit variable organic/inorganic affinity.
- (2) For elements with multiple oxidation states;
 - (A) If the IP's for all of the oxidation states fall well within either the organic or inorganic field the element will exhibit a high organic or inorganic affinity, respectively.
 - (B) If the IP's for all the oxidation states fall



 within either the organic or inorganic field
 but also approach the $IP=0.05$ boundary the
 element will exhibit some variability but
 will show a preference for the organic or
 inorganic fraction, respectively.

(C) If the IP's for all the oxidation states
 straddle the $IP=0.05$ boundary the element
 will show extreme variability in
 organic/inorganic affinity.



CHAPTER VIII: CONCLUSIONS

The processes responsible for the geochemistry of a given coal are extremely variable both within and between different coals. It would not be a gross overstatement to say that comparing coals from different localities is like comparing apples and oranges.

The peats which now make-up the coals of the Cretaceous Emery Coal Field, Utah and the Paleocene Powder River Basin Coal Field, Wyoming accumulated in very different paleoenvironments. The transgressive/regressive setting of the constructive delta plain on which the Utah peats were deposited received numerous influxes of detritus and marine waters, both of which contributed to the higher ash content of these coals, average 8.2%. Conversely, the Wyoming peats were deposited in a quiescent fluvio-lacustrine setting, protected from major sedimentary events. In addition, the tectonic setting of the Wyoming Structural Province at the time (Turonian) must have been in dynamic equilibrium, with subsidence occurring at only a slightly higher rate than emergence of the surrounding Precambrian uplifts. Accordingly, vast, thick coals resulted with relatively low ash contents, averaging 4.4% for this study.

Iron Sulfide nodules in the Utah coals host unusually high concentrations of some of the potentially environmentally

harmful trace elements. Arsenic, Se and Hg are present at greater than order of magnitude concentrations relative to the whole coals. Zinc and Cd were not detected in either the coals or nodules. Antimony was detected in both coals but not in the nodules. Uranium was present at approximately the same concentrations in both coals and the nodules. Geld, Co and W were also present at "unusually high" concentrations in the nodules (no numbers reported).

Overburden and clinker associated with the Wyoming coals are geochemically similar to each other and to other fine grained rocks within the Powder River Basin. The geochemistry of the clinker and overburden is controlled, to a large extent, by the presence of clays and associated elements. Furthermore, there appears to have been little change, geochemically, in the clinker during burning.

The mineralogy of the two coals is appreciably different based on SEM/EDS analyses of discrete grains. The Utah coals contain clays (kaolinite, illite, mixed layer and glauconite/montmorillonite), silicates (quartz, zircon, plagioclase feldspar, alkali feldspar and a mixed Ca/Ti/Fe-silicate), carbonates (Ca+Mg+Fe), oxides (rutile and cassiterite), sulfides (pyrite/marcasite) and sulfates (barite and celestite). The Wyoming coals contain quartz, pyrite/marcasite, barite and rutile similar to the Wyoming samples. In addition, the Wyoming coals contain oxides of

Cr/Fe/Ni. Unlike the Utah coals the Wyoming samples contain appreciable amounts of Al, Si and Ca in the "clean" coal matrix.

Mineral paragenesis resulting from the oxidation of Fe-sulfide, contained in the nodules of Utah coal, to hydrous Fe-sulfates include szomolnokite and halotrichite. Szomolnokite is the typical secondary phase which develops on "clean" Fe-sulfide while halotrichite results from the oxidation of Fe-sulfide in the presence of clays. The growth of halotrichite appears to have occurred in the near surface environment of the nodules. The origin of the nodules can be inferred from mineralogical and textural relationships within and adjacent to the nodules.

The bulk geochemistry of the two coals is reflected in the higher ash content for the Utah samples. On average, the Utah coals contain higher concentrations of 27 elements, in decreasing order of enrichment, Fe, La, U, Th, Ce, Na, Eu, Hf, Nd, Cl, Cr, Sm, Al, S, Lu, Sb, Dy, Yb, Mo, Rb, Zr, Sc, Ga, As, Ti, Mn and Mg while 13 elements, Ca, Se, V, Ni, Pb, Sr, Zn, Cs, Br, Cu, Ba, Co and Au are more concentrated in the Wyoming Coals. In general, neither coal is significantly different from geographically similar coals. For that matter, these two coals are much more similar than different seams from with the same coal at other locations.

Comparisons of 16 elements plus ash for the two coals show that Al, Ga, Cr, ash, V, Ti, Ni, Zr and Cu exhibit positive ($R > 0.5$) correlations for all the elements taken together both within and between the two coals. Calcium, Rb, Ba, Mn, Co, Pb and Sr do not show significant correlation ($-0.5 < R < 0.5$). Only S exhibits a large negative correlation ($R = 0.58$) between the two coals. Interpretation of these data is complicated. Obviously, mineralogy, ash content, diagenesis, groundwater, weathering and the geochemical nature of the element are all factors. However, it is likely that the major factor controlling the tendency of an element to be positively correlated with the other elements in one coal while negatively correlated with the same elements in another coal is a function of the organic/inorganic affinity of the element in question at the time of emplacement.

The environmental impact of coal utilization has been greatly underestimated based on bulk analyses of waste products retained in combustion facilities. The toxicology of inhaled particles emitted from power plants is enhanced owing to the preferential concentration and distribution of carcinogenic/mutagenic trace elements on the surfaces of the emitted particulates. Over 47,000 metric tons of Zn+As+Se+Cd+Sb+Hg+Pb are mobilized yearly as a result of coal utilization in North America and more than 3,000 tons of this reach the atmosphere. A new term is proposed to more correctly identify the hazards associated with coal

utilization: the "Effective Coal Concentration" of an element is here defined as the total amount of the element mobilized yearly as a result of coal utilization. This term can be adapted to local situations.

The organic/inorganic affinity of an element appears to be controlled, in part, by the ionic potential ($IP = \text{charge}/\text{ionic radius}$) of the element at the time of emplacement. Elements which exhibit $IP > 0.05$ favor organic affinities while those with $IP < 0.05$ show higher inorganic affinities. Elements which exhibit multiple oxidation states, i.e., IP values above and below 0.05, also show the greatest variability in organic/inorganic affinity.

BIBLIOGRAPHY

- Adriano, D.C., Page, L.A., Elsewi, A.A., Chang, A.C. and Straugham, I., (1980). Utilization and disposal of fly ash and other coal residues in terrestrial ecosystems: a review. *Journal of Environmental Quality*, v. 9, no. 3, p. 333-344.
- Affolter, R.H. and Hatch, J.R., (1980). Chemical analyses of coal from the Dakota and Straight Cliffs Formations of SW Utah. United States Geological Survey Open-File Report 80-138, p. 29-32.
- Affolter, R.H., J.R. Hatch and T.A. Ryer, (1979). Chemical Analyses of Coal and Shale from the Ferron Sandstone Member of the Mancos Shale, Emery Coal Field, Emery County, Utah. United States Geological Survey, Open-File Report 79-858, 35 p.
- Allen, R.M., and VanderSande, J.B., (1983). Analysis of sub-micron mineral matter in coal via scanning transmission electron microscopy. *Fuel*, v. 62.
- Anderson, L.A. and Smith, K.B., (1980). Dynamics of mercury at coal-fired power plant and adjacent cooling lake. *Environmental Science and Technology*, v. 11, no. 1, p. 75-85.
- Andren, C.F. and Klein, D.H., (1975). Selenium in coal-fired steam plant emissions. *Environmental Science and Technology*, v. 9, no. 9, 856-858.
- Aranyi, C.F., Miller, F.J., Andrea, F., Ehrlich, R., Fenters, J., Gardner, D.E. and Waters, M.D., (1979). Cytotoxicity to alveolar macrophages of trace metals absorbed on fly ash. *Environmental Research*, v. 20, p.14-23.
- Armstrong, R.L., (1968). Sevier Orogenic Belt in Nevada and Utah. *Geological Society of America Bulletin*, v. 79, p. 429-458.
- Bardin, S.W. and Bish, D.L., (1983). The occurrence of calcium oxalate minerals within aquatic macrophytes from Okefenokee Swamp, in R. Raymond and M. Andrejko (eds.), *Mineral matter in peat, its occurrence, form and distribution*. Los Alamos National Laboratory, LA-9907-OBES, Los Alamos, New Mexico, 242 p.
- Basolo, F. and Pearson, R.G., (1968). *Mechanisms of inorganic reactions: Study of metal complexes in solution*. John Wiley and Sons, Inc., New York, 426 p.

Berry, L.G. and Mason, B., (1959). Mineralogy, concepts, descriptions and determinations. W.H. Freeman and Company, San Francisco, 630 p.

Bertine, K.K. and Goldber, E.D., (1971). Fossil fuel combustion and the major sedimentary cycle. Science, v. 173, p. 233-235.

Billings, C.B. and Matson, W.R., (1972). Mercury emission from coal combustion. Science, v. 176, p. 1232-1233.

Bol'shakov, A.P. and Ptushko, L.I., (1971). Alteration products of melanterite from Nikitov mercury ore deposits. International Geological Review, 13, p. 849-854.

Bolton, N.E., Carter, J.A., Emery, F.J., Feldman, C., Fulkerson, W., Hulett, L.D. and Lyon, W.S., (1975). Trace element mass balance around a coal-fired steam plant, in S.P. Babu (ed.), Trace elements in fuel, American Chemical Society, Advances in Chemistry, Series, 141, p. 175-191.

Breger, I.A., Deul, M. and Rubinstein, S., (1955). Geochemistry and mineralogy of a uraniferous lignite. Economic Geology, v. 50, p. 206-226.

Brownlow, A.H., (1979). Geochemistry. Prentice-Hall, 498 p.

Campbell, J.A., Laul, J.C., Nielson, K.K. and Smith, R.D., (1978). Separation and chemical characterization of finely-sized fly-ash particles. Analytical Chemistry, v. 50, no. 8, p. 1032-1040.

Coates, D.A., (1980). Formation of clinker by natural burning of coal beds in the Powder River Basin, Wyoming, in L.M. Carter (ed.), Proceedings of the 4th Symposium on the Geology of Rocky Mountain Coal. Colorado Geological Survey Resource Series 10 (1980), p. 37-40.

Coates, D.A., and Naeser, C.W., (1980). Fission-track ages of clinker development, eastern Powder River Basin, Campbell County, Wyoming: Geological Society of America, Abstracts with Programs, Rocky Mountain Section Meeting, Provo, Utah.

Cody, R.D. and Biggs, D.L., (1973). Halotrichite, szomolnokite, and rozenite from Kolliver State Park, Iowa. Canadian Mineralogist, v. 11, p. 958-970.

- Coles, K.G., Ragaini, J.M., Ondov, J.M., Fisher, G.L., Silbermann, D. and Prentice, B.A., (1979). Chemical studies of stack fly ash from a coal-fired power plant. *Environmental Science and Technology*, v. 13, no. 4, p. 455-459.
- Cotter, E., (1976). The role of deltas in the evolution of the Ferron Sandstone and its coals, Castle Valley, Utah. *Brigham Young University Studies*, v. 22, pt. 3, p. 15-41.
- Curry, W.H., III, (1971). Laramide structural history of the Powder River Basin, Wyoming. Twenty-Third Annual Field Conference; 1971 Wyoming Geological Association Guidebook, p. 49-60.
- Davison, R.L., Natusch, D.F.S., Wallace, J.R. and Evans, C. A., (1974). Trace elements in fly ash, dependence of concentration on particle size. *Environmental Science and Technology*, v. 8, no. 13, p. 1107-1113.
- Doelling, H.H., (1972). Central Utah coal fields: Sevier-Sanpete, Wasatch Plateau, Book Cliffs and Emery. *Utah Geological and Mineralogical Survey Monograph 3*, p. 416-469.
- Doelling, H.H., (1971). Emery Coal Field, Utah. *Journal of Sedimentary Petrology*, v. 41, p. 43-44.
- Drain, A., (1861). Notice sur les cristaux d'albite renfermes dans les calcaires magnesiens des environs de modane. *Soc. Geol. France Bull.*, v. 18, ser. 2, p. 804-805. Cited in Kastner, 1971.
- Ebens, R.J., and McNeal, J.M., (1977). Geochemistry of Fort Union shale and sandstone in outcrop in the Northern Great Plains Coal Province, in *Geochemical survey of the Western Energy Regions*, fourth annual progress report: U.S. Geological Survey Open-File Report 77-872, p. 185-197.
- Estep, P.A., Kovach, J.J. and Karr Jr., C., (1968). Quantitative infrared multicomponent determination of minerals occurring in coal. *Analytical Chemistry*, v. 40, no. 2, p. 358-363.
- Ethridge, F.G., Jackson, T.J. and Youngberg, A.D., (1981). Floodbasin sequence of a fine-grained meander belt subsystem: The coal-bearing Lower Wasatch and Upper Fort Union Formations, Southern Powder River Basin, Wyoming. *Society of Economic Paleontologists and Mineralogists Special Publication No. 31*, p. 191-209.

- Fanshawe, J.R., (1971). Structural evolution of Big Horn Basin. Twenty-Third Annual Field Conference; 1971 Wyoming Geological Association Guidebook, p. 35-37.
- Fisher, G.L., Chang, D.P.L. and Brummer, M., (1976). Fly ash collected from electrostatic precipitators: microcrystalline structures and the mystery of the spheres. Science, v. 197, p. 553-554.
- Flores, R.M., (1981). Coal deposition in fluvial paleoenvironments of the Paleocene Tongue River Member of the Fort Union Formation, Powder River area, Powder River Basin, Wyoming and Montana. Society of Economic Paleontologists and Mineralogists Special Publication No. 31, p. 169-190.
- Flores, R.M., (1980). Comparison of depositional models of Tertiary and Upper Cretaceous coal-bearing rocks in some western interior basins of the United States. 1980 Proceedings of the 4th Annual Symposium on the Geology of Rocky Mountain Coals, Colorado Geological Survey, p. 17-20.
- Flores, R.M., (1979). Coal depositional models in some Tertiary and Cretaceous coal fields in the U.S. western interior. Organic Geochemistry, v. 1, p. 225-235.
- Frazer, F.W. and Belcher, C.B., (1972). Quantitative determination of the mineral-matter content of coal by a radiofrequency-oxidation technique. Fuel, v. 52, p. 41-46.
- Fyfe, W.S., (1987). University of Western Ontario, personal communication.
- Glass, G.B., (1981). Coal deposits of Wyoming. Thirty-Second Annual Field Conference; 1981 Wyoming Geological Association Guidebook, p. 181-236.
- Glass, G.B., (1979). Coal development in Powder River Basin, Wyoming (Abs.). American Association of Petroleum Geologists Bulletin, v. 63, no. 5, p. 827-828.
- Glass, G.B., (1978). Wyoming coal fields, 1978. Wyoming Geological Survey, Public Information Circular no. 9, 21 p.
- Glass, G.B., (1976). Update of the Powder River Coal Basin. Twenty-eighth annual field conference; 1976 Wyoming Geological Association Guidebook, p. 209-220.

- Glaze, R.E. and Keller, E.R., (Chairmen) (1965). Geologic history of the Powder River Basin: Wyoming Geological Association Technical Studies Committee, Casper, Wyoming. American Association of Petroleum Geologists Bulletin, v. 49, no. 11, p. 1893-1907.
- Gluskoter, H.J., (1975). Mineral matter and trace elements in coal, in S.P. Babu (ed.), Trace elements in fuel: American Chemical Society, Washington, D.C., Advances in Chemistry Series No. 141, p. 1-22.
- Gluskoter, H.J., (1965). Electric low-temperature ashing of bituminous coal: Fuel, v. 44, p. 285-291.
- Gluskoter, H.J., Ruch, R.R., Miller, W.G., Cahill, R.A., Dreher, G.B. and Kuhn, J.K., (1977). Trace elements in coal: occurrence and distribution. Illinois State Geological Survey Circular 499, 154 p.
- Goldschmidt, V.M., (1937). The principles of distribution of chemical elements in minerals and rocks. Journal of the Chemical Society, 227, p. 655-673.
- Goldschmidt, V.M., (1935). Rare elements in coal ashes: Industrial and Engineering Chemistry, v. 27, no. 9, p. 1100-1102.
- Goldstein, J.I., and Yakowitz, H., (1975). Practical scanning electron microscopy. Plenum Books.
- Greenwood, N.N. and Earnshaw, A., (1984). Chemistry of the elements. Pergamon Press, Great Britain; 1542 p.
- Hatch, J.R., Affolter, R.H. and Davis, F.D., (1980). Chemical analyses of coal from the Blackhawk Formation, Wasatch Plateau Coal Field, Carbon, Emery, Sevier Counties, Utah. Utah Geological and Mineral Survey Special Study 49, p. 99-102.
- Hatch, J.R. and Swanson, V.E., (1977). Trace elements in Rocky Mountain coals, in D.K. Murray (ed.), Geology of Rocky Mountain coal - A Symposium. Colorado Geological Survey Resource Series 1, p. 143-165.
- Herring, J.R., (1980). Geochemistry of clinker, naturally burning coal, and mine fires, in L.M. Carter (ed.), Proceedings of the 4th Symposium on the Geology of Rocky Mountain Coal. Colorado Geological Survey Resource Series 10 (1980), p. 41-44.

Hinkley, T.K., Herring, J.R., and Ebens, R.J., (1980). Chemical character and practical pre-mining sampling needs, Fort Union Formation coal overburden rock, in L.M. Carter (ed.), Proceedings of the 4th Symposium on the Geology of Rocky Mountain Coal. Colorado Geological Survey Resource Series 10 (1980), p. 45-49.

Hinkley, T.K., and Ebens, R.J., (1977). Geochemistry of fine-grained rocks in cores of the Fort Union Formation, in Geochemical survey of the Western Energy Regions, 4th Annual Progress Report, July 1977: U.S. Geological Survey Open-File Report 77-872, p. 169-172.

Hinkley, T.K., and Ebens, R.J., (1976). Mineralogy of fine-grained rocks in the Fort Union Formation, in Geochemical Survey of the Western Energy Regions: U.S. Geological Survey Open-File Report 76-729, p. 10-13.

Horton, L. and Aubrey, K.V., (1950). The distribution of minor elements in vitrain: Three vitrains from the Barnsley seam. Society of Chemical Industry, Journals and Transactions, Supplementary Issue No. 1, v. 69, p. S41-S48.

Houston, R.S., (1971). Regional tectonics of the Precambrian rocks of the Wyoming Province and its relationship to Laramide structure. Twenty-Third Annual Field Conference; 1971 Wyoming Geological Association Guidebook, p. 19-27.

Huggins, F.E., Huffman, G.P. and Lin, M.C., (1983). Observations on low temperature oxidation of minerals in bituminous coals. International Journal of Coal Geology, 3, p. 157-182.

Kaakinen, J.W., Jorden, R.M., Lawasani, N.H. and West, R.E., (1975). Trace element behavior in coal-fired power plants. Environmental Science and Technology, v. 9, no. 10, p. 862-869.

Kalb, G.W., (1975). Total mercury mass balance at a coal-fired power plant, in S.P. Babu (ed.), American Chemical Society, Washington, D.C., Advances in Chemistry Series 141, p. 154-174.

Kastner, M., (1971). Authigenic feldspars in carbonate rocks. American Mineralogist, v. 56, p. 1401-1441.

Klein, D.H., Andren, A.W., Carter, J.A., Emery, F.J., Feldman, C., Furkerson, W., Lyon, W.S., Ogle, J.C., Talai, Y., VanHook, R.I. and Bolton, N., (1975). Pathways of thirty-seven trace elements through a coal-fired power plant. Environmental Science and Technology, v. 9, no. 7, p. 643-647.

- Krauskopf, K.B., (1967). Introduction to geochemistry. McGraw-Hill Inc., 721 p.
- Kronberg, B.I., Murray, F.H., Fyfe, W.S., Winder, C.G., Brown, J.R. and Powell, M., (1987). Geochemistry and petrology of the Mattagami Formation lignites (northern Ontario), in A. Volborth (ed.), Coal Science and Chemistry. Elsevier Science Publishing B.V., Amsterdam, p. 245-263.
- Kuhn, J.K., Fiene, F.L., Cahill, R.A., Gluskoter, H.J., and Shimp, N.F., (1980). Abundance of trace and minor elements in organic and mineral fractions of coal. Illinois State Geological Survey, Environmental Geology Notes 88, 67 p.
- Lee, R.E., Crist, H.L., Riley, A.E. and MacLeod, K.E., (1975). Concentration and size of trace metal emissions from a power plant, a steel plant and a cotton gin. Environmental Science and Technology, v. 9, no. 7, p. 643-647.
- Linton, R.W., Loh, A., Natusch, D.F.S., Evans, C.A. and Williams, P., (1976). Surface predominance of toxic elements in airborne particles. Science, v. 191, p. 852-854.
- Lupton, C.T., (1916). Geology and coal resources of Castle Valley in Carbon, Emery and Sevier counties, Utah. United States Geological Survey Bulletin, v. 628, 84 p.
- McGookey, D.P., compiler, (1972). Cretaceous System, in, W.W. Malloy (ed.), Geologic Atlas of the Rocky Mountain Region. Rocky Mountain Association of Geologists, p. 190-228.
- McGrew, P.O., (1971). The Tertiary history of Wyoming. Twenty-third annual field conference; 1971 Wyoming Geological Association Guidebook, p. 29-33.
- Mellor, D.P. and Maley, L., (1948). Order of stability of metal complexes. Nature, v. 161, p. 436-437.
- Miller, R.N. and Given, P.H., (1987). The association of major, minor and trace inorganic elements with lignites. II. Minerals, and major and minor element profiles, in four seams. Geochimica et Cosmochimica Acta, v. 51, p. 1311-1322.
- Miller, R.N., Yarzab, R.F. and Given, P.H., (1979). Determination of mineral-matter contents of coals by low-temperature ashing. Fuel, v. 58, p. 4-10.

- Mitchell, R.S. and Gluskoter, H.J., (1976). Mineralogy of ash of some American coals: variations with temperature and source. *Fuel*, v. 55, p. 90-96.
- Naevel, R.C., (1981). Origin, petrology and classification of coal, in: M. Elliott (ed.), *Chemistry of coal utilization*, Volume 2. Wiley Interscience, p. 91-158.
- Natusch, D.F.S., (1978). Potentially carcinogenic species emitted to the atmosphere by fossil-fueled power plants. *Environmental Health Perspectives*, v. 22, p. 79-90.
- Natusch, D.F.S. and Wallace, J.R., (1974). Urban aerosol toxicity: the influence of particle size. *Science*, v. 186, no. 4165, p. 695-699.
- Natusch, D.F.S., Wallace, J.R. and Evans, C.A., (1974). Toxic trace elements: Preferential concentration in respirable particles. *Science*, v. 183, p. 202-204.
- Nicholls, G.D., (1968). The geochemistry of coal-bearing strata, in D. Murchison and T.S. Westoll (eds.), *Coal and coal-bearing strata*. Elsevier, New York, p. 269-307.
- O'Gorman, J.V. and Walker Jr., P.L., (1971). Mineral matter characteristics of some American coals. *Fuel*, v. 50, p. 135-151.
- Ondov, J.M., Ragaini, R.C. and Biermann, A.H., (1979a). Elemental emissions from a coal-fired power plant: comparison of a Venturi wet scrubber system with a cold-sided electrostatic precipitator. *Environmental Science and Technology*, v. 13, no. 5, p. 598-607.
- Ondov, J.M., Ragaini, R.C. and Biermann, A.H., (1979b). Emissions and particle size distributions of minor and trace elements at two western coal-fired power plants equipped with cold-sided electrostatic precipitators. *Environmental Science and Technology*, v. 13, no. 8, p. 946-953.
- Page, A.L., Elsewi, A.A. and Straughan, I.R., (1979). Physical and chemical properties of fly ash from coal-fired power plants with reference to environmental impact, in *Residue Reviews*, v. 71, p. 83-120.
- Painter, P.C., Coleman, M.M., Jenkins, R.G., Whang, P.W. and Walker Jr., P.W., (1978). Fourier transform infrared study of mineral matter in coal. A novel method of quantitative mineralogical analysis. *Fuel*, v. 57, p. 337-344.

- Piperno, E., (1975). Trace element emissions: aspects of environmental toxicology, in S.P. Babu (ed.), Trace elements in fuel. American Chemical Society Advances in Chemistry Series 141, p. 192-209.
- Rankama, K. and Sahama, Th.G., (1950). Geochemistry. University of Chicago Press, Chicago, 912 p.
- Rao, C.P. and Gluskoter, H.J., (1976). Occurrence and distribution of minerals in Illinois coals. Illinois State Geological Survey Circular 476, 56 p.
- Raymond Jr., R., Andrejko, M.J. and Bardin, S.W., (1983). Occurrence of szomolnokite in Kentucky No. 14 coal and possible implications concerning formation of iron sulfides in peats and coals, in R. Raymond and M. Andrejko (eds.), Mineral matter in peat, its occurrence, form and distribution. Los Alamos National Laboratory, LA-9907-OBES, Los Alamos, New Mexico, p. 158-168.
- Robinson, P., compiler, (1972). Tertiary History, in, W.W. Mallory (ed.), Geologic Atlas of the Rocky Mountain region. Rocky Mountain Association of Geologists, p. 233-242.
- Rose, G., (1865). Uber die krystallform des albite von dem roc tourne und von bonhomme in savoyen und des albite in Allgemeinen. Pogg. Ann. Phys. Chem., v. 25, p. 457-468. Cited in Kastner, 1971.
- Roy, W.R., Thiery, R.G., Schuller, R.M. and Suloway, J.J., (1981). Coal fly ash: a review of the literature and proposed classification system with emphasis on environmental impacts. Illinois Geological Survey, Environmental Geology Notes 96, 69 p.
- Ruch, R.R., Gluskoter, H.J. and Shimp, N.F., (1974). Occurrence and distribution of potentially volatile trace elements in coal: A final report. Illinois Geological Survey Environmental Geology Note 72, 96 p.
- Ruch, R.R., Gluskoter, H.J. and Shimp, N.F., (1973). Occurrence and distribution of potentially volatile trace elements in coal: An interim report. Illinois Geological Survey Environmental Geology Note 81, 43 p.
- Ryer, T.A., (1983). Transgressive-regressive cycles and the occurrence of coal in some Upper Cretaceous strata of Utah. Geology, v. 11, p. 207-210.
- Ryer, T.A., (1981). Deltaic coals of the Ferron Sandstone Member of Mancos Shale: Predictive model for Cretaceous coal-bearing strata of western interior. American

Association of Petroleum Geologists Bulletin, v. 65,
no. 11, p. 2323-2340.

- Sawyer, R.K. and Griffin, G.M., (1983). The source and origin of the mineralogy of the northern Florida Everglades, in R. Raymond and M. Andrejko (eds.), Mineral matter in peat, its occurrence, form and distribution. Los Alamos National Laboratory, LA-9907-OBES, Los Alamos, New Mexico, p. 189-198.
- Smith, A.D., (1981). Muddy Creek coal drilling project, Wasatch Plateau, Utah. Utah Geological and mineral Survey Special Studies, 55, p. 15-16.
- Smith, R.D., Campbell, J.A. and Nielson, K.K., (1979). Concentration dependence upon particle-size of volatilized elements in fly ash. Environmental Science and Technology, v. 13, no. 5, p. 553-558.
- Swanson, V.E., Medlin, J.H., Hatch, J.R., Coleman, S.L., Wood, G.H., Woodruff, S.D. and Hildebrand, R.T., (1976). Collection, chemical analysis, and evaluation of coal samples in 1975. United States Geological Survey Open-File Report 76-468, 503 p.
- U.N. Energy Yearbook, (1984).
- Weichman, B.E., Glaze, R.E. and Keller, E.R., (1965). Geological history of Powder River Basin. American Association of Petroleum Geologists Bulletin, v. 49, no. 11, p. 1893-1907.
- Weise Jr., R.G., Powell, M.A. and Fyfe, W.S., (1987). Spontaneous formation of hydrated iron sulfates on laboratory samples of pyrite- and marcasite-bearing coals. Chemical Geology, v. 63, p. 29-38.
- Zodrow, E.L., Wiltshire, J. and McCandlish, K., (1979). Hydrated sulfates in the Sydney Coalfield of Cape Breton, Nova Scotia. II. Pyrite and its alteration products. Canadian Mineralogist, v. 17, p.63-77.
- Zodrow, E.L. and McCandlish, K., (1978). Hydrated sulfates in the Sydney Coalfield, Cape Breton, Nova Scotia. Canadian Mineralogist, v. 16, p. 17-22.
- Zubovic, P., (1976). Geochemistry of trace elements in coal, in F.A. Ayer (compiler), Symposium proceedings: Environmental aspects of fuel conversion technology, II: (December 1975), Washington D.C. U.S. Environmental Protection Agency, Environmental Protection Technology Series EPA-600/2-76-149, p. 47-63.

Zubovic, P., (1966a). Minor element distribution in coal samples of the Interior Coal Province. Advances in Chemistry Series 55, p. 231-247.

Zubovic, P., (1966b). Physicochemical properties of certain minor elements as controlling factors of their distribution in coal. Advances in Chemistry Series 55, p. 221-230.

Zubovic, P., Stadnichenko, T. and Sheffey, N.B., (1961). The association of minor element associations in coal and other carbonaceous sediments. United States Geological Survey Professional Paper 424-D, Article 411, P. D345-D348.